

Earth Systems Data and Models

Kripamoy Sarkar  
Sarada Prasad Pradhan  
Trilok Nath Singh *Editors*

# Landslides: Analysis, Modeling and Mitigation


 Springer

# Earth Systems Data and Models

## Volume 7

### Series Editors

Bernd Blasius, Institute for Chemistry and Biology of the Marine Environment,  
Carl von Ossietzky University of Oldenburg, Oldenburg, Niedersachsen, Germany

Avelino Núñez-Delgado , Soil Science and Agricultural Chemistry, University of  
Santiago de Compostela, Lugo, Spain

Dimitri P. Solomatine, UNESCO—IHE Institute for Water Education, Delft, The  
Netherlands



The book series *Earth Systems Data & Models* publishes state-of-the-art research and technologies aimed at understanding processes and interactions in the earth system. A special emphasis is given to theory, methods, and tools used in earth, planetary and environmental sciences for: modeling, observation and analysis; data generation, assimilation and visualization; forecasting and simulation; and optimization. Topics in the series include but are not limited to: numerical, data-driven and agent-based modeling of the earth system; uncertainty analysis of models; geodynamic simulations, climate change, weather forecasting, hydroinformatics, and complex ecological models; model evaluation for decision-making processes and other earth science applications; and remote sensing and GIS technology. The series publishes monographs, edited volumes and selected conference proceedings addressing an interdisciplinary audience, which not only includes geologists, hydrologists, meteorologists, chemists, biologists and ecologists but also physicists, engineers and applied mathematicians, as well as policy makers who use model outputs as the basis of decision-making processes.

Kripamoy Sarkar · Sarada Prasad Pradhan ·  
Trilok Nath Singh  
Editors

# Landslides: Analysis, Modeling and Mitigation

*Editors*

Kripamoy Sarkar  
Department of Applied Geology  
Indian Institute of Technology (Indian  
School of Mines), Dhanbad  
Dhanbad, Jharkhand, India

Sarada Prasad Pradhan  
Department of Earth Sciences  
Indian Institute of Technology Roorkee  
Roorkee, Uttarakhand, India

Trilok Nath Singh  
Indian Institute of Technology Patna  
Patna, Bihar, India

ISSN 2364-5830

ISSN 2364-5849 (electronic)

Earth Systems Data and Models

ISBN 978-3-031-78895-6

ISBN 978-3-031-78896-3 (eBook)

<https://doi.org/10.1007/978-3-031-78896-3>

© The Editor(s) (if applicable) and The Author(s), under exclusive license to Springer Nature Switzerland AG 2025

This work is subject to copyright. All rights are solely and exclusively licensed by the Publisher, whether the whole or part of the material is concerned, specifically the rights of translation, reprinting, reuse of illustrations, recitation, broadcasting, reproduction on microfilms or in any other physical way, and transmission or information storage and retrieval, electronic adaptation, computer software, or by similar or dissimilar methodology now known or hereafter developed.

The use of general descriptive names, registered names, trademarks, service marks, etc. in this publication does not imply, even in the absence of a specific statement, that such names are exempt from the relevant protective laws and regulations and therefore free for general use.

The publisher, the authors and the editors are safe to assume that the advice and information in this book are believed to be true and accurate at the date of publication. Neither the publisher nor the authors or the editors give a warranty, expressed or implied, with respect to the material contained herein or for any errors or omissions that may have been made. The publisher remains neutral with regard to jurisdictional claims in published maps and institutional affiliations.

This Springer imprint is published by the registered company Springer Nature Switzerland AG  
The registered company address is: Gewerbestrasse 11, 6330 Cham, Switzerland

If disposing of this product, please recycle the paper.

# Foreword

I am pleased to learn that Springer Publishing Company is releasing a new book on landslides as part of the Earth Systems Data and Models series. This book, titled *Landslides: Analysis, Modeling and Mitigation*, is edited by **Kripamoy Sarkar, Sarada Prasad Pradhan, and Trilok Nath Singh**, who are renowned experts in landslide hazard assessment.

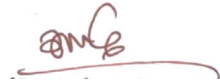
In the recent past, on July 30, 2024, the Landslide in Wayanad, Kerala, causing a death of hundreds of people besides the landslide on August 26, 2024, in North Gondar (Ethiopia) and on August 27, 2024, in Phuket, Thailand, are the cases that need be pondered upon. Both natural- and human-induced factors have contributed to these events. It has been noticed that landslides and related mass movements can occur in various settings. As has been evident, the consequences of Wayanad hazard have severely impacted the ecology, economy, and environment. In a country like India, with its diverse topography and climate, the unpredictability of landslides and rockfall hazards pose a significant concern. The book addresses these concerns quite effectively.

The book comprises fifteen chapters that explore different aspects of landslide hazard mechanisms and assessment. These chapters are organized into four sections and each focused on a major theme:

- **First Part: Understanding the Basics of Landslides and Their Causative Factors**—This part covers the fundamental mechanisms of landslide hazards and the factors leading to slope failures.
- **Second Part: Some Traditional Techniques of Landslide Assessment**—This part discusses conventional methods for assessing slope stability, including widely used rock mass and slope mass classification systems.
- **Third Part: Simulation of Slope Mass Movements Including Numerical Methods**—This part addresses modeling slope mass movements and evaluating their stability using techniques such as limit equilibrium methods and numerical methods like finite and distinct element methods.

- **Fourth Part: Machine Learning Methods for Landslide and Slope Stability Prediction**—This part explores how advanced machine learning models can be developed and applied to predict slope instability and landslide susceptibility in specific regions.

The book represents a collaborative effort by numerous authors, researchers, and experts in the field of landslide studies from across the country. The editors have done an exemplary job in gathering, compiling, and presenting these contributions in book form. I extend my warm congratulations to everyone involved in this publication and commend Springer Publishing Company on the launch of this important work.



August 2024

Dr. Uday Kant  
Vice Chairman  
Bihar State Disaster Management Authority  
Patna, Bihar, India

# Preface

The diverse topography of India witnesses several natural calamities. One of the most severe among them is the occurrences of landslides. Defined as mass movements down the hill slopes, landslides are very frequent in the country, especially in the hilly terrains. These mainly include the Himalayan regions (northern and north-eastern), the eastern ghats, and the western ghats. Various natural and man-made factors come into play during the initiation of slope failures, which include both landslides and rock fall hazards. For instance, weak lithology, unfavourable structural conditions, and extreme climatic conditions, including cloudbursts and seismic events, often trigger landslides. Often, human intervention in the form of unplanned construction, and engineering activities results in the occurrence of these unfortunate events. Landslides and rockfall events not only result in the loss of human lives, but are also responsible for damaging infrastructures and transportation facilities, impacting the overall socio-economic conditions of the country.

In an attempt to provide better insights into the subject of landslides hazards, this book presents a comprehensive effort accomplished not only to understand the issue, but also to help in the analysis, modeling and effective prediction of the same. This book emphasizes on the mechanisms involved in the initiation of slope failures, the various modes of slope failures, the methods used to analyse and predict the occurrence of landslides—which range from the traditional methods of stability assessment, the numerical methods, to the state-of-the-art machine learning techniques—and the mitigation measures that could be adopted to reduce the possibilities of such failures.

The book consists of fifteen chapters from various contributors across the country, which have been broadly classified into four parts. The first part gives an understanding of the mechanisms of the landslide hazards, and the various causative factors like orientation of structural discontinuities, rainfall, and microstructural characteristics. The second part deals with the basic methods used for assessing the stability of slopes. This includes empirical methods, slope mass and rock mass characterization techniques, and photogrammetry methods. The third part gives an understanding of the simulation methods adopted in landslide hazard evaluation, with insights into the traditional limit equilibrium methods, and the numerical methods adopted like

the finite and the distinct element methods. The fourth part consists of some state-of-the-art machine learning applications in prediction of slope stability, as well as landslide hazard susceptibility. Many chapters consist of specific case studies with respect to the occurrences of landslides from various parts of India, which will help in reinforcing the overall motive behind the genesis of this book.

We express our deepest gratitude to all the authors for their indispensable contributions in the form of highly motivating chapters to this book. We thank them again for sharing their immense knowledge and expertise. We are also much indebted to reviewers for their valuable suggestions and comments.

And above all, we express our exuberant gratitude to Springer Publication Ltd. for believing in our work and enabling it for publication.

We are much beholden to Avishek Dutta for offering his editorial assistantship in the making of the book.

Dhanbad, India  
Roorkee, India  
Patna, India

Kripamoy Sarkar  
Sarada Prasad Pradhan  
Trilok Nath Singh

# Contents

## **Understanding the Basics of Landslides and Their Causative Factors**

### **Navigating Hydrological Factors in Understanding and Mitigating Landslide Hazards in the Indian Himalayas: A Short Review ..... 3**

Amulya Ratna Roul, Ajit Kumar Behera, Rudra Mohan Pradhan,  
and Sarada Prasad Pradhan

### **Geological and Microstructural Controls on a Landslide in Ghat Region Along NH-09, Kumaun Himalaya ..... 25**

Piyush Kumar Singh and Sarada Prasad Pradhan

### **Rainfall Induced Landslides in Bangapani Tehsil of Pithoragarh District, Kumaun Himalaya, India ..... 49**

Rahul Negi, Pooja Saini, and R. A. Singh

### **A Comparative Analysis of Landslide Characteristics of the Himalayan and Western Ghat Mountain Belts ..... 77**

N. K. Rai, P. K. Singh, Ravi Shankar, and Digvijay Singh

## **Some Traditional Techniques of Landslide Assessment**

### **Applications of Photogrammetry Technique in Slope Stability Investigation ..... 103**

Jaspreet Singh, Amulya Ratna Roul, Saurabh Prakash Aher,  
Sarada Prasad Pradhan, and Vikram Vishal

### **Empirical Method Based Geotechnical Assessment of Engineered Slopes Along National Highway-58, Rajasthan, India ..... 123**

Tariq Siddique, Aquib Shamshad, Tuba Fatima,  
Pirzada Mohammad Haris, and Md. Erfan Ali Mondal



<b>Slope Stability Evaluation Through Slope Mass Rating and Its Extension</b> .....	145
Amit Jaiswal, Md Shayan Sabri, Amit Kumar Verma, Ashutosh Pratap Shastri, Komal Kumari, and T. N. Singh	
<b>Simulation of Slope Mass Movements Including Numerical Methods</b>	
<b>Assessment of Progressive Behaviour of Deep-Seated Kotropi Landslides (Himachal Pradesh) Using the 3D Limit Equilibrium Method</b> .....	165
Saurabh Kumar, Saurabh Prakash Aher, Sarada Prasad Pradhan, and B. D. Patni	
<b>Simulating Failure Modes in a Jointed Rock Slope Using Distinct Element Modeling—A Case Study from the Himachal Himalayas in India</b> .....	189
Avishek Dutta, Kripamoy Sarkar, and T. N. Singh	
<b>Two-Dimensional Finite Element Modelling for an Optimum Engineered Design for Portal Slopes</b> .....	209
Ravi Kumar Umrao, Rajesh Singh, L. K. Sharma, and T. N. Singh	
<b>Finite Element Modeling for Rock Slope Stability Assessment in North-Eastern India</b> .....	225
Kripamoy Sarkar and Avishek Dutta	
<b>Effect of Ditch Design on Rockfall Hazard Using Rigid Body Model</b> ....	241
Anurag Niyogi, Kripamoy Sarkar, and T. N. Singh	
<b>Probabilistic Stability Analysis of Opencast Coal Mine Dump Slopes from Lower Gondwana Region, India: A Case Study</b> .....	253
Prasanta Kr. Behera, Ashok Kr. Singh, and Kripamoy Sarkar	
<b>Machine Learning Methods for Landslide and Slope Stability Prediction</b>	
<b>An Emerging Machine Learning Approach for Predicting Risk and Stability on Susceptible Terrain</b> .....	271
Sanjay Singh, Amit Kumar Verma, and Jayraj Singh	
<b>Comparative Assessment of XGBoost Model and Hyper-Parameter Optimization Techniques in Landslide Susceptibility Mapping—A Case Study of Aglar Watershed, Part of Lesser Himalaya</b> .....	287
Dipika Keshri, Kripamoy Sarkar, and Shovan Lal Chattoraj	

# Editors and Contributors

## About the Editors

**Kripamoy Sarkar** is an Associate professor in the Department of Applied Geology in the Indian Institute of Technology (Indian School of Mines) Dhanbad. He is an accomplished and trained Engineering Geologist by profession with unique blend of industry and academic experience and has contributed significantly in the field of natural hazard investigations and soft computing applications in landslides. A few noteworthy contributions of Prof. Sarkar include improvements in rock mass characterization systems, and application of numerical modelling techniques to solve slope instability problems in the Indian Himalayas. His list of publications includes 90 scientific papers in various national and international journals and conference proceedings of repute. He has also published 4 edited book chapters that reflect advanced studies on the assessment of the landslide hazards. Prof. Sarkar has been the principal investigator of 5 major projects on landslide vulnerability analysis and rockfall hazard assessment sponsored by the Ministry of Earth Sciences, DST, and IIT (ISM) Dhanbad in the Northern and North-Eastern parts of the Indian Himalayas. He is the recipient of the prestigious Inder Mohan Thapar Research Award (2021 and 2022) from IIT (ISM) Dhanbad. He is an Associate Editor of the *Journal of Earth System Science*.

**Sarada Prasad Pradhan** is currently working as an Associate Professor in Indian Institute of Technology (IIT) Roorkee, India, in the Department of Earth Sciences. He obtained his M.Sc. (Applied Geology) and Ph.D. from IIT Bombay (India). He worked as a Reservoir Engineer in Oil and Natural Gas Corporation Ltd. (ONGC) for around 5 years where he was associated with many projects of national importance. He was recipient of Outstanding Young Faculty Award by IIT Roorkee, Melpadom Attumalil Georgekutty Young Scientist Award, Young Scientist Award from CAFET INNOVA Technical Society and Award of excellence from ONGC Ltd. His research findings have been well received by the scientific community and published more than 100 research papers and abstracts in leading national, international journals,

book chapters and conference proceedings. He has been investigating major research and consultancy projects on slope stability sponsored by Govt. of India, Govt. of Uttarakhand and private industries. His major research interests are Rock Mechanics, Engineering Geology, Slope Stability, Reservoir Geo-mechanics, Petroleum Geo-science and Carbon Dioxide Sequestration.

**Trilok Nath Singh** is currently working as Director of IIT Patna and the Institute Geoscience Chair Professor in the Department of Earth Sciences, IIT Bombay, Mumbai, and is an expert in the field of rock mechanics, mining geology, and clean energy. He received his Ph.D. degree from the Institute of Technology BHU, Varanasi, in 1991 and subsequently served the institute until 2003. He is a recipient of many prestigious awards such as the National Mineral Award, the first P. N. Bose Mineral Award, the SEAGATE Excellence Award for Geo-Engineering, and the GSI Sesquicentennial Commemorative Award. He has nearly 28 years of experience in research and teaching with 40 doctoral theses completed under his supervision and has authored more than 350 publications in various journals and conferences of national and international repute. He is currently leading projects of immense scientific and industrial importance related to coalbed methane, carbon sequestration, shale gas, nuclear waste repositories, and mine slope stability, to name a few. He is on the governing and advisory councils of several national institutes and universities.

## Contributors

**Saurabh Prakash Aher** Department of Earth Sciences, Indian Institute of Technology Roorkee, Roorkee, India

**Ajit Kumar Behera** Groundwater Hydrology Division, NIH Roorkee, Uttarakhand, India

**Prasanta Kr. Behera** Geological Survey of India (GSI), Kolkata, West Bengal, India

**Shovan Lal Chattoraj** Geosciences and Disaster Management Studies Group, IIRS, Dehradun, Dehradun, India

**Avishek Dutta** Indian Institute of Technology (Indian School of Mines), Dhanbad, Jharkhand, India

**Tuba Fatima** Department of Geology, Aligarh Muslim University, Aligarh, India

**Pirzada Mohammad Haris** Department of Geology, Aligarh Muslim University, Aligarh, India

**Amit Jaiswal** Department of Civil Engineering, National Institute of Technology, Patna, Patna, Bihar, India

**Dipika Keshri** Department of Civil Engineering, School of Engineering and Technology (SOET), DIT University, Dehradun, Uttarakhand, India

**Saurabh Kumar** Department of Earth Sciences, IIT Roorkee, Roorkee, India

**Komal Kumari** Department of Civil and Environmental Engineering, Indian Institute of Technology Patna, Bihta, Patna, Bihar, India

**Md. Erfan Ali Mondal** Department of Geology, Aligarh Muslim University, Aligarh, India

**Rahul Negi** Department of Geology, L.S.M. Government P.G. College Pithoragarh, Pithoragarh, Uttarakhand, India

**Anurag Niyogi** Department of Applied Geology, Indian Institute of Technology (Indian School of Mines), Dhanbad, Jharkhand, India;  
Department of Earth and Environmental Sciences, Indian Institute of Science Education and Research, Bhopal, Madhya Pradesh, India

**B. D. Patni** NHPC Limited, Faridabad, India

**Rudra Mohan Pradhan** Department of Geology and Geophysics, IIT Kharagpur, Kharagpur, India

**Sarada Prasad Pradhan** Department of Earth Sciences, Indian Institute of Technology Roorkee, Roorkee, India

**N. K. Rai** Department of Earth and Planetary Sciences, University of Allahabad, Prayagraj, Uttar Pradesh, India

**Amulya Ratna Roul** Department of Earth Sciences, Indian Institute of Technology Bombay, Mumbai, India;  
Department of Earth Sciences, Indian Institute of Technology Roorkee, Roorkee, India

**Md Shayan Sabri** Department of Civil and Environmental Engineering, Indian Institute of Technology Patna, Bihta, Patna, Bihar, India

**Pooja Saini** Department of Geology, L.S.M. Government P.G. College Pithoragarh, Pithoragarh, Uttarakhand, India

**Kripamoy Sarkar** Department of Applied Geology, Indian Institute of Technology (Indian School of Mines), Dhanbad, Jharkhand, India

**Aquib Shamsad** Department of Geology, Aligarh Muslim University, Aligarh, India

**Ravi Shankar** Department of Science and Humanities, Bakhtiyarpur College of Engineering, Patna, Bihar, India

**L. K. Sharma** Geological Survey of India, Eastern Region, State Unit: Jharkhand, Ranchi, India;  
Indian Institute of Technology Bombay, Mumbai, India

**Ashutosh Pratap Shastri** Department of Civil and Environmental Engineering, Indian Institute of Technology Patna, Bihta, Patna, Bihar, India

**Tariq Siddique** Department of Geology, Aligarh Muslim University, Aligarh, India

**Ashok Kr. Singh** CSIR-Central Institute of Mining and Fuel Research, Regional Research Centre, Roorkee, Uttarakhand, India

**Digvijay Singh** Department of Earth and Planetary Sciences, University of Allahabad, Prayagraj, Uttar Pradesh, India

**Jaspreet Singh** Department of Earth Sciences, Indian Institute of Technology Roorkee, Roorkee, India

**Jayraj Singh** CAIRO, Universiti Teknologi Malaysia, Kuala Lumpur, Malaysia; NIIT University, Neemrana, Rajasthan, India

**P. K. Singh** Department of Earth and Planetary Sciences, University of Allahabad, Prayagraj, Uttar Pradesh, India

**Piyush Kumar Singh** Department of Earth Sciences, IIT Roorkee, Roorkee, India

**R. A. Singh** Government Degree College Churiyala, Haridwar, Uttarakhand, India

**Rajesh Singh** Department of Geology, University of Lucknow, Lucknow, India; Indian Institute of Technology Bombay, Mumbai, India

**Sanjay Singh** Department of Civil and Environmental Engineering, Indian Institute of Technology, Patna, India

**T. N. Singh** Department of Civil and Environmental Engineering, Indian Institute of Technology Patna, Bihta, Patna, Bihar, India;  
Indian Institute of Technology Patna, Bihta, Bihar, India

**Ravi Kumar Umrao** School of Environmental Sciences, Jawaharlal Nehru University, New Delhi, India;  
Indian Institute of Technology Bombay, Mumbai, India

**Amit Kumar Verma** Department of Civil and Environmental Engineering, Indian Institute of Technology Patna, Bihta, Patna, Bihar, India

**Vikram Vishal** Department of Earth Sciences, Indian Institute of Technology Bombay, Mumbai, India

# **Understanding the Basics of Landslides and Their Causative Factors**

# Navigating Hydrological Factors in Understanding and Mitigating Landslide Hazards in the Indian Himalayas: A Short Review



Amulya Ratna Roul, Ajit Kumar Behera, Rudra Mohan Pradhan,  
and Sarada Prasad Pradhan

**Abstract** Landslides represent a significant geological hazard in the Indian Himalayan region, particularly in the Northeastern Himalayas and Northwestern Himalayas, posing substantial risks to human settlements, infrastructure, and natural ecosystems. Understanding the complex interplay between hydrological factors, such as rainfall and groundwater, and their influence on landslide occurrences is imperative for effective mitigation strategies and disaster management in these vulnerable regions. Rainfall, characterized by its intensity, duration, and spatial distribution, plays a pivotal role in triggering landslides in the Indian Himalayas. The steep topography coupled with the monsoonal climate regime results in intense rainfall events, particularly during the monsoon season, which significantly increases the susceptibility of the region to landslides. Moreover, the variability of rainfall patterns across different seasons further exacerbates landslide risks, with prolonged wet periods leading to saturation of the soil and increased pore water pressure, ultimately culminating in slope instability and landslide occurrences. Groundwater dynamics also exert a profound influence on landslide susceptibility in the Indian Himalayan region. The complex interaction between geological formations, hydrogeological properties, and groundwater flow regimes influences the stability of slopes. Groundwater infiltration into the subsurface can weaken slope materials, reduce soil cohesion, and lubricate potential slip surfaces, thereby facilitating landslide initiation and propagation. Additionally, fluctuations in groundwater levels, influenced by seasonal variations in precipitation and land use practices, contribute to temporal variations in landslide occurrences. This chapter aims to provide a thorough resource for researchers

---

A. R. Roul (✉)

Department of Earth Sciences, IIT Bombay, Powai 400 076, India

e-mail: [amulya.did@gmail.com](mailto:amulya.did@gmail.com)

A. K. Behera

Groundwater Hydrology Division, NIH Roorkee, Uttarakhand 247 667, India

R. M. Pradhan

Department of Geology and Geophysics, IIT Kharagpur, Kharagpur 721 302, India

S. P. Pradhan

Department of Earth Sciences, IIT Roorkee, Uttarakhand 247 667, India

and stakeholders working in or planning to work in the Indian Himalayas. It aims to underscore both the limitations and strengths inherent in current research endeavours. It also offers insights into the critical areas requiring urgent attention for advancing landslide risk reduction efforts in the region.

**Keywords** Landslide assessment · Northeastern Himalaya · Northwestern Himalaya · Indian Himalaya · Rainfall threshold

## 1 Introduction

The Indian Himalayan region encompasses approximately 16.2% of the nation's total geographical expanse and sustains a population exceeding 31 million individuals (Dikshit et al. 2020). The Himalayas, characterized by a fragile ecosystem and a delicate geological structure undergoing contemporary crustal adjustments, coupled with factors such as heavy precipitation, diverse slopes, and challenging hydro-geological conditions, are highly prone to landslides. This susceptibility is exacerbated by escalating anthropogenic activities (Gupta, 2009; Hasegawa et al. 2009; Bhambri et al. 2017). Despite the apparent stability of Himalayan slopes, they undergo continual processes of erosion and weathering. Advances in scientific understanding have challenged the traditional notion that landslides primarily affect steep slopes, leading to the conclusion that even gentle slopes can become highly susceptible to landslides under unfavourable conditions such as high annual precipitation and seismic activity (Komadja et al. 2020, 2021). Over time, numerous studies have investigated the relationship between weathering processes and landslide occurrence in the Himalayas. Gerrard (1994), Naithani and Rawat (2009), and Chaudhary et al. (2010) have all attributed the formation of various clay minerals from bedrock weathering to intense rainfall in the region, which can contribute to slope failure.

Rainfall patterns in the Himalayan region exert a profound influence on groundwater levels, which in turn significantly impact the occurrence of landslides on the Indian Himalayan side. The Himalayas experience diverse rainfall regimes due to their complex topography and unique climatic conditions. Intense monsoon rains during the summer months contribute to substantial groundwater recharge, saturating the soil and increasing pore pressure within the subsurface layers. This increased pore pressure, especially in regions with steep slopes and unstable geological formations, lessens the effective stresses in the soil mass. Consequently, the weakened soil becomes more susceptible to landslides, especially in regions where the groundwater table intersects with the potential slip surface. Furthermore, prolonged or heavy rainfall events can lead to rapid groundwater rise, exacerbating the risk of slope instability and landslide occurrence (Fig. 1). Conversely, extended periods of drought or reduced rainfall can cause groundwater depletion, resulting in soil desiccation and loss of slope stability. The intricate interplay between rainfall infiltration, groundwater levels, and slope stability underscores the complex nature of landslide hazard assessment in the Indian Himalayas. Effective management strategies for landslide



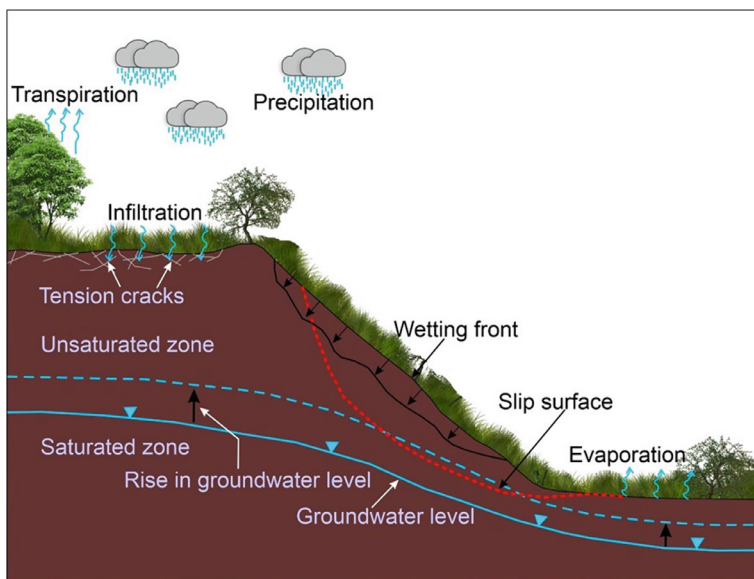


**Fig. 1** A schematic representation of potential slope failure in the mountainous region due to hydrological factors

mitigation must consider the dynamic relationship between rainfall-induced groundwater fluctuations and slope instability to enhance resilience and minimize the socio-economic impacts of landslides in the region. Through comprehensive monitoring, modeling, and early warning systems, efforts can be directed toward mitigating the adverse effects of rainfall-induced landslides and fostering sustainable development in the vulnerable Himalayan landscape.

The rise in pore pressure induced by rainfall and fluctuations in groundwater levels diminishes the effective stresses within materials (Germer and Braun, 2011). Variations in pore pressure within slopes during rainfall events are closely associated with groundwater flow and fluctuations. These variations are impacted by various factors, including slope topography, precipitation patterns, and geomaterial properties such as porosity, permeability, anisotropy, and saturation degree (Yeh et al. 2020). Intense rainfall events that raise groundwater levels in the vadose zone cause a decrease in effective stresses, which in turn promotes the initiation of shallow landslides. During the monsoon and dry seasons, mountainous areas undergo notable variations in the water table, resulting in saturated conditions beneath the water table and elevated pore pressures. The water table's depth significantly influences potential failure surfaces and slope stability. Rainfall infiltration raises groundwater levels and increases pore pressure or decreases matric suction in unsaturated soils. Matric suction is critical for the stability of unsaturated slopes (Fredlund and Rahardjo, 1993). Slope failures and landslides can occur as a result of reduced matric suction and increased pore pressure, which reduce shear strength. These occurrences' failure mechanisms, which

include both shallow and deep-seated slips, are impacted by loose fill, the thickness of the remaining soil, rainfall patterns, and other variables (Cai and Ugai, 2004). When positive pore water pressure is present at the slip surface, seasonal fluctuations in groundwater levels have an impact on the stability of deep-seated landslides (Matsuura et al. 2008). Using three distinct groundwater table locations that correspond to usual, wet, and dry times in Singapore, Rahardjo et al. (2010) examined the effects of rainfall intensities, soil characteristics, and groundwater table position on slope stability. By simulating groundwater levels and pore water pressures in slopes before and after rainfall, Yeh et al. (2020) showed a decrease in the factor of safety linked to increasing pore pressure and groundwater table elevation. They achieved this by using three-dimensional finite element modelling. Latief and Zainal (2019) investigated the stability of highway embankments using finite element analysis and came to the conclusion that the factor of safety against sliding may be maintained by decreasing the water table level while decreasing the cross-sectional area. Many studies have examined different aspects of landslide research in different parts of the Indian Himalayas, but a cohesive framework is significantly missing. This paper provides a comprehensive overview of landslide research in the Indian Himalayan region, highlighting the assessments and mitigating landslide hazards. It emphasizes the need for further research and collaboration to enhance landslide monitoring, forecasting, and mitigation strategies in the region.

## 2 Indian Himalayan Geology

One of the most varied and heterogeneous regions in India is the Himalayan region, which is particularly prone to landslides due to its differences in lithology, geology, rainfall distribution, land use/cover, soil characteristics, and road and river networks (Fig. 2). According to the Ministry of Environment, Forest and Climate Change, Government of India, this region covers ten states and accounts for around 16.2% (or nearly 500,000 km<sup>2</sup>) of the landmass of India. It is located between latitudes 26° 20' and 35° 40' N and longitudes 74° 50' and 95° 40' E. Along with the hill stations of Assam, Sikkim, Arunachal Pradesh, Meghalaya, Nagaland, Manipur, Mizoram, and West Bengal in the Northeastern region, it encompasses the Union Territory of Jammu and Kashmir, and the state of Uttarakhand, Himachal Pradesh in Northern region.

A notable feature of the Himalayan orogeny is the extensive lateral continuity of its major tectonic elements (Sati, 2014). The Himalaya is traditionally segmented into four distinct tectonic units that can be traced continuously for over 2400 km along the belt (Fig. 3).

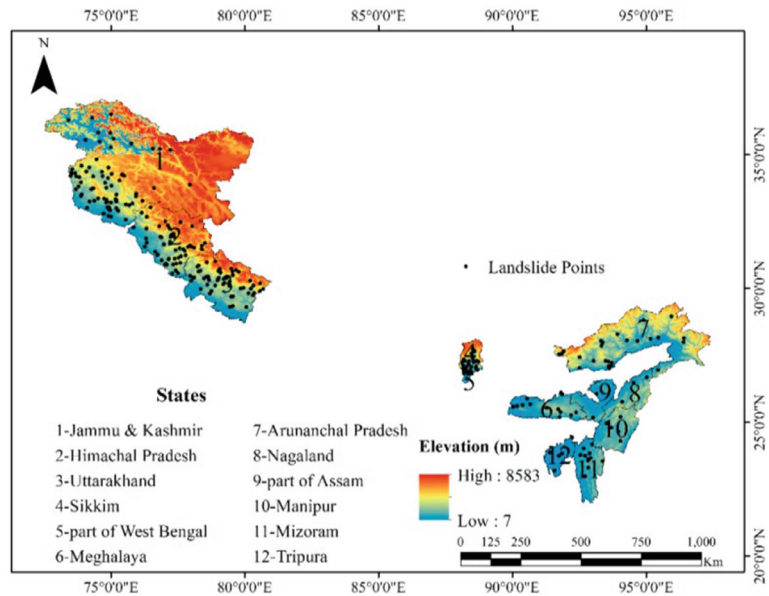


**Fig. 2** Rainfall-induced landslides are marked in the Indian Himalayan Region (Dikshit et al. 2020)

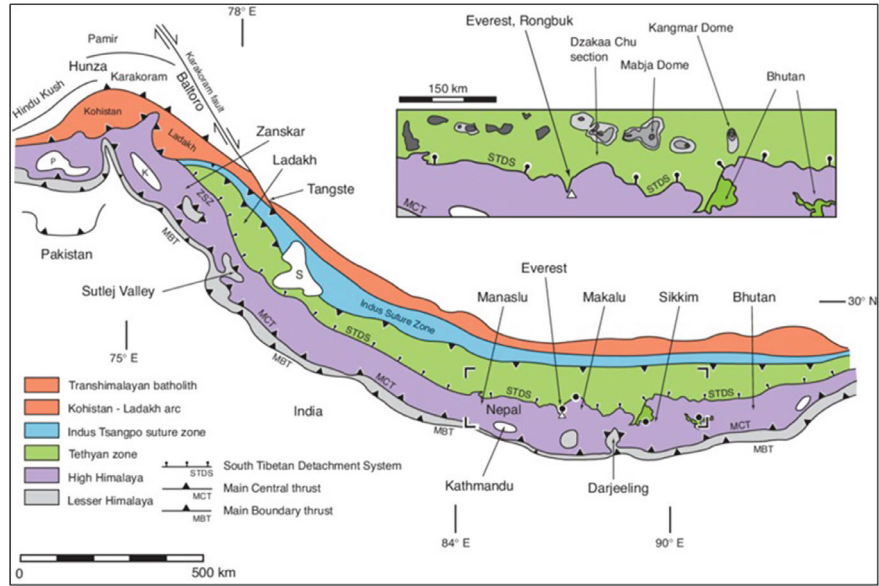


**Fig. 3** Geological map of the Indian Himalayan region (Searle, 2013)

## ***2.1 Sub-Himalayan Tectonic Plate***

In past, the Sub-Himalayan tectonic plate is sometimes called the Cis-Himalayan tectonic plate. This plate forms the southern foothills of the Himalayan Range and consists predominantly of Miocene to Pleistocene molassic sediments, which originated from the erosion of the Himalaya. These sediments, referred to as the “Murree and Sivaliks Formations,” are internally folded and imbricated. The Sub-Himalayan Range is thrust over the Quaternary alluvium deposited by rivers such as the Ganges, Indus, and Brahmaputra along the Main Frontal Thrust, indicating that the Himalaya remains a highly active orogenic region.

## ***2.2 Lesser Himalaya (LH) Tectonic Plate***

The Lesser Himalaya (LH) tectonic plate predominantly comprises Upper Proterozoic to Lower Cambrian detrital sediments derived from the passive Indian margin, alongside granites and acid volcanics dated around  $1840 \pm 70$  Ma (Pradhan et al. 2006). These sedimentary formations are thrust over the Sub-Himalayan range along the Main Boundary Thrust (MBT) (DeCelles et al. 2016). The Lesser Himalaya is often observed in tectonic windows, such as the Kishtwar or Larji-Kulu-Rampur windows, within the broader High Himalaya Crystalline Sequence.

## ***2.3 Central Himalayan Domain, (CHD) or High Himalaya Tectonic Plate***

The Central Himalayan Domain constitutes the core of the Himalayan orogen and includes regions with the greatest topographic relief, including the highest peaks. It is typically divided into four distinct zones (Chakrabarti, 2016).

**High Himalayan Crystalline Sequence (HHCS).** This unit comprises a 30-km-thick sequence of medium- to high-grade metamorphic metasedimentary rocks, extensively intruded by granites from the Ordovician (~500 Ma) and early Miocene (~22 Ma) periods. While most of the metasediments in the HHCS date from the late Proterozoic to early Cambrian, significantly younger metasediments are present in certain regions, such as Mesozoic sediments in the Tandi syncline of Nepal and Warwan Valley of Kistwar in Kashmir, Permian sediments in the “Tschuldo slice,” and Ordovician to Carboniferous sediments in the “Sarchu area” on the Leh-Manali Highway. The HHCS forms a major nappe, which is thrust over the Lesser Himalaya along the “Main Central Thrust” (MCT).

**Tethys Himalaya (TH).** The Tethys Himalaya is an approximately 100-km-wide synclinorium characterized by strongly folded, imbricated, and weakly metamorphosed sedimentary series. Within this unit, several nappes, referred to as the “North Himalayan Nappes,” have been identified. The sediments of the TH preserve an almost complete stratigraphic record from the Upper Proterozoic to the Eocene. Stratigraphic analysis of these sediments provides crucial insights into the geological history of the northern continental margin of the Indian subcontinent, tracing its evolution from the Gondwanan period to its continental collision with Eurasia (Thakur, 1987). The transition from the generally low-grade sediments of the “Tethys Himalaya” to the underlying low- to high-grade rocks of the “High Himalayan Crystalline Sequence” is typically gradual. However, in many areas along the Himalayan belt, this transition zone is marked by a significant structure known as the “Central Himalayan Detachment System,” also referred to as the “South Tibetan Detachment System” or “North Himalayan Normal Fault,” which exhibits both extensional and compressional features. See the ongoing geologic studies section below for more details.

**Nyimaling-Tso Morari Metamorphic Dome (NTMD).** In the Ladakh region, the “Nyimaling-Tso Morari Metamorphic Dome” represents a gradual transition from the “Tethys Himalaya synclinorium” to a large dome of greenschist to eclogite facies metamorphic rocks. Similar to the HHCS, these metamorphic rocks are the metamorphic equivalents of the sediments at the base of the Tethys Himalaya. Additionally, the “Precambrian Phe Formation” in this area is intruded by several Ordovician granites, dated to approximately 480 Ma age.

**Lamayuru and Markha Units (LMU).** The Lamayuru and Markha Units consist of flyschs and olistholiths that were deposited in a turbiditic environment on the northern part of the Indian continental slope and within the adjacent Neotethys basin. These sediments date from the Late Permian to the Eocene.

### 3 Landslide Monitoring Techniques

Particularly in the Indian Himalayan region, where slopes are naturally prone to abrupt failure driven by rainfall or seismic events landslide monitoring is an essential component of landslide assessment. Three main types of monitoring techniques are commonly employed: ground-based observation, remote sensing and GIS, and geophysical methods (Chae et al. 2017).

#### 3.1 Ground-Based Observations

Ground-based observations play a crucial role in monitoring landslides and understanding their mechanisms. Field surveys are conducted to assess slope stability,



**Fig. 4** Instruments used for the ground-based observation in slope stability monitoring

identify potential landslide triggers, and monitor ground movements. Researchers use various instruments, such as extensometers, inclinometers, tiltmeters, and piezometers, to measure ground movements, tilt, water level meter, moisture meter, and pore water pressure within the landslide area (Fig. 4, Hunger et al. 2014). These instruments provide valuable data for evaluating the stability of slopes and detecting early signs of potential landslide activity. One of the key advantages of ground-based observations is their ability to provide real-time data on slope conditions. This allows for immediate response and mitigation efforts in case of an impending landslide. Ground-based observations also help in validating data obtained from remote sensing techniques, ensuring the accuracy of landslide monitoring and assessment (Martha et al. 2017; Dikshit and Satyam, 2018; Yhokha et al. 2018). Additionally, these observations provide valuable insights into the geological and hydrological factors influencing landslide occurrence, aiding in the development of effective mitigation strategies. However, the security of the instruments and their installation on a broad area is a key challenge in ground-based observations.

### 3.2 Remote Sensing and GIS Techniques

Remote sensing techniques have revolutionized the investigation of landslides by providing valuable data on landslide extent, morphology, and dynamics over large

areas. Satellite imagery, LiDAR (Light Detection and Ranging), and RADAR (Radio Detection and Ranging) are commonly used remote sensing tools for landslide investigation (van Westen and Sato, 2017). Satellite imagery, especially high-resolution optical imagery, is used to monitor changes in the landscape before and after landslides. These images can reveal subtle surface movements and changes in vegetation cover, aiding in the identification of potential landslide areas. LiDAR technology provides detailed 3D terrain models, allowing researchers to analyze terrain characteristics and identify potential landslide triggers such as steep slopes or weak geological formations. RADAR satellites, on the other hand, can penetrate through clouds and vegetation, providing all-weather monitoring capabilities for landslide-prone areas. Integration of remote sensing data with GIS (Geographic Information System) allows for the creation of detailed landslide inventory maps, which are essential for hazard assessment and mitigation planning. These maps provide valuable information for land use planning and infrastructure development in landslide-prone areas.

### ***3.3 Geophysical Methods***

Geophysical methods such as Ground Penetrating Radar (GPR) and Electrical Resistivity Tomography (ERT) have been employed for subsurface investigations (Mondal et al. 2008; Falae et al. 2019). Ground Penetrating Radar (GPR) is used to investigate subsurface features and detect potential slip surfaces within landslides. It can provide high-resolution images of the subsurface, allowing researchers to identify internal structures and potential failure mechanisms (Fallah et al. 2017). Electrical Resistivity Tomography (ERT) is another widely used geophysical method for landslide investigation. It measures variations in subsurface electrical resistivity, which can indicate the presence of water-saturated zones or geological structures associated with landslides.

## **4 Landslide Studies of The Recent Decades**

### ***4.1 Assessment of Major Landslide Events***

The Himalayan region is susceptible to frequent landslides, with Uttarakhand being one of the most extensively studied areas. Notable landslide events in Uttarakhand include the devastating August 1998 landslide in the Okhimath area of the Mandakini Valley, triggered by heavy rainfall, resulting in 103 fatalities and damage to 47 villages. Subsequent events, such as the July 2001 cloudburst, caused over 200 landslides and affected nearly 4000 individuals (Naithani et al. 2002). In September 2012, heavy rainfall led to 473 landslides and claimed 51 lives (Martha et al. 2012),

while June 2013 witnessed significant rainfall, particularly impacting the Chamoli and Rudraprayag districts (Martha et al. 2015). Himachal Pradesh, particularly the Katropi area, has also experienced recurring landslides, with a major event in August 2017 resulting in 46 fatalities (Roy et al. 2018; Pradhan et al. 2019). Between 2005 and 2014, the Pawari landslip zone, which is situated in the southeast of the state, increased by 7% (Kumar et al. 2018). Other notable landslides include the Luggarbhathi and Dharla events, claiming 65 and 62 casualties respectively. In the union territory of Jammu and Kashmir, major cloudbursts, such as those in Leh Nalla (2005, 2006), Leh (2010), and Baggar (2011), have resulted in significant damage (Banerjee and Dimri, 2010). In the northeastern part of the region, Darjeeling and Sikkim have been particularly prone to landslides, with historical occurrences dating back to the late nineteenth century. Darjeeling witnessed major events in 1950 and 1968, resulting in substantial loss of life (Mondal and Mandal, 2019). Similar to this, Meghalaya's National Highways NH-40 and NH-44 have seen substantial instability, while Sikkim has experienced multiple landslides, including the Lanta Khola disaster (Anbarasu et al. 2010; Sarkar et al. 2016a, b; Umrao et al. 2017; Bera et al. 2019). In Mizoram, NH-44A has experienced recurrent landslides in recent years (Sardana et al. 2019). These events underscore the region's vulnerability to landslides and highlight the need for effective mitigation strategies to minimize loss of life and property damage.

The assessment and categorization of landslides before and after their occurrence play a crucial role in hazard analysis, aiding in the evaluation of rescue and relief efforts (Cruden and Varnes, 1996; Martha et al. 2010a, b). Traditionally, landslide damage assessments relied on field visits and simplistic categorizations, neglecting contextual morphometry. However, researchers are now using image classification techniques for landslide mapping due to the availability of high-resolution data and the advancement of remote sensing technologies. Researchers at the National Remote Sensing Centre (NRSC) have focused most of their efforts on post-landslide detection in the Indian Himalayas, using high-quality remote sensing images to identify changes like vegetation loss and the exposure of new rock and soil (Vinod et al. 2008; Martha et al. 2012). Pixel-based and object-based methods are used to evaluate damages using pre- and post-event images for the landslide event. While pixel-based methods involve spectral information for change detection, object-based approaches consider spectral, spatial, and contextual properties, making them more suitable for irregularly shaped natural events like landslides. In the Indian Himalayan region, object-based picture classification has been widely applied, with particular emphasis on landslide detection in the immediate aftermath of an event and the creation of landslide inventory databases from archived images of the site. The accuracy of these techniques depends on factors such as segmentation techniques, resolution of satellite images, and the application of computational techniques like Machine Learning (ML) and Artificial Neural Networks (ANN) (Martha et al. 2016). However, there remains a need for further research to validate and apply these techniques across different Himalayan regions for enhanced understanding and reliability.

The assessment of landslide hazards is essential to comprehending the probability and possible extent of landslide incidents (Reichenbach et al. 2018). This is typically



achieved through landslide susceptibility mapping, which evaluates various predisposing factors' spatial distribution. Different classification techniques have been employed over time, including qualitative, semi-quantitative, quantitative, and deterministic methods (Kanungo et al. 2008; Sarkar et al. 2016a, b). Qualitative methods rely on subjective assessments, while semi-quantitative approaches assign weights to significant factors. Deterministic analysis involves assessing physical and mechanical soil properties to determine slope stability. Quantitative models, such as logistic regression, rely on landslide density under influencing factors. The parameters used for susceptibility analysis include geological, geomorphological, environmental, and anthropogenic factors (Table 1).

## 4.2 *Rock Mass Classification in Himalayan Landslide Study*

Rock mass classification plays a crucial role in assessing and mitigating landslide hazards in the Indian Himalayas, particularly concerning hydrological factors. By categorizing rock masses based on their geological properties, structural characteristics, and stability parameters, researchers can better understand the susceptibility of slopes to landslides triggered by hydrological processes such as intense rainfall, snowmelt, and glacial movements. Classifications like the Rock Mass Rating (RMR) or Geological Strength Index (GSI) provide quantitative measures that aid in identifying potential landslide-prone areas and assessing the magnitude of risk.

In the Himalayan region, where complex geological formations and tectonic activities influence slope stability, rock mass classification helps in delineating zones susceptible to landslides exacerbated by hydrological factors. For instance, areas with fractured, weathered rock masses are more prone to erosion and failure under the influence of rapid runoff or groundwater saturation during monsoons. Understanding these classifications allows researchers to prioritize areas for detailed hydrological monitoring and implement appropriate mitigation measures, such as slope stabilization techniques or early warning systems. Moreover, integrating hydrological data with rock mass classifications facilitates dynamic hazard mapping and forecasting models (Kumar et al. 2017a, b; Siddique et al. 2020; Jaiswal et al. 2024). These models can predict potential landslide occurrences based on real-time rainfall data, groundwater fluctuations, and changes in glacier dynamics, thereby supporting proactive measures to mitigate risks to infrastructure, communities, and ecosystems in the fragile Himalayan terrain (Table 2).

## 5 Mitigation Approach

Landslide forecasting stands as a pivotal component in disaster risk reduction efforts, particularly in the challenging terrain of the Indian Himalayan region where rainfall-triggered shallow landslides are prevalent (Kanungo and Sharma, 2014; Dikshit and

**Table 1** Some of the noted landslide studies consider the hydrological factor in the Indian Himalayan region

References	Study site	Methods used	Remarks
Shah et al. 2024	Kasmir Himalaya	Threshold analysis	Statistics-based approach for landslide prediction
Saha and Bera, 2024	Garhwal Himalaya	Threshold analysis	Statistics-based approach for landslide prediction
Kumari et al. 2023	Lesser Himalaya	Numerical analysis (THRESH)	Statistics-based approach for landslide prediction
Sarkar et al. 2023	Uttarkashi (NW Himalaya)	Threshold analysis	Statistics-based approach for landslide prediction
Paswan and Shrivastava, 2022	Shimla, Himachal Pradesh	Physical model analysis	Numerical-based study for the early warning system
Dutta et al. 2021	Sikkim Himalaya	Threshold analysis	Statistics-based approach for landslide prediction
Abraham et al. 2020b	Darjeeling Himalaya	Threshold analysis	Statistics-based approach for landslide prediction
Abraham et al. 2020c	Kalimpong town, West Bengal	Threshold analysis	Statistics-based approach for landslide prediction
Teja et al. 2019	Darjeeling Himalaya	Threshold analysis	Algorithm-based approach for landslide prediction
Sharma et al. 2019	Himalaya	Remote sensing and machine learning	Landslide susceptibility mapping of the Himalayan watershed
Sardana et al. 2019	Mizoram, NE Himalaya	Quantitative analysis	Landslide stability prediction of the road-cut slopes
Peethambaran et al. 2019	NW Himalaya	Remote sensing and machine learning	Landslide susceptibility zonation
Mondal and Mandal, 2019	Darjeeling Himalaya	Remote sensing	Landslide susceptibility mapping
Meena et al. 2019	Kullu Valley, Himachal Pradesh	Remote sensing and machine learning	Landslide susceptibility mapping
Kumar et al. 2019a, b	Satluj Valley, NW Himalaya	Remote sensing	Landslide mapping
Kannaujiya et al. 2019	Garhwal Himalaya	Remote sensing and Ground-based observation	Characterization of landslide
Harilal et al. 2019	Sikkim, India	Threshold analysis	Landslide prediction and real-time monitoring
Falae et al. 2019	Garhwal Himalayas	Ground-based observation	Landslide prediction from the slope movement

(continued)

**Table 1** (continued)

References	Study site	Methods used	Remarks
Dikshit and Satyam, 2019	Chibo, NE Himalaya	Remote sensing	Probabilistic rainfall threshold
Bera et al. 2019	Namchi, Sikkim	Remote sensing	Landslide hazard zonation mapping
Banerjee and Dimri, 2019	Ladakh, Jammu and Kashmir	Identification and preliminary study	Leh cloudburst event
Yhokha et al. 2018	Nainital, Uttarakhand	Remote Sensing	Identify the slope movement for landslide prediction
Roy et al. 2018	Katropi, Himachal Pradesh	Identification and preliminary study	46 lives were lost
Mandal et al. 2018	Sikkim Himalayas	Remote sensing	Modeling and mapping landslide susceptibility
Kumar et al. 2018	Satluj Valley, Himachal Pradesh	Identification and preliminary study	62 lives were lost
Dikshit et al. 2018b	Kalimpong, Darjeeling Himalayas	Ground-based observation	Landslide prediction from the slope movement
Dikshit et al. 2018a	Darjeeling Himalaya	Threshold analysis	Probabilistic analysis for landslide occurrences
Chawla et al. 2018	Darjeeling Himalaya	Remote sensing and machine learning	Landslide susceptibility mapping
Umrao et al. 2017	Meghalaya, NE Himalaya	Quantitative analysis	Landslide stability analysis along the road
Sahana and Sajjad 2017	Rudraprayag, Uttarakhand	Remote sensing and machine learning	Landslide susceptibility zonation mapping
Pham et al. 2017b	Uttarakhand, NW Himalaya	Remote sensing and machine learning	Landslide susceptibility assessment
Pham et al. 2017a	NW Himalaya	Remote sensing and machine learning	Landslide susceptibility assessment
Kumar et al. 2017b	Garhwal Himalaya	Remote sensing and machine learning	Landslide susceptibility mapping and prediction
Kumar et al. 2017a	Jammu and Kashmir Himalaya	Threshold analysis	Landslide prediction from mean rainfall event
Sarkar et al. 2016b	Darjeeling Himalayas	Remote sensing	Landslide susceptibility assessment
Sarkar et al. 2016a	Jaintia Hill, Meghalaya	Quantitative analysis	Landslide stability analysis in and around Jaintia Hill

(continued)

**Table 1** (continued)

References	Study site	Methods used	Remarks
Mathew et al. 2016b	Lesser Himalaya	Ground-based observation	Stability analysis of the unstable slopes
Martha et al. 2016a	Chamoli and Rudraprayag, Uttarakhand	Remote sensing	Identification of new landslides
Gupta et al. 2016	Garhwal Himalaya	Numerical simulation	Stability analysis of the unstable slopes
Balamurugan et al. 2016	Manipur, NE Himalaya	Remote sensing and machine learning	Landslide susceptibility zonation mapping
Sarkar et al. 2015	Alaknanda valley	Remote sensing and machine learning	Landslide hazard assessment
Martha et al. 2015	Chamoli and Rudraprayag	Identification and Preliminary study	43 lives were lost
Singh et al. 2014	Arunachal Pradesh, NE Himalaya	Remote sensing and machine learning	Landslide hazard zonation mapping
Sharma et al. 2014	Sikkim Himalaya	Remote sensing and machine learning	Landslide hazard vulnerability assessment and zonation
Mathew et al. 2014	Garhwal Himalaya	Threshold analysis	Landslide prediction from intensity and cumulative rainfall
Kanungo and Sharma, 2014	Garhwal Himalaya, Uttarakhand	Threshold analysis	Landslide prediction from intensity rainfall
Ramakrishnan et al. 2013	Kumaon Himalaya	Remote sensing and machine learning	Landslide susceptibility assessment
Mondal et al. 2013	Darjeeling Himalaya	Remote sensing and machine learning	Landslide susceptibility zonation mapping
Martha et al. 2013	Okhimath, Uttarakhand	Remote sensing	Landslide hazard and risk assessment
Martha et al. 2012	Rudraprayag, Uttarakhand	Remote sensing	Pre- and post-landslide impact analysis
Das et al. 2012	Himalaya	Remote sensing and machine learning	Landslide susceptibility mapping along the road corridors
Ghosh et al. 2011	Darjeeling Himalayas	Remote sensing	Empirical modelling for landslide susceptibility
Das et al. 2011	Northern Uttarakhand	Remote sensing and machine learning	Probabilistic landslide hazard assessment
Sharma et al. 2010	North Sikkim	Ground-based observation	Landslide analysis based on subsurface ground condition

(continued)

**Table 1** (continued)

References	Study site	Methods used	Remarks
Sengupta et al. 2010	North Sikkim, NE Himalaya	Threshold analysis	Landslide prediction from cumulative rainfall
Martha et al. 2010b	Okhimath	Identification and preliminary study	51 lives were lost and 473 landslides
Martha et al. 2010a	NW Himalaya	Remote sensing	Volumetric analysis of Landslide
Chauhan et al. 2010	Garhwal Himalaya	Remote sensing and machine learning	Landslide susceptibility zonation mapping
Anbarasu et al. 2010	Lanta Khola, Sikkim	Quantitative analysis	Identify the mechanism of activation of the landslide
Mathew et al. 2009	Garhwal Himalaya	Remote sensing and machine learning	Landslide susceptibility zonation mapping
Vinod et al. 2008	Uttarkashi, NW Himalaya	Remote sensing	Overall study of landslide
Sarkar and Anbalagan 2008	Garhwal Himalaya	Remote sensing and machine learning	Landslide hazard zonation mapping
Mondal et al. 2008	Garhwal Himalaya	Ground-based observation	Stability analysis of the unstable slopes
Kanungo et al. 2008	Darjeeling Himalayas	Remote sensing	Landslide risk assessment
Mathew et al. 2007	Garhwal Himalaya	Remote sensing	Landslide susceptibility mapping
Kanungo et al. 2006	Darjeeling Himalaya	Remote sensing and machine learning	Landslide susceptibility zonation
Naithani et al. 2002	Rudraprayag, Garhwal Himalaya	Identification and preliminary study	27 lives were lost and 4000 people affected
Gupta and Anbalagan, 1997	Tehri Dam Reservoir	Remote sensing	Landslide hazard zonation mapping

Satyan, 2018). Including hydromechanical variables in landslide studies is crucial for accurately accounting for water flux. These variables, which describe the interaction between mechanical and hydraulic processes in a geological system, are essential for predicting the system's behavior. Hydromechanical variables include factors such as pore water pressure, soil and rock permeability, stress–strain relationships, and the mechanical properties of materials. These parameters influence how water moves through and interacts with the geological medium, making them vital for comprehensive landslide analysis. The primary approach for predicting the occurrence of landslides is precipitation analysis, which includes slope stability analysis, subsurface monitoring, and estimation of minimum rainfall requirements. In this context, minimum rainfall conditions also referred to as thresholds, which must be defined using empirical or physical approaches. (Guzzetti et al. 2007; Dikshit et al. 2019).

**Table 2** Some of the noted rainfall thresholds are estimated for the Indian Himalayan region

Sr. no.	Empirical equation	Time range	Study area	Scale	Source
1	$I = 1.38D^{-0.126}$	$48 < D < 240$	Garhwal Himalaya	Local	Saha and Bera, <a href="#">2024</a>
2	$I = 1.19D^{-0.352}$ $I = 1.74D^{-0.329}$	$24 < D < 480$	Kashmir Himalaya	Local	Shah et al. <a href="#">2024</a>
3	$I = 14.82D^{-0.39}$	$0.167 < D < 500$	Lesser Himalaya	Local	Kumari et al. <a href="#">2023</a>
4	$E = 7.761D^{0.8587}$	$24 < D < 240$	Uttarkashi (NW Himalaya)	Local	Sarkar et al. <a href="#">2023</a>
5	$E = 1.50D^{0.65}$	$12 < D < 200$	Darjeeling Himalaya	Local	Abraham et al. <a href="#">2020b</a>
6	$E = 4.2D^{0.56}$	$12 < D < 300$	Kalimpong town, West Bengal	Local	Abraham et al. 2020c
7	$I = 1.82D^{-0.23}$	$24 < D < 336$	Garhwal Himalaya, India	Local	Kanungo and Sharma, <a href="#">2014</a>
8	$I = 58.7D^{-1.12}$	$0.9 < D < 100$	Garhwal Himalaya, India	Local	Mathew et al. <a href="#">2014</a>
9	$I = 14.82D^{-0.39}$	$0.167 < D < 500$	North Sikkim, India	Local	Sengupta et al. <a href="#">2010</a>
10	$E = 0.012D^{1.54}$	$20 < D < 600$	Lanta Khola, North Sikkim, India	Local	Sengupta et al. <a href="#">2010</a>

Physical models, which often do not have the large datasets required in the Indian Himalayas, evaluate the relationship between rainfall conditions and soil hydrological parameters impacting slope stability. On the other hand, empirical methods, although simpler to apply, rely on statistical analyses of precipitation and landslide data to determine threshold levels (Segoni et al. [2018](#)). The methodology employed, the density of rain gauges, and the quality of the data all have an impact on threshold estimation. Notably, there is little research on rainfall thresholds in the Himalayan area of India. A number of empirical methods have been examined, including the use of rainfall intensity-duration (ID) thresholds for areas like Garhwal and Kalimpong, and the estimation of cumulative event rainfall to mean annual rainfall ratio (EMAP) for the Sikkim Himalayas (Harilal et al. [2019](#); Teja et al. [2019](#)). However, concerns persist regarding the spatial distribution of rain gauges and the temporal resolution of precipitation data, which may lead to underestimation of rainfall thresholds and an increased number of false alarms in early warning systems. Antecedent rainfall, particularly over 15–30 days, has been identified as a significant factor influencing slope destabilization, accentuating the importance of considering historical rainfall patterns in landslide forecasting. Regional and local thresholds need further investigation, with variations observed across different regions of the study area. Defining rainfall thresholds at smaller, local scales may offer more effective landslide early

warning systems due to the heterogeneous nature of rainfall patterns in the Himalayan region (Mathew et al. 2014; Kumar et al. 2017a, b). Despite progress, significant gaps remain in understanding and predicting landslide occurrences in this geologically complex and vulnerable region, underscoring the urgent need for continued research and collaboration to enhance landslide forecasting capabilities and mitigate the impacts of such natural hazards. The trend has shifted towards more sophisticated computational techniques like Support Vector Machine (SVM), Artificial Neural Networks (ANN), and Machine Learning (ML) which have shown promising results, particularly in regions like the Uttarakhand Himalayas (Mathew et al. 2007; Das et al. 2012; Pourghasemi et al. 2018; Sharma and Mahajan, 2019). However, the adoption of these computational methods varies across different Himalayan regions, highlighting the need for further research and standardized guidelines for landslide hazard assessment.

The estimated Rainfall Intensity-Duration (ID) thresholds for various regions within the Indian Himalayas indicate significant local variability in rainfall intensity required to trigger slope failures. Similarly, the Rainfall Event-Duration (ED) thresholds exhibit comparable patterns across the Himalayan region. These findings suggest that both ID and ED thresholds are crucial for understanding the dynamics of rainfall-induced landslides in susceptible areas of the Indian subcontinent.

## Declarations

**Conclusions** The review paper provides a comprehensive overview of ongoing studies in the Indian Himalayan region, highlighting its significant contribution to global rainfall-induced landslides. Emphasizing the importance of rainfall-triggered landslide activity, the paper suggests that such landslides can be managed effectively through early warnings and forecasting models. However, it also underscores areas needing significant growth, including studies on climate change, the use of high-resolution data, and the adoption of novel techniques.

In the assessment of landslide aspects, the review calls for a directional shift towards automated approaches and the utilization of higher temporal resolution datasets. It stresses the need for localized rainfall threshold studies and the integration of empirical and physical models to improve understanding and facilitate the establishment of operational landslide early warning systems. While landslide monitoring employs various methods, there is a need for a comprehensive, multi-scale approach covering the entire region.

Despite advancements in computational technologies, the review suggests the adoption of large data analytics and hybrid models to handle geographical heterogeneity and uncertainty in landslide susceptibility studies. It also addresses the data deficiency in ground-based rainfall data in significant portions of the Himalayan region, suggesting the use of remote sensing data as a potential solution.

In conclusion, the review paper provides some bulleted points, highlighting the areas for improvement and offering recommendations to enhance understanding and management of landslide hazards in the region:

- **Data Collection:** Implement comprehensive and consistent data collection protocols for rainfall, groundwater levels, and slope stability indicators.
- **Monitoring Systems:** Establish advanced and real-time monitoring systems using modern sensors and remote sensing technology to detect early signs of landslides.
- **Hydrological Modeling:** Enhance hydrological models to better predict the impact of intense rainfall events on groundwater levels and slope stability.
- **Soil and Rock Properties:** Conduct detailed studies on the mechanical properties of soil and rock to understand their behavior under varying moisture conditions.

- **Public Awareness:** Increase public awareness and education about landslide risks and preventive measures, especially in vulnerable communities.
- **Early Warning Systems:** Develop and implement early warning systems based on real-time data and predictive models to provide timely alerts to at-risk populations.
- **Slope Stabilization:** Invest in slope stabilization techniques, such as retaining walls, drainage systems, and vegetation cover, to reduce the likelihood of landslides.
- **Interdisciplinary Research:** Foster interdisciplinary research collaborations to combine expertise from geology, hydrology, engineering, and social sciences for a holistic approach to landslide hazard management.
- **Community Engagement:** Engage local communities in landslide risk assessment and mitigation efforts to ensure their active participation and resilience building.
- **Policy Development:** Formulate and enforce policies that mandate regular maintenance of infrastructure and implementation of landslide mitigation measures in prone areas.
- **Training and Capacity Building:** Provide training and capacity building for local authorities, emergency responders, and community leaders on landslide preparedness and response strategies.

Valuable insights into the current landscape of landslide research in the Indian Himalayan region. It highlights areas for improvement and offers recommendations to enhance understanding and management of landslide hazards in the region.

The authors declare no conflict of interest.

## References

- Abraham MT, Satyam N, Kushal S, Rosi A, Pradhan B, Segoni S (2020) Rainfall threshold estimation and landslide forecasting for Kalimpong India Using SIGMA Model. *Water* 12(4):1195
- Anbarasu K, Sengupta A, Gupta S, Sharma SP (2010) Mechanism of activation of the Lanta Khola landslide in Sikkim Himalayas. *Landslides* 7:135–147
- Balamurugan G, Ramesh V, Touthang M (2016) Landslide susceptibility zonation mapping using frequency ratio and fuzzy gamma operator models in part of NH-39, Manipur, India. *Nat Hazards* 84:465–488
- Banerjee A, Dimri AP (2019) Comparative analysis of two rainfall retrieval algorithms during extreme rainfall event: a case study on cloudburst, 2010 over Ladakh (Leh), Jammu and Kashmir. *Nat Hazards* 97:1357–1374
- Bera A, Mukhopadhyay BP, Das D (2019) Landslide hazard zonation mapping using multi-criteria analysis with the help of GIS techniques: a case study from Eastern Himalayas, Namchi, South Sikkim. *Nat Hazards* 96:935–959
- Cai F, Ugai K (2004) Numerical analysis of rainfall effects on slope stability. *Int J Geomech* 4:69–78
- Chae BG, Park HJ, Catani F, Simoni A, Berti M (2017) Landslide prediction, monitoring and early warning: a concise review of state-of-the-art. *Geosci J* 21:1033–1070
- Chaudhary S, Gupta V, Sundriyal YP (2010) Surface and sub-surface characterization of Byung landslide in Mandakini valley Garhwal Himalaya. *Himalayan Geology* 31(2):125–132
- Chauhan S, Mukta S, Arora MK (2010) Landslide susceptibility zonation of the Chamoli region, Garhwal Himalayas, using logistic regression model. *Landslides* 7:411–423
- Chawla A, Chawla S, Pasupuleti S, Rao ACS, Sarkar K, Dwivedi R (2018) Landslide susceptibility mapping in Darjeeling Himalayas, India. *Adv Civ Eng* 1–17
- Cruden DM, Varnes DJ (1996) Landslides: investigation and mitigation. In: National research council transportation research board special report (Book 247), Turner AK, Schuster RL (eds) Transportation research board: Washington, DC, USA, pp 36–75



- Das I, Stein A, Kerle N, Dadhwal VK (2011) Probabilistic landslide hazard assessment using homogeneous susceptible units (HSU) along a national highway corridor in the northern Himalayas, India. *Landslides* 8:293–308
- Das I, Stein A, Kerle N, Dadhwal VK (2012) Landslide susceptibility mapping along road corridors in the Indian Himalayas using Bayesian logistic regression models. *Geomorphology* 179:116–125
- DeCelles PG, Carrapa B, Gehrels GE, Chakraborty T, Ghosh P (2016) Along-strike continuity of structure, stratigraphy, and kinematic history in the Himalayan thrust belt: the view from Northeastern India. *Tectonics* 35:2995–3027
- Dikshit A, Satyam N (2019) Probabilistic rainfall thresholds in Chibo, India: estimation and validation using monitoring system. *J Mt Sci* 16:870–883
- Dikshit A, Satyam DN, Towhata I (2018) Early warning system using tilt sensors in Chibo, Kalimpong, Darjeeling Himalayas India. *Nat Hazards* 94:727–741
- Dikshit A, Sarkar R, Pradhan B, Segoni S, Alamri AM (2020) Rainfall induced landslides studies in Indian Himalayan region: a critical review. *Appl Sci* 10:2466
- Dikshit A, Satyam DN (2018) Estimation of rainfall thresholds for landslide occurrences in Kalimpong, India. *Innov Infrastruct Solut* 3
- Dikshit A, Sarkar R, Satyam N (2018a) Probabilistic approach toward Darjeeling Himalayas landslides-a case study. *Cogent Eng* 5
- Dutta K, Wanjari N, Misra AK (2021) Study of qualitative stability analysis and rainfall thresholds for possible landslide occurrence: a case study of Sikkim Himalaya. *J Taibah Univ Sci* 15(1):407–422
- Falae PO, Kanungo DP, Chauhan PKS, Dash RK (2019) Electrical resistivity tomography (ERT) based subsurface characterisation of Pakhi Landslide, Garhwal Himalayas India. *Geomorphol Nat Hazards Environ Earth Sci* 78:430
- Fallah N, Momeni A, Nazari H (2017) Investigation of landslides using geophysical methods: a review. *Appl Geophys* 142:37–48
- Fredlund DG, Rahardjo H (1993) Soil mechanics for unsaturated soils. Wiley, New York
- Germer K, Braun J (2011) Effects of saturation on slope stability: laboratory experiments utilizing external load. *Vadose Zo J* 10:477–486
- Gerrard J (1994) The landslide hazard in the Himalayas: geological control and human action. *Geomorphol Nat Hazards* 10:221–230
- Ghosh S, Carranza EJM, van Westen CJ, Jetten VG, Bhattacharya DN (2011) Selecting and weighting spatial predictors for empirical modeling of landslide susceptibility in the Darjeeling Himalayas (India). *Geomorphology* 131:35–56
- Gupta P, Anbalagan R (1997) Slope stability of Tehri Dam Reservoir area, India, using landslide hazard zonation (LHZ) mapping. *Q J Eng Geol* 30:27–36
- Gupta V, Bhasin RK, Kaynia AM, Kumar V, Saini AS, Tandon RS, Pabst T (2016) Finite element analysis of failed slope by shear strength reduction technique: a case study for Surabhi Resort Landslide, Mussoorie township Garhwal Himalaya. *Geomat Nat Hazards Risk* 7:1677–1690
- Guzzetti F, Peruccacci S, Rossi M, Stark CP (2007) Rainfall thresholds for the initiation of landslides in central and southern Europe. *Meteorol Atmos Phys* 98:239–267
- Harilal GT, Madhu D, Ramesh MV, Pullarkatt D (2019) Towards establishing rainfall thresholds for a real-time landslide early warning system in Sikkim, India. *Landslides* 16:2395–2408
- Jaiswal A, Verma AK, Singh TN (2024) Evaluation of slope stability through rock mass classification and kinematics analysis of some major slopes along NH-1A from Ramban to Banihal, North Western Himalayas. *J Rock Mech Geotech Eng* 16:167–182
- Kannaujiya S, Chatteraj SL, Jayalath D, Ray PKC, Bajaj K, Podali S, Bisht MPS (2019) Integration of satellite remote sensing and geophysical techniques (electrical resistivity tomography and ground penetrating radar) for landslide characterization at Kunjethi (Kalimath), Garhwal Himalaya India. *Nat Hazards* 97:1191–1208
- Kanungo DP, Sharma S (2014) Rainfall thresholds for prediction of shallow landslides around Chamoli-Joshimath region, Garhwal Himalayas, India. *Landslides* 11:629–638

- Kanungo DP, Arora MK, Sarkar S, Gupta RP (2006) A comparative study of conventional, ANN black box, fuzzy and combined neural and fuzzy weighting procedures for landslide susceptibility zonation in Darjeeling Himalayas. *Eng Geol* 85:347–366
- Kanungo DP, Arora MK, Gupta R, Sarkar S (2008) Landslide risk assessment using concepts of danger pixels and fuzzy set theory in Darjeeling Himalayas. *Landslides* 5:407–416
- Komadja GC, Pradhan SP, Oluwasegun AD, Roul AR, Stanislas TT, Laibi RA, Adebayo B, Onwualu AP (2021) Geotechnical and geological investigation of slope stability of a section of road cut debris-slopes along NH-7, Uttarakhand India. *Results Eng* 10:100227
- Komadja GC, Pradhan SP, Roul AR, Adebayo B, Habinshuti JB, Glodji LA, Onwualu AP (2020) Assessment of stability of a Himalayan road cut slope with varying degrees of weathering: a finite-element-model-based approach. *Heliyon* 6(11)
- Kumar A, Asthana AL, Priyanka RS, Jayangondaperumal R, Gupta AK, Bhakuni SS (2017) Assessment of landslide hazards induced by extreme rainfall event in Jammu and Kashmir Himalaya, northwest India. *Geomorphology* 284:72–87
- Kumar D, Thakur M, Dubey CS, Shukla DP (2017) Landslide susceptibility mapping & prediction using support vector machine for Mandakini River Basin, Garhwal Himalaya, India. *Geomorphology* 295:115–125
- Kumar V, Gupta V, Jamir I (2018) Hazard evaluation of progressive Pawari landslide zone, Satluj valley, Himachal Pradesh India. *Nat Hazards* 93:1029–1047
- Kumar V, Gupta V, Jamir I, Chatteraj SL (2019) Evaluation of potential landslide damming: case study of Urni landslide, Kinnaur, Satluj valley, India. *Geosci Front* 10:753–767
- Kumar V, Gupta V, Sundriyal YP (2019) Spatial interrelationship of landslides, litho-tectonics, and climate regime, Satluj valley, Northwest Himalaya. *Geol J* 54:537–551
- Kumari S, Chaudhary A, Shankar V (2023) Modelling of rainfall threshold for the initiation of landslides in lesser Himalayan region using THRESH. *Model Earth Syst Environ* 9:3207–3215
- Latief RH, Zainal AKE (2019) Effects of water table level on slope stability and construction cost of highway embankment. *Eng J* 23:1–12
- Mandal S, Mandal K (2018) Modeling and mapping landslide susceptibility zones using GIS based multivariate binary logistic regression (LR) model in the Rorachu river basin of eastern Sikkim Himalaya, India. *Modeling Earth Syst Environ* 4:69–88
- Martha TR, Kerle N, Jetten V, van Westen CJ, Kumar KV (2010) Landslide volumetric analysis using cartosat-1-derived DEMs. *Ieee Geosci Remote Sens Lett* 7:582–586
- Martha TR, Kerle N, Jetten V, van Westen CJ, Kumar KV (2010) Characterising spectral, spatial and morphometric properties of landslides for semi-automatic detection using object-oriented methods. *Geomorphology* 116:24–36
- Martha TR, Kerle N, van Westen CJ, Jetten V, Kumar KV (2012) Object-oriented analysis of multi-temporal panchromatic images for creation of historical landslide inventories. *Isprs J Photogramm Remote Sens* 67:105–119
- Martha TR, van Westen CJ, Kerle N, Jetten V, Kumar KV (2013) Landslide hazard and risk assessment using semi-automatically created landslide inventories. *Geomorphology* 184:139–150
- Martha TR, Roy P, Govindharaj KB, Kumar KV, Diwakar PG, Dadhwal VK (2015) Landslides triggered by the June 2013 extreme rainfall event in parts of Uttarakhand state, India. *Landslides* 12:135–146
- Martha TR, Kamala P, Jose J, Kumar KV, Sankar GJ (2016) Identification of new landslides from high resolution satellite data covering a large area using object-based change detection methods. *J Indian Soc Remote Sens* 44:515–524
- Martha TR, Reddy PS, Bhatt CM, Raj KBG, Nalini J, Padmanabha EA, Narender B, Kumar KV, Muralikrishnan S, Rao GS, Diwakar PG, Dadhwal VK (2017) Debris volume estimation and monitoring of Phuktal river landslide-dammed lake in the Zaskar Himalayas, India using Cartosat-2 images. *Landslides* 14:373–383
- Mathew J, Jha VK, Rawat GS (2007) Application of binary logistic regression analysis and its validation for landslide susceptibility mapping in part of Garhwal Himalaya, India. *Int J Remote Sens* 28:2257–2275

- Mathew J, Jha VK, Rawat GS (2009) Landslide susceptibility zonation mapping and its validation in part of Garhwal Lesser Himalaya, India, using binary logistic regression analysis and receiver operating characteristic curve method. *Landslides* 6:17–26
- Mathew J, Babu DG, Kundu S, Kumar KV, Pant CC (2014) Integrating intensity-duration-based rainfall threshold and antecedent rainfall-based probability estimate towards generating early warning for rainfall-induced landslides in parts of the Garhwal Himalaya, India. *Landslides* 11:575–588
- Matsuura S, Asano S, Okamoto T (2008) Relationship between rain and/or meltwater, pore-water pressure and displacement of a reactivated landslide. *Eng Geol* 101:49–59
- Meena SR, Mishra BK, Piralilou ST (2019) A hybrid spatial multi-criteria evaluation method for mapping landslide susceptible areas in Kullu Valley, Himalayas. *Geosciences* 156
- Mondal S, Mandal S (2019) Landslide susceptibility mapping of Darjeeling Himalaya, India using index of entropy (IOE) model. *Appl Geomat* 11:129–146
- Mondal SK, Sastry RG, Pachauri AK, Gautam PK (2008) High resolution 2D electrical resistivity tomography to characterize active Naitwar Bazar landslide, Garhwal Himalaya, India. *Curr Sci* 94:871–875
- Naithani AK, Rawat GS (2009) Investigations of bunga landslide and its mitigation—a case study from pinder valley, Garhwal Himalaya Uttarakhand. *Indian Landslides* 2(1):9–22
- Naithani AK, Kumar D, Prasad C (2002) The catastrophic landslide of 16 July 2001 in Phata Byung area, Rudraprayag district, Garhwal Himalaya, India. *Curr Sci* 82:921–923
- Paswan AP, Shrivastava AK (2022) Modelling of rainfall-induced landslide: a threshold-based approach. *Arab J Geosci* 15:795
- Peethambaran B, Anbalagan R, Shihabudheen KV, Goswami A (2019) Robustness evaluation of fuzzy expert system and extreme learning machine for geographic information system-based landslide susceptibility zonation: a case study from Indian Himalaya. *Environ Earth Sci* 78
- Pham BT, Bui DT, Pourghasemi HR, Indra P, Dholakia M (2017) Landslide susceptibility assessment in the Uttarakhand area (India) using GIS: a comparison study of prediction capability of naïve bayes, multilayer perceptron neural networks, and functional trees methods. *Theor Appl Climatol* 128:255–273
- Pham BT, Bui DT, Prakash I, Dholakia MB (2017) Hybrid integration of multilayer perceptron neural networks and machine learning ensembles for landslide susceptibility assessment at Himalayan area (India) using GIS. *CATENA* 149:52–63
- Pourghasemi HR, Yansari ZT, Panagos P, Pradhan B (2018) Analysis and evaluation of landslide susceptibility: a review on articles published during 2005–2016 (periods of 2005–2012 and 2013–2016). *Arab J Geosci* 11:193
- Pradhan B, Singh R, Buchroithner M (2006) Estimation of stress and its use in evaluation of landslide prone regions using remote sensing data. *Adv Space Res* 37:698–709
- Rahardjo H, Nio AS, Leong EC, Song NY (2010) Effects of groundwater table position and soil properties on stability of slope during rainfall. *J Geotech Geoenviron Eng* 136:1555–1564
- Ramakrishnan D, Singh TN, Verma AK, Gulati A, Tiwari KC (2013) Soft computing and GIS for landslide susceptibility assessment in Tawaghat area, Kumaon Himalaya, India. *Nat Hazards* 65:315–330
- Roy P, Martha TR, Jain N, Kumar KV (2018) Reactivation of minor scars to major landslides—a satellite-based analysis of Kotropi landslide (13 August 2017) in Himachal Pradesh India. *Curr Sci* 115:395
- Saha S, Bera B (2024) Rainfall threshold for prediction of shallow landslides in the Garhwal Himalaya India. *Geo Geo* 3:100285
- Sahana M, Sajjad H (2017) Evaluating effectiveness of frequency ratio, fuzzy logic and logistic regression models in assessing landslide susceptibility: a case from Rudraprayag district, India. *J Mt Sci* 14:2150–2167
- Sardana S, Verma A, Singh A (2019) Comparative analysis of rockmass characterization techniques for the stability prediction of road cut slopes along NH-44A, Mizoram, India. *Bull Eng Geol Environ* 78:5977–5989

- Sarkar S, Anbalagan R (2008) Landslide hazard zonation mapping and comparative analysis of hazard zonation maps. *J Mt Sci* 5:232–240
- Sarkar S, Kanungo DP, Sharma S (2015) Landslide hazard assessment in the upper Alaknanda valley of Indian Himalayas. *Geomat Nat Hazards Risk* 6:308–325
- Sarkar K, Buragohain B, Singh T (2016) Rock slope stability analysis along NH-44 in Sonapur area, Jaintia hills district, Meghalaya. *J Geol Soc India* 87:317–322
- Sarkar S, Roy AK, Raha P (2016) Deterministic approach for susceptibility assessment of shallow debris slide in the Darjeeling Himalayas, India. *CATENA* 142:36–46
- Sarkar S, Chandna P, Pandit K, Dahiya N (2023) An event-duration based rainfall threshold model for landslide prediction in Uttarkashi region, North-West Himalayas, India. *Int J Earth Sci* 112:1923–1939
- Sati VP (2014) Towards sustainable livelihoods and ecosystems in mountain regions. Springer, Berlin, Germany
- Searle M (2013) Crustal melting, ductile flow, and deformation in mountain belts: cause and effect relationships. *Lithosphere* 5(6):547–553
- Segoni S, Piciullo L, Gariano SL (2018) A review of the recent literature on rainfall thresholds for landslide occurrence. *Landslides* 15:1483–1501
- Sengupta A, Gupta S, Anbarasu K (2010) Rainfall thresholds for the initiation of landslide at Lanta Khola in north Sikkim, India. *Nat Hazards* 52:31–42
- Shah B, Bhat MS, Alam A, Malik UF, Ali N, Sheikh HA (2024) Establishing the landslide-triggering rainfall thresholds for the Kashmir Himalaya. *Nat Hazards* 120:1319–1341
- Sharma S, Mahajan AK (2019) A comparative assessment of information value, frequency ratio and analytical hierarchy process models for landslide susceptibility mapping of a Himalayan watershed, India. *Bull Eng Geol Environ* 78:2431–2448
- Sharma SP, Anbarasu K, Gupta S, Sengupta A (2010) Integrated very low-frequency EM, electrical resistivity, and geological studies on the Lanta Khola landslide, North Sikkim, India. *Landslides* 7:43–53
- Sharma LP, Patel N, Ghose MK, Debnath P (2014) Application of frequency ratio and likelihood ratio model for geo-spatial modelling of landslide hazard vulnerability assessment and zonation: a case study from the Sikkim Himalayas in India. *Geocarto Int* 29:128–146
- Siddique T, Mondal MEA, Pradhan SP, Salman M, Sohail M (2020) Geotechnical assessment of cut slopes in the landslide-prone Himalayas: rock mass characterization and simulation approach. *Nat Haz* 104:413–435
- Singh C, Kohli A, Kumar P (2014) Comparison of results of BIS and GSI guidelines on macro level landslide hazard zonation—a case study along highway from Bhalukpong to Bomdila, West Kameng district, Arunachal Pradesh. *J Geol Soc India* 83:688–696
- Teja TS, Dikshit A, Satyam N (2019) determination of rainfall thresholds for landslide prediction using an algorithm-based approach: case study in the Darjeeling Himalayas, India. *Geosciences* 302
- Thakur VC (1987) Plate tectonic interpretation of the western Himalaya. *Tectonophysics* 134:91–102
- Umrao RK, Singh R, Sharma L, Singh T (2017) Soil slope instability along a strategic road corridor in Meghalaya, north-eastern India. *Arab J Geosci* 10:260
- van Westen CJ, Greiving S (2017) Multi-hazard risk assessment and decision making. In: N.R. Dalezios (ed), *Environmental hazards methodologies for risk*, Int Water Assoc. (IWA) Publishing, London, pp 31–94
- Vinod kumar K, Lakhera RC, Martha TR, Chatterjee RS, Bhattacharya A (2008) Analysis of the 2003 Varunawat landslide, Uttarkashi, India using earth observation data. *Environ Geol* 55:789–799
- Yeh PT, Lee KZZ, Chang KT (2020) 3D Effects of permeability and strength anisotropy on the stability of weakly cemented rock slopes subjected to rainfall infiltration. *Eng Geol* 266:105459
- Yhokha A, Goswami PK, Chang CP, Yen JY, Ching KE, Aruche KM (2018) Application of persistent scatterer interferometry (PSI) in monitoring slope movements in Nainital, Uttarakhand Lesser Himalaya, India. *J Earth Syst Sci* 127

# Geological and Microstructural Controls on a Landslide in Ghat Region Along NH-09, Kumaun Himalaya



Piyush Kumar Singh and Sarada Prasad Pradhan

**Abstract** Landslides are one of the most common and hazardous geological events in hilly terrains around the world. The interplay of geological and structural factors significantly influence slope stability. The geological features, such as faults, joints, bedding planes and microstructures, along with geotechnical properties of the rock mass play a crucial role in determining the propensity of slope failure. This study analyzed geotechnical, microstructural and geological controls on a slope in the Ghat region along NH-09, Pithoragarh, Kumaun Himalaya. By integrating field observations, microstructural analysis, and numerical modelling in FEM, this study aims to elucidate the specific factors contributing to slope failure. Field observations and kinematic analysis identified wedge failure caused by the intersection of joint and bedding plane. The mesostructures and microstructures were correlated with the help of rose diagram and kinematic analysis. A strong correlation emerged between the microstructures and the mesostructures, which impacts the slope from a small scale to a large scale. The stability of the slope was evaluated through Finite Element Method (FEM), which revealed that the slope is stable when unsaturated condition is considered, but the slope becomes unstable in dynamic and saturated condition with  $SRF < 1$ .

**Keywords** Slope stability · Rock mass classification · Kinematic analysis · Microstructure · Numerical modelling

---

P. K. Singh (✉) · S. P. Pradhan  
Department of Earth Sciences, IIT Roorkee, Roorkee, India 247667  
e-mail: [piyush\\_s@es.iitr.ac.in](mailto:piyush_s@es.iitr.ac.in)

S. P. Pradhan  
e-mail: [sppradhan@es.iitr.ac.in](mailto:sppradhan@es.iitr.ac.in)

## 1 Introduction

One of the most common and damaging geological concerns is landslides, which can seriously jeopardize infrastructure, human life, and the environment (Hung et al., 2014; Froude and Petley, 2018). These gravity-driven mass movements of rock, debris, or earth down a slope can be triggered by a variety of factors, including intense precipitation, seismic activity, erosion, and human activities such as construction or mining (Highland and Bobrowsky, 2008; Vishal et al., 2010; Xiong and Huang, 2022). Understanding the factors that control the initiation and behaviour of landslides is crucial for effective hazard assessment, risk mitigation, and early warning systems development (Fell et al., 2008; Guzzetti et al., 2012). Among them, the slope materials' geological, geotechnical, and microstructural properties are crucial in determining slope stability and the likelihood of landslides (Calcaterra and Parise, 2010). These controls are intricate and site-specific, underscoring the significance of thorough site investigations and meticulous characterization of slope materials. The frequency and features of discontinuities considerably impact a rock slope's stability (Priest, 1993). Around the world, slope stability is a complex problem that results in both ecological damage and human casualties in mountainous terrains (Panikkar and Subramanyam, 1997). The Himalaya is one such mountainous region characterised by intense tectonic and seismic activity. It is traversed by numerous thrusts, causing the rocks in the region to be highly fragmented. This is why landslides are such a devastating natural disaster in the Himalayas which affect tourists and inhabitants. Large-scale widening of roads through unplanned excavations has increased the risk of slope failure (Umrao et al., 2011). 66.5% of landslides occur in India's North-west Himalayas, with Uttarakhand having the most landslide incidents, followed by Jammu & Kashmir and Himachal Pradesh (Jain et al., 2023). The Uttarakhand Himalaya is a tectonically unstable region, making it vulnerable to frequent disasters (Dudeja et al., 2017). A highly deformed and tectonically active zone, the Lesser Himalayan region is characterized by generations of joints, fractures, faults, folds and shear planes (Negi et al., 2021). To better comprehend such complicated Himalayan terrain, thorough field research and accurate geological and geotechnical assessments of the rock slopes are rudiments.

For the building of a road network, determining safe cut slopes and using the proper excavation techniques are essential. The stability of slopes is generally assessed through several geo-mechanical classification techniques. The classification techniques used in this study to analyze the slope's stability include Rock Mass Rating (RMR) (Bieniawski, 1989), Slope Mass Rating (SMR) (Romana, 1985) and CSMR (Continuous Slope Mass Rating) (Tomás et al., 2007). Among the other geo-mechanical classification methods, RMR serves as deformability of rock masses and is employed in calculating other slope stability classification methods such as SMR and CSMR. The RMR system assigns a rating to the rock mass based on the relative importance of various factors contributing to the stability. Despite using multiple parameters to estimate rock mass quality, RMR still presents difficulties. For gauging the slope stability, SMR (Slope Mass Rating) developed by Romana (1985) relies

on RMR and adjustment factors for orientation parameters. CSMR is a modified version of SMR that uses continuous functions in the calculation of slope rating instead of discrete functions. These classification techniques combine structural and geotechnical properties to provide empirical estimates of rock mass qualities and slope failure propensities.

Several researchers used numerical modelling approaches to examine the slope stability precisely. The Finite Element Method (FEM) is a powerful tool that enables the investigation of stress distributions, failure mechanisms, and slope deformation while taking into account material heterogeneity, groundwater conditions, and external loading scenarios (Griffiths and Lane, 1999; Zheng et al., 2005). FEM discretizes the slope into a large quantity of small elements and solves the governing equations of deformation and equilibrium for each element. The Limit Equilibrium Method (LEM) and FEM uses shear strength reduction (SSR) method for slope stability evaluation to scrutinize safety factor (Dawson et al., 1999; Kumar et al., 2020). LEM can't deal with complex problems related to stress, so FEM is used to monitor the effect of stress and seismic impact on the rock slope (Cheng et al., 2007). FEM is recommended for slope stability analysis as it has good accuracy and high efficiency compared to LEM.

In this study, we investigated the geological, geotechnical and microstructural controls on a slope in the ghat region along NH-09, Pithoragarh, Kumaun Himalaya, Uttarakhand, India. By integrating field observations, laboratory analyses, and numerical modelling in RS2, we aim to elucidate the specific factors that contribute to slope failure. Field investigations were conducted to ascertain the distribution and orientation of discontinuities in order to perform kinematic analysis along with the calculation of rock mass characteristics to analyze the slope stability by RMR, SMR and CSMR. Since the rock's mechanical strength and its deformation behaviour are highly influenced by its mineral composition and fabric, a proper microstructural investigation was conducted to analyze the mineral composition, arrangement, orientation of minerals and microfaults.

## 2 Study Area

This research was carried out on a road-cut slope situated on the National Highway-09 (NH-09) southwest of Pithoragarh city, Kumaun Himalaya within the Uttarakhand state of India, having coordinates of 29°31'18.05"N latitude and 80°8'9.72"E longitude (Fig. 1). Thousands of tourists and pilgrims utilize this road annually, making it a crucial connecting route between Pithoragarh and other destinations. Field data encompassing both structural and geotechnical aspects was gathered. Samples representative of the area was procured and subsequently analyzed at the Geotechnical Laboratory, Department of Earth Sciences, IIT Roorkee, for rock mass characterization and additional experiments.

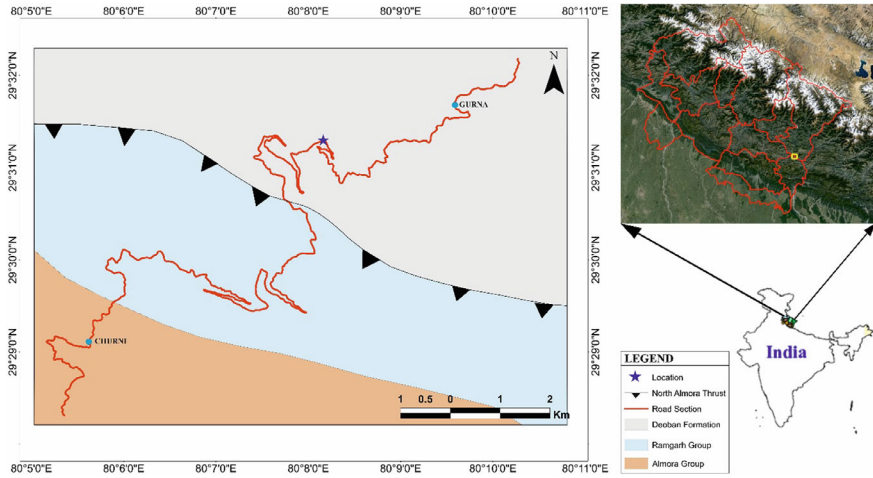


**Fig. 1** Map of the study area (modified after Geological Survey of India (2024))

## 2.1 Geological Framework

The Himalayan orogenic belt was created when the Indian and Eurasian continental plates collided. They are roughly 2400 kms long and between 250–300 kms in width and are bounded in the NE (Namcha Barwa and the Tsangpo Gorge) and NW (Nanga Parbat and the Indus Gorge) by tectonic kinks (Saini et al., 2018). It is traversed by several thrusts, viz, Main Frontal Thrust, Main Boundary Thrust, Main Central Thrust and Indus-Yarlung-Tsangpo Suture Zone, and several normal faults as well as other thrusts like Almora Thrust, Askot Thrust, Munsiyari Thrust, etc. The age of the Himalayas ranges from Precambrian (Basement) to Pleistocene (Shiwaliks) (Saini et al., 2018).

The area being studied is situated within the Kumaun Himalayas of Uttarakhand, located in India's Lesser Himalayas. The boundaries of the Lesser Himalayas are delineated by the Main Boundary Thrust to the south and the Main Central Thrust to the north. The rocks of the Lesser Himalayan Sequence consist of meta-sedimentary rocks, meta-volcanic strata, and Augen gneiss, as outlined by Gupta and Mukherjee (2022). The stratigraphy of the Lesser Himalayan sequence is presented in Table 1.

The study area features exposure of the Deoban Formation within the Tejam Group rocks, with noticeable influence from the nearby North Almora Thrust (NAT). Dolomitic limestone predominates as the major lithology along the slope, showcasing distinctive folds, lineations and faults.



**Table 1** Stratigraphy of lesser himalaya (Valdiya, 1980)

Lesser Himalayan metasedimentary zone	Tejam group	Deoban / mandhali formation	Limestone, dolomite and phyllite/slate
	Damtha group	Rautgara formation	Quartzite with penecontemporaneous mafic metavolcanic intruded by epidiorite
	Ramgarh group	Debguru porphyroid, bhatwari unit	Biotite-granite and tourmaline granite, schistose quartzite and chlorite schist
	North almora thrust (NAT)		
	Jaunsar group	Chandpur formation	Pauri phyllite, bhainswara quartzite
	Almora group	Dudhatoli crystalline	Schistose gneiss, biotite-garnet schist and garnetiferous gneiss

## 2.2 Climate and Seismicity

Himalayas experience extensive climates, from humid subtropical in the foothills towards the Indo-Gangetic plain to a cold, dry desert climate on the Tibetan (northern) side of the range. The most characteristic feature of the climate of the Himalayan Mountains is monsoon, which brings rain to the eastern side of the Himalayas. It is the primary reason for the monsoonal rainfall in the Indian subcontinent. The region experiences an annual rainfall from 850 to 1280 mm, with the majority occurring from June to September (Khanduri, 2022). Located in seismic zone V, characterized by high seismic activity, the area is prone to seismicity. Given its variation in landscape and regional climate, this region in the Pithoragarh District is among the most vulnerable areas.

## 3 Methodology

The methodology carried out during the study is given in the flow chart in Fig. 2. A field survey was carried out to gather samples for microstructural and strength analysis and to document geological, geotechnical, and structural parameters pertinent to slope stability. Kinematic analysis was conducted utilizing the discontinuity and slope orientation data acquired from the field. Based on field conditions, the Rock Mass Rating (RMR), Slope Mass Rating (SMR), and Continuous Slope Mass Rating (CSMR) are computed to evaluate the quality of the rock mass, categorize the slope as stable or unstable, and provide the likelihood of collapse. As per the recommended procedures by ISRM (ISRM, 1978, 1981), the Uniaxial Compressive Strength (UCS) of the rock samples was ascertained by converting the Schmidt hammer rebound number. After that, thin section analysis was conducted to recognize the significant minerals and microstructures in the rock sample and assess their

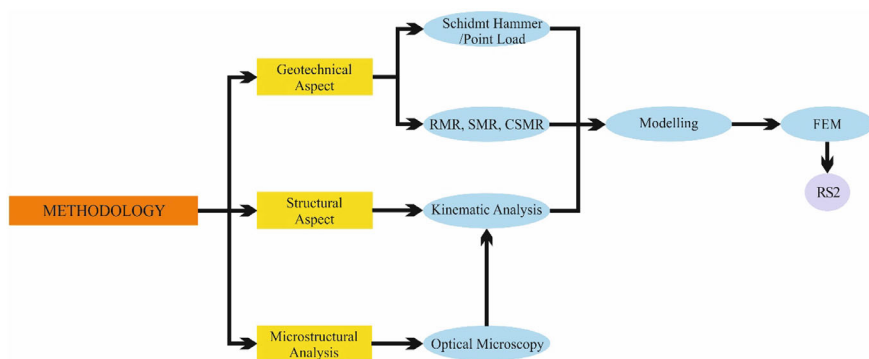


**Fig. 2** Methodology chart used in the study

orientation within the rock. The microstructures were correlated with the mesostructures through kinematic analysis and rose diagram to depict their distribution visually. Finally, the program based on Finite Element (RS2) was used to carry out numerical modelling. Because the Limit Equilibrium Method (LEM) only considers the Factor of Safety (FoS), FEM overcomes these constraints by providing calculations for the slope's maximum shear strain, total displacement, and yield components (Bekele and Meten, 2022).

### 3.1 Microstructural Analysis

Thin sections were created from the oriented rock samples acquired from the study area for conducting the microstructural analysis. This analysis facilitated the understanding of the anisotropy and inhomogeneity of the rocks, attributed to variations in the rock's mineralogy and texture, as well as the presence of microcracks, faults, and folds. The rock sample was sliced into multiple thin sections, each oriented perpendicular to the foliation. One thin section was aligned with the strike of the foliation, while another was positioned along the vertical plane in the direction of the foliation's dip. Thin section analysis is instrumental in elucidating various rock properties, including the mineralogical composition, the interrelationship between rock-forming minerals, grain size, grain shape, grain orientation, and the presence of microcracks, micro-faults, micro-folds, and porosity structure (Budennyy et al., 2017). The microstructural analysis also aided in establishing their relationship with the mesostructures through kinematic analysis. After that, the thin section analysis was conducted under a polarized optical microscope, and Leica 4.4.0 software was used to capture the pictures.

### 3.2 *Kinematic Analysis*

Kinematics refers to a body's geometrically possible motion without considering the forces involved (Goodman, 1989). Joint orientation-related rock slope failure types can be assessed by kinematic analysis (Hoek and Bray, 1981; Goodman and Bray, 1976). Its drawbacks include failing to take external influences and the characteristics of rocks and joints (Yoon et al., 2002). Rock slopes that are structurally regulated can fail in three different ways: planar, wedge, and toppling. Planar mode of failure is a type of gliding failure that happens in slopes having discontinuity having strike almost parallel ( $\pm 15^\circ$ ) to the slope's strike with discontinuity dip flatter as compared to the slope angle and steeper when compared to friction angle (Fig. 3a). When two discontinuities overlap, wedge failure happens when the angle of inclination is steeper when compared to the friction angle and flatter than the slope angle (Fig. 3b). The toppling mode of failure occurs when the slope's strike is close to ( $\pm 20^\circ$ ) the discontinuity's strike, yet the discontinuity dip is contrary to the slope face (Fig. 3c). In the RocScience program DIPS 6.0, an equal area stereonet is used to determine the mode and the direction of failure.

### 3.3 *Rock Strength Test*

Schmidt Hammer Rebound—It is a tool to gauge the elastic strength or qualities of rock or concrete. It first evaluates surface hardness and penetration resistance (Aydin and Basu, 2005). This method of determining the compressive strength of rock is non-destructive. A graded scale is used to measure the rebound value. Rock of lower strength absorbs more energy, which lowers the rebound value, and vice versa. Schmidt hammers come in two varieties: L- and N-type. When compared to L-type hammer, N-type hammer generates less data dispersion, making it more effective in estimating UCS and Young's modulus (Aydin and Basu, 2005). Researchers (Aufmuth, 1973; Xu et al., 1990; Deere and Miller, 1966; Beverly et al., 1979; Kahraman, 2001; Katz et al., 2000; Shorey et al., 1984) have provided several relationships that link UCS and Schmidt hammer. Deere and Miller (1966) gave a graph showing the link between Uniaxial Compressive Strength (UCS) and Schmidt hammer rebound number while considering the rock's unit weight and hammer orientation.

### 3.4 *Rock Mass Rating*

In 1973, Bieniawski, at the South African Council of Scientific and Industrial Research (CSIR), developed the Rock Mass Rating (RMR) based on his observations

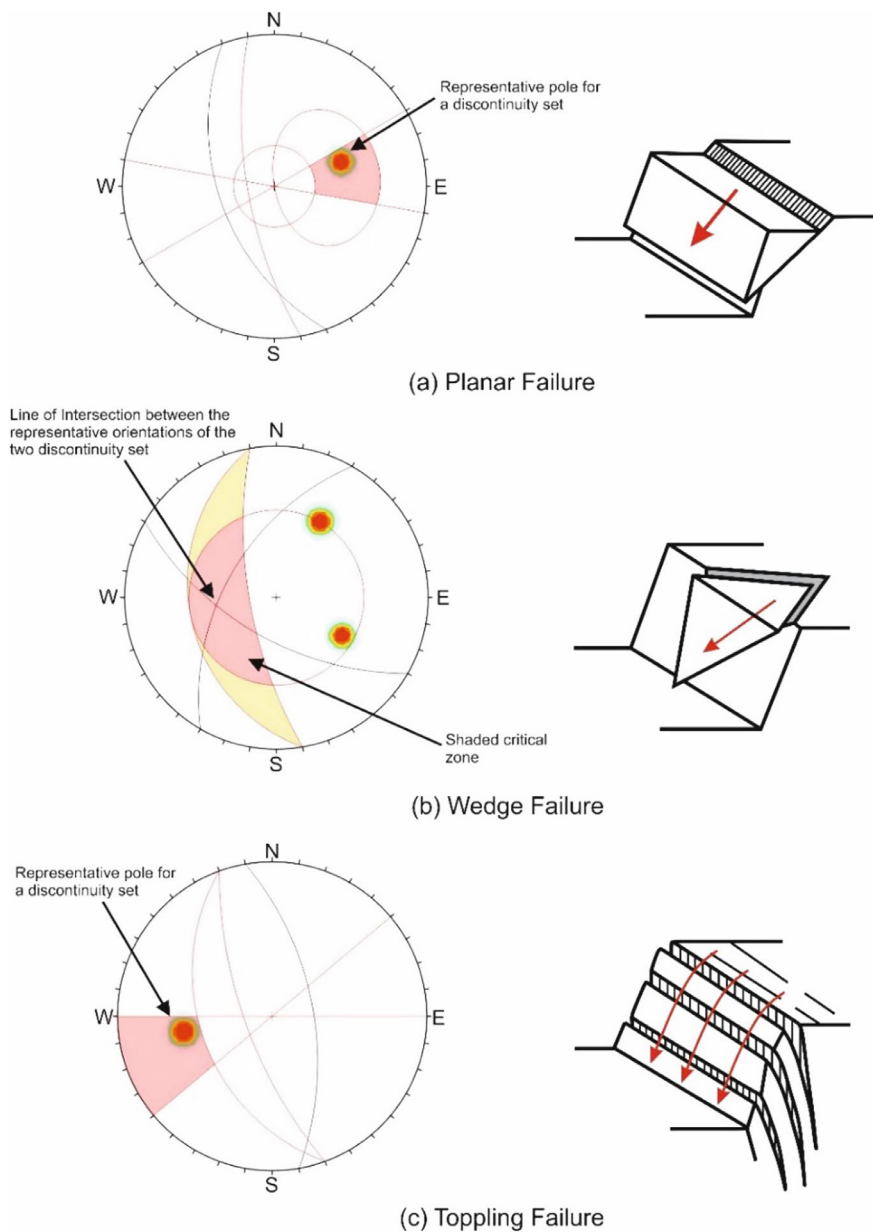


**Fig. 3** Stereographic plot showing requirements for **a** Planar failure, **b** Wedge failure (Hoek and Bray, 1981), **c** Toppling failure (Goodman, 1989)

**Table 2** Classification table for RMR

RMR	Class	Rock quality
0–20	I	Very poor
21–40	II	Poor
41–60	III	Fair
61–80	IV	Good
81–100	V	Very good

from working in shallow tunnels (Kaiser et al., 1986). At that time, the classification was also referred to as geomechanical classification. RMR underwent several significant changes in 1974, 1975, 1976, 1978, 1979, 1984, 1989, and 1993. RMR uses six parameters for defining the rock and discontinuity condition. These parameters (of representing causative factors) are (1) UCS of intact rock material, (2) Rock Quality Designation (RQD), (3) Discontinuity Spacing, (4) Discontinuity condition, (5) Groundwater condition, and (6) Discontinuity orientation. These parameters have ratings varying from 0 to 30, with UCS having ratings ranging from 0 to 15 (Bieniawski, 1979, 1984), RQD ratings ranging from 3 to 20 (Bieniawski, 1979), Joint spacing range 5–20 (Bieniawski, 1979), joint condition from 0 to 30 (Bieniawski, 1979), groundwater condition from 0 to 15 (Bieniawski, 1993) and 0 to (–60) rating was given to joint orientation (Bieniawski, 1979). A higher rating value indicates better rock quality compared to those with lower values. RMR rating is expressed with ratings in the range of 0–100 with a similar way of defining rock quality, with higher values indicating better rock mass (Bieniawski, 1973, 1989). RMR categorizes the rock mass into five classes on the basis of the ratings obtained by the addition of ratings of different parameters. To calculate the  $RMR_b$  (basic Rock Mass Rating), the first five parameters' ratings are summed. Table 2 shows the ratings of RMR, rock quality and its class.

### 3.5 Slope Mass Rating

Bieniawski's (1973, 1989) RMR system was not well suited for assessing slope stability because it was primarily intended for use in tunnels and dams. The Slope Mass Rating (SMR) categorization system was developed by Romana (1985) to assess the safety of rock slopes. Correction parameters from the joint-slope relationship are added in Bieniawski's RMR method, and an excavation-dependent factor is also added to determine slope stability. The SMR consists of  $RMR_b$  system, three adjustment components and a factor of excavation method.

$$SMR = RMR_b + (F_1 * F_2 * F_3) + F_4$$

where  $RMR_b$  = basic Rock Mass Rating, which is evaluated on the basis of Bieniawski (1973, 1989). The adjustment components, F1, F2, F3, and F4, are specified as follows.:

F<sub>1</sub> for planar and toppling failure relies on the parallelism between slope's direction ( $\alpha_s$ ) and discontinuity's dip direction ( $\alpha_j$ ). In contrast, for wedge failure, the trend of line of intersection ( $\alpha_i$ ) of discontinuities is considered. The value ranges from 0.15 to 1.00.

F<sub>2</sub> for planar and toppling failure depends on the amount of dip of discontinuity ( $\beta_j$ ). For wedge failure, the plunge of the line of intersection of discontinuities is taken ( $\beta_i$ ). Its value also ranges from 0.15 to 1.00, but for toppling failure, it is 1.00.

F<sub>3</sub> depends on how slope dip ( $\beta_s$ ) and dip amount of discontinuity ( $\beta_j$ ) are related. It tells about discontinuity's probability to daylight. For toppling failure, the values  $\beta_j$  and  $\beta_s$  are added, whereas for planar and wedge failure, it is deducted. The value ranges from 0 to (−60) for all types of failures.

The F<sub>4</sub> stands for the adjustment factor, which varies based on the slope-cutting technique. It includes different types of blasting techniques. Its value ranges from (−8) to (+15).

### 3.6 Continuous Slope Mass Rating

Romana's (1985) SMR has certain limitations because it divides the slope into discrete classes according to pre-established intervals, resulting in a step-by-step analysis that occasionally ignores minute changes in slope conditions. To eliminate the limitations, Tomás et al. (2007) presented CSMR, which uses continuous functions for F1, F2, and F3 to provide smooth and continuous evaluation of the slope stability parameters. With the ability to detect minute variations in the characteristics of the rock mass and slope geometry, CSMR enables a more accurate and thorough evaluation of slope stability. It also enhances the sensitivity of the analysis, which aids in detecting instabilities of small scale and provides a more accurate reflection of slope's actual conditions.

The difference between the adjustment factors of discrete and continuous functions can be seen through the graph (Fig. 4). F<sub>4</sub> (excavation method) is the same as that defined by Romana (1985).

The sigmoidal continuous functions are:

$$F1 = \frac{16}{25} - \frac{3}{500} - \text{atan}\left(\frac{1}{10}(|A| - 17)\right) \quad (1)$$

$$F2 = \frac{9}{16} + \frac{1}{195}\text{atan}\left(\frac{17}{100}B - 5\right) \quad (2)$$

$$F3 = -30 + \frac{1}{3}\text{atan}C \quad (3)$$

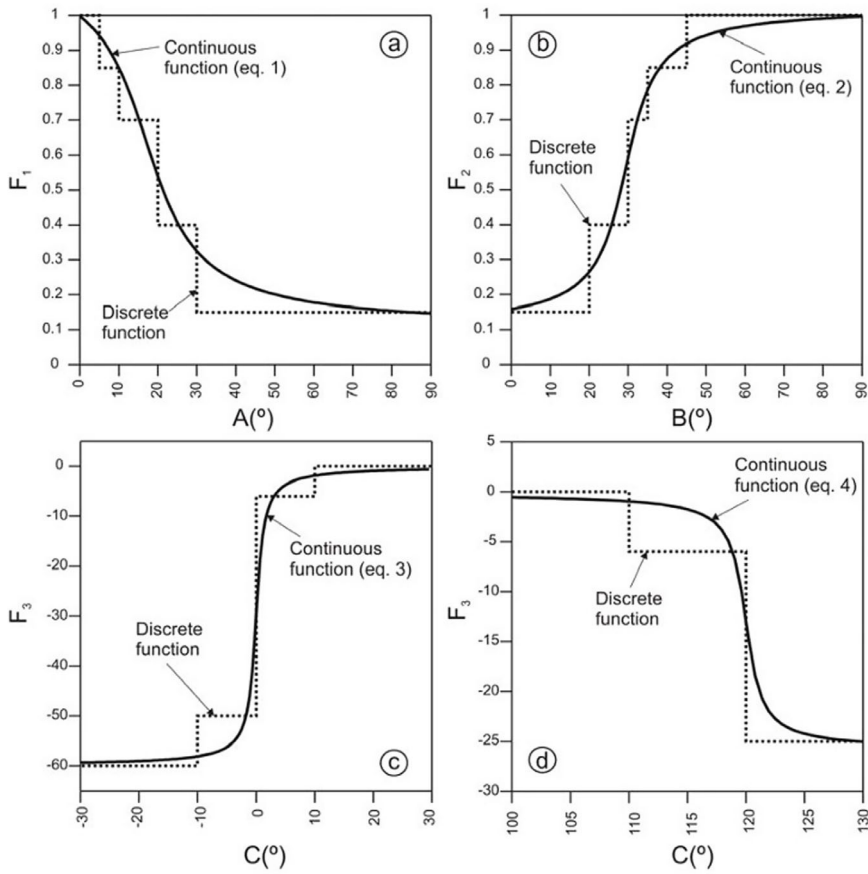


**Fig. 4** Graph showing the difference between the adjustment factors as discrete and continuous functions (Tomás et al., 2007)

$$F3 = -30 - \frac{1}{7} \text{atan}(C - 120) \quad (4)$$

where, A is the parallelism (A) between the slope's direction ( $\alpha_s$ ) and the discontinuity's dip direction ( $\alpha_j$ ) (or the trend of line of intersection ( $\alpha_i$ ) for wedge failure), B is the value of discontinuity dip ( $\beta_j$ ) or the azimuth of line of intersection of discontinuities ( $\beta_i$ ) for wedge failure and C is the relation between slope face ( $\beta_s$ ) and discontinuity dip ( $\beta_j$ ) as defined by Romana. For parameter F3, in the event of planar or wedge failure, Eq. (3) is applied, whereas in the event of a toppling failure, Eq. (4) is applied.

### 3.7 Numerical Modelling

Numerical modelling has evolved into a crucial tool for assessing slope stability and forecasting potential failure mechanisms. It employs mathematical models and computer simulations to scrutinize intricate interactions among soil or rock materials, groundwater, and external loads. Various types of numerical modelling techniques include limit equilibrium method (LEM), finite difference method (FDM), finite element method (FEM), discrete fracture network method (DFM), distinct element method (DEM), particle flow code (PFC) and boundary element method (BEM) (Jing and Hudson, 2002). Out of this, FEM is used in this study and is a type of elasto-plastic numerical approach for solving complex problems. A shear strength reduction approach is used with the FEM to evaluate slope stability (Griffiths and Lane, 1999). It has gained popularity due to its versatility, efficiency, and ability to handle problems with complex geometries and boundary conditions. The FE analysis of slopes emphasizes deformation rather than slope stability (Griffiths and Lane, 1999). The actual geometry of slope is discretized into finite elements as the first stage in a finite element analysis. Collection of the nodes, formed by connected points and finite elements, is called mesh. Mesh is generally triangular or quadrilaterals for 2D, while tetrahedra or hexahedra for 3D problems. The FEM formulation entails developing a set of governing equations that characterize the system's behaviour as it responds to external loads and boundary conditions (Cook et al., 2001). After obtaining the numerical solution, post-processing techniques, that include calculating stresses, strains, displacements, etc., are used to extract valuable information. Finite element approach has the following advantages over limit equilibrium methods—no assumptions should be made with respect to the position of the surface of failure since failure occurs when the applied shear forces exceed the rock's shear strength, no assumption is required about slice side forces, and it can track progressive failure (Griffiths and Lane, 1999). The software used in this study for finite element analysis is RocScience's RS2.

## 4 Results and Discussions

This research integrates geological (geological structures, lithology and topography) and geotechnical components to assess rock slope stability resulting from road excavation. The rock slope was identified as unstable during the reconnaissance survey and the major slope failure observed was wedge type of failure due to the interaction of the bedding plane and a joint plane. Deoban Formation's meta-sedimentary rocks make up the lithology of the rock slope, with rock type primarily being thick dolomitic limestone intercalated between thin laminations of phyllite. The road cut slope consists of 2 major sets of discontinuities having orientations:  $J_1$ — $85^\circ/080^\circ$ ,  $J_2$ — $41^\circ/260^\circ$  and the bedding plane with orientation  $74^\circ/010^\circ$ , making it structurally regulated. The slope is about 35 m high, having the orientation of  $67^\circ/340^\circ$ , with two



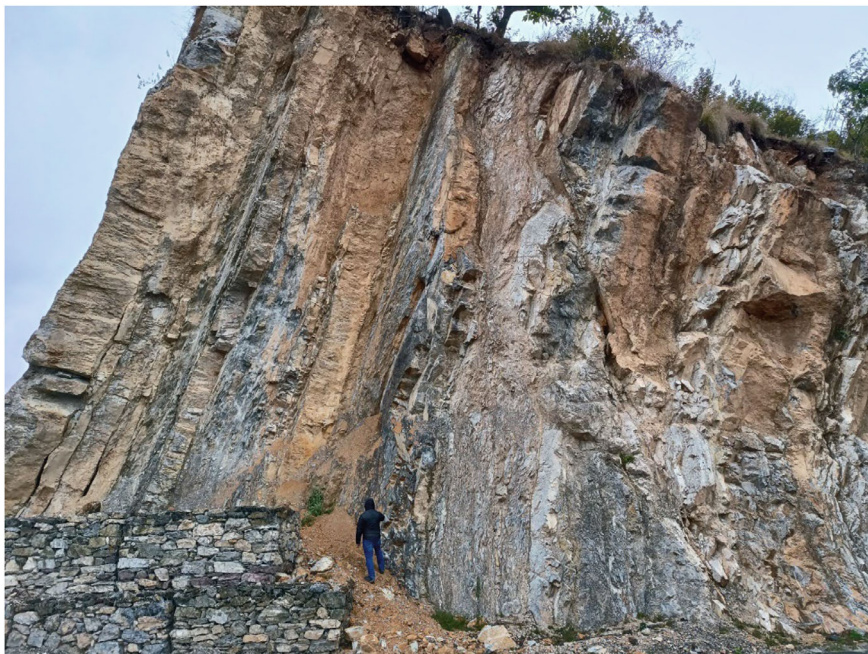


**Fig. 5** Field photograph of the slope depicting thick dolomitic limestone intercalated with thin laminations of phyllite with two prominent joint planes and a distinct bedding plane

sides that face the road. One side of the slope is stable, while the other side exhibits wedge failure (Fig. 5). Adjacent to the slope, the road has a width of around 5 m. Due to the considerable height of the slope compared to the width of the road, a substantial volume of rock mass could potentially be displaced onto the road during the event of slope failure. Hence, when planning stable cut slopes, it's essential to carefully consider both the height of the slope and the width of the road. (Gupta and Mukherjee, 2022).

#### **4.1 Microstructural Analysis**

The microstructural study of rock was conducted on the thin sections prepared from the oriented samples, aiding in understanding its heterogeneity and anisotropy encompassing textural, mineralogical and structural changes. Thin sections of oriented dolomitic limestone samples were prepared and seen under a polarising microscope to find the orientation of microstructures and the major minerals.

The dolomitic limestone is a compact, fine grained rock with the presence of mineral dolomite, which is calcium magnesium carbonate ( $\text{CaMg}(\text{CO}_3)_2$ ). It is formed through the process of dolomitization, where the original limestone is altered

by the replacement of calcium ions with magnesium ions. It exhibits a distinct crystalline texture and is generally more resistant to weathering and erosion compared to pure limestone. Dolomitic limestone present in the studied slope is metamorphosed and, thus, is hard and compact. It is composed mainly of calcite and dolomite as major minerals that can be seen under the polarising microscope. Micritic grains, formed through chemical precipitation of carbonate mud, were present primarily as matrix in the rocks of the study area, along with some coarse sparite crystals present between the open spaces or cracks parallel to the bedding plane, as can be seen in Fig. 6a–d.

Detailed analysis of thin section reveals that the sparite crystals are precipitated along cracks (following J2) (Fig. 6a, d) and bedding plane (Fig. 6b–d), wherever there is availability of open spaces, with the variation in orientation of approximately  $\pm 20^\circ$ . This excessive distribution of sparite crystals throughout the sample introduces heterogeneities or planes of weakness, potentially reducing the rock's strength. It can be seen from Fig. 6a that the layer of sparite crystals is folded, which depicts that compressive stress has acted on the rocks of the study area with the stress direction being perpendicular to the bedding plane (i.e., along  $100^\circ$ – $280^\circ$ ). The compressive

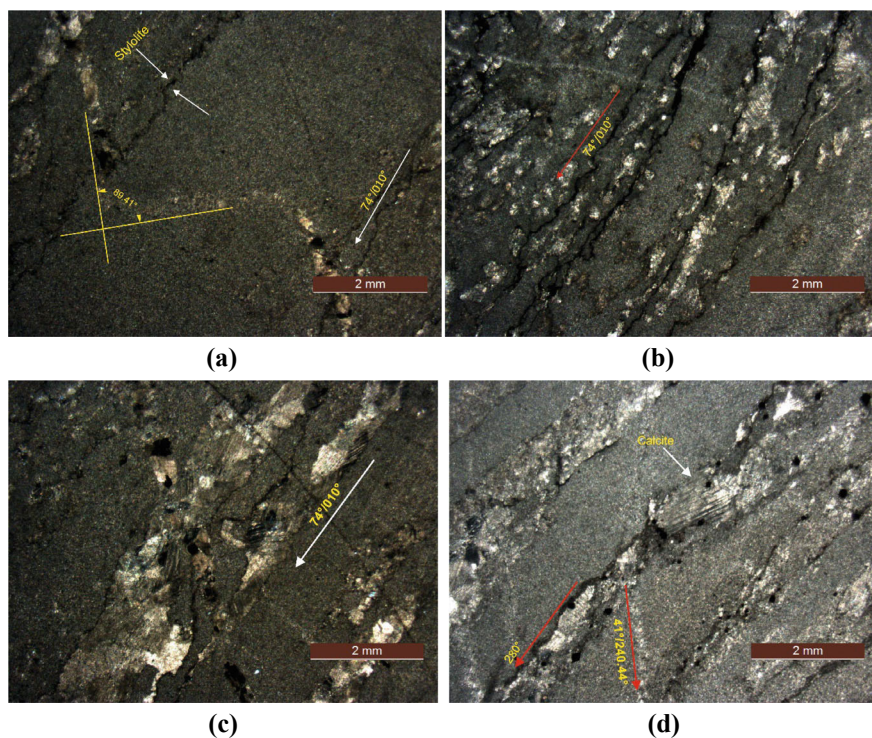


**Fig. 6** Thin section images showing the orientation of minerals, **a**, **b** and **c** were made across the foliation parallel to its strike; **d** parallel to the dip direction of foliation

stress must have been high enough to form an open fold with an interlimb angle of  $\sim 90^\circ$ . The slope failure can be caused by the dissolution of sparite crystals present along the joint J2 ( $41^\circ/260^\circ$ ) as well as along the bedding plane ( $74^\circ/010^\circ$ ), which will be confirmed through kinematic analysis in the next section of this study.

The presence of stylolites can be seen in the thin sections (Fig. 6a, b) in the direction parallel to the bedding plane and sparitic layer. It indicates the zone of dissolution and pressure solution, which causes insoluble residues to concentrate and discontinuities or weak points to form inside the rock mass. The presence of stylolite aids in confirming the stress direction to be around  $100^\circ$ – $280^\circ$ , depicting that the area occurs in the region of high tectonic activity. These stylolitic seams can act as potential failure planes, reducing the overall strength and cohesion of the rock mass. The presence of stylolites also introduces anisotropy and heterogeneity in the rock mass.

## 4.2 Kinematic Analysis

The orientation data for the structural discontinuities was recorded during the field survey and used in the kinematic analysis. The kinematic analysis aids in understanding the probability, specific kind and zone of failure the slope displays by plotting the discontinuities' orientation data on stereographic projections. The slope is present at the bend of the road, i.e., two sides of the slope are daylighting, with one side of the slope being stable and the other side showing wedge type of slope failure with one critical intersection of joint, J2 and the bedding plane (Fig. 7). The intersection line runs nearly parallel to the slope direction, with the plunge being less than the slope angle but greater than the angle of friction. The plunge and trend of the critical intersection line is  $37^\circ/292^\circ$ . The result of kinematic analysis helps in calculation of the SMR and CSMR.

## 4.3 Correlation Between Mesostructures and Microstructures

The orientation of the minerals, intrusion, and sparite layers was ascertained from the thin sections of orientated samples. The orientations were noted and used to determine the correlation between microstructures and mesostructures. The correlation was made possible by plotting the orientation data in the rose diagram and kinematic analysis.

The strike of mesostructures was plotted on the rose diagram (Fig. 8a) along with the orientation of microstructures, seen under the polarised microscope, in different rose diagrams (Fig. 8b) for comparison. On comparison, it can be seen that the microstructures follow a similar trend as the mesostructures, with some variation in the orientation. When the orientation of microstructures was depicted, some of the microstructures were not following the same trend as that of the bedding plane,

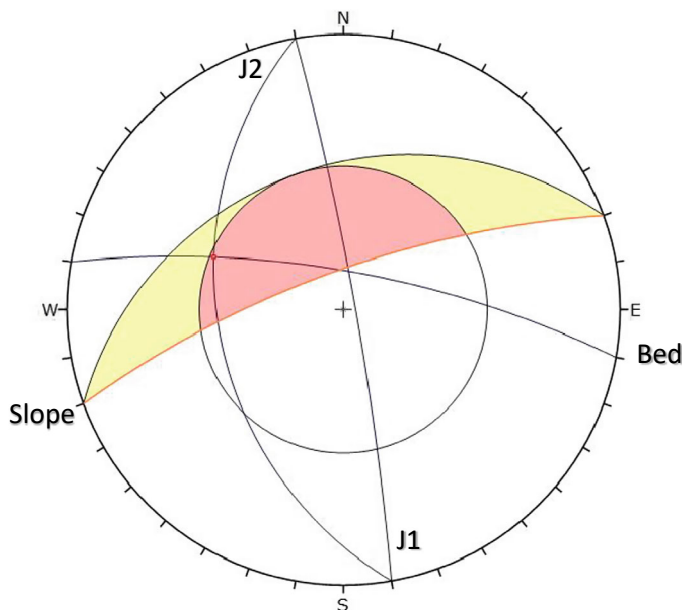


**Fig. 7** Kinematic Analysis of the slope showing wedge failure with one critical intersection point

instead, there was a variation of  $\pm 10^\circ$ . However, most of them followed the trend of the bedding plane and joint planes, as can be seen from the rose diagram. The similar orientation implies that the development of mesostructures stemmed from the coalescence of the microstructures, and any alteration in the structures or orientation at the micro level can have a significant impact at the meso-level. Apart from these, some minor cracks were not following the discontinuities, rather, they were oriented along N-S or NE-SW direction. There was an absence of mesostructures following these microstructural trends, and since we know that microstructures coalesce to form mesostructures, it can be said that a new joint plane can be formed in future with strike direction following the trend of NE-SW.

The orientation of microstructures was utilized to conduct kinematic analysis (Fig. 9), accessing how the microstructural features influence the stability of slope at a small scale. This stereographic projection of kinematic analysis was employed for comparison with the kinematic analysis conducted by using geological structures (Fig. 7). The orientation of microstructures with high frequency, as seen from the rose diagram in Fig. 8b, was used for kinematic analysis. The kinematic analysis of the microstructures shows three crucial intersections indicating wedge-type failure. On comparison with the kinematic analysis of the slope, it can be seen that the microstructural orientation causing wedge failure has a fairly similar orientation with the joint plane J2 and bedding plane, confirming that the microstructures do coalesce to form mesostructures. It is evident from appropriate thin section analysis



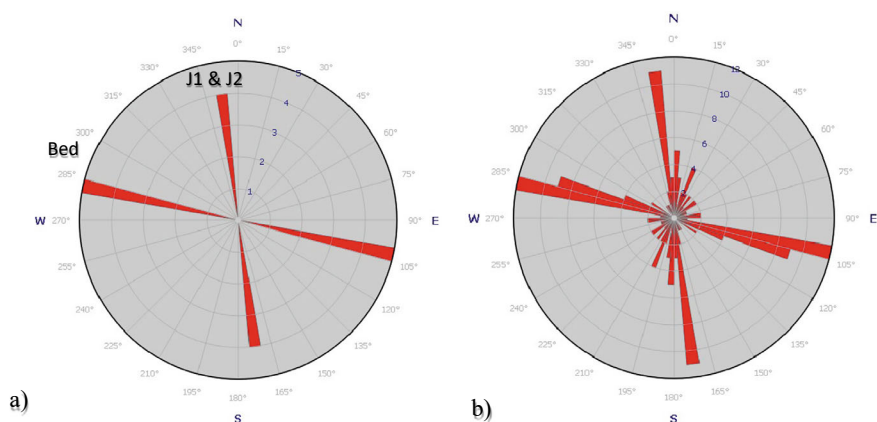


**Fig. 8** Rose diagram for the orientation of discontinuities in **a** Meso-scale **b** Micro-scale. The mesostructures follow the orientation of microstructures, which shows that the microstructures coalesce to form mesostructures

that two additional microstructure orientations are not seen at large scales: one orientation is nearly parallel to the bedding plane, while the other orientation is  $55^\circ/110^\circ$ . When further stress is applied, these microstructures may combine to form further discontinuities, which will result in the creation of two more crucial wedge failure junction locations.

#### 4.4 Rock and Slope Mass Classifications

The RMR estimates the quality and mechanical behaviour of rock masses by considering both the geological and geotechnical features. Schmidt Hammer was used to find the UCS of the rock with the help of the rebound value and unit weight of rock. The  $H_r$  and UCS values for the slope are 36.4 and 88 MPa, respectively. Utilizing field data, the  $RMR_b$  and RMR values were computed to be 46 and 41, respectively. The RMR categorizes the rocks of the slope as belonging to the ‘fair rock’ category, specifically Class III. SMR and CSMR are estimated with the help of  $RMR_b$ .

Given that the RMR system was initially intended for applications in tunnels and dams and may not be ideal for evaluating slope stability, the Slope Mass Rating (proposed by Romana in 1985) was employed. This approach assesses the safety of rock slopes by considering the relationship between joints and slopes, as well as the method of excavation. Table 3 presents the results of SMR and CSMR for the slope. The type of failure has been identified through field observations as wedge failure, which was subsequently confirmed through kinematic analysis. The SMR value for the slope indicating wedge failure is 38.35, suggesting its instability with a probability of failure estimated at 0.6.

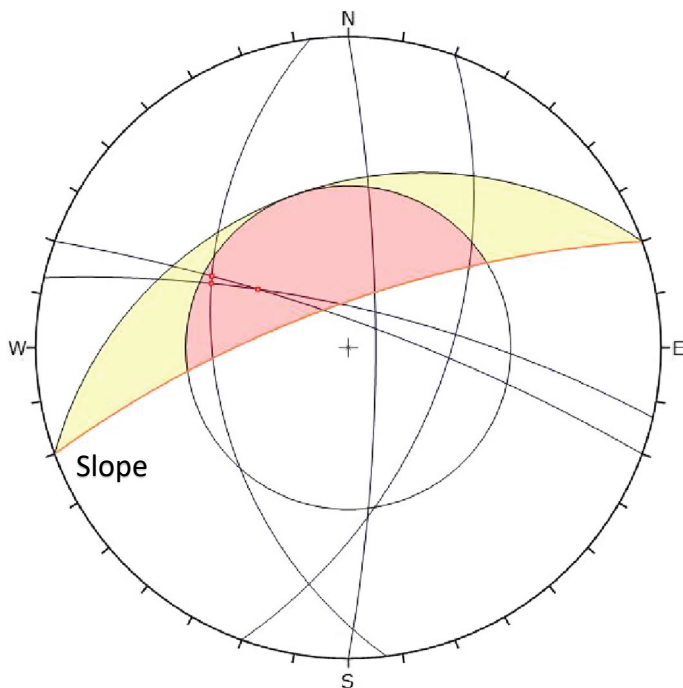


**Fig. 9** Kinematic analysis done through the orientation of microstructures showed wedge type of failure with three critical points due to the intersection of microstructures, which is somewhat oriented in the same direction as J2 and bedding plane

**Table 3** SMR and CSMR calculation table for the slope with adjustment factors

	$RMR_b$	$F_1$	$F_2$	$F_3$	$F_4$	SMR/ CSMR	Class	Stability	Probability of failure
SMR	46	0.15	0.85	-60	0	38.35	IV	Unstable	0.6
CSMR	46	0.18	0.87	-59.2	0	36.7	IV	Unstable	0.6

The SMR method introduced by Romana (1985) is constrained by its utilization of discrete functions. Conversely, the Continuous Slope Mass Rating (CSMR), proposed by Tomás et al. (2007), overcomes these limitations by employing continuous functions for  $F_1$ ,  $F_2$ , and  $F_3$  instead of discrete ones, while  $F_4$  remains unchanged. The CSMR value for wedge failure is 36.7, slightly differing from the SMR value. However, despite this variance, the instability and failure probability of the slope remain consistent.

## 4.5 Numerical Modelling

Numerical simulation was done using finite equilibrium modelling approach in Rocscience's RS2 software. The slope was modelled and simulated to do the stability analysis and compute the Strength Reduction Factor (SRF). The models were simulated in saturated and unsaturated conditions while considering both static and dynamic settings to emulate real circumstances. This was done to find the minimum SRF of the slope when considering several conditions to know its most unstable condition. The modelling also helped in evaluation of the displacement or deformation of the slope. The slope is simulated using Generalised Hoek–Brown (GHB) criteria as it gives better results compared to Mohr–Coulomb when jointed rock slope is considered (Pradhan and Siddique, 2020).

According to the slope's simulation results, the slope is unstable when considering static-saturated conditions, whereas it is stable when considering static-unsaturated conditions (Fig. 10). The simulation was also conducted considering dynamic settings because the slope is located in Zone V of the seismic zones of India. During dynamic setting, the slope was critically stable in unsaturated condition and unstable in saturated condition (Fig. 10) with the FoS given in Table 4.

Figure 10 reveals the unstable portion of the slope. The RS2 model depicts that the most unstable condition in which there is a high chance of slope failure is dynamic saturated condition. This means that the slope will fail if seismic activity is followed by high amount of rainfall.

## 5 Conclusion

The study demonstrated the effect of geological structures and microstructures on rock slope stability located in Pithoragarh district, Kumaun Himalaya, India. The field observations and kinematic analysis showed the failure type of the slope as wedge formed due to the intersection of the discontinuity plane—J2 and bedding plane. A strong correlation was observed between the kinematic analysis of mesostructures and microstructural orientations. However, additional wedges were formed when considering microcracks. The microstructural analysis depicted the presence of sparitic veins precipitated along joint—J2, and bedding plane. The presence of stylolites also influences the rock mass and it was found parallel to the direction of bedding plane. Thus, it is concluded that these veins and stylolites act as planes of weakness and introduce anisotropy and heterogeneity in the rock mass, reducing the rock's strength. The rock mass characterization depicted that the rock quality falls under the 'fair' category and the slope mass characterization depicted that the slope was unstable with the probability of failure of 0.6. The numerical modelling based on FEM revealed that the slope is stable in unsaturated condition with SRF being just greater than 1, but in dynamic setting and saturated conditions, it is unstable.

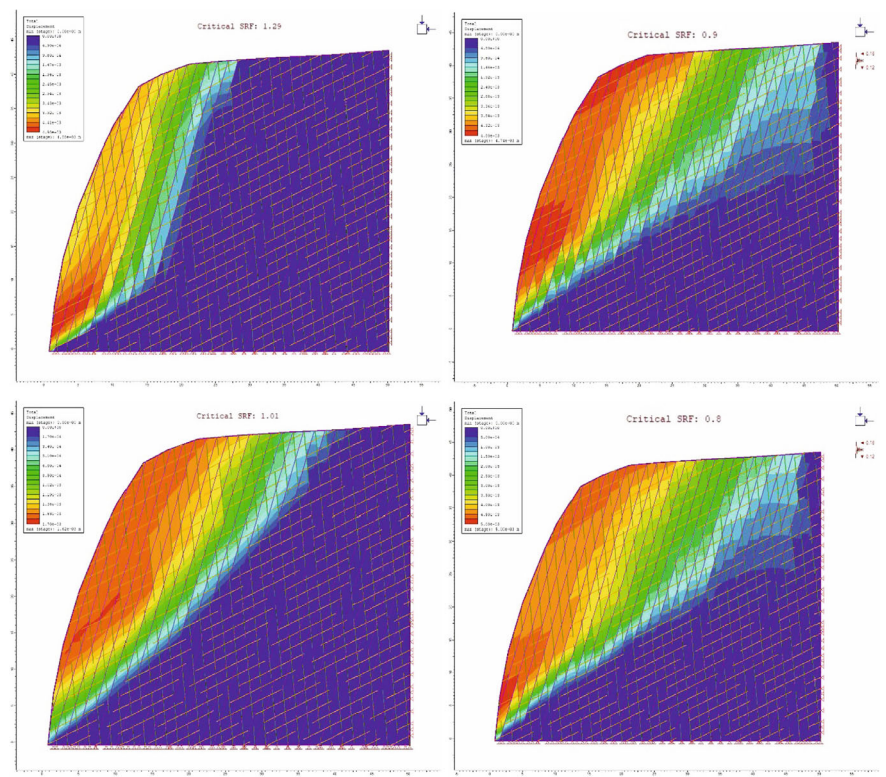


**Fig. 10** 2D FEM model in RS2 software for the slope showing the displacement contours in different conditions: unsaturated (SRF—1.29), dynamic unsaturated (SRF—1.01), saturated (SRF—0.9), and dynamic saturated (SRF—0.8)

**Table 4** The factor of safety from FEM by RS2 in different conditions

		FoS
Static	Unsaturated	1.29
	Saturated	0.9
Dynamic	Unsaturated	1.01
	Saturated	0.8

**Acknowledgements** The authors extend their heartfelt gratitude to the Department of Earth Sciences, IIT Roorkee for granting access to essential laboratory and computer resources. A special thanks to Mr. Sharique Siddique, Geotechnical Laboratory, Department of Earth Sciences, IIT Roorkee, India, for accompanying during the field.

**Declarations**

**Conflict of Interest** On behalf of all the authors, the corresponding author states that there are no conflicts of interest. The authors have no relevant financial or non-financial interests to disclose.



**Ethical Approval** All authors have read, understood, and have complied as applicable with the statement on Ethical responsibilities of Authors as found in the Instructions for Authors and are aware that with minor exceptions, no changes can be made to authorship once the paper is submitted.

**Consent to Publish**

This manuscript does not contain any individual data in any form.

## References

- Aufmuth RE (1973) Geotechnical study of rock glaciers. Ohio state university
- Aydin A, Basu A (2005) The Schmidt hammer in rock material characterization. *Eng Geol* 81(1):1–14. <https://doi.org/10.1016/j.enggeo.2005.06.006>
- Bekele A, Meten M (2022) Modeling rock slope stability using kinematic, limit equilibrium and finite-element methods along Mertule Maryam-Mekane Selam road, central Ethiopia. *Model Earth Syst Environ*. <https://doi.org/10.1007/s40808-022-01563-8>
- Beverly EJ, Thompson TW, Anderson LR, Haas CJ, Hinze WJ, Clayton CR (1979) Discussion: engineering classification of in-situ rock. In: *Proc Engng. Found Conf Univ of Missouri-Rolla*
- Bieniawski ZT (1973) Engineering classification of jointed rock masses. *Trans South Afr Inst Civil Eng* 15:335–344
- Bieniawski ZT (1984) The design process in rock engineering. *Rock Mech Rock Engng* 17:183–190. <https://doi.org/10.1007/BF01042549>
- Bieniawski ZT (1979) The geomechanics classification in rock engineering applications. In: *Proceeding of 4th international congress on rock mechanics of ISRM*, pp 55–95
- Bieniawski ZT (1989) Engineering rock mass classifications: a complete manual for engineers and geologists in mining, civil, and petroleum engineering
- Bieniawski ZT (1993) Classification of rock masses for engineering: the RMR system and future trends. In: *Comprehensive rock engineering*. 3, pp 553–573. <https://doi.org/10.1016/b978-0-08-042066-0.50028-8>
- Budennyy S, Pachezhertsev A, Bukharev A, Erofeev A, Mitrushkin D, Belozarov B (2017) Image processing and machine learning approaches for petrographic thin section analysis. *Society of petroleum engineers—SPE russian petroleum technology conference 2017*. <https://doi.org/10.2118/187885-ms>
- Calcaterra D, Parise M (2010) Weathering as a predisposing factor to slope movements. *Geological Society, Engineering Geology Special Publications*, London, 23(1), pp 141–159.
- Cheng YM, Lansivaara T, Wei WB (2007) Two-dimensional slope stability analysis by limit equilibrium and strength reduction methods. *Comput Geotech* 34:137–150
- Cook RD, Malkus DS, Plesha ME, Witt RJ (2001) *Concepts and applications of finite-element analysis* 4th ed. Wiley
- Dawson EM, Roth WH, Drescher A (1999) Slope stability analysis by strength reduction. *Géotechnique* 49(6):835–840. <https://doi.org/10.1680/geot.1999.49.6.835>
- Deere DU, Miller RP (1966) Engineering classification and index properties for intact rock (No. TR-AFWL-TR-65-116). Air Force Weapons Lab (AFWL/LN), Kirtland AFB, NM
- Dudeja D, Bhatt SP, Biyani AK (2017) Stability assessment of slide zones in Lesser Himalayan part of Yamunotri pilgrimage route, Uttarakhand, India. *Environ Earth Sci* 76(1). <https://doi.org/10.1007/s12665-016-6366-y>
- Fell R, Corominas J, Bonnard C, Cascini L, Leroi E, Savage WZ (2008) Guidelines for landslide susceptibility, hazard and risk zoning for land use planning. *Eng Geol* 102(3–4):85–98
- Froude MJ, Petley DN (2018) Global fatal landslide occurrence from 2004 to 2016. *Nat Hazard* 18:2161–2181. <https://doi.org/10.5194/nhess-18-2161-2018>
- Geological survey of India, 2024 (GSI). <https://www.bhukosh.gsi.gov.in>
- Goodman RE (1989) *Introduction to rock mechanics*, 2nd edn. Wiley

- Goodman RE, Bray JW (1976) Toppling of rock slopes. In: Rock engineering for foundations and slopes. ASCE, pp 201–234
- Griffiths DV, Lane PA (1999) Slope stability analysis by finite elements. *Géotechnique* 49(3):387–403. <https://doi.org/10.1680/geot.1999.49.3.387>
- Gupta AK, Mukherjee MK (2022) Evaluating road-cut slope stability using newly proposed stability charts and rock microstructure: an example from Dharasu-Uttarkashi roadway, lesser Himalayas India. *Rock Mech Rock Eng* 55(7):3959–3995. <https://doi.org/10.1007/s00603-022-02846-3>
- Guzzetti F, Mondini AC, Cardinali M, Fiorucci F, Santangelo M, Chang KT (2012) Landslide inventory maps: new tools for an old problem. *Earth Sci Rev* 112(1–2):42–66
- Highland LM, Bobrowsky P (2008) The landslide handbook—a guide to understanding landslides. Reston, VA: US geological survey
- Hoek E, Bray JW (1981) Rock slope engineering, vol 358. Institution of mining and metallurgy, London
- Hung O, Leroueil S, Picarelli L (2014) The Varnes classification of landslide types, an update. *Landslides* 11(2):167–194
- ISRM (1978) Suggested methods for the quantitative description of discontinuities in rock masses. *Int J Rock Mech Min Sci Geomech Abstr* 15:319–368
- ISRM (1981) Rock characterization testing and monitoring. In: Brown E (ed). Pergamon Press, Oxford, pp 211
- Jain N, Roy P, Martha TR, Jalan P, Nanda A (2023) Landslide Atlas of India (Mapping, monitoring and advance techniques using space-based inputs). NRSC special publication. NRSC/ISRO. Document number: NRSC-RSA-GSG-GMED-FEB 2023-TR-0002167-V1.0
- Jing L, Hudson JA (2002) Numerical methods in rock mechanics. *Int J Rock Mech Min Sci* 39(4):409–427. [https://doi.org/10.1016/S1365-1609\(02\)00065-5](https://doi.org/10.1016/S1365-1609(02)00065-5)
- Kahraman S (2001) A brittleness index to estimate fracture toughness of rocks. *J South Afr Inst Min Metall* 101(3):141–142
- Kaiser PK, Mackay C, Gale AD (1986) Evaluation of rock classifications at B.C. rail tumbler ridge tunnels. *Rocks Mechanics and Rock Engineering* 19:205–234
- Katz O, Reches ZE, Roegiers JC (2000) Evaluation of mechanical rock properties using a Schmidt Hammer. *Int J Rock Mech Min Sci* 37(4):723–728
- Khanduri S (2022) Rain-induced slope instability: case study of monsoon 2020 affected villages in pithoragarh District of Uttarakhand, India. *Int J Earth Sci Knowl Appl* 4(1):1–18
- Kumar A, Sharma RK, Mehta BS (2020) Slope stability analysis and mitigation measures for selected landslide sites along NH-205 in Himachal Pradesh, India. *J Earth Syst Sci* 129(1). <https://doi.org/10.1007/s12040-020-01396-y>
- Negi R, Singh RA, Saini P, Singh PK, Khali H (2021) Landslide investigations along the road corridor between Nandprayag and Gopeshwar, Chamoli district, Uttarakhand Lesser Himalaya. In: Shandilya AK, Singh VK, Bhatt SC, Dubey CS (eds) Geological and geo-environmental processes on earth. Springer, pp 315–324
- Panikkar SV, Subramanyan V (1997) Landslide hazard analysis of the area around Dehradun and Mussorie. *Uttar Pradesh Current Sci* 73(12):1117–1123
- Pradhan SP, Siddique T (2020) Stability assessment of landslide-prone road cut rock slopes in Himalayan terrain: a finite element method based approach. *J Rock Mech Geotech Eng* 12(1):59–73
- Priest SD (1993) Discontinuity analysis for rock engineering. Chapman & Hall, London
- Romana M (1985) New adjustment ratings for application of Bieniawski classification to slopes. In: International symposium on the role of rock mechanics ISRM, pp 49–53
- Saini P, Negi R, Singh RA, Singh PK (2018) Himalaya and its climate & biodiversity. *Shodh Sadhna Shodh Patrika* 5(1):78–84
- Shorey PR, Signer SP, Baul RL, Jeffries MS (1984) Slope stability study for the brock bridge railroad relocation project. *Geotech Test J* 7(3):117–128

- Tomás R, Delgado J, Serón JB (2007) Modification of slope mass rating (SMR) by continuous functions. *Int J Rock Mech Min Sci* 44(7):1062–1069. <https://doi.org/10.1016/j.ijrmms.2007.02.004>
- Umrao RK, Singh R, Ahmad M, Singh TN (2011) Stability analysis of cut slopes using continuous slope mass rating and kinematic analysis in Rudraprayag District. Uttarakhand. *Geomaterials* 01(03):79–87. <https://doi.org/10.4236/gm.2011.13012>
- Valdiya KS (1980) Stratigraphic scheme of the sedimentary units of Kumaun Lesser Himalaya
- Vishal V, Pradhan SP, Singh TN (2010) Instability assessment of mine slope—a finite element approach. *Int J Earth Sci Eng* 3(6):11–23
- Xiong L, Huang RQ (2022) Landslide susceptibility mapping using frequency ratio and logistic regression models in Xi'an, China. *Geomat Nat Haz Risk* 13(1):1024–1043
- Xu S, Grasso P, Mahtab A (1990) Use of Schmidt hammer for estimating mechanical properties of rocks. *Proc Rock Mech* 6:511–519
- Yoon WS, Jeong UJ, Kim JH (2002) Kinematic analysis for sliding failure at multi-faced rock slopes. *Eng Geol* 68(1–2):51–73
- Zheng H, Liu DF, Li CG (2005) Slope stability analysis by combining the finite element method and limit analysis. *Geotech Geol Eng* 23(5):527–545

# Rainfall Induced Landslides in Bangapani Tehsil of Pithoragarh District, Kumaun Himalaya, India



Rahul Negi, Pooja Saini, and R. A. Singh

**Abstract** Landslide is one of the most common disasters in the Himalayan terrain. The Himalaya is renowned for heavy rainfall during the monsoon. Due to the growth of population and developmental activities, people have a limited choice to construct the civil structures in safe places in the Himalayan region. Many village settlements are also situated on old landslide zones. These are prone to small/large landslide incidences causing damage to infrastructures and loss of lives. Pithoragarh district of Uttarakhand in India is highly prone to landslide disasters, and it has witnessed a large number of disastrous landslides every year because of the climatic conditions, geological and structural frameworks. Rainfall-induced landslides are a prominent event in the Pithoragarh district. The present study of landslides has been carried out in seven villages of the Bangapani tehsil of Pithoragarh. During the year 2020, 17 people and 23 cattle were killed by the landslide disaster. In the last 50 years (from 1971 to 2020), 433 people and 248 cattle were killed by the landslide disaster, and almost all landslides are induced by rainfall/cloudburst. The study describes the mechanism of rainfall-induced landslides. We have analyzed daily/monthly rainfall data for 2020, classified into pre-monsoon, during-monsoon, post-monsoon, and winter monsoon. Excess rainfall in the region makes it more susceptible to conditions for slope failure. The current study focuses on the actual causes of landslides in the area and estimates the damage at all locations. The rainfall records, structural data, surface geology, weathering, erosion, slope, aspect, and kinematic analysis have carried out systematic analyses for landslide occurrence. The study results describe how rainfall acts as the main triggering factor for the landslide. For analyzing all landslides, pre and post-monsoon satellite imagery of sentinel-2B has been used. The final output of the study indicates that landslides have been triggered during heavy rainfall in this region.

---

R. Negi (✉) · P. Saini

Department of Geology, L.S.M. Government P.G. College Pithoragarh, Pithoragarh, Uttarakhand, India

e-mail: [rahulnegi005@gmail.com](mailto:rahulnegi005@gmail.com)

R. A. Singh

Government Degree College Churiyala, Haridwar, Uttarakhand, India

e-mail: [singhdr.ramautar@gmail.com](mailto:singhdr.ramautar@gmail.com)

**Keywords** Landslide · Rainfall · Bangapani · Pithoragarh · Himalaya

## 1 Introduction

Landslide is one of the most common natural disasters which affects at least 15% of the Indian landmass. The landslide occurrence affects several mountainous regions globally, especially in the monsoon season. The frequency of landslide occurrences in the Himalayas is more than in other parts of mountainous regions in India. The fragile rocks and steep slopes make the vulnerable conditions of the Himalayan terrain. Every year in this region, landslide hazards damage infrastructures, agricultural lands, roads, bridges, and cattle and lose human lives. Many field studies indicate that many human settlements on the Himalayan terrain are either on old landslide mass or in-prone areas. In these areas, many people have been affected by small to large-scale landslide incidences from time to time, particularly during the rainy season. Some good publications are also available worldwide regarding the general relationship between landslide and rainfall viz., Brand et al. (1984), Sarma and Bora (1994), Lee et al. (2014), Dikshit et al. (2020), Mandal et al. (2021), Paswan and Shrivastava (2022). The previous study indicates that most of the landslides in the Pithoragarh district were triggered by rainfall/cloudburst (Khanduri 2017; Sajwan et al. 2017; Khanduri et al. 2018; Negi et al. 2018). The present area comes under subtropic regions. The Inter-Tropical Convergence Zone (ITCZ) reaches in June–July during the monsoon season. Due to this, ITCZ low-pressure zones form in the area, and heavy rainfall occurs during the monsoon.

Pithoragarh district of Uttarakhand is prone to landslide disasters. The district witnessed a large number of disastrous landslides every year due to climatic conditions and geological and structural frameworks. Generally, most of the slopes are moderate to very steep in the mountainous region of the Himalayas. Hence, people have a limited choice for their livelihood construction in suitable places, and of course, the population growth rate has been increased by 5.13% in the district. Major or minor recent developmental activities along the fragile slopes of the Himalayas create instability in many places. According to available data in the literature, rainfall-induced landslides have killed 416 people, 225 cattle and devastated many agricultural lands as well as infrastructures from 1971 to 2018 (Singh 2013; Sajwan et al. 2017; Khanduri et al. 2018; Sajwan and Khanduri 2018; Negi et al. 2018). Some examples of major devastating landslide incidences that occurred in the district are presented in Table 1.

Landslide refers to the downslope movement of the earth's surface materials under the influence of gravity. This phenomenon occurs naturally or due to human causes or a combination of both. Besides the surface geology, slope failure also depends on the quantity of rainfall and the safety factor. With the increase in slope, the shear strength of the material decreases, and the chances of slope instability increase. Shear strength is a force that can hold the material in its own place, but shear stress influences downward, and the combination of both is referred to as the factor of

**Table 1** Historical 50 years record of devastating landslides in pithoragarh

Landslide disaster event date/year	Event location	Casualties	References
July 1971	Dobata	12 People	Sajwan and Khanduri (2018)
26 July 1996	Raintoli	16 People	Sajwan and Khanduri (2018)
August 1998	Malpa	221 People	Sajwan and Khanduri (2018)
July 2001	Khetgaon	5 People	Sajwan and Khanduri (2018)
5 September 2007	Baram	14 People	Sajwan and Khanduri (2018)
8 August 2009	La-Jhekla	42 People	Singh (2013)
August 2010	Munsiyari	38 People	Khanduri et al. (2018)
18 September 2010	Munsiyari	19 People	Khanduri et al. (2018)
1 July 2016	Bastri, Didihat and Naulra villages	21 People and 174 cattle	Sajwan et al. (2017)
14 August 2017	Malpa and Mangti	27 People and 51 cattle	Khanduri et al. (2018)
3 July 2018	Gaila	1 person	Negi et al. (2018)
19 July 2020	Tanga, Bindi, Bata and Gaila villages in Bangapani Tehsil	14 People and 23 cattle	Discussed in this paper
27 August 2020	Dhami and Mori villages in Bangapani Tehsil	3 People	

safety. The factor of safety (FoS) is represented by the ratio of the shear strength to shear stress. Rainfall, erosion, road cuts, quarries, previous landslide, the weight of buildings, swelling clay, seismicity, and blasting may increase shear stress, whereas pore water pressure, weathering decrease the strength of the material. Many types of surface features are vulnerable to landslides during torrential rainfall including natural slope, huge boulders present on the steep slope, rock-cut slope, soil cut slope, earth fill retaining wall, steep slope, and highly weathered rocks are more prone (Brand et al. 1984). Most landslides have been active during the monsoon period in the hilly terrain of the Himalaya. Thus, the relationship between rainfall infiltration and the initiation of landslides is important. The present study focussed on the rainfall-induced landslides in Bangapani tehsil of Pithoragarh.

## 2 Study Area

The study area lies in the Bangapani tehsil of Pithoragarh district in Kumaun Himalaya. Pithoragarh is one of the remotest areas of Uttarakhand, India. The present investigation of landslide carried out from Tanga (N 30° 01' 05'', E 80° 19' 50''), Gaila (N 30° 04' 28.3'', E 80° 19' 29.6''), Bindi (N 30° 02' 00'', E 80° 20' 25''), Lodi (N 30° 01' 20.36'', E 80° 20' 15.34''), Bata (N 30° 02' 06'', E 80° 18' 53''), Dhami (N 29° 54' 46'', E 80° 17' 49'') and Mori (N 29° 54' 20.59'', E 80° 18' 42.39'') villages of Bangapani tehsil (Fig. 1). These villages were heavily damaged during the landslide disaster in 2020. These locations fall under Survey of India toposheet No 62B/8. The Gori Ganga is a major river flowing in the study area, whereas the Mandakini River and Paina Gad are the main tributaries. The study area comes under the seismic zone V. It experienced earlier earthquakes of 6.1 magnitudes in 1980 and 5.5 magnitudes in 1997 at the Indo-Nepal border, which induced several landslides in the Dharchula region (Sajwan and Khanduri 2018). Most earthquake-induced landslides/rockfalls happen on convex slopes, whereas rain-induced landslides are more common on concave slopes. About 20–30% of losses during earthquakes in hilly terrains have been attributed to landslides (Parkash 2013).

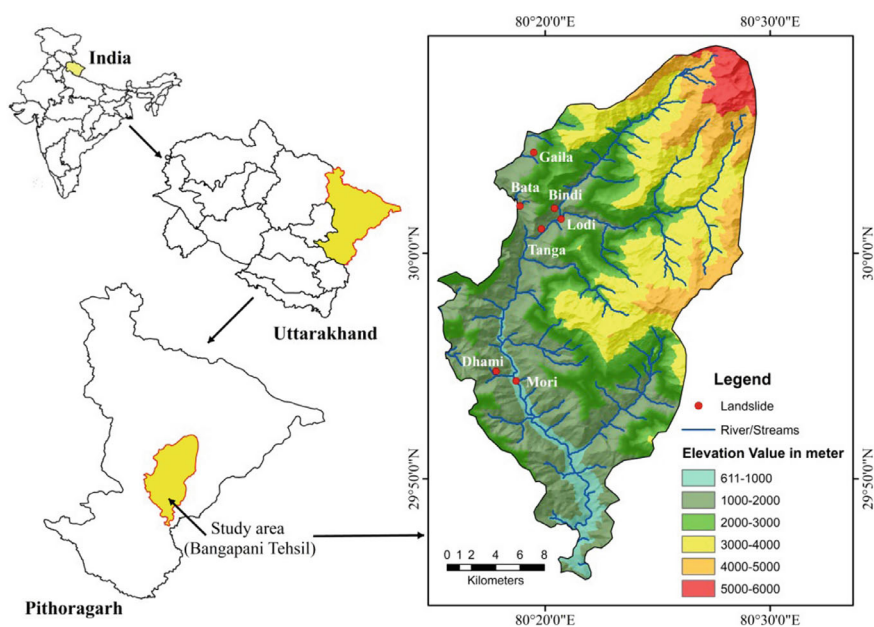


**Fig. 1** Location and relief map of the study area

3 Methodology

Present work has been accomplished in three parts: pre-field, during the field, and post-field (Fig. 2). The rigorous fieldwork was carried out during the monsoon period in 2020. The main objective of the pre-field is a literature survey, preparing a base map for making different maps and interpretations of the landslides. Firstly, information on landslide events has been collected from daily news and newspapers. After that, field investigations have been done regarding the collection of data related to landslides, such as the attitude of rocks, morphological data of landslides, hydrological conditions, etc. Survey of India toposheet No. 62B/8 has been used as a base map for the preparation of the geological map of the area. During the fieldwork, landslides were marked on the base map with the help of the Global Positioning System (GPS). During fieldwork, an analysis of damage estimation due to the disaster has also been made. Information about landslide events has also been collected from local government agencies and locally affected people. In the post-field work, we identified the mechanism of landslides by using various parameters such as slope, aspect, surface geology, weathering, erosion, and rainfall. The history of these landslides has also been analyzed with the help of Google Earth. Analysis of daily/monthly rainfall data for 2020 and kinematic analysis of slope failure have also been used for the detailed investigation of only one landslide. The pre-monsoon and post-monsoon

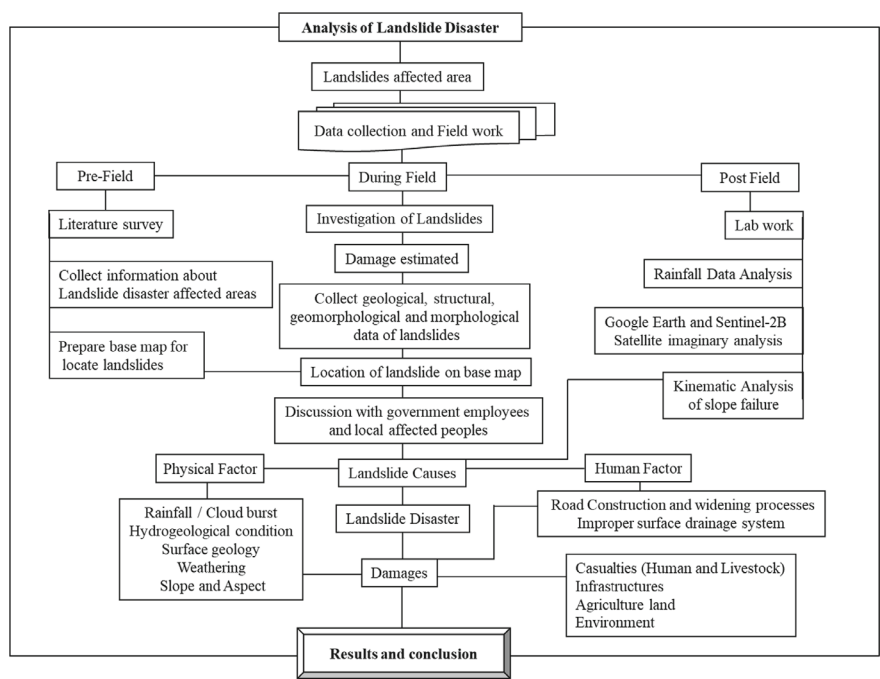


Fig. 2 Research framework chart for the study



imaginary studies of each landslide have been carried out by the Sentinel-2B satellite data, which makes it easier to know when the landslide was active/reactive. Some remedial measures or rehabilitation for the affected area have been suggested.

### 4 Geological Setup of the Area

Himalaya is one of the youngest mountains and is still dynamic since the collision of the Indian Plate with the Eurasian plate (Gansser 1964; Valdiya 1980; Yin 2006). Previously many researchers have broadly divided Himalayan Mountain into Siwalik, Lesser Himalaya, Higher Himalaya, Tethyan Himalaya, and Trans Himalaya. The Bangapani tehsil covers some parts of lesser and Higher Himalayan zones (Fig. 3). Geologically, the present study of all landslides are comes under Lesser Himalayan Zone. Many workers have given the structural, geological, and stratigraphical framework of Kumaun Himalaya. The lithology of the study area consists of sedimentary, metamorphic, and also igneous intrusions. The rock types belong to the Jaunsar, Tejam, Damtha, Almora and Vaikrita Groups (Valdiya 1980). The slate, phyllite, dolomitic limestone, and calcareous quartzite are dominant rock types which belong to Mandhali and Deoban formations of the Tejam group. These rocks are widely

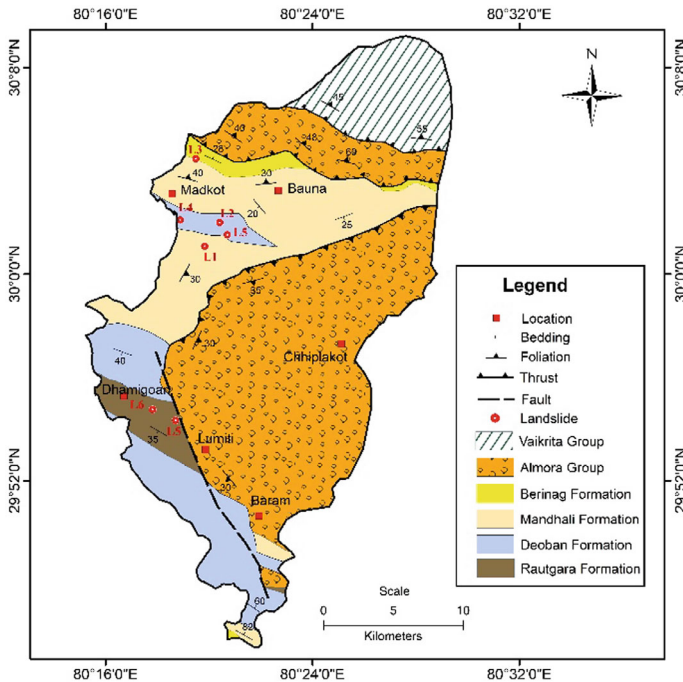


Fig. 3 Generalized geological map of Bangapani tehsil (modified after Valdiya 1980)

present around the Tanga, Bindi, Lodi, Bata, Dhami, and Mori villages. The quartzite and schist of Berinag Formation are exposed dominantly in the Gaila village. The structural features observed such folds, faults, thrusts, fractures, joints, boudinage, pinch, and swell in the rocks of the area. In general, the Uttarakhand Himalaya is tectonically active terrain where landslides are also triggered by tectonic stresses and structural discontinuities (Gupta 2005; Singh et al. 2021a, b). Tectonic stress and structural discontinuity also contribute to slope instability in the area.

## 5 Investigation of Landslide Disaster

Landslide is a natural disaster that refers to the downslope movement of rock, debris, rock cum debris or earth materials. The movement of materials depends on the type of landslides such as fall, flow, slide, subsidence, and creeping. Landslides have been classified based on the type of movement and type of materials (Varnes 1978; Highland and Bobrowsky 2008). In the Himalayan region, torrential rainfall and geological settings are the major triggering factors behind the activation of landslides. Previously many workers have carried out landslide studies using various methods and techniques in the Himalayan region (Gupta 2005; Singh 2013; Pachauri 2016; Kumar et al. 2017; Siddique and Pradhan 2019; Pradhan and Siddique 2020; Negi and Singh 2020, 2021; Saini et al. 2021; Singh et al. 2021a, b).

In the present study area, landslides frequently occur after heavy rainfall. Analysing of the last 48 years of landslide records of the Pithoragarh district clearly indicates that most of the slides were rainfall-induced. Landslide disaster killed 17 people in Tanga, Gaila, Dhami, and Mori villages of Bangapani tehsil during the year 2020. The morphological classification of each landslide event is described below:

### 5.1 *Landslide-1 at Tanga Village*

Tanga village is situated on the hill slope at the right bank of Paina Gad. The landslide is present at N 30° 01' 05'', E 80° 19' 50'' at an altitude of 1320 m (Fig. 4a, b). This village was affected by the landslide disaster in 2020. After continuous rain on the night of 19–20 July, a cloud burst occurred in which many landslides were triggered at the upslope side of the village. From the uphill side, debris materials entered the village, and 11 people, and 13 cattle lost their lives. Due to the cloud burst, an estimated 33,000 m<sup>3</sup> of debris material resting on the village and approximately 305,320 m<sup>2</sup> area have been affected by the landslide. Almost 90% of houses and about 3 hectares of agricultural land were damaged, and around 287 people were affected during this event (source: DDMO Pithoragarh). This is a debris flow and debris slide type of landslide, and it contains boulders up to about 5 × 3 m in size. During the field investigation of the village, it was noticed that water seeps along the schistosity planes, and the moisture content in the soil is high. The mechanism

of the Tanga landslide is well illustrated in Fig. 11. Slate and phyllite are present in Tanga village, but dolomitic limestone is dominant in the east direction in Danibagad village. Fractures, cleavages, and joints are present in the rocks. The schistosity dips  $30^\circ$  towards ESE, and the prominent joints dip  $70^\circ$  towards South,  $88^\circ$  towards ENE, and  $70^\circ$  towards WNW. The dip of schistosity plane in the mountain slope and the landslide movement direction is ESE. The kinematic analysis shows plane failure conditions (Fig. 4c). Before this incident, there was a big landslide present



(a)

**Fig. 4** **a** Tanga landslide, **b** NRDMS rescue team at a damaged house, **c** kinematic analysis of different discontinuities ( $J_0$ ,  $J_1$ ,  $J_2$ ,  $J_3$ ) along with slope showing plane failure condition and shaded portion showing the direction of failure at Tanga village, **d** pre-monsoon and post-monsoon imaginaries of Tanga landslide

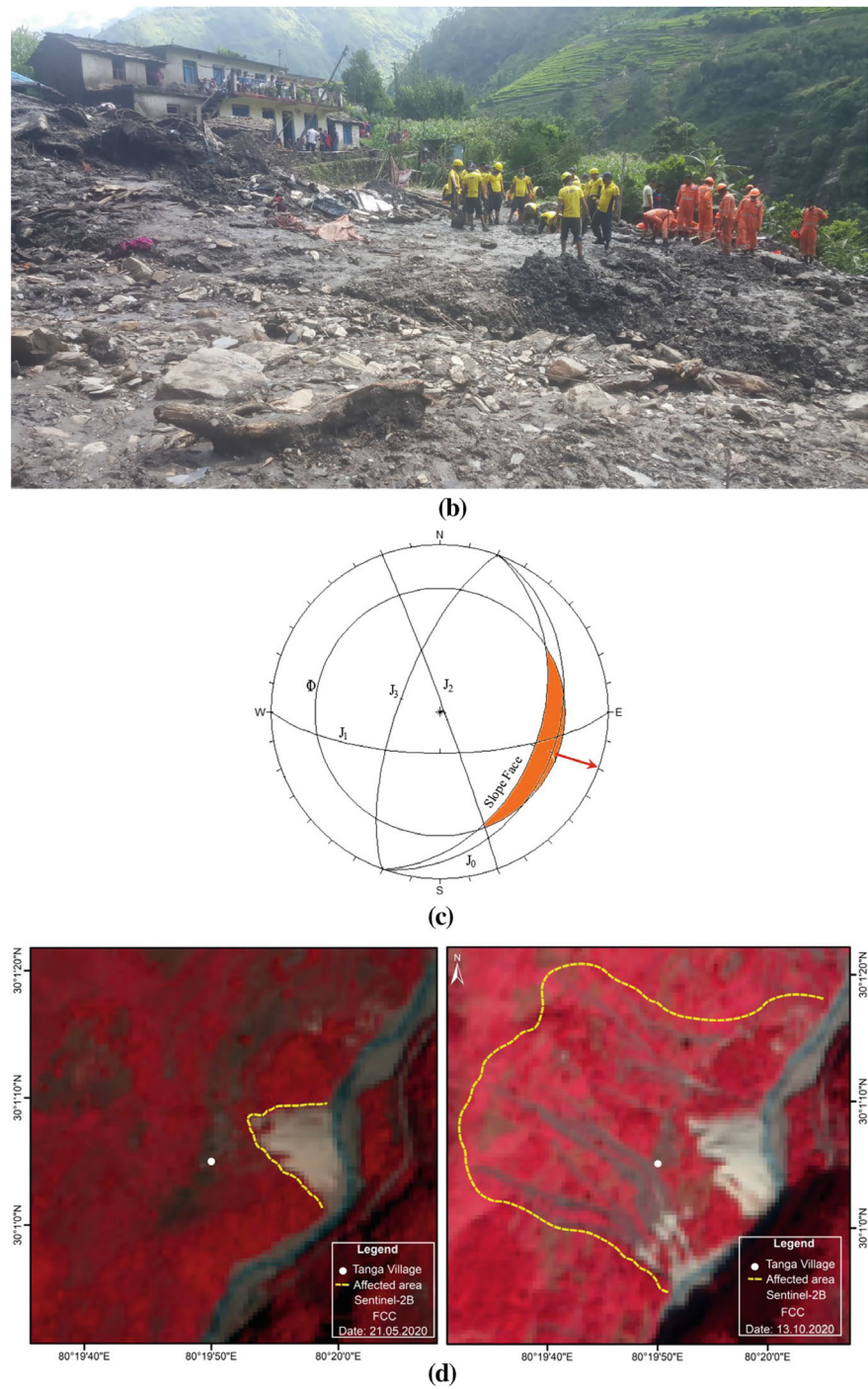


Fig. 4 (continued)



in the downslope of the village. Analysis of the satellite imagery and information gathered from local government agencies, and village people conformed that firstly the landslide in the downslope of the village began in 2013. Initially, the dimension was less, and the movement rate of the landslide was slow in the year between 2014 and 2017. After 2018, the movement rate of landslide increased, and the dimension of their also increased. Sentinel-2B satellite imagery has been used to know about landslide conditions in pre-monsoon and post-monsoon periods. It was observed that a landslide was present in pre-monsoon image, but its dimension was increased as well as some new landslides were also active during the monsoon (Fig. 4d). Before the monsoon 2020, an estimated area of 42,600 m<sup>2</sup> was affected by a landslide on the downside of the village. Tanga village is located in the crown part of the landslide, and the distance between the crown and the nearest house is only 5 m (Fig. 4a). Up to 30 cm subsidence and 10 cm wide cracks are observed in the crown part of the landslide. The motor road was also built in the village under the Pradhan Mantri Gram Sadak Yojana (PMGSY). Hairpin bends are present on this road at eight places and prepared after cutting the mountain slope. Due to the unplanned and excessive road cut of the slope, this village was in vulnerable conditions, and during the sliding road was damaged in many places. The Seragaht Dam Hydro-power project which is built over the Paina Gad was damaged due to heavy rainfall in 2013. Again, the dam was destroyed due to a cloud burst in the area on 2 July 2018 (Negi et al. 2018) and 19 July 2020. After the burst of the artificial dam at Paina Gad, the water level suddenly increased, and did more toe cutting in the Tanga village. In every monsoon period, Paina Gad does the toe cutting of the village. Before the incident cloud burst, the village was in susceptible condition due to continuous toe cutting since 2013. The main causes of this landslide are torrential rainfall/cloud burst and toe cutting by the Paina Gad. The remedial measures could be prepared on the down hillside of the village (slope), including a gabion wall, plantation, and proper surface drainage. In addition to that, rock bolting and netting treatment can be done on the uphill side of the village. Some of the houses were destroyed by landslides that needed to be relocated to safe places in this village.

## 5.2 *Landslide-2 at Bindi Village*

Bindi village is present on the right bank of the Paina Gad and in the North-East direction of the Tanga village and it has an altitude of 1380 m (Fig. 5a). Due to continuous rain, landslides were triggered at midnight on 19–20 July 2020. Dolomitic limestone is dominantly present in the village, overlain by thick soil. Sentinel-2B satellite imagery have been used for analysing pre-monsoon and post-monsoon conditions of landslide. It was observed that a landslide occurred in the post-monsoon image but was not seen in the pre-monsoon image (Fig. 5b). Due to this landslide, 600 m<sup>2</sup> area has been affected. Three houses were damaged, and two cattle were lost during this incident. Another house present near the landslide is also in a vulnerable condition. The slope of the area is steep in the eastern direction. During the fieldwork,

it has been observed that landslide type is a debris slide and the main causes of this landslide are rainfall and steep slope. For remedial measures, gabion wall and proper surface drainage should be prepared. Due to the landslide, some houses were damaged and in the worst condition. Therefore, rehabilitation of affected families should be done in a safe place.



(a)

**Fig. 5** a Bindi landslide, b Pre-monsoon and post-monsoon imaginaries of bindi landslide

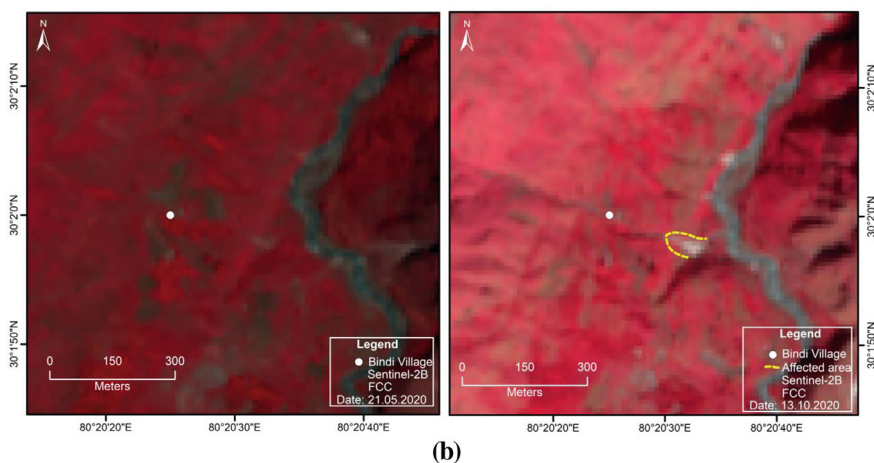


**Fig. 5** (continued)

### 5.3 Landslide-3 at Gaila Village

The Gaila village experienced a landslide incidence on 19–20 July 2020. This landslide is present at N 30° 04' 28.3'', E 80° 19' 29.6'' and an altitude of 1853 m. This village is situated uphill side and left bank of the Mandakini Gad. Geologically, the area is situated below the Main Central Thrust. Quartzite and schist are the main rock types at this place in which quartzite is in weathered condition due to the presence of clay minerals. The quartzite and schist dips 30° towards NNW. Four joint sets have been observed in the quartzite. The PMGSY road has been under construction since 2017. Road cuts affected the mountain slope in many places. During torrential rainfall on 19–20 July 2020, the retaining wall of the road was broken, and sliding took place (Fig. 6a). Another house has been damaged by the instability of the road cut section (Fig. 6b). Due to this incident, three people were killed after being buried in debris materials. Two houses were completely destroyed during the incident. For identifying pre-monsoon and post-monsoon situations, Sentinel-2B satellite imagery has been used for this slide (Fig. 6c). It was observed that no landslide was present in the pre-monsoon, but some new landslides were also present in the post-monsoon image. Due to the landslide, 3100 m<sup>2</sup> area had been affected. The movement of the landslide towards the west direction. Main causes of the landslide are heavy rainfall, poor surface drainage along the road, and a less stable retaining wall. For remedial measures, retaining wall and proper surface drainage along the roadside should be prepared. Some houses were also damaged by a landslide which needs to prepare in any safe place.





(a)



(b)

**Fig. 6** **a** Buried house under landslide at Gaila village, **b** damaged house due to the instability of road cut slope at Gaila village, **c** pre-monsoon and post-monsoon imaginaries of Gaila landslide



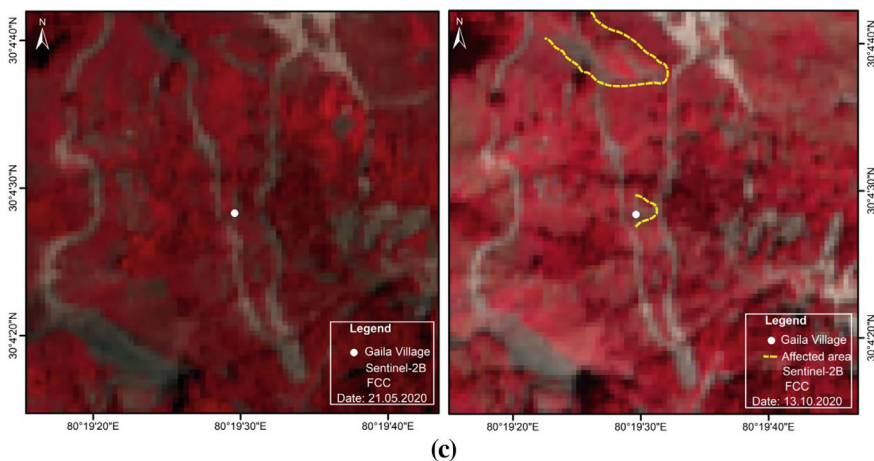


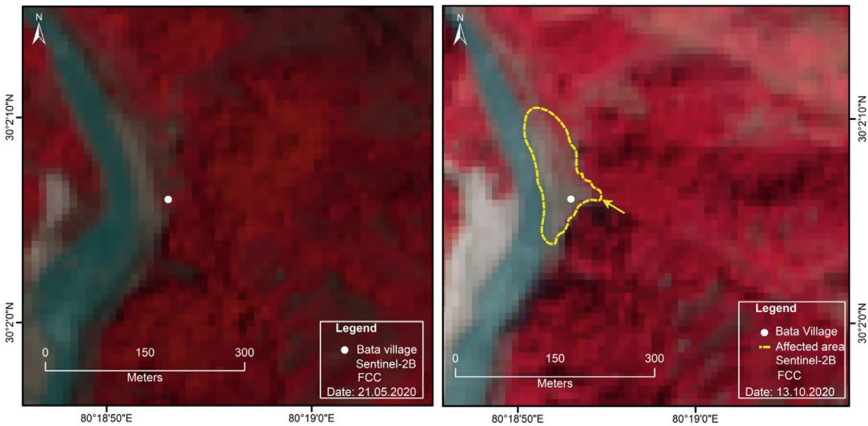
**Fig. 6** (continued)

#### 5.4 Landslide-4 at Bata Village

Bata village landslide incidence occurred on midnight of 19–20 July 2020, the landslide occurred at Bata village. This landslide located at N 30° 02' 06'' and E 80° 18' 53'' at an altitude of 1164 m. Slate is present at this location and dips 40° towards NNW. Three joint sets were also observed, which dip 50° towards NNE, 70° towards west and 85° towards NW. The slope of the mountain is very steep towards NW and the landslide movement is also towards NW. A house damaged due to this landslide was situated on the left terrace of the Gori River. That house occurs just below and right side of the waterfall of an ephemeral stream and not maintaining a safe distance from the stream (Fig. 7a). This stream flows in the NW direction and further joins with the Gori River. The damaged house is located towards the dip direction of the slate. After continuous rainfall, a cloudburst incident occurred on the uphill side of the village. At midnight of 19–20 July 2020, suddenly water gradient increased in the stream due to which a house was damaged, and 1400 m<sup>2</sup> of agricultural land was affected by the flash flood. In this incident, 8 cattle were feared buried. On that day, the area received 125 mm of rainfall (Fig. 12) Torrential rainfall is the major cause of this landslide. Pre-monsoon and post-monsoon imaginary of this landslide has been analyzed with the help of Sentinel-2B satellite. It is observed that landslide is present in post-monsoon but not seen in pre-monsoon imaginary (Fig. 7b). For safety, the damaged house needs to relocate to any other safe place. It is highly recommended that houses should be constructed at a safe distance from rivers/streams.



(a)



(b)

**Fig.7** **a** A house damaged by flash-flood at bata village, **b** pre-monsoon and post-monsoon imaginaries of bata landslide

**5.5 Landslide-5 at Lodi Village**

The Lodi village is present on the left terrace of the Paina gad. The village is situated at N 30° 01' 20.36'', E 80° 20' 15.34'' at an elevation of 1280 m. The Seragaht Dam Hydro-power project has been built just upstream side of the Paina Gad. This dam was burst during monsoon periods in 2013, 2018, and 2020 and subsequently, after each bursting of the dam Paina Gad eroded the base of the village due to toe cutting. The local people and Google earth information have also confirmed it. By the Gad flooding had already washed out two houses, and other remaining 7 houses of the village are present in unsafe conditions (Fig. 8a). During 19–20 July 2020, the

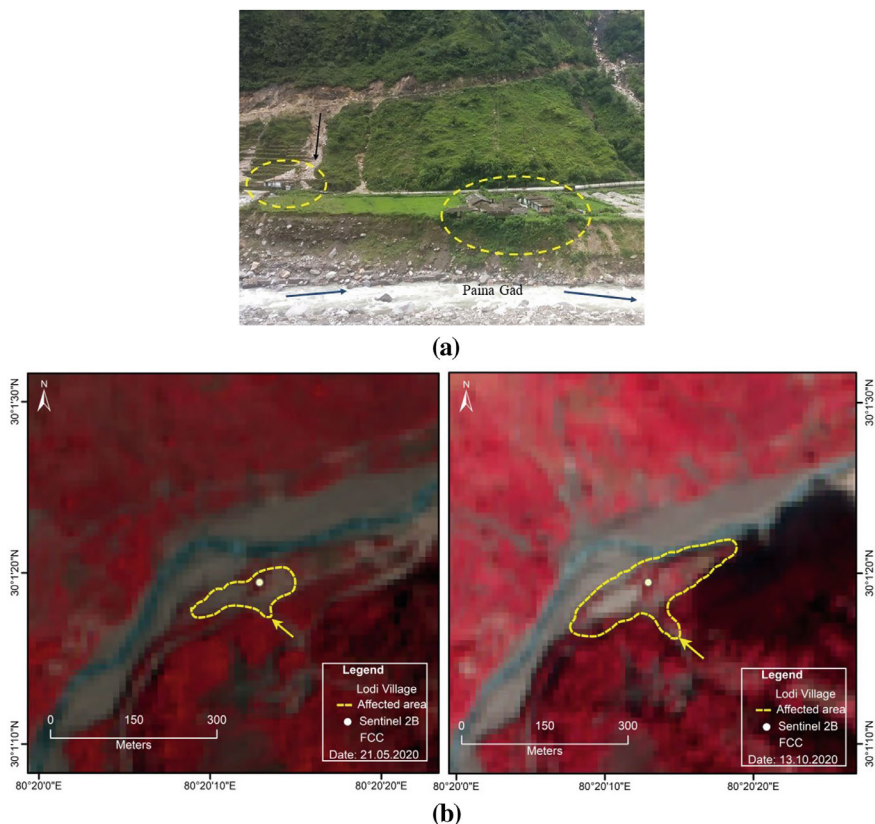


**Fig. 8** **a** Hazardous situation lodi village due to toe cutting, **b** pre-monsoon and post-monsoon imaginaries of lodi landslide

agricultural land was damaged by debris flow, and the 9000 m<sup>2</sup> area was affected. The landslide is observed both pre-monsoon and post-monsoon imaginary of Sentinel-2B satellite, but in post-monsoon, the dimension of landslide is increased (Fig. 8b). Heavy rainfall, the dam burst, and toe cutting by Paina Gad are the major causes of this landslide. For remedial measures, either strong concrete retaining wall should be prepared at the toe-cutting side of the river or rehabilitation of the affected family of all these seven houses should be done at any safe place.

## 5.6 Landslide-6 at Dhami Village

The landslide incidence has occurred in Dhami village. This landslide is active during the heavy precipitation on 27 July 2020 and located at N 29° 54' 46", E 80° 17' 49". This landslide is situated at the left bank and uphill side of Patali Gad which is the

present at right bank side of the Gori River. During 27 July 2020, a huge landslide activated after torrential rainfall due to where two people were killed after being buried. The approximate total length of the landslides is 500 m. A huge mass of debris moves along the west side of the village, but due to some obstacle, a branch of this slide entered the village, and a family along with the house was completely buried. A total of two houses were destroyed by landslide disaster (Fig. 9a). The slope of the area is steep towards the southern direction. A total 57,000 m<sup>2</sup> area had been affected by this landslide. This is a debris slide type of landslide which contains boulders up to 8 × 5 m in size. This landslide was started during a heavy rainfall period it is also confirmed by Sentinel-2B satellite imagery of the pre-monsoon and post-monsoon (Fig. 9b). During the field investigation, it has been observed that the village rests over the buried landslide, and at places, water seeps from the ground. Dolomitic limestone and calcareous quartzite are present in the area which is in highly weathered conditions. After the study of satellite imagery, it has been confirmed that another landslide is also present below the village since 2004 (Fig. 9c). Heavy rainfall and loose materials are the major causes of this landslide. For remedial measures, retaining wall, soil nailing, and proper surface drainage should be prepared at the bottom part of the landslide. Do not quarry in the bottom part of the village. The affected people of damaged houses need rehabilitation at any other safe place.

### 5.7 *Landslide-7 at Mori Village*

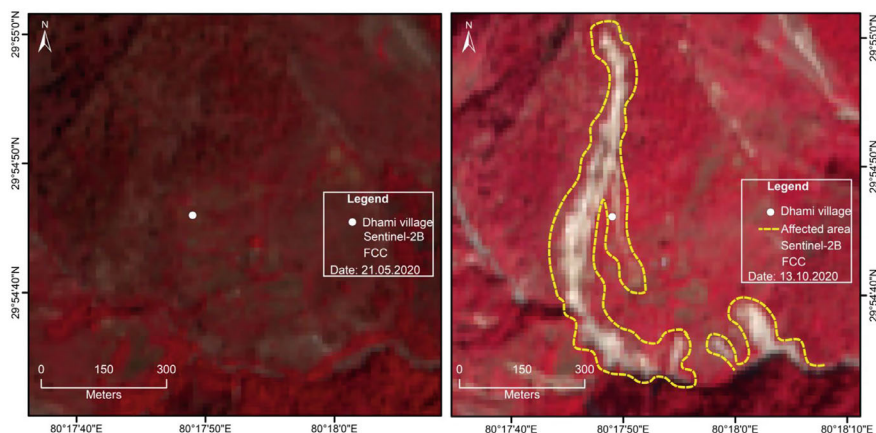
The Mori village is located at N 29° 54' 20.59'', E 80° 18' 42.39'' on the left side of the Gori Ganga River. A seasonal stream flows near the north direction of the village. On 27 July 2020, the landslide formed on the uphill side of the village after continuous torrential rainfall. A Flash flood occurred in the village after a cloud burst at around 4:30 AM. The entire Mori village was buried, and in many places, roads and bridges were damaged between Jauljibi and Munsiyari (Fig. 10a). During this event, one person died, and 24 houses, two motor vehicles, and most of the agricultural lands were damaged. Due to this incidence, 815 people, as well as about 63,739 m<sup>2</sup> area, were affected. Due to this flash flood, 134,000 m<sup>3</sup> of debris material is resting on the village. This landslide was active during the monsoon it is also confirmed by the Sentinel-2B satellite imagery of the pre-monsoon and post-monsoon (Fig. 10b). The downslope or towards the east in the village, approximately 36,000 m<sup>2</sup> of agricultural land was washed out by the Gori River in 2013 (by analysing Google earth imagery). During the field investigation, we observed that up to 20 m thick debris materials are present with approximately up to 5 × 2 m boulders of high-grade rocks. The Gori River turns approximately at the right angle when the debris materials enter the river. There was exceptionally high rainfall (889 mm) in the month of July 2020 (Fig. 12). Similarly, a huge landslide has been observed at Lumiti village towards the SSE of the Mori village. The Lumiti village is present at a crown part of the slide with coordinate N 29° 54' 15.16'', E 80° 19' 58.15''. After analysis of Google earth images, it was revealed that this huge landslide occurred during



the monsoon season of 2020. The 513,000 m<sup>3</sup> debris materials have damaged the approximately 689,000 m<sup>2</sup> land area of Lumiti village. The detailed investigations of the field and satellite data reveal that most of the houses are present either along the drainage or over the buried old landslide materials. Thus, some houses are present in susceptible conditions for the landslide. The main causes of the landslide are cloud burst, fragile lithology, and houses did not maintain a safe distance from the seasonal stream/Gori River.



(a)



(b)

**Fig. 9** **a** A house damaged by landslide at dhami village, **b** pre-monsoon and post-monsoon imaginaries of dhami landslide, **c** active landslide below the dhami village



(c)

Fig. 9 (continued)

## 6 Rainfall-Landslide Relationship

During the fieldwork, detailed information on landslides was collected at all locations. Rainfall data were collected from DDMO Pithoragarh to perform the relationship between rainfall and landslides. The monsoon season extends from June to September in the study area, but rainfall reaches its peak point during July and August (Fig. 12). The slope map of the area implies that most of the slopes are moderate to very steep (Fig. 13a, b). As the slope increases, the shear strength of the overburden decreases, and the chance of slope failures also increases. During the rainy period, infiltration of water can reduce the frictional force as well as increase the shear force due to which material can move downward. Rainwater also adds significant weight to the slope as it seeps into the ground and raises the water table. The rapid change in underground water level along the slope also affects the triggering of landslides. During a long time of rain shower, infiltration or seepage of water acts as a function of hydraulic force (Sarma and Bora 1994). When rain waters enter the tension cracks, it exerts additional hydraulic pressure, contributing to slope failure (Fig. 11). Thus, rainwater acts as a key factor behind the activation of landslides. Rainfall may influence landslides directly or indirectly (Sarma and Bora 1994). Water saturation, excess pore water pressure within soil and rock, and erosion of the earth

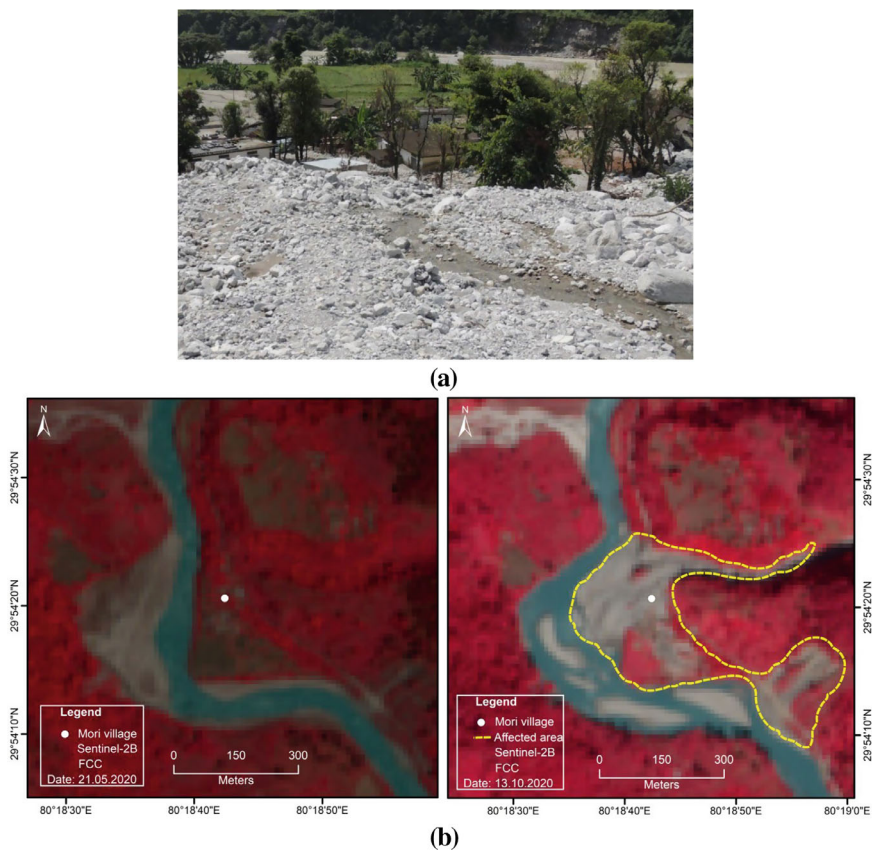


**Fig. 10** **a** Flash flood at mori village, **b** pre-monsoon and post-monsoon imaginaries of mori landslide

surface directly influence the landslides, whereas weathering influences landslides indirectly. During the field investigation, it was observed that moisture content in soil was present extensively at all landslides implying that the slope was highly saturated. With the increase of saturation, the pore-water pressure increases and reduces the shear strength of the material, which causes slope instability. The rate of saturation of materials significantly depends on the degree of weathering.

The factor of safety (FoS) depends on the shear strength and shear stress of the materials. In rainfall-induced landslide mechanism, three conditions may arise, i.e.,  $FoS > 1$ ,  $FoS = 1$ , and  $FoS < 1$ , as given in Fig. 11. In the first condition, when  $FoS > 1$ , no landslide takes place, it means the slope is safe (Fig. 11a). In the second condition, when  $FoS = 1$ , it is on the verge situation for sliding (Fig. 11b). In the last condition, when  $FoS < 1$ , the slope is unstable and a landslide occurs (Fig. 11c). During rainfall, water infiltrates into the slope, pore-water pressure increases, as well as the shear strength of the material decreases successively. Due to these, tensional cracks are



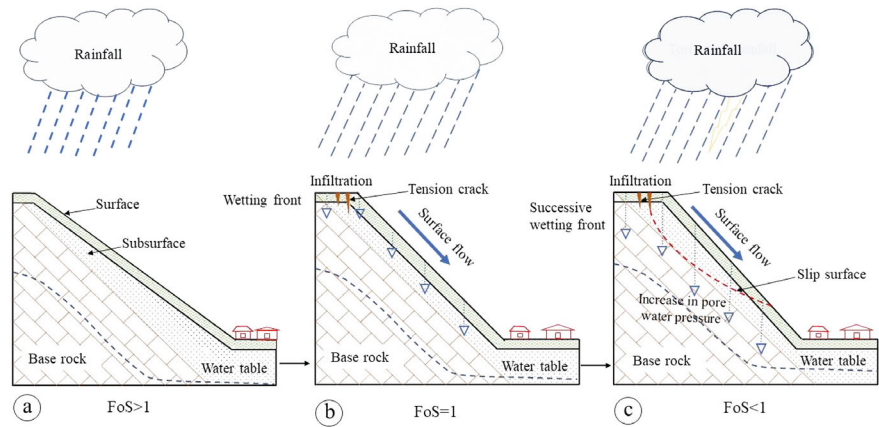


**Fig. 11** Mechanism of rainfall-induced landslides. **a** The factor of safety ( $FoS$ )  $> 1$ , shows stable slope condition, **b**  $FoS = 1$ , shows slope is at point of failure, **c**  $FoS < 1$ , shows unstable slope condition

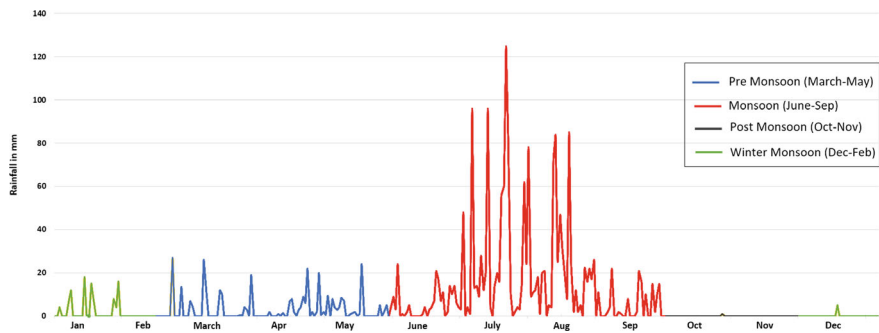


**Fig. 12** Daily/monthly rainfall distribution pattern in 2020

developed, and the slope may become susceptible to failure. The steep mountain slope is vulnerable and the probability of landslides is higher during rainfall. This type of situation occurred at Tanga village on 19 July 2020.

A daily rainfall map has been prepared for analysing rainfall effects on landslides (Fig. 12). It has been seen that during monsoon, most of the landslides either activate or increase their dimension. At the villages (Bindi, Gaila, Bata, Dhimi, and Mori) there was no landslide in pre-monsoon images, but landslides are present in post-monsoon images (Figs. 5b, 6c, 7b, 9b, and 10b). At villages (Tanga and Lodi), landslides have already existed in pre-monsoon, but their dimension was increased in post-monsoon images (Figs. 4d and 8b).



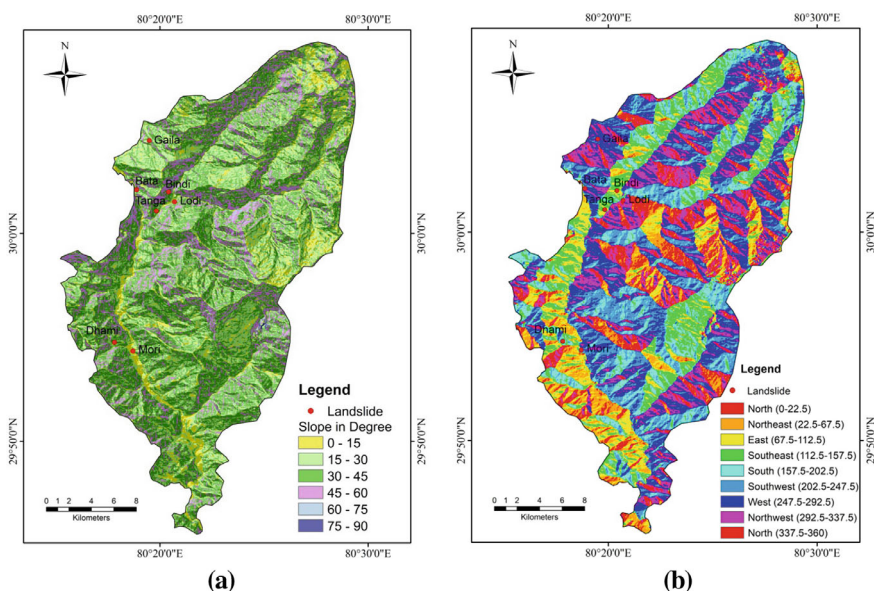


**Fig. 13** **a** Slope map of the Bangapani Tehsil, **b** aspect map of the Bangapani Tehsil

## 7 Triggering Factors of Landslide

Detailed investigation of landslides has been done during the fieldwork as well as lab work. We found some important triggering factors that are responsible for landslides. Both natural and human causative parameters of landslides are classified. Rainfall is the prime important causative factor of the landslide, which has been already discussed, but some other triggering factors describe below:

### 7.1 Surface Geology

Surface geology is an important controlling factor in the activation of landslides. The rock types and their attitude, strength, structures, porosity, and permeability are also responsible for slope stability or instability. Some rocks have numerous fractures, cleavages, and joints, due to which rocks become weaker and vulnerable to slope failure. The land use, type of soil, and thickness above the base rock is related to landslide activation. People have limited choices in constructing houses in suitable places in the study area. It has been observed that most of the houses as well as some villages rest over the old landslide materials, e.g., Tanga, Lumiti, Dhami and Mori villages (Figs. 4a, 8a, 9c and 10a).

## **7.2 Weathering**

Rainwater is one of the most important agents for weathering rocks. With the presence of water, rock undergoes physical (by contraction and expansion) and chemical weathering or both. Dolomitic limestone and low-grade metamorphic rocks are dominant in landslide areas. In low-grade metamorphic rocks, the clay group of minerals such as mica, chlorite, sericite etc. is the primary product of weathering (Singh et al. 2021a, b). The dolomitic limestone is also weathered by rainwater. Acidic rains produce an acidic solution that dissolves the carbonate rocks. In the present area at Gaila village, quartzite rock is in highly weathered conditions due to the presence of clay minerals. This rock erodes easily during rains. In the downslope part of Dhami Village, dolomitic limestone and calcareous quartzite are also in highly weathered conditions (Fig. 9c). In the area, the physical/mechanical weathering process is continuously due to diurnal temperature variation in different seasons. Due to this, at places the effects of frost wedging, where water seeps inside the rocks and freezes. As the water freezes, it expands, cracking the rock from the inside. This is one of the reasons for initiating landslides.

## **7.3 Erosion**

Rainfall also leads the soil erosion, and the erosion of the hill slope may lead to slope instability. Splash, rill, and gully types of erosion take place during the period of heavy rainfall. After continuous erosion of vegetated slope, rills and gullies are developed, and thus slopes assume to be unstable (Fig. 4a). Due to soil erosion, overburden containing many boulders becomes unstable and falls downslope (Fig. 10a). However, scrub, grass, and vegetation cover on land surface control the erosion activity. Toe erosion is another contributing factor for land-sliding, which acts more during the rainfall period at Tanga and Lodi. During the rainfall period, water from all streams enters the river causing more erosion along the river banks (Figs. 4a and 8a).

## **7.4 Slope and Aspect**

Slope and aspect are other important contributing factors to landslides. The slope and aspect map of the study area has been prepared by Aster DEM and using with RS and GIS techniques (Fig. 13a, b). In the Himalayan terrain, most of the slopes are moderate to steep. Due to endogenic and exogenic activities, the steep slopes are more vulnerable to landslides. The slope map of the study area represents a moderate to steep slope. Aspect refers to the direction of mountain slopes. The slope aspect is directly related to the biochemical or weathering process. In general, northern

slopes in the Himalaya have more moisture content and dense forest cover than the southern slopes, which have less moisture content and deficiency of large trees. Thus, the mountain aspect is also controlling slope failure. In the landslides at Tanga, Bindi, Gaila, Bata, Lodi, Dharni, and Mori, aspect refers to E, E, W, W, NW, S, and SW, respectively (Fig. 13a, b).

## 7.5 Human Factors

The present study of landslides belongs to the Lesser Himalayan zone which is a neotectonically active terrain. Thousands of people live on the fragile slope of the Himalaya, whereas many villages rest over the old landslides zone. The rapid developmental activities and growth of populations, people have a limited choice to construct a house in a safe place in the Himalayan terrain. Many villages are affected by small to large-scale landslide incidences, particularly in the rainy season. Rising population and civilization, humans are tempering with nature and inviting landslides day by day. Increasing development activities such as road construction and road widening at Tanga and Gaila villages make them vulnerable to slope failure. Nowadays every villager demands the construction of the road due to which mountain slope cuts at many places. The dynamic changes in the slope geometry of mountains are more susceptible to landslides. Joints and cracks in the rock become wider due to these construction activities; thus, water seepage through it. Due to the availability of rain, pore water pressure increases which are also responsible for slope instability in the study area. Thus, most landslides occurred along or near the road section of the area. In the present study area at Tanga, Gaila, Lodi, and Bata locations, rainfall, and human activities were responsible for the landslide disaster.

## 8 Results and Discussion

The present investigation of landslides has been carried out at seven villages in the Bangapani tehsil. We have analysed the various natural and human factors such as slope, aspect, surface geology, weathering, erosion, anthropogenic activities, and rainfall pattern of the area. Most of the landslides are triggered by prolonged rainfall at Tanga, Bindi, Gaila, Bata, Lodi, Dharni, and Mori. Landslides present in all seven villages have occurred during the monsoon period of 2020. We elucidate monthly rainfall patterns of the area, which is broadly classified as pre-monsoon, during-monsoon, post-monsoon, and winter (Fig. 12). In the year 2020, the highest 889 mm rainfall was recorded in July; after that, 613.5 mm rainfall occurred in August. The landslide at Tanga, Bindi, Gaila, Bata, and Lodi on 19 July 2020 (Figs. 4a, 5a, 6a, 6b, 7a and 8a) and Dharni and Mori on 27 July 2020 (Figs. 9a and 10a) have occurred during the high rainfall period. The area received 125 mm rainfall on 19 July and 62 mm rainfall on 27 July 2020 (Fig. 12). The monsoon reaches in the

area between June to September, but it at peak during July and August months. In 2020, total 81% of rainfall occurred between June to September, while 66% of rainfall occurred in July and August. For detailed analysis we have used Sentinel-2B satellite imageries and prepared pre-monsoon and post-monsoon maps of all seven landslides dated 21.05.2020 and 13.10.2020, respectively. It can be clearly seen in pre-, and post-monsoon satellite imaginary that in villages (Bindi, Gaila, Bata, Dhami, and Mori) initially, there were no landslides, but landslides are present in post-monsoon imaginary. In contrast, in some villages (Tanga and Lodi) initially, landslides were already present, which were increased in their dimension due to heavy rainfall. Hence at all these locations, landslides were developed during the monsoon.

The high rainfall of the area is a good indicator for predicting the landslides in the study area, and most of the old landslides also occurred during the highest rainfall. During successive rains, soil infiltration results in a reduction in the shear strength of the materials. The gradually decreasing the factor of safety of the slope may increase the triggering of the landslides. During fieldwork observations, we found that all landslides occurred along the drainage, river terraces, and road sections. Some villages/houses also rested over fragile geology and did not maintain a safe distance from seasonal streams/ivers, which are more prone to landslide disasters (Figs. 4a, 7a, 8a, and 10a). In this paper, the mechanism of rainfall-induced landslides has been investigated. In the above-discussed villages, 17 people and 23 cattle lost their lives, and many infrastructures, agricultural land, road, and pathways were damaged by the landslide disaster in 2020. Due to this disastrous event total 99 families were affected in Tanga, Bindi, Gaila, Lodi, Bata, Dhami, and Mori villages and live in very susceptible zones. At many places, new seasonal nala have been developed in the affected villages after the befalling of the cloudburst (Fig. 4a).

## 8.1 Kinematic Analysis

Kinematic analysis is a method that uses forecasts the probability of slope failure. The analysis is related to the orientation of discontinuity and mountain slope to determine the condition of a possible mode of plane, wedge and topple failures (Hoek and Bray 1981). This method of slope failure has been done in equal area net by using Dips software from Rocscience. The structural data of all discontinuity planes and slope geometry have been analysed in the lower hemisphere of the equal area net. This method has been applied in all places, but only appropriate results show at Tanga village. Four joint sets ( $J_0$ ,  $J_1$ ,  $J_2$ ,  $J_3$ ) were obtained in Tanga village with dips of  $30^\circ/110^\circ$ ,  $70^\circ/180^\circ$ ,  $88^\circ/70^\circ$ , and  $70^\circ/290^\circ$ , respectively. For kinematic analysis, the friction angle ( $\Phi$ ) of slate rock is taken  $27^\circ$ . The mountain slope at the location is  $40^\circ$  towards the ESE direction. The orientations of all data obtained were plotted on the stereographic projection that shows plane failure. The shaded area shows the direction of failure (Fig. 4c), which also matches the direction of planar landslide movement. The condition of plane failure is present in Tanga village. On 19 July

2020, due to the presence of excess water at Tanga village, the shear strength of the material was reduced, resulting in a heavy landslide.

## 9 Conclusion

The present investigation of landslides has been done in the Bangapani tehsil of the Pithoragarh district in Uttarakhand. The study of landslides and daily/monthly rainfall data for 2020 indicate that all seven landslides have been activated/reactivated after heavy rainfall. The landslide at Tanga, Bindi, Gaila, Bata, and Lodi villages occurred on 19 July, 2020, and at Dhami and Mori had been occurred on 27 July 2020 during the high rainfall threshold. The daily/monthly rainfall distribution chart can give the most reliable prediction for the landslide present in the Bangapani tehsil. The area received 125 mm of rainfall on 19 July, whereas 62 mm of rainfall was received on 27 July 2020. Sentinel-2B satellite imageries for pre-monsoon and post-monsoon clearly indicate that all seven landslides were activated/reactivated during monsoon. Thus, all landslides can be considered as rainfall-induced. Another important factor is that the landslides are dependent on the duration as well as the intensity of rainfall. Based on this analysis, we conclude that the rainfall intensity is primarily responsible for the slope failure in these areas. While the mechanism of rainfall-induced landslide varies from place to place. Besides the rains, natural factors such as slope, weathering and erosion, lithology, and their structural parameter or anthropogenic factors such as road construction are also responsible for triggering the landslides.

**Acknowledgements** Authors are thankful to District Disaster Management Office (DDMO) Pithoragarh for providing rainfall data of the district and officers from the Department of Geology and Mining Unit Dehradun, Uttarakhand, for support during fieldwork. Also, we thank the anonymous reviewers for their feedback during the manuscript preparation.

## References

- Brand EW, Premchitt J, Phillipson HB (1984) Relationship between rainfall and landslides in Hong Kong. In: Proceedings of the 4th international symposium on landslides, Toronto, pp 276–284
- Dikshit A, Satyam N, Pradhan B, Kushal S (2020) Estimating rainfall threshold and temporal probability for landslide occurrences in Darjeeling Himalayas. *Geosciences J* 24:225–233
- Gansser A (1964) The geology of the Himalayas. Wiley Interscience, New York, p 289
- Gupta V (2005) The relationship between tectonic stresses, joint patterns and landslides in the higher Indian Himalaya. *J Nepal Geol Soc* 31:51–58
- Highland LM, Bobrowsky P (2008) The landslide handbook—a guide to understanding landslides, vol 1325. U.S. Geological Survey Circular, Reston, Virginia, p 129
- Hoek E, Bray J W (1981) Rock slope engineering, revised 3rd edn. The Institution of Mining and Metallurgy, London, pp 341–351

- Khanduri S (2017) Disaster hit Pithoragarh District of Uttarakhand Himalaya: causes and implications. *J Geogr Nat Disasters* 7(3):1–5
- Khanduri S, Sajwan KS, Rawat A (2018) Disastrous events on Kelash-Mansarowar route, Dharchula Tehsil in Pithoragarh District, Uttarakhand in India. *J Earth Sci Clim Change* 9:463
- Kumar M, Rana S, Pant PD, Patel RC (2017) Slope stability analysis of Balia Nala landslide, Kumaun Lesser Himalaya, Nainital, Uttarakhand, India. *J Rock Mech Geotech Eng* 9(1):150–158. <https://doi.org/10.1016/j.jrmge.2016.05.009>
- Lee ML, Ng KY, Huang YF, Li WC (2014) Rainfall-induced landslides in Hulu Kelang area, Malaysia. *Nat Hazards* 70:353–375
- Mandal P, Sarkar S (2021) Estimation of rainfall threshold for the early warning of shallow landslides along National Highway-10 in Darjeeling Himalayas. *Nat Hazards* 105:2455–2480
- Negi R, Singh RA (2020) Landslide: a study from NH-7. *Anusandhan Vigyan Sodh Patrika* 8(1):29–34
- Negi R, Singh RA (2021) Landslide in Didihat tehsil of Pithoragarh district in Kumaun Himalaya. *Anusandhan Vigyan Sodh Patrika* 9(1):1–7
- Negi R, Singh RA, Singh PK, Saini P (2018) Study of landslides in Uttarakhand during rainy season of 2018. *Anusandhan Vigyan Sodh Patrika* 6(1):74–82
- Pachauri AK (2016) Disaster management of landslides in the Indian Himalaya. *J Ind Geol Cong* 8(1):27–48
- Parkash S (2013) Earthquake related landslides in the Indian Himalaya: experiences from the past and implications for the future. In: Mardottini C, Canuti P, Sassa K (eds) *Landslide science and practice*. Springer, Heidelberg. [https://doi.org/10.1007/978-3-642-31427-8\\_42](https://doi.org/10.1007/978-3-642-31427-8_42)
- Paswan AP, Shrivastava A (2022) Modelling of rainfall-induced landslide: a threshold-based approach. *Arab J Geosci* 15:795. <https://doi.org/10.1007/s12517-02210024-6>
- Pradhan SP, Siddique T (2020) Stability assessment of landslide-prone road cut rock slopes in Himalayan terrain: a finite element method based approach. *J Rock Mech Geotech Eng* 12(1):59–73. <https://doi.org/10.1016/j.jrmge.2018.12018>
- Saini P, Negi R, Singh RA, Rani R, Singh PK (2021) Landslide studies between Askot and Jauljibi along NH-9, Pithoragarh, Kumaun Himalaya. In: Singh RA, Singh PK (eds) *ASR Publications*, Lucknow, pp 124–134. ISBN: 978-93-83247-95-0
- Sajwan KS, Khanduri S, Bhaisora B (2017) Some significant aspect of cloudburst with especial reference to devastating landslides at Bastari, Naulra and Didihat region, Pithoragarh district Kumaon Himalaya, Uttarakhand. *Int J Curr Res* 9(07):54255–54262
- Sajwan KS, Khanduri S (2018) Investigation of hydro-metrological disaster affected Malpa and Mangti area, Pithoragarh district, Uttarakhand, India. *J Geogr Nat Disaster* 8(2). <https://doi.org/10.4172/2167-0587.1000228>
- Sarma A, Bora PK (1994) Influence of rainfall on landslide. In: *International conference on landslides, slope stability and the safety of infra-structures*, CAMS, Malaysia, pp 311–316
- Siddique T, Pradhan SP (2019) Road widening along National Highway-58, Uttarakhand, India. *Curr Sci* 117(8):1267–1269. <https://doi.org/10.4172/2381-8719>
- Singh RA, Negi R, Singh PK, Singh TN (2021a) Landslide studies between Devprayag and Pali along National Highway-7, Tehri District, Garhwal Lesser Himalaya. *J Sci Res* 65(1):32–38
- Singh RA, Negi R, Singh PK, Singh TN (2021b) Landslide studies between Pali to Bagwan along National highway-7, Tehri District, Garhwal Lesser Himalaya. In: Singh RA, Singh PK (eds) *ASR Publications* Lucknow, pp 80–92. ISBN: 978-93-83247-95-0
- Singh RA (2013) La-Jhekla landslides, Pithoragarh district, Uttarakhand, India. In: Singh RA (ed) *Landslides and environmental degradation*. Gyanodaya Prakashan, Nainital, pp 141–149, ISBN: 81-85097-90-9
- Valdiya KS (1980) *Geology of Kumaun Lesser Himalaya*. Wadia Institute of Himalayan Geology, Dehradun, p 291
- Varnes DJ (1978) Slope movement type and processes, landslides analysis and control; special report 176. Transportation Research Board, Washington, DC, pp 11–80

Yin A (2006) Cenozoic tectonic evolution of the Himalayan orogen as constrained by along-strike variation of structural geometry, exhumation history, and foreland sedimentation. *Earth-Sci Rev* 79:1–131

**Rahul Negi** obtained his M.Sc. (Geology) from Govt. P.G. College Gopeshwar, which is affiliated to HNB Garhwal University, Uttarakhand in 2015. He worked as a Project fellow in DST sponsored project entitled 'Large Scale Geological and Structural Mapping between Devprayag to Srinagar (35 km) along Rishikesh-Kedarnath Highway'. He has PGDDM (Post Graduated Disaster Management Diploma) from Uttarakhand Open University in 2017. He has also worked as a project Geologist with the DGM Uttarakhand to find out landslide affected areas/villages, their mitigation and rehabilitation. He has been pursuing Ph.D. from Kumaun University, Nainital since 2018 entitled 'Structure and tectonics between Saknidhar and Srinagar area, Garhwal Lesser Himalaya, India'. He has published 8 national and international research papers. Currently serving as a District Mines Officer in the Geological and Mines Department of Uttarakhand'.

**Pooja Saini** completed her M.Sc. (Geology) from Kurukshetra University, Haryana. She has been pursuing PhD from Kumaun University, Nainital since 2017 entitled 'Structure and Strain analysis across Askot klippe, Kumaun Lesser Himalaya'. She has published 3 national/international research papers.

# A Comparative Analysis of Landslide Characteristics of the Himalayan and Western Ghat Mountain Belts



N. K. Rai, P. K. Singh, Ravi Shankar, and Digvijay Singh

**Abstract** The landslides in the Himalayas and the Western Ghats are prime examples of devastating hazards in India and potentially across the globe. Studies conducted globally report that India, along with its neighboring countries, experiences the highest number of landslides and fatalities due to these events. The geographical position of the Himalayan belt places it in a collision zone where stresses and resulting deformation are very high. External triggering forces such as earthquakes, rainfall, storms, and avalanches make the area prone to landslide activities. In the present study, a comparison has been made between the spatial distribution, size, and characteristics of landslides in the Kangra district of Himachal Pradesh and the Idukki district of Kerala in India. Both regions are hill stations that attract many tourists every year. They are distinct in terms of geology, geomorphology, and tectonic activities, making them suitable counterparts for analyzing landslide activities. Idukki is predominantly a gneissic terrain with intense chemical weathering and high monsoonal rains, while Kangra's geology mostly belongs to the Lower Sivaliks, consisting of sandstone, shales, conglomerates, etc., and is sandwiched between two major thrust zones. Landslide activities in both areas are a major concern, mostly arising due to rapid urbanization, unplanned excavation, and intense rainfall, a major triggering factor of landslides. The study shows that lower elevation and steeper slopes are more critical factors in Idukki, while gentle slopes are more critical in Kangra. The size of the landslide is important as large volumes of dislodged material can lead to large-scale devastation. The slope angle, elevation, and slopes far from road networks largely control the size of landslides in these areas.

**Keywords** Landslides · Himalayas · Western Ghats

---

N. K. Rai · P. K. Singh (✉) · D. Singh

Department of Earth and Planetary Sciences, University of Allahabad, Prayagraj, Uttar Pradesh, India

e-mail: [pk Singh@allduniv.ac.in](mailto:pk Singh@allduniv.ac.in)

R. Shankar

Department of Science and Humanities, Bakhtiyarpur College of Engineering, Patna, Bihar, India



## 1 Introduction

The mountainous regions, such as the Himalayas, are considered as the zones of high energy environments often characterized by instability and variability (Gerrard 1994). Mass movements have been argued to be one of the significant processes in the denudation of mountainous terrain (Dortch et al. 2009). The magnitude of mass movement in the Himalaya varies, ranging from the vast extension of entire mountain ranges due to gravity tectonics, to the tiniest slope failures, to the sackung failure of individual peaks (Shroder and Bishop 1998). Mass movements in various forms such as falls, slides, flows, avalanches, creep etc. is the major cause of instability and designated as a major hazard in these areas (Rautela and Lakhera 2000; Singh et al. 2016a; Kainthola et al. 2021). The Western Ghats mountain ranges are considered as the second most landslide prone area after the Himalayas (Kuriakose et al. 2009; Martha et al. 2021). Both the Himalayan and the Western Ghat mountain range present distinct topography carved by long term denudational processes and are the zones of extreme mass movement activities. The Himalayas present a topography deeply cut by erosion, valley and glaciers of enormous size, steep sided lofty peaks, very complex geological structures owing to its genesis and are geodynamically very aggressive (Zeitler et al. 2001). The Western Ghats, a passive margin escarpment older than the Himalayas, have subdued relief with an average elevation of 1200 m. The seaward slopes are steep which rise abruptly from the coastal plains and the plateaus and peaks are highly dissected by the streams. The continual growth of hill slopes in nations with high population densities leads mountain ecosystems to experience significant land use changes (Chuang and Shiu 2018). Idukki district of Kerala and Kangra district of Himachal Pradesh (H.P.) are one of the fastest developing districts in India with high population density and are highly prone to landslide hazards. Several instances of landslide hazards have been noted along the anthropogenically modified slopes of both the districts leading to loss of lives and economic damages. The Geological Survey of India postulates that economic losses in many developing nations due to landslide activities may reach up to 1–2% of gross national product.

### *1.1 Landslide Characteristics of Kangra, Himachal Pradesh*

The hilly terrain of Himachal Pradesh is geologically young, tectonically very less stable, and steep in nature. Therefore, landslides are more frequent and hence cause massive disruption of life and properties in this terrain (Sana et al. 2024). The heavy rainfall in the monsoon season coupled with inappropriate anthropogenic interventions in the form of deforestation, unscientific road cutting, terracing, and changes in land use/land cover have significantly aggravated the problem of landslides in this area (Singh et al. 2016a; Kainthola et al. 2021; Sharma et al. 2024). Dharamshala and its suburbs in the Kangra valley is prone to high landslide hazard due to unplanned

development and urbanization, modifications of land use land cover (LULC) patterns (increase in agriculture land and settlements) and the major triggering force has been heavy to very heavy rainfall (Sharma et al. 2015; Sharma and Mahajan 2019). Singh et al. (2020) used satellite images to analyse a very famous Kotrupi landslide (Mandi district) which has been reactivated several times in the past with the most devastating slide in 2017 killing over 50 people. The study also highlighted the role of multiple factors such as earthquake, rainfall, tension cracks and sheared rock mass for the reactivation of landslide. So, apart from rainfall, earthquake also serve as triggering factor to the landslides in Himachal Pradesh. Gupta et al. (2022) highlights a case of severe landslide in the Bhagsu nala in McLeod Ganj area of Dharamshala due to extreme rainfall event leading to flash floods. The catchment of Bhagsu nala is small but has higher drainage density and circular shape making it susceptible to peak flow in short duration. The Soldha landslide, lying between Lower and Middle Siwalik sandstone with clay intercalations, of 2013 in Kangra district was triggered by heavy rainfall but the gradual slope failure is also accompanied by disturbances caused due to continuous seismic activities in the region (Mahajan et al. 2022). A local thrust, Jwalamukhi thrust, passing along the toe of this landslide is thought to be responsible for tectonic damage of the lithological layers of the Upper and Middle Siwalik promoting high rate of weathering and reduction in rock mass strength. Khanduri and Verma (2018) reported that the presence of tectonically active main boundary fault (MBF), Main Central Thrust (MCT), Krol, the Giri, Jutogh, and Nahan thrusts, and several other small faults make the area highly susceptible to earthquakes and earthquake-induced landslides. The ever-increasing road network in hilly terrains play significant role in the socio-economic development of an area however, slopes upon exposure become a source of different forms of landslide activity. Rockfall and rockslides have also become very common along the cut slopes as the highly jointed rock mass is exposed and are capable of detaching from the slope face (Singh et al. 2016b). Moreover, the weathering state, type of rock, strength, predefined plane of weakness, jointing pattern, barren land over rock units also control the type and nature of landslides (Rautela and Lakhera 2000; Mahanta et al. 2016). Several authors have performed landslide hazard zonation by selecting several predisposing factors for attaining economic benefits and desired safety measures (Singh and Kumar 2018; Banshtu et al. 2020; Sweta et al. 2022).

## ***1.2 Landslide Characteristics of Western Ghat, Kerala***

The geologically stable Western Ghat is very prone to landslide hazards and in fact is second most landslide prone zone in India after the Himalayas. The western ghats, the major orographic feature, passes through Kerala occupying around 47% of the total landmass. Kerala has 14 districts of which 13 are known for landslide hazards. Thampi et al. (1995) emphasizes that only about 8% of the total area of the Western Ghats is critical zone for landslide hazards. The state experiences nearly all major types of landslides, the most notable reported in the literature are rockfalls, rock slips,

slumps, creeps, debris flows and in a few cases, rotational types of slides (Kuriakose et al. 2009). Some of the major factors for landslide hazards in Kerala are reportedly precipitation, high weathering rate, landuse and landcover changes, anthropogenic factors, geology and geomorphology. The Himalayan landslides are found in all size ranging from very small to catastrophic, displacing very large volume of material. Sliding of mass in most cases may involve overburden along with underlying rock. The Western Ghat landslides tend to be comparatively small and generally involves movement of the top overburden (Thampi et al. 1998). Majority of landslides have been recorded during monsoon in the western slopes of the Western Ghat while the eastern slopes witness occasional landslides due to cyclonic events. Overall, the failure is associated with heavy rainfall leading to oversaturation of the top material (Sajinkumar et al. 2011; Martha et al. 2015). Kuriakose et al. (2008) working on shallow landslides of Kottayam and Idukki districts analysed that debris flow is the most common type of landslide which originate in highly saturated concave depressions with dimensions limited to  $10 \times 10$  m and a soil thickness of about 1–1.5 m. It was also noticed that reactivation of landslides was rare compared to event based landslides. Ramasamy et al. (2021) working on the role of geomorphology to landslide proneness highlighted that fractures associated with repeated deformation and increase in pore water pressure by entry of rainwater through the fractures are the major cause of landslide in the Western Ghat. Heavy precipitation, temperature, plateau like topography, presence of structural discontinuities makes the Western Ghat highly susceptible to intense chemical weathering of bedrocks. Sajinkumar et al. (2011) working on influence of weathering on landslides analysed hornblende gneiss, granite gneiss and their altered derivative products. Different variety of soil such as laterites, loam, alluvium etc. cover the top of Precambrian basement rocks in the Western Ghats. It was noted that gibbsite is dominant product in soil derived from both rock types owing to high alumina content. The degree to which chemical weathering affects the rock mass depends on the mineralogy, fractures, precipitation, climate, topography etc. Unconsolidated overburden with variable geotechnical properties and thickness can be found all along the Western Ghat topography. Land use and land cover change due to afforestation, road widening, agriculture practices etc. accelerates the process of chemical weathering promoting landslides in Kerala. Jha et al. (2000) estimated significant land use changes in the southern parts of Western Ghat during 1973–1995 through satellite image. Land use change has been most rapid in Kerala probably due to high population density. The decrease in forest cover has been attributed to increase in plantation and agriculture. Kumar (2005) connects changing land use land cover pattern to frequent flash floods, soil erosion, silting of reservoirs and landslide. Landslides associated with the semi circular escarpments are also common due to heavy headward erosion by the tributaries of the river flowing into Arabian sea. The results of landslide hazard zonation employing geospatial techniques in Idukki district highlights that around  $49.5 \text{ km}^2$  of the total study area ( $438 \text{ km}^2$ ) lie in fragile to highly fragile category of landslides (Biju Abraham and Shaji 2013). Kanungo et al. (2020) noted the lack of scientific intervention for sustainable development as the major cause of landslide activity causing loss of life and property. Problems such as lack of protection of hill slopes, interference with

natural drainage, heavy loading of slope are some of the major causes of unscientific engineering practices. Achu et al. (2021) presented preliminary analysis of Pettimudi landslide. Earthquakes have been known to cause significant landslide hazard around the world. In India, most earthquake triggered landslide studies have been restricted to the Himalayas. Kerala lies in seismic zone III indicating a moderate risk zone. Ramasamy et al. (2019) conducted studies on reservoir induced seismicity in Kerala and highlighted that the region is tectonically active. Several studies point to the fact that NS to NNW-SSE faults are prone to seismicity in Kerala (Ganesha Raj et al. 2001; Ramasamy et al. 2019). The entire Kerala state has a characteristic thin veneer of soil cover over the Precambrian crystalline rocks.

## 2 Geology of Idukki and Kangra

Idukki is located in the southern-central region of Kerala. It has the second-largest geographical region among all the districts in Kerala. This region is extremely vulnerable to avalanches, consequently being the most prone area in the Western Ghats. More than half of its entire surface is encompassed by forest (Kanungo et al. 2020). Geologically, the district can be separated into three sections from north to south: (1) Peninsular gneissic complex in the north, (2) Charnokite group of rocks in the south, and (3) Migmatitic complex in between. The oldest rocks belong to the Peninsular Gneissic Complex, represented by granitic gneiss. These rocks are foliated and show folding on a regional scale. The Khondalite group is characterised by calc-granulite and quartzite. These rocks occur in linear bands or as enclaves mostly within gneissic terrain. The Charnokite group consists of orthopyroxene granite and magnetite quartzite among which Charnokite is widespread with intermediate to acidic in composition. Central, south-east, and north-east parts of Idukki are dominated by a migmatitic complex of rocks (Sulal and Archana 2019).

The Kangra basin lies in the Siwalik Lesser Himalayan tectonic zone between  $31^{\circ} 40' - 32^{\circ} 25'$  North latitude and  $70^{\circ} 35' - 77^{\circ} 5'$  East longitude having an elevation range varying from 500 to 5500 m from mean sea level. The region is characterized by a well-defined series of almost parallel hill ranges that rise in height towards the northeast. Hence, the Kangra Basin is an example of an intermontane basin situated in the northernmost part of the Siwalik foreland basin (Thakur et al. 2020). Along with the Main Central Thrust (MCT), the closely spaced Main Boundary Thrust (MBT) constitutes another significant geomorphic element of the basin. The Main Boundary Thrust (MBT) separates the Tertiary Formations to the south and Pre-Tertiary Formations to the north. In further north, the well-known Dhauladhar Range of the Lesser Himalaya skirts the basin (Gupta and Thakur 1974). The Dhauladhar Range has a general trend of NW–SE and is situated between the Beas and Ravi Rivers. The rocks of this region have characteristic steeper scraps separated by a regional thrust towards the north and are predominantly comprised of middle and upper Sivaliks litho-units. In the south, the overall geomorphology is mainly comprised of steep

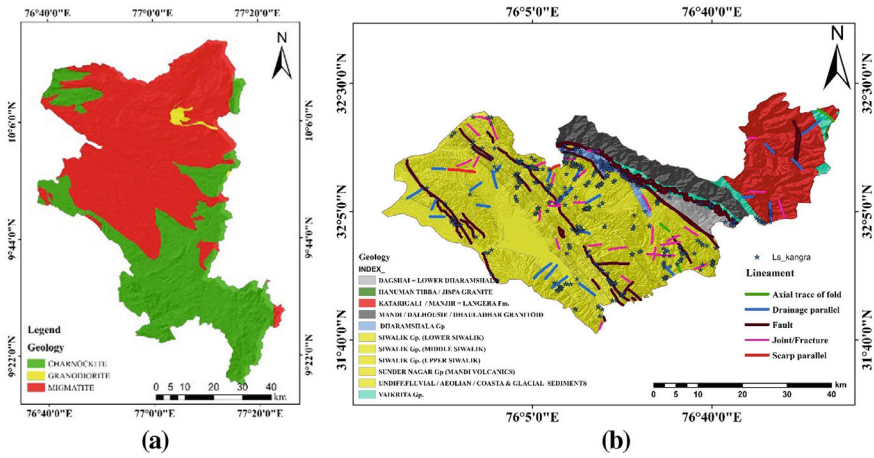


**Fig. 1** Simplified geology map showing different lithology and structures in, **a** Idukki, Kerala, **b** Kangra, H.P. India

valleys which are generally filled with alluvial sand, slate, and recent boulder material. Apart from the above-mentioned thrust planes, the area has been traversed by characteristic transverse lineaments viz. Dehar lineament and Gaj lineament. Such interesting intersecting patterns have made the region tectonically interesting (Singh et al. 2006). The simplified geological map of Idukki and Kangra showing different lithology and structures is depicted in Fig. 1.

### 3 Methodology

This research extensively examines the occurrence and distribution of catastrophic landslides from a geospatial perspective and further seeks to understand the role of various predisposing factors that typically influence their spatial distribution. We have recognized significant patterns and trends associated with landslide incidents through extensive assessment of the landslide inventory utilizing advanced spatial analytical methods. In the present investigation, we have utilized the SRTM–DEM having a resolution of 30 m which was further processed in a GIS environment. The DEM is pre-processed and rectified using GIS and different thematic maps like drainage buffer, slope angle, rainfall, and distance to road, etc. have been created using the GIS tool (Fig. 2). In addition, the thematic maps of geology and the lineament have been prepared by acquiring the respective shapefiles from “BHUKOSH”, the Geological Survey of India website. The rainfall maps for both the study areas are prepared for the years 2011–2020 using data from the Climate Hazards Group InfraRed Precipitation with Station data (CHIRPS).

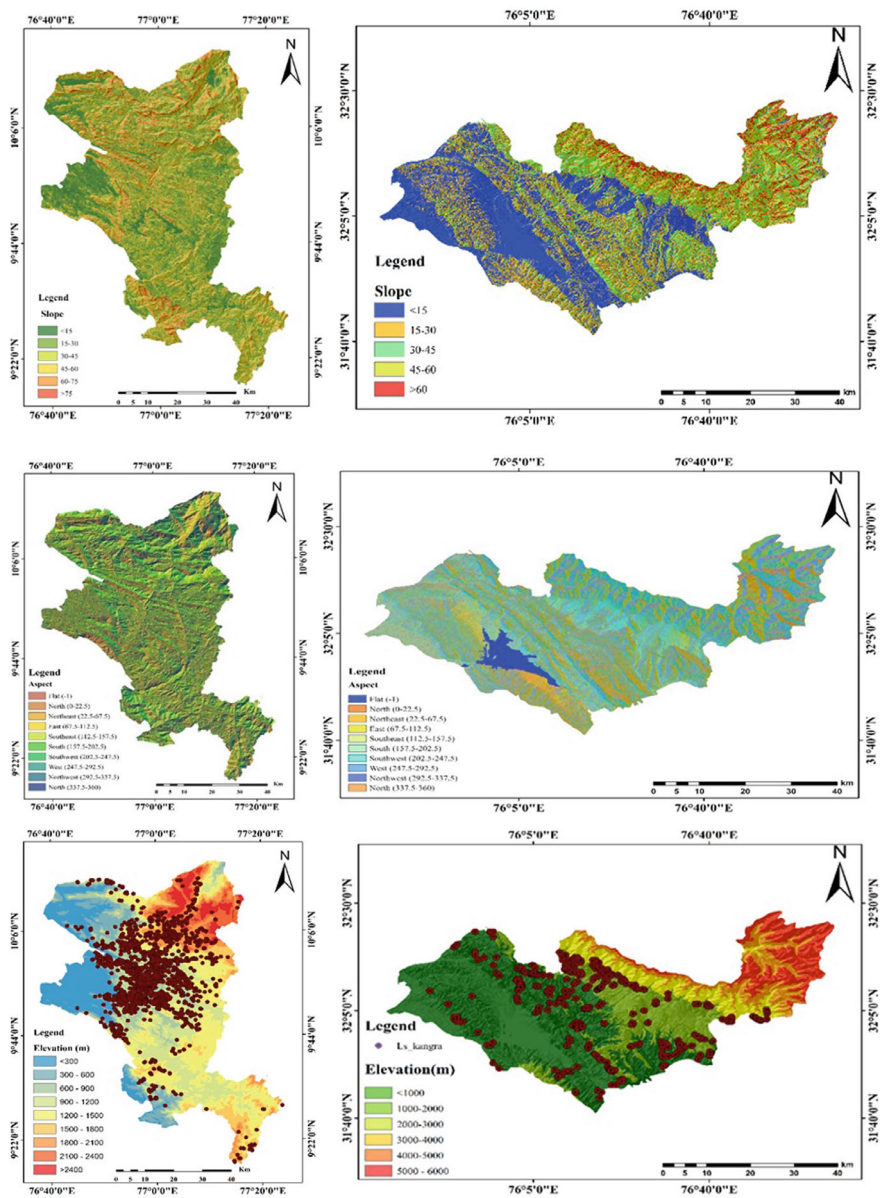


**Fig. 2** Various thematic maps derived from SRTM-DEM for the studied locations i.e., Idukki on the left side and Kangra on the right side



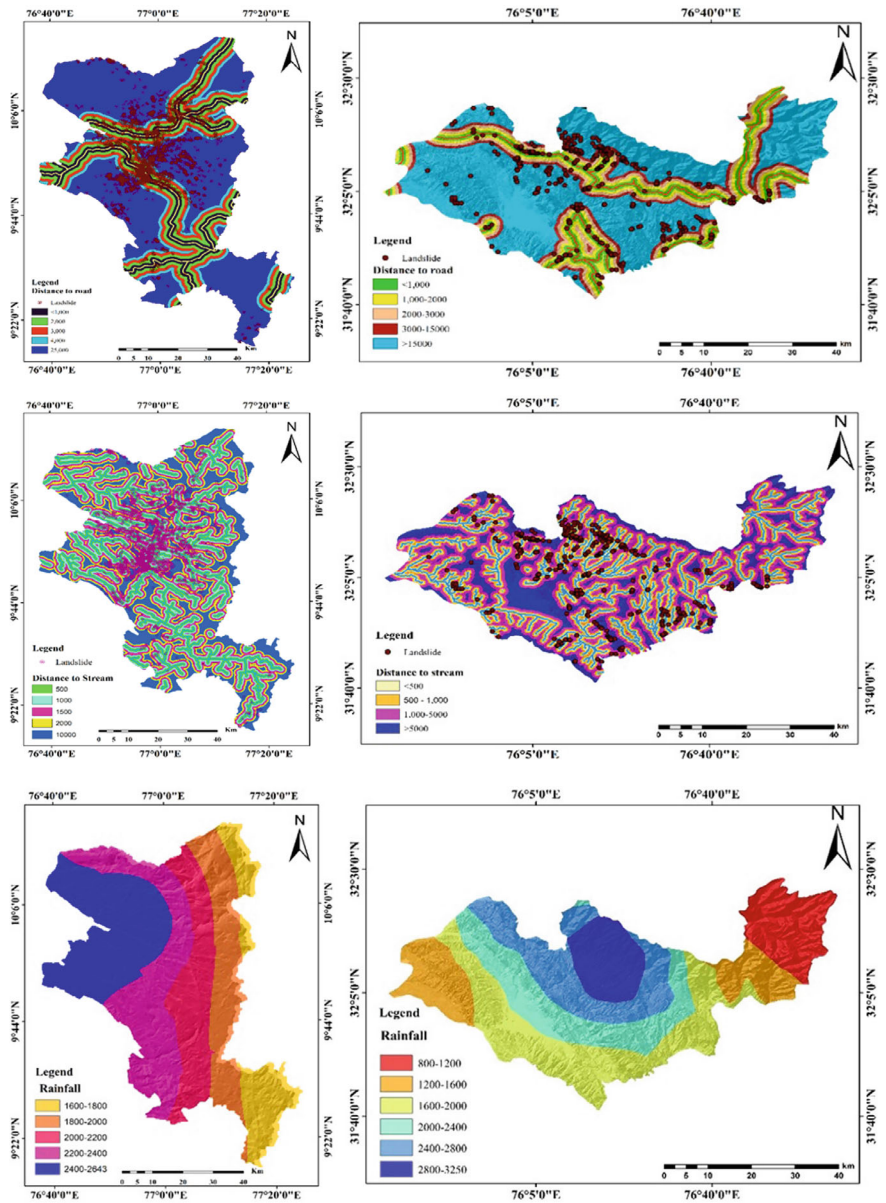


Fig. 2 (continued)

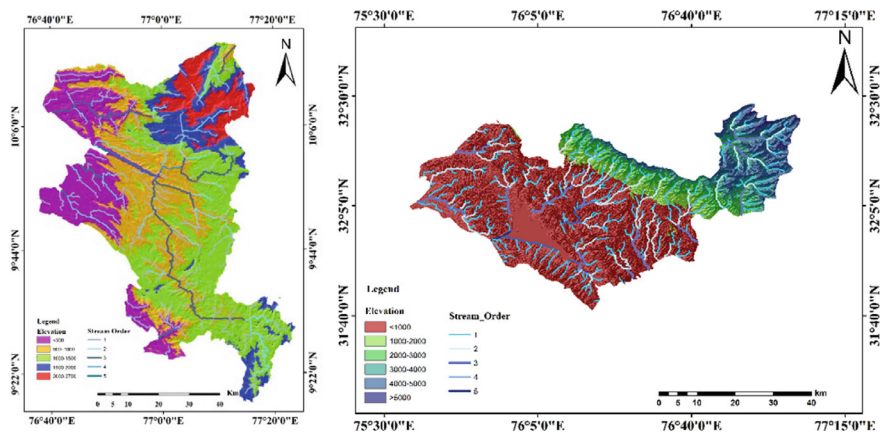


Fig. 2 (continued)

In this study, two completely different geomorphic terrains, both prone to landslides of different size and frequency, have been analyzed. The first location is Kangra, one of the most significant districts of the Himachal Himalayas. The other area is the Idukki district in Kerala, which is an important terrain of the Western Ghats in the southern region of India. We have downloaded landslide inventory data containing various significant parameters such as location, cause of landslide, length, width, height, area, land use land cover etc. from BHUKOSH and Hao et al. (2020). The landslide inventory of Idukki is an event triggered landslide of the 2018 rainfall event while the historical inventory of Kangra is used in absence of availability of an event triggered inventory. The statistical analysis of each inventory is presented in Table 1. The landslides in both the areas are mostly triggered by rainfall thereby helping us in presenting a case study to analyze the critical factors responsible for varying frequency, size and spatial distribution of landslides.

Furthermore, the analysis of landslide area and size is conducted using frequency-area distribution curves and box plots. For the box plots, landslide area data exported from a specific thematic map in a GIS environment is used to analyze the control of landslide size. Frequency-area distribution (FAD) plots are employed to compare the two rainfall-triggered landslide inventories. Previously, many authors have analysed the FAD of landslides following inverse power law where statistics of landslides can

**Table 1** Statistics parameters of the analysed landslide inventory of Kangra and Idukki

Elements	Kangra	Idukki
Number of landslides	521	1987
Maximum area of landslide	100,000 m <sup>2</sup>	80,300 m <sup>2</sup>
Minimum area of landslide	4 m <sup>2</sup>	16 m <sup>2</sup>
Total area of the landslides	658,110	4,631,446.792
Average area of landslides	1263.17	2330.87



be assessed using both cumulative and non-cumulative distribution (Malamud et al. 2004; Tanyaş et al. 2019). In a non-cumulative frequency size distribution, a rollover point and a cut-off is generally observed making it a more popular statistical model (Malamud et al. 2004; Guzzetti et al. 2008; Tanyaş et al. 2019). Malamud et al. (2004) proposed a three-parameter inverse gamma distribution which can fit entire landslide inventory. The distribution has an exponential rollover for small landslides while decays as inverse power law for medium and large-scale landslides (Eq. 1).

$$p(A_L; \rho, a, s) = \frac{1}{a\Gamma(\rho)} \left[ \frac{a}{A_L - s} \right]^{\rho+1} \exp \left[ -\frac{a}{A_L - s} \right] \quad (1)$$

In the above equation,  $\rho$  is the parameter controlling power-law decay for medium and large landslides,  $\Gamma(\rho)$  is the gamma function of  $\rho$ ,  $A_L$  is landslide area ( $\text{m}^2$ ),  $a$  is essentially a rollover point ( $\text{m}^2$ ),  $s$  is the exponential decay for small landslide areas ( $\text{m}^2$ ), and  $-(\rho + 1)$  is the power-law exponent.

## 4 Results and Discussion

Kangra is situated in a seismically active zone, influenced by the tectonic activity of the Indian Plate colliding with the Eurasian Plate (Thakur et al. 2000). This tectonic activity has resulted in the uplift of the Himalayan range and frequent earthquakes. The region features a variety of rock types, including sedimentary, metamorphic, and igneous rocks. The Lower Sivalik Hills, part of the Kangra district, are predominantly composed of sedimentary rocks such as sandstones, shales, and conglomerates, deposited during the Tertiary period. The geology Kangra is also marked by significant geological structures like thrusts and folds. The geological framework becomes further complex by the presence of major faults like Main Boundary Thrust (MBT) and the Main Central Thrust (MCT). Idukki is part of the Western Ghats, one of the oldest mountain ranges in India. The predominant rock types in the region are granite gneiss, hornblende biotite gneiss, and charnockite gneiss which are high grade metamorphic rocks. The climatic condition of Idukki is responsible for high rates of weathering and the weathering products are present in entire Kerala in the form of overlying unconsolidated material on top of parent rocks. Idukki falls in seismic zone III and has witnessed small to moderate size earthquake. Moyar and Bhavani (MSZ/BSZ) shear zones, as well as Noyil-Kaveri (NK) and Karur-Kambam-Painavu-Trichur (KKPT) shear zones, dominate the region's northern boundary. On the other side, the Madurai Block (MB) and Kerala Khondalite Block (KKB) mostly encompass the southern portion (Saikia et al. 2024).

## 4.1 Analysis of Frequency of Landslides

Amid various geoenvironmental factors, the slope plays a crucial role in destabilizing a terrain, making it susceptible to erosion and, consequently, vulnerable to multiple natural hazards (Mahajan and Virdi 2000; Nakileza and Nedala 2020). The slope/slope angle is a very important topographic attribute for landslide susceptibility studies as well as hazard assessments (van Westen et al. 2008). The steepness of the slope angle is very much responsible for the increase in the downslope component of gravity which in turn increases the shear stress in the slope, intensifying the probability of landslide occurrence (Dai and Lee 2002; Donati and Turrini 2002; Lee and Choi 2004; He and Beighley 2008). However, slopes having lower slope angles generally have a lower probability of slope failure (Lee and Talib 2005; Lee and Sambath 2006). Çellek (2022) suggested that slope significantly influences the formation, development, and landslide susceptibility. While studying landslides in the Himalayas, Kahlon et al. (2014) suggested that higher slopes under the influence of triggering factors such as monsoonal rain, earthquake, etc., provide the prospect for slope failure. In addition, slope angle also influences surface runoff, which is considered an important erosional agent in mountainous terrain (Korup et al. 2005).

In the studied locations, the higher frequency of landslides is found associated with slope angles of  $20^{\circ}$ – $25^{\circ}$  for the Kangra region (Fig. 3). Sharma and Mahajan (2019) studied the landslide characteristics of the Dharamshala region, Kangra Valley in the northwestern Himalayas, and observed that the maximum frequency of landslides is associated with a slope angle of  $21^{\circ}$ – $30^{\circ}$ . Further, for the areas in and around Idukki, the maximum frequency of landslides is found associated with slopes  $25^{\circ}$ – $35^{\circ}$ . Jacinth Jennifer and Saravanan (2022) suggested that the critical slope angle of  $20^{\circ}$ – $35^{\circ}$  are highly accountable for triggering landslides. More landslides are observed on steeper slopes in Idukki compared to Kangra, suggesting that either not all landslides have been mapped in the latter case or there is a difference in the failure mechanisms.

The observation from the slope directions on which landslides have occurred when plotted against the frequency of landslides shows that the south, southeastern, and southwestern-facing slopes experience the maximum frequency of landslides for the Kangra Valley region. The south, southeast, and southwest are generally warmer in Indian subcontinents due to maximum exposure to the sun. Sharma et al. (2023) in their study of Landslide Susceptibility assessment along India's National Highway 58 around Uttarakhand suggested that south-facing slopes receive more sunlight and rainfall, making them warm, wet, and therefore more susceptible to landslides (Chawla et al. 2018). However, the landslide frequency is independent of slope directions in the case of the Idukki region and occurs almost in every slope direction. This may be attributed to the fact that in addition to the slope direction, the landslide probability also depends upon other parameters such as rainfall geology, etc. (Çellek 2022).

The landslide frequency when analyzed against the mean annual rainfall of the two studied basins presents contrasting observations. The rainfall intensities have

a feeble influence on the landslide frequencies in the Kangra basin since higher landslide frequency has been observed randomly i.e., in lower, medium as well as higher rainfall intensity distribution (Fig. 3). However, in the case of the Idukki region, the rainfall intensity has a substantial influence on landslide frequency i.e. higher landslide frequency has been observed towards greater rainfall intensity end. (Jacinth Jennifer and Saravanan 2022) while studying the rainfall-triggered landslide

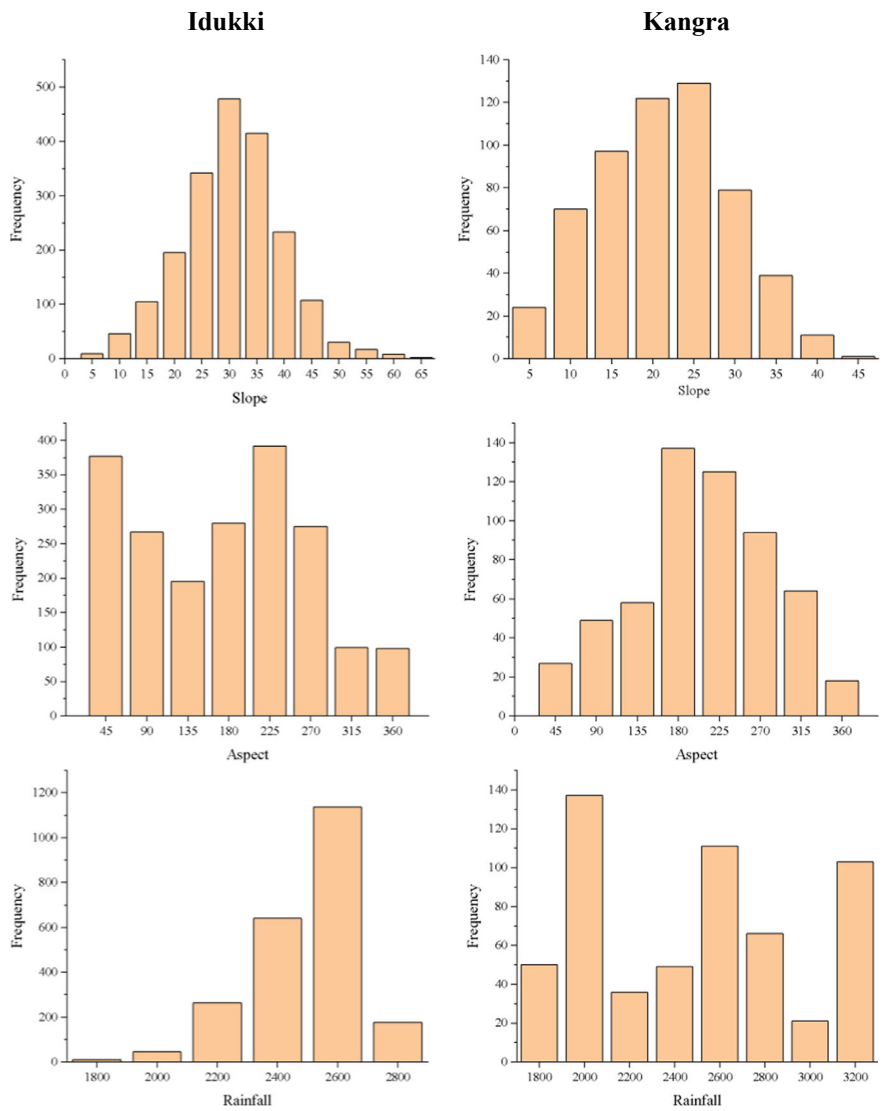


**Fig. 3** Frequency of landslides with different geomorphological parameters in Idukki and Kangra

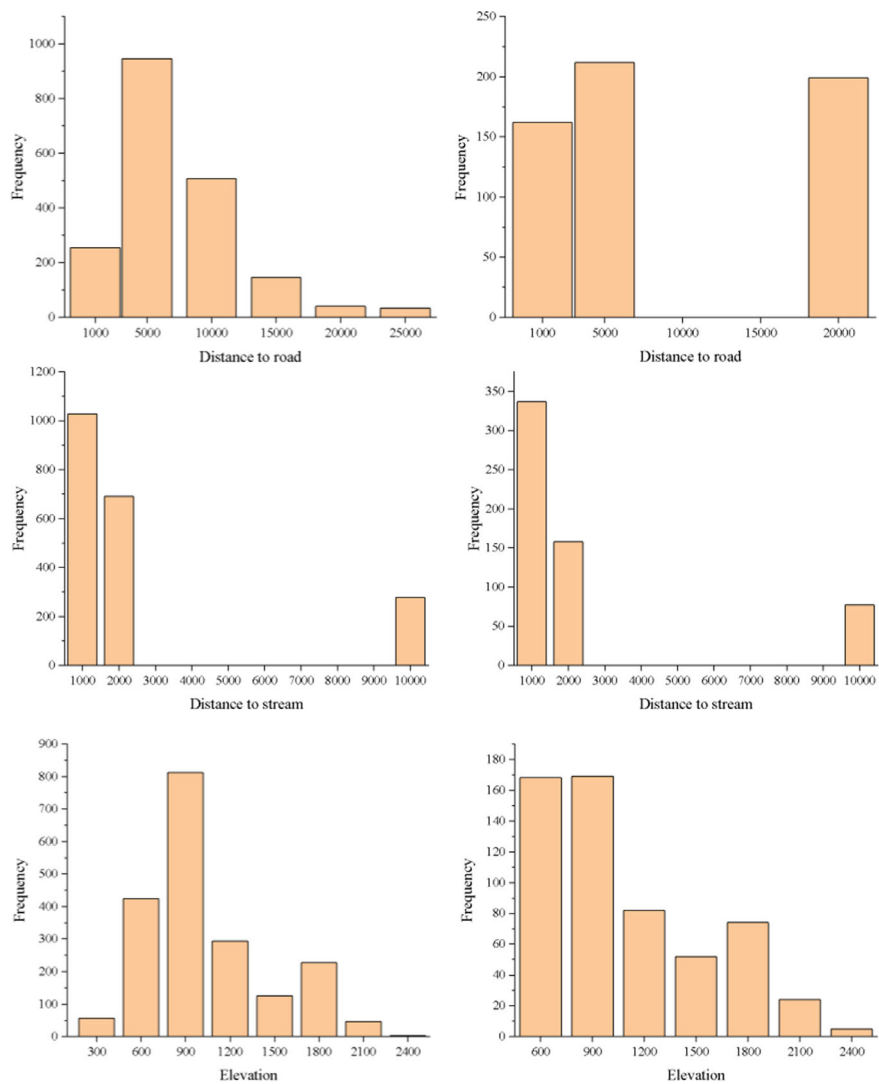


Fig. 3 (continued)

in Kerala-Karnataka in August 2018 suggested that the prolonged incessant rainfall of more than an average of 600 mm triggers landslides and debris flow in these areas.

The distance of the active landslide from the linear features such as roads, faults, and streams is an important factor in a landslide (Çellek 2023). It is generally observed that road/highway construction considerably alters the natural topography of a terrain as well as affects the stability of slope (Dragičević et al. 2015; Aghdam et al. 2016). Landslide generally occurs around the edges of slopes that are affected by roads or slopes where roads intersect (Yilmaz et al. 2012; Alemdag et al. 2015; Meinhardt

et al. 2015). Many researchers have suggested that the construction of roads in mountainous terrains increases the probability of landslide hazards (Dugonji 2014). The observations in the present study also support the earlier findings as in the case of both areas, higher frequency of landslides have been observed in close vicinity of roads/highways (Fig. 3). This observation also advocates the anthropogenic influences on landslide occurrence. Additionally, the vibration created due to traffic causes loosening and fragmentation of the newly excavated slope, which further leads to landslides.

Similarly, a strong correlation exists between landslide frequency and their distance from the stream (Huntley 2022; Mersha and Meten 2020). Different authors have suggested that the frequency of landslides will be higher in the proximity of streams and the frequency decreases linearly with an increase in distance from the stream (Dai and Lee 2002; Mossa et al. 2005; Xu and Xu 2012; Çellek 2023). Streams promote landslide hazards by eroding the slope base and saturating the underwater section of the slope-forming material (Akgün and Türk 2011; Shankar et al. 2022). A similar pattern has been observed in both study areas, where a higher frequency of landslides is located in close proximity to the stream network (Fig. 3).

A higher frequency of landslides has been observed on lower elevations in the case of both the districts i.e., Idukki and Kangra. Studies suggest that in general, higher elevation seems to be devoid of frequent landslides (Nakileza and Nedala 2020; Shankar et al. 2022; Pei et al. 2023).

## 4.2 Analysis of Control of Landslide Size

In order to accurately predict landslides, it is crucial to take into account their size, which is a powerful predictor of the runout distance for many distinct types of landslides (Medwedeff et al. 2020). The landslide size tends to increase with increase in slope angle for both areas however, the median landslide size is on the higher side for Idukki region (Fig. 4). The high-grade metamorphic rocks are able to support steeper slope in Idukki while Lower Sivalik anisotropic sedimentary rocks are unable to support steeper slopes in Kangra. The landslides on gentle slopes are particularly due to slip in overlying unconsolidated material, a situation prevalent in both the regions. Several authors have reported high rate of weathering in gneissic terrain causing the build-up of thick pile of unconsolidated material over the bedrock (Sajinkumar et al. 2011; Regmi et al. 2013, 2014). Kasai and Yamada (2019) analysed the frequency area distribution of an earthquake triggered landslides and showed that landslide size tend to increase first till a slope angle of 25° followed by a decreasing trend at steeper slopes. In a study conducted by Chen et al. (2016) on the relationship between slope angle and landslide size using limit equilibrium analysis, it was concluded that increasing the slope angle modifies the potential critical slip surface, which may influence the amount of material available for sliding.

Slope direction appears to be significant in Idukki, as landslide size decreases on north and east-facing slopes while increasing on south and west-facing slopes.

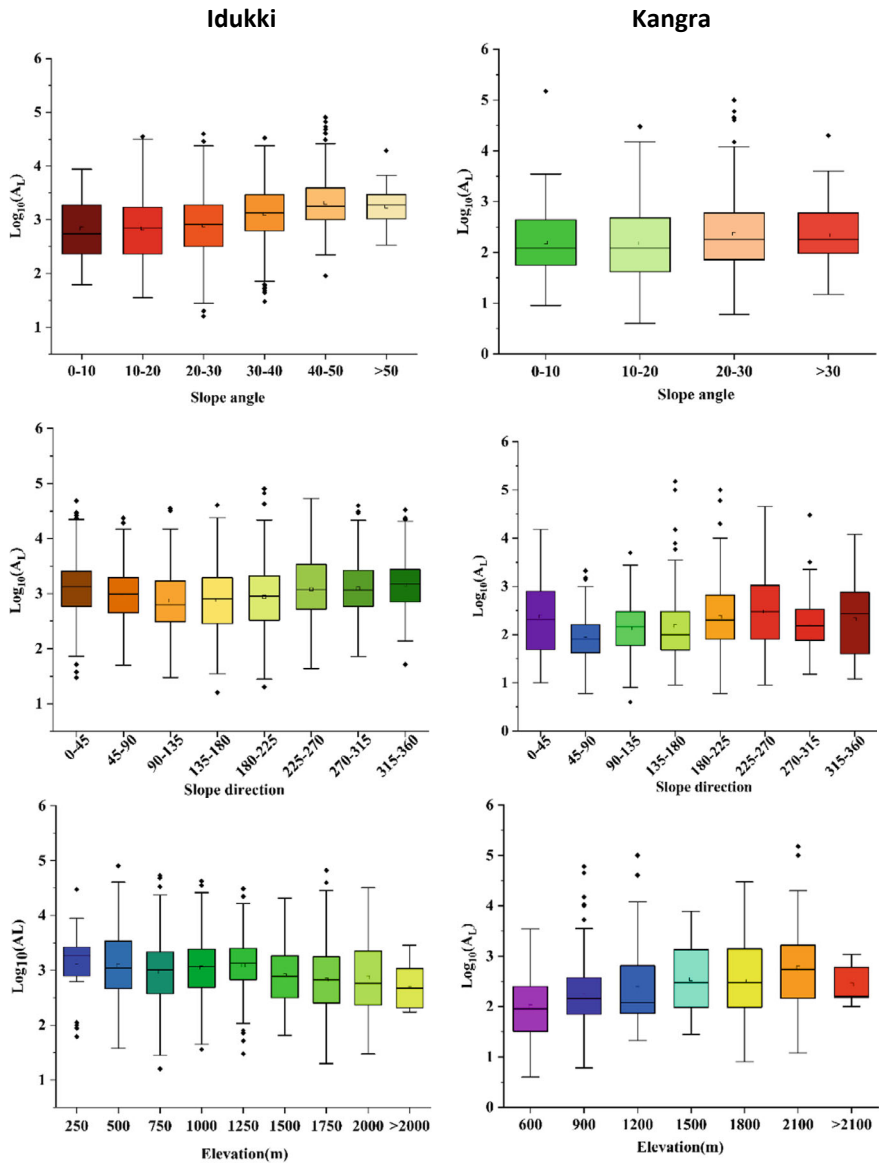


**Fig. 4** Box plot showing variation of landslide area ( $\text{m}^2$ ) with different geomorphological parameters for Idukki and Kangra

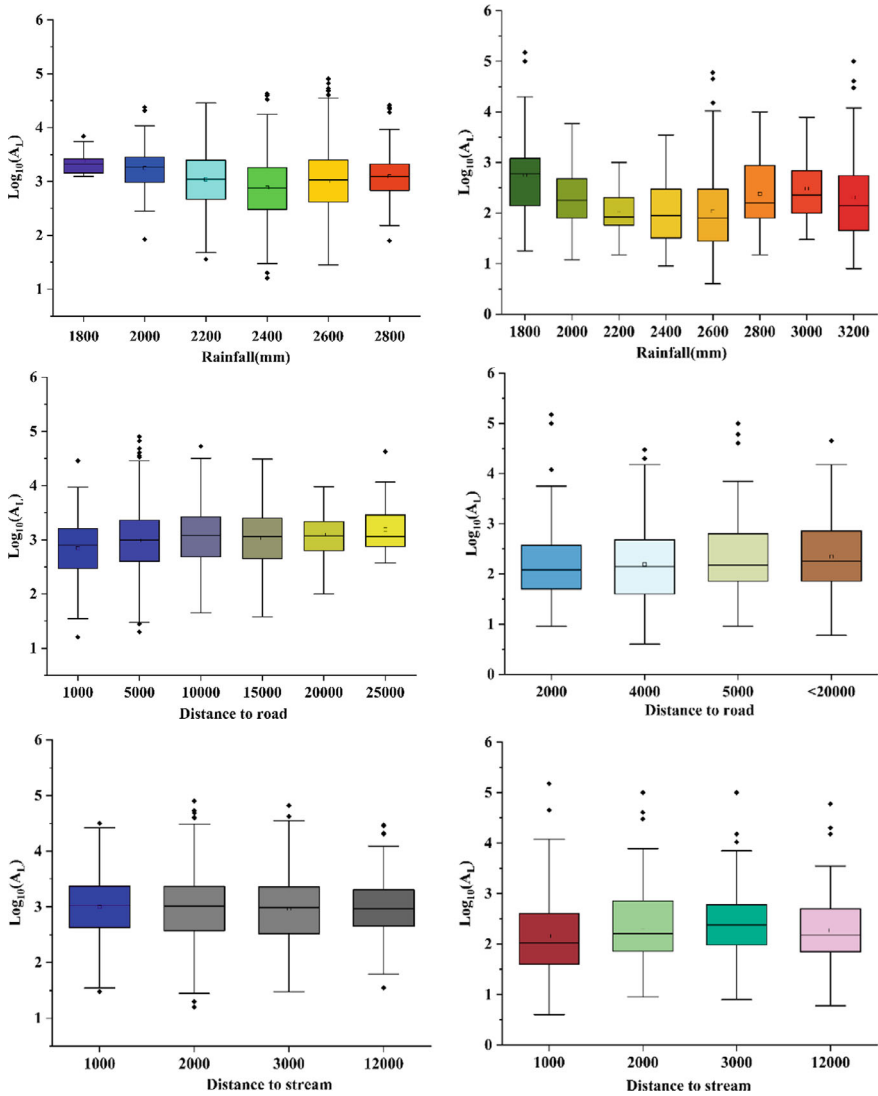


Fig. 4 (continued)

In contrast, landslide size in Kangra shows no significant correlation with slope direction and follows a rhythmic trend. Although both areas are at similar elevations, elevation trends differ between the regions. In Idukki, landslide size shows an overall decreasing trend, whereas an overall increasing trend is observed in Kangra.

Since rainfall-triggered landslides are characteristic of both hill stations, rainfall is a crucial factor in analyzing such landslides. When the 10-year average rainfall is plotted against landslide size, similar trends are observed in both areas. A decrease in

landslide size is seen with increasing rainfall, followed by an increase. The tropical climate facilitates intense chemical weathering, and the monsoon acts as one of the most significant triggering agents. Deforestation in Idukki has also led to a deeper weathering profile, where increased pore pressure during the monsoon results in a loss of shear strength and subsequent failure. In their study, Sajinkumar et al. (2011) observed that hornblende gneiss was more susceptible to landslides than granite gneiss in Idukki. The two thrusts bounding Kangra makes the rocks highly folded and fractured. Deformation in rock mass is aided by fracturing, urbanization, and unscientific modification of steep slopes making the area a hotbed for the development of pore pressure during monsoon effectively leading to landslides (Sharma et al. 2015).

In both areas, small landslides are common near road cuts, while larger landslides are observed farther from road networks. Several numerical and field analyses have shown a dominance of shallow or small-scale failures along cut slopes, primarily in the form of plane or wedge failures (Ahmad et al. 2013; Singh et al. 2015; Mori et al. 2017). In unplanned excavation, rockfall has found to be one of the most common types of landslide (Ansari et al. 2014; Singh et al. 2016a; Siddique et al. 2017). The landslide size seems unrelated to streams in both areas indicating that larger landslides may not be a result of the vicinity to streams.

### ***4.3 Comparison of Frequency Area Distribution***

The frequency area distribution can be used to characterize the severity of landslide event (Malamud et al. 2004). The slope of medium and large-scale landslides in both the areas follows three parameter inverse gamma distribution however, the position of rollover seems to be very different. The rollover for Idukki is attained at about 392 m<sup>2</sup> while for Kangra it hovers around 35 m<sup>2</sup> (Fig. 5). The cut-off for Idukki is obtained at 5696 m<sup>2</sup>, past this medium and large-scale landslides decays with a power law exponent of  $\sim 2.4$ . Most medium and large scale landslides show a power law tail with an exponent of  $\sim 2.3 \pm 0.6$  (Eeckhaut et al. 2007). A small power law exponent implies more contribution of large landslide to the inventory. The historical landslide inventory of Kangra is not mapped properly and is likely to be incomplete. It is possible that many landslides are missing from the inventory of entire Himachal Pradesh, making it very difficult for analysing FAD of this area. The rollover position in the FAD curve of landslides is a critical point where the distribution deviates from the power law relationship, typically for small landslides. Several explanations have been proposed for this deviation, of which geomorphological factors and failure process seems to be more important in the present analysis (Kasai and Yamada 2019; Tanyaş et al. 2019). In Idukki, landslides are primarily attributed to the intense weathering patterns of the gneissic terrain, whereas in Kangra, the low-strength interbedded rocks of the Lower Sivaliks, exhibiting anisotropic behavior, largely control landslide occurrences. Rock anisotropy has been linked to modifying the failure process of landslides, where failure is predominantly guided by the anisotropy



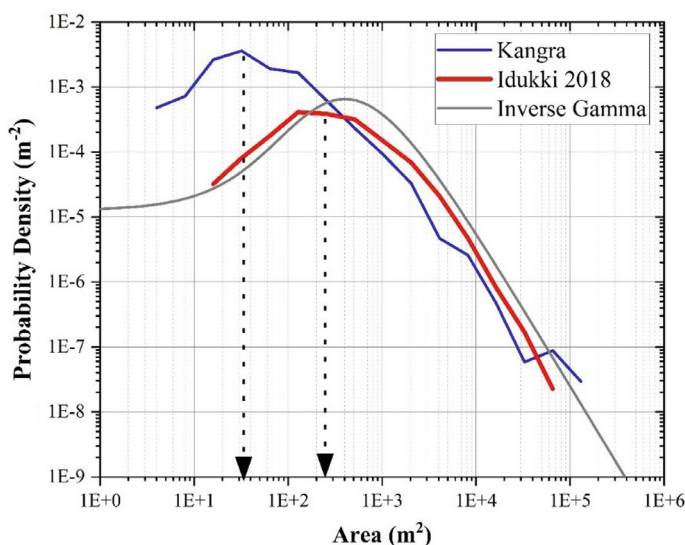


**Fig. 5** Frequency area distribution plot for two different inventories of Idukki and Kangra along with three parameter inverse gamma curve proposed by Malamud et al. (2004)

angle and interface shear strength (Singh et al. 2017). However, an in-depth analysis of failure mechanism needs to be conducted to validate the above inference.

## 5 Conclusion

In this study, a comparative analysis has been conducted to understand the spatial distribution, frequency, and size of landslides in two distinct tectonic, geologic, and geomorphic terrains. Kangra in Himachal Pradesh and Idukki in Kerala serve as good examples to develop an understanding of the factors responsible for landslides in these hilly regions. The landslide size tends to increase with the slope angle in both areas; however, the median landslide size is higher in the Idukki region. Slope direction appears to be significant in Idukki, as the size decreases on north and east-facing slopes while increasing on south and west-facing slopes. In Idukki, landslide size shows an overall decreasing trend, whereas an increasing trend is observed in Kangra. In both areas, smaller landslides are common near road cuts, while larger landslides are found farther from road networks. Slopes with angles between  $20^\circ$  and  $35^\circ$  are more prone to landslides and attract more failures. Lower elevation supports more landslides in both areas. In both cases, a higher frequency of landslides is located near stream networks. The FAD curve for both inventories, when plotted as non-cumulative size distribution, shows a typical power-law tail followed by a rollover at smaller landslides. The rollover and cutoff size vary for both areas, smaller rollover

being observed in Kangra. The power-law exponent is  $-2.4$ , closely aligning with previous research results.

**Acknowledgements** Authors thankfully acknowledge the support provided by the Geological Survey of India “BHUKOSH” and CHIRPS Data Portal for providing data freely. The authors are very much thankful to the anonymous reviewers for the comment which modified the chapter in the current form.

The authors declare that they have no conflict of interest.

## References

- Achu AL, Joseph S, Aju CD, Mathai J (2021) Preliminary analysis of a catastrophic landslide event on 6 August 2020 at Pettimudi, Kerala state, India. *Landslides* 18:1459–1463. <https://doi.org/10.1007/s10346-020-01598-x>
- Aghdam IN, Varzandeh MHM, Pradhan B (2016) Landslide susceptibility mapping using an ensemble statistical index (Wi) and adaptive neuro-fuzzy inference system (ANFIS) model at Alborz Mountains (Iran). *Environ Earth Sci* 75:1–20. <https://doi.org/10.1007/S12665-015-5233-6/FIGURES/14>
- Ahmad M, Umrao RK, Ansari MK et al (2013) Assessment of rockfall hazard along the road cut slopes of state highway-72, Maharashtra, India. *Geomaterials* 3:15–23. <https://doi.org/10.4236/gm.2013.31002>
- Akgün A, Türk N (2011) Mapping erosion susceptibility by a multivariate statistical method: a case study from the Ayvalık region, NW Turkey. *Comput Geosci* 37:1515–1524. <https://doi.org/10.1016/J.CAGEO.2010.09.006>
- Alemdag S, Kaya A, Karadag M et al (2015) Utilization of the limit equilibrium and finite element methods for the stability analysis of the slope debris: an example of the Kalebasi district (NE Turkey). *J African Earth Sci* 106:134–146. <https://doi.org/10.1016/j.jafrearsci.2015.03.010>
- Ansari MK, Ahmad M, Singh TN (2014) Rockfall risk assessment for pilgrims along the circum-ambulatory pathway, Saptashrungi Gad Temple, Vani, Nashik Maharashtra, India. *Geomatics Nat Hazards Risk* 5:81–92. <https://doi.org/10.1080/19475705.2013.787657>
- Banshtu RS, Versain LD, Pandey DD (2020) Risk assessment using quantitative approach: Central Himalaya, Kullu, Himachal Pradesh, India. *Arab J Geosci* 13:1–11. <https://doi.org/10.1007/S12517-020-5143-0/FIGURES/9>
- Biju Abraham P, Shaji E (2013) Landslide hazard zonation in and around Thodupuzha-Idukki-Munnar road, Idukki district, Kerala: a geospatial approach. *J Geol Soc India* 82:649–656. <https://doi.org/10.1007/s12594-013-0203-7>
- Çellek S (2022) Effect of the slope angle and its classification on landslides. *Himal Geol* 43:85–95
- Çellek S (2023) Linear parameters causing landslides: a case study of distance to the road, fault, drainage. *Kocaeli J Sci Eng* 6:94–113. <https://doi.org/10.34088/kojose.1117817>
- Chawla A, Chawla S, Pasupuleti S et al (2018) Landslide susceptibility mapping in Darjeeling Himalayas, India. *Adv Civ Eng* 2018. <https://doi.org/10.1155/2018/6416492>
- Chen XL, Liu CG, Chang ZF, Zhou Q (2016) The relationship between the slope angle and the landslide size derived from limit equilibrium simulations. *Geomorphology* 253:547–550. <https://doi.org/10.1016/J.GEOMORPH.2015.01.036>
- Chuang YC, Shiu YS (2018) Relationship between landslides and mountain development—integrating geospatial statistics and a new long-term database. *Sci Total Environ* 622–623:1265–1276. <https://doi.org/10.1016/J.SCITOTENV.2017.12.039>

- Dai FC, Lee CF (2002) Landslide characteristics and slope instability modeling using GIS, Lantau Island, Hong Kong. *Geomorphology* 42:213–228. [https://doi.org/10.1016/S0169-555X\(01\)00087-3](https://doi.org/10.1016/S0169-555X(01)00087-3)
- Donati L, Turrini MC (2002) An objective method to rank the importance of the factors predisposing to landslides with the GIS methodology: application to an area of the Apennines (Valnerina; Perugia, Italy). *Eng Geol* 63:277–289. [https://doi.org/10.1016/S0013-7952\(01\)00087-4](https://doi.org/10.1016/S0013-7952(01)00087-4)
- Dortch JM, Owen LA, Haneberg WC et al (2009) Nature and timing of large landslides in the Himalaya and Transhimalaya of northern India. *Quat Sci Rev* 28:1037–1054. <https://doi.org/10.1016/j.quascirev.2008.05.002>
- Dragičević S, Lai T, Balram S (2015) GIS-based multicriteria evaluation with multiscale analysis to characterize urban landslide susceptibility in data-scarce environments. *Habitat Int* 45:114–125. <https://doi.org/10.1016/J.HABITATINT.2014.06.031>
- Dugonji S (2014) Landslide risk increasing caused by highway, pp 333–342
- Eeckhaut M, Van Den, Poesen J, Govers G et al (2007) Characteristics of the size distribution of recent and historical landslides in a populated hilly region. *Earth Planet Sci Lett* 256:588–603. <https://doi.org/10.1016/j.epsl.2007.01.040>
- Ganesha Raj K, Paul MA, Hegde VS, Nijagunappa R (2001) Lineaments and seismicity of Kerala—a remote sensing based analysis. *J Indian Soc Remote Sens* 29:203–211. <https://doi.org/10.1007/BF02995725/METRICS>
- Gerrard J (1994) The landslide hazard in the Himalayas: geological control and human action. *Geomorphology* 10:221–230. [https://doi.org/10.1016/0169-555X\(94\)90018-3](https://doi.org/10.1016/0169-555X(94)90018-3)
- Gupta VJ, Thakur VC (1974) Geology of the area around Dharmasala, Kangra district, H.P India. *Geol Rundschau* 63:548–558. <https://doi.org/10.1007/BF01820829/METRICS>
- Gupta V, Ram BK, Kumar S, Sain K (2022) A case study of the 12 July 2021 Bhagsunath (McLeod Ganj) flash flood in Dharamshala, Himachal Pradesh: a warning against constricting natural drainage. *J Geol Soc India* 98:607–610. <https://doi.org/10.1007/S12594-022-2033-Y/METRICS>
- Guzzetti F, Ardizzone F, Cardinali M et al (2008) Distribution of landslides in the Upper Tiber River basin, central Italy. *Geomorphology* 96:105–122. <https://doi.org/10.1016/j.geomorph.2007.07.015>
- Hao L, Rajaneesh A, Van WC et al (2020) Constructing a complete landslide inventory dataset for the 2018 monsoon disaster in Kerala, India, for land use change analysis. *Earth Syst Sci Data* 2:1–32. <https://doi.org/10.5194/essd-2020-83>
- He Y, Beighley RE (2008) GIS-based regional landslide susceptibility mapping: a case study in southern California. *Earth Surf Process Landforms* 33:380–393. <https://doi.org/10.1002/ESP.1562>
- Huntley D (2022) Progress in landslide research and technology
- Jacynth Jennifer J, Saravanan S (2022) Contribution of SAR-driven displacement measurement in assessing the triggering factors of rainfall-induced landslides. *Geocarto Int* 37:2821–2841. <https://doi.org/10.1080/10106049.2020.1844313>
- Jha CS, Dutt CBS, Bawa KS (2000) Deforestation and land use changes in Western Ghats, India. *Curr Sci* 79:231–238
- Kahlon S, Chandel VBS, Brar KK (2014) Landslides in Himalayan mountains: a study of Himachal Pradesh, India. *Int J Eng Appl Sci Res (IJEASR)* 3(9):28–34
- Kainthola A, Sharma V, Pandey VHR et al (2021) Hill slope stability examination along Lower Tons Valley, Garhwal Himalayas, India. *Geomatics Nat Hazards Risk* 12:900–921. <https://doi.org/10.1080/19475705.2021.1906758>
- Kanungo DP, Singh R, Dash RK (2020) Field observations and lessons learnt from the 2018 landslide disasters in Idukki District, Kerala, India. *Curr Sci* 119:1797. <https://doi.org/10.18520/cs/v119/i11/1797-1806>
- Kasai M, Yamada T (2019) Topographic effects on frequency—size distribution of landslides triggered by the Hokkaido Eastern Iburi earthquake in 2018. *Earth, Planets Sp* 8. <https://doi.org/10.1186/s40623-019-1069-8>

- Khanduri VS, Verma S (2018) Assessment of landslides occurred in Himachal Pradesh over last two decades. *J Emerg Technol Innov Res* 5:23–30
- Korup O, Schmidt J, McSaveney MJ (2005) Regional relief characteristics and denudation pattern of the western Southern Alps, New Zealand. *Geomorphology* 71:402–423. <https://doi.org/10.1016/J.GEOMORPH.2005.04.013>
- Kumar BM (2005) Land use in Kerala: changing scenarios and shifting paradigms. *J Trop Agric* 42:1–12
- Kuriakose SL, Jetten VG, van Westen CJ et al (2008) Pore water pressure as a trigger of shallow landslides in the Western Ghats of Kerala, India: some preliminary observations from an experimental catchment. *Phys Geogr* 29:374–386. <https://doi.org/10.2747/0272-3646.29.4.374>
- Kuriakose SL, Sankar G, Muraleedharan C (2009) History of landslide susceptibility and a chorology of landslide-prone areas in the Western Ghats of Kerala, India. *Environ Geol* 57:1553–1568. <https://doi.org/10.1007/s00254-008-1431-9>
- Lee S, Choi J (2004) Landslide susceptibility mapping using GIS and the weight-of-evidence model. *Int J Geogr Inf Sci* 18:789–814. <https://doi.org/10.1080/13658810410001702003>
- Lee S, Sambath T (2006) Landslide susceptibility mapping in the Damrei Romel area, Cambodia using frequency ratio and logistic regression models. *Environ Geol* 50:847–855. <https://doi.org/10.1007/S00254-006-0256-7/FIGURES/4>
- Lee S, Talib JA (2005) Probabilistic landslide susceptibility and factor effect analysis. *Environ Geol* 47:982–990. <https://doi.org/10.1007/S00254-005-1228-Z/TABLES/4>
- Mahajan AK, Viridi NS (2000) Preparation of landslides hazard zonation map of Dharamshala town & adjoining areas. District Kangra (H.P.): technical report, 45. Wadia Institute of Himalayan Geology, Dehradun. Ref No. Endst/281/MA dt 27/2/99
- Mahajan AK, Sharma S, Patial S et al (2022) A brief address of the causal factors, mechanisms, and the effects of a major landslide in Kangra valley, North-Western Himalaya, India. *Arab J Geosci* 159(15):1–12. <https://doi.org/10.1007/S12517-022-10163-W>
- Mahanta B, Singh HO, Singh PK et al (2016) Stability analysis of potential failure zones along NH-305, India. *Nat Hazards* 83:1341–1357. <https://doi.org/10.1007/s11069-016-2396-8>
- Malamud BD, Turcotte DL, Guzzetti F, Reichenbach P (2004) Landslide inventories and their statistical properties. *Earth Surf Process Landforms* 29:687–711. <https://doi.org/10.1002/esp.1064>
- Martha TR, Roy P, Govindharaj KB et al (2015) Landslides triggered by the June 2013 extreme rainfall event in parts of Uttarakhand state, India. *Landslides* 12:135–146. <https://doi.org/10.1007/s10346-014-0540-7>
- Martha TR, Roy P, Jain N et al (2021) Geospatial landslide inventory of India—an insight into occurrence and exposure on a national scale. *Landslides* 18:2125–2141. <https://doi.org/10.1007/s10346-021-01645-1>
- Medwedeff WG, Clark MK, Zekkos D, West AJ (2020) Characteristic landslide distributions: an investigation of landscape controls on landslide size. *Earth Planet Sci Lett* 539:116203. <https://doi.org/10.1016/j.epsl.2020.116203>
- Meinhardt M, Fink M, Tünschel H (2015) Landslide susceptibility analysis in central Vietnam based on an incomplete landslide inventory: comparison of a new method to calculate weighting factors by means of bivariate statistics. *Geomorphology* 234:80–97. <https://doi.org/10.1016/j.geomorph.2014.12.042>
- Mersha T, Meten M (2020) GIS-based landslide susceptibility mapping and assessment using bivariate statistical methods in Simada area, Northwestern Ethiopia. *Geoenvironmental Disasters* 7:1–22. <https://doi.org/10.1186/S40677-020-00155-X/FIGURES/11>
- Mori A, Subramanian SS, Ishikawa T, Komatsu M (2017) A case study of a cut slope failure influenced by snowmelt and rainfall. *Procedia Eng* 189:533–538. <https://doi.org/10.1016/j.proeng.2017.05.085>
- Mossa S, Capolongo D, Pennetta L, Wasowski J (2005) A GIS-based assessment of landsliding in the Daunia Apennines, southern Italy. *Polish Geol Inst Spec Pap* 86–91

- Nakileza BR, Nedala S (2020) Topographic influence on landslides characteristics and implication for risk management in upper Manafwa catchment, Mt Elgon Uganda. *Geoenvironmental Disasters* 7. <https://doi.org/10.1186/s40677-020-00160-0>
- Pei Y, Qiu H, Zhu Y et al (2023) Elevation dependence of landslide activity induced by climate change in the eastern Pamirs. *Landslides* 20:1115–1133. <https://doi.org/10.1007/S10346-023-02030-W/FIGURES/11>
- Ramasamy SM, Gunasekaran S, Rajagopal N et al (2019) Flood 2018 and the status of reservoir-induced seismicity in Kerala, India. *Nat Hazards* 99:307–319. <https://doi.org/10.1007/s11069-019-03741-x>
- Ramasamy S, Gunasekaran S, Saravanavel J et al (2021) Geomorphology and landslide proneness of Kerala, India a geospatial study. *Landslides* 18:1245–1258. <https://doi.org/10.1007/s10346-020-01562-9>
- Rautela P, Lakhera RC (2000) Landslide risk analysis between Giri and Tons rivers in Himachal Himalaya (India). *Int J Appl Earth Obs Geoinf* 2:153–160. [https://doi.org/10.1016/S0303-2434\(00\)85009-6](https://doi.org/10.1016/S0303-2434(00)85009-6)
- Regmi AD, Yoshida K, Dhital MR, Devkota K (2013) Effect of rock weathering, clay mineralogy, and geological structures in the formation of large landslide, a case study from Dumre Besei landslide, Lesser Himalaya Nepal. *Landslides* 10:1–13. <https://doi.org/10.1007/s10346-011-0311-7>
- Regmi AD, Yoshida K, Dhital MR, Pradhan B (2014) Weathering and mineralogical variation in gneissic rocks and their effect in Sangrumba landslide, East Nepal. *Environ Earth Sci* 71:2711–2727. <https://doi.org/10.1007/s12665-013-2649-8>
- Saikia U, Menon AS, Das R, Mittal H (2024) Estimation of source parameters of local earthquakes originated near Idukki reservoir, Kerala. *Acta Geophys* 1–14. <https://doi.org/10.1007/S11600-024-01348-W/FIGURES/7>
- Sajinkumar KS, Anbazhagan S, Pradeepkumar AP, Rani VR (2011) Weathering and landslide occurrences in parts of Western Ghats, Kerala. *J Geol Soc India* 78:249–257. <https://doi.org/10.1007/s12594-011-0089-1>
- Sana E, Kumar A, Robson E et al (2024) Preliminary assessment of series of landslides and related damage by heavy rainfall in Himachal Pradesh, India, during July 2023. *Landslides* 21:919–931. <https://doi.org/10.1007/s10346-023-02209-1>
- Shankar R, Satyam GP, Singh PK et al (2022) Impact of geomorphometric parameters on the occurrence and distribution of landslides in Yamuna river basin, North-Western Himalaya, India. *J Mt Sci* 19:2374–2396. <https://doi.org/10.1007/s11629-021-7081-z>
- Sharma S, Mahajan AK (2019) Information value based landslide susceptibility zonation of Dharamshala region, northwestern Himalaya, India. *Spat Inf Res* 27:553–564. <https://doi.org/10.1007/s41324-019-00259-z>
- Sharma M, Upadhyay RK, Tripathi G et al (2023) Assessing landslide susceptibility along India's national highway 58: a comprehensive approach integrating remote sensing, GIS, and logistic regression analysis. *Conservation* 3:444–459. <https://doi.org/10.3390/conservation3030030>
- Sharma M, Das S, Pain A et al (2024) Preliminary assessment of the Shiv Bawdi landslide in Shimla, Himachal Pradesh, India. *Landslides* 21:1591–1601. <https://doi.org/10.1007/S10346-024-02234-8/TABLES/2>
- Sharma R, Sharma UK, Mahajan AK (2015) Rainfall and anthropogenically accelerated mass movement in the outer Himalaya, north of Dharamshala town, Kangra district, Himachal Pradesh, India. A cause of concern. *J Geol Soc* 563–569
- Shroder JF, Bishop MP (1998) Mass movement in the Himalaya: new insights and research directions. *Geomorphology* 26:13–35. [https://doi.org/10.1016/S0169-555X\(98\)00049-X](https://doi.org/10.1016/S0169-555X(98)00049-X)
- Siddique T, Pradhan SP, Vishal V et al (2017) Stability assessment of Himalayan road cut slopes along national highway 58, India. *Environ Earth Sci* 76:1–18. <https://doi.org/10.1007/S12665-017-7091-X/FIGURES/6>

- Singh K, Kumar V (2018) Hazard assessment of landslide disaster using information value method and analytical hierarchy process in highly tectonic Chamba region in bosom of Himalaya. *J Mt Sci* 15:808–824. <https://doi.org/10.1007/S11629-017-4634-2/METRICS>
- Singh S, Sharma DK, Dhar S, Randhawa SS (2006) Geological significance of soil gas radon: a case study of Nurpur area, district Kangra, Himachal Pradesh, India. *Radiat Meas* 41:482–485. <https://doi.org/10.1016/J.RADMEAS.2005.10.009>
- Singh PK, Kainthola A, Singh TN (2015) Rock mass assessment along the right bank of river Suttlej, Luhri, Himachal Pradesh, India. *Geomatics Nat Hazards Risk* 6:212–223. <https://doi.org/10.1080/19475705.2013.834486>
- Singh PK, Singh KK, Singh TN (2017) Slope failure in stratified rocks: a case from NE Himalaya, India. *Landslides* 14:1319–1331. <https://doi.org/10.1007/s10346-016-0785-4>
- Singh N, Gupta SK, Shukla DP (2020) Analysis of landslide reactivation using satellite data: a case study of Kotrupi landslide, Mandi, Himachal Pradesh, India. *Int Arch Photogramm Remote Sens Spat Inf Sci-ISPRS Arch* 42:137–142. <https://doi.org/10.5194/isprs-archives-XLII-3-W11-137-2020>
- Singh PK, Kainthola A, Panthee S, Singh TN (2016a) Rockfall analysis along transportation corridors in high hill slopes. *Environ Earth Sci* 75:1–11. <https://doi.org/10.1007/s12665-016-5489-5>
- Singh PK, Kainthola A, Panthee S, Singh TN (2016b) Rockfall analysis along transportation corridors in high hill slopes. *Environ Earth Sci* 75. <https://doi.org/10.1007/s12665-016-5489-5>
- Sulal N, Archana K (2019) Note on post disaster studies for landslides occurred in june 2018 at Idukki district, Kerala. Thiruvananthapuram
- Sweta K, Goswami A, Nath RR, Bahuguna IM (2022) Performance assessment for three statistical models of landslide susceptibility zonation mapping: a case study for Dharamshala region, Himachal Pradesh, India. *J Earth Syst Sci* 131:1–16. <https://doi.org/10.1007/S12040-022-01881-6/FIGURES/7>
- Tanyaş H, van Westen CJ, Allstadt KE, Jibson RW (2019) Factors controlling landslide frequency–area distributions. *Earth Surf Process Landforms* 44:900–917. <https://doi.org/10.1002/esp.4543>
- Thakur VC, Sriram V, Mundeji AK (2000) Seismotectonics of the great 1905 Kangra earthquake meizoseismal region in Kangra-Chamba, NW Himalaya. *Tectonophysics* 326:289–298. [https://doi.org/10.1016/S0040-1951\(00\)00126-8](https://doi.org/10.1016/S0040-1951(00)00126-8)
- Thakur VC, Joshi M, Suresh N (2020) Linking the Kangra piggy-back basin with reactivation of the Jawalamukhi thrust and erosion of Dhauladhar range, Northwest Himalaya. *Episodes* 43:335–345. <https://doi.org/10.18814/epiiugs/2020/020020>
- Thampi PK, Mathai J, Sankar G (1995) Landslides (Urul Pottal) in Western Ghats: some field observations. In: *Proc: Seventh Kerala Science Congress, Palakkad*, pp 97–99
- Thampi PK, Mathai J, Sankar G, Sidharthan S (1998) Debris flow in Western Ghats—A regional evaluation. In: *Final Proc. Tenth Kerala Science Congress, Kozhikode*, pp 73–75
- van Westen CJ, Castellanos E, Kuriakose SL (2008) Spatial data for landslide susceptibility, hazard, and vulnerability assessment: an overview. *Eng Geol* 102:112–131. <https://doi.org/10.1016/J.ENGGEOL.2008.03.010>
- Xu C, Xu XW (2012) Spatial prediction models for seismic landslides based on support vector machine and varied kernel functions: a case study of the 14 April 2010 Yushu earthquake in China. *Acta Geophys Sin* 55:666–679. <https://doi.org/10.1002/cjg2.1761>
- Yilmaz C, Topal T, Süzen ML (2012) GIS-based landslide susceptibility mapping using bivariate statistical analysis in Devrek (Zonguldak-Turkey). *Environ Earth Sci* 65:2161–2178. <https://doi.org/10.1007/s12665-011-1196-4>
- Zeitler PK, Meltzer AS, Koons PO et al (2001) Erosion, Himalayan geodynamics, and the geomorphology of metamorphism. *GSA Today* 11:4–9. <https://doi.org/10.1109/IEMBS.2009.5332464>

**Mr. Nilesh Kumar Rai** is a research scholar at the Department of Earth and Planetary Sciences, University of Allahabad, Prayagraj, India. Mr. Rai has completed his undergraduate studies in 2017 and postgraduate studies in 2019 at the University of Allahabad. Mr. Rai's interests lie in understanding spatial characteristics of landslide in complex weathered terrain. He has published few research papers to his credits. Mr. Rai has attended various conferences and training courses significant to his research work. Mr. Rai along with his team participated in a quiz on National Science Day in 2023 where the team was placed third in the poster presentation category.

**Dr. Prakash Kumar Singh** is an Assistant Professor in the Department of Earth and Planetary Sciences at the University of Allahabad. He has received his Doctorate degree from Indian Institute of Technology Bombay and Master of Science degree from Indian Institute of Technology Kharagpur. His research interests primarily focus on Engineering Geology, Rock Mechanics, and Slope Stability. Dr Singh is presently working on landslide characteristics of stratified rock mass and highly weathered terrain. Dr. Singh has authored several journal articles and conference papers, contributing significantly to the fields of rock mechanics and geotechnical engineering. Dr. Singh is a life member of the Indian Society for Rock Mechanics and Tunnelling Technology and the Indian Science Congress Association. Dr. Singh's work has been widely cited, reflecting his impact on the scientific community.

**Dr. Ravi Shankar** is Ph.D. from the Indian Institute of Technology (ISM) Dhanbad and currently works as an Assistant Professor at Bakhtiyarpur College of Engineering (Department of Science and Technology, Government of Bihar). His research interests include the application of Remote Sensing and GIS in Geomorphological, Neotectonic as well as hazard assessments. Dr. Shankar has authored many journal articles as well as conference papers, contributing significantly to his area of research. Dr. Shankar has industrial experience of about four years at the Rock Excavation Engineering Division of CSIR-CIMFR where he was a part of various challenging projects of rock excavation/controlled blasting of national significance. Further, he worked as an Engineering Geologist at Geoconsult India Private Limited for about three years where he was involved in NATM tunnel construction for Indian Railways.

**Mr. Digvijay Singh** is a research scholar at the Department of Earth and Planetary Sciences, University of Allahabad, Prayagraj, India. Mr. Singh completed his undergraduate studies in 2017 and post graduate studies in 2019 from the University of Allahabad. He has qualified UGC NFSC JRF fellowship in 2022. Mr. Singh has attended several workshops and conferences related to his research work. Presently, Mr. Singh is working on landslide characteristics of stratified rock mass and engineering material characterization of weathered rocks. Mr. Singh has also published few research articles and presented several papers in national and international conference.

# **Some Traditional Techniques of Landslide Assessment**



# Applications of Photogrammetry Technique in Slope Stability Investigation



Jaspreet Singh, Amulya Ratna Roul, Saurabh Prakash Aher,  
Sarada Prasad Pradhan, and Vikram Vishal

**Abstract** The advancement in computational power has led to the substantial input of modern technological tools in data processing, generation, and analysis. Incorporating remote sensing practices such as photogrammetry and LiDAR in mining and geological engineering practices for landslide studies, rock slope analysis and monitoring has increased enormously. Photogrammetry is an inexpensive way to remotely fetch data related to geological characterization and hazard assessment of slopes even in rugged geological terrains using unmanned aerial vehicles (UAV) or terrestrial tools. Structure from motion (SfM) is a range imaging technique that uses a sequence of 2D images acquired using a simple camera to generate 3D point clouds for examining 3D structures. The generated point cloud can be used in multi-dimensional perspectives such as DEM generation, structural data extraction, slope deformation monitoring, and 3D mesh generation to develop realistic numerical models. This manuscript critically reviews the application, principle and limitations associated with the use of photogrammetry in slope failure and hazard assessment.

**Keywords** Remote sensing · Photogrammetry · Slope stability · Landslides

## 1 Introduction

Landslides are one of the common geological hazards affecting the hilly regions. The data record globally shows that due to 4862 different landslide events total of 55,997 people were killed globally between 2004 and 2016 (Melanie and David 2018). Together with fatal incidents, there are billions of dollars in infrastructure and economic loss globally every year. Specifically, in the Asian region, the spatial distribution of landslides is very heterogeneous, if we see the world landslide hazard

---

J. Singh (✉) · A. R. Roul · S. P. Aher · S. P. Pradhan

Department of Earth Sciences, Indian Institute of Technology Roorkee, Roorkee 247667, India  
e-mail: [jsingh1@es.iitr.ac.in](mailto:jsingh1@es.iitr.ac.in)

A. R. Roul · V. Vishal

Department of Earth Sciences, Indian Institute of Technology Bombay, Mumbai 400076, India

zonation map Himalayan region shows the highest contribution. Along with the catastrophic landslides the small-scale events of rock fall or slope failure events are more commonly encountered and are left unreported. These small events may lead to serious cause of accidents and may propagate in larger catastrophic landslides in the future. The slope stability specifically in rock slope is influenced by geological conditions. The presence of structural discontinuities such as joints, foliations, bedding planes, veins and faults intersect the rock mass into blocks. The kinematic stability of the blocks in the slope are controlled by the relative orientation of slope face and joints and the mechanical properties of the rock and joints. Traditional field measurements conducted using scanline survey use the Brunton compass or other instruments for collecting the relevant data.

With the advancement in technology, computational techniques have gained a significant importance and provided wider applicability. Remote sensing techniques such as LiDAR and photogrammetry are commonly used these days for landslides and slope stability investigation (Jaboyedoff et al. 2012; Tannant 2015; Riquelme et al. 2015; Donati et al. 2018; Francioni et al. 2019). Photogrammetry is a simple and economical way to generate 3D models by acquiring multiple overlapping photographs. Structure from Motion or SfM is a photogrammetry technique that generates three-dimensional models from series of two-dimensional images using geometrical analysis. The unmanned aerial vehicle (UAV) mounted with cameras, lenses and other sensors provides with ample data even in rugged and inaccessible locations. The terrestrial photogrammetry and high-resolution photography have been used at a wide range of engineering scales from laboratory to field for analysing highway cuts, single bench to overall pit slopes, major landslides, mine pillars and underground excavation faces (Casson et al. 2003; Donati et al. 2018; Scaioni et al. 2014). Xu et al. (2020) implemented multitemporal UAV based photogrammetry to detect and monitor the landslide. The continuous measurements of the deformation in the surface offer an effective way to characterize the slope movement for providing effective mitigations (Cenni et al. 2021; Donati et al. 2020; Lissak et al. 2020; Peternel et al. 2017; Demoulin 2006; Warrick et al. 2019; Lato et al. 2015b). Other remote sensing techniques such as aerial/terrestrial laser scanning and space/ground based synthetic aperture radar have also been effectually used to monitor the surface deformation (Lato et al. 2015a; Cigna et al. 2013; Mateos et al. 2017; Jaboyedoff et al. 2012; Gordon et al. 2001; Fobert et al. 2021; Cenni et al. 2021; Mateos et al. 2017). The point cloud developed from photogrammetry can be used to get the engineering geological data related to joint orientation, roughness, slope face orientation and conducting scanline survey (Francioni et al. 2019; Singh et al. 2022; Haneberg 2008; Kim et al. 2016; Bistacchi et al. 2011). Donati et al. (2018) discussed the application of high-resolution photography, thermal imaging and hyperspectral imaging for damage characterization in rock slopes. Francioni et al. (2019) compared the point cloud generated using photogrammetry with the laser scanner for the slope outcrop and found that the models were precise for measurement. Salvini et al. (2016) discussed the geological implementation of laser scanning and UAV photogrammetry in Marble quarrying. The point clouds developed using photogrammetry are also used to regenerate the geometric topography by creating DEM/mesh of the surface (Sarro

et al. 2018). The function of topography in slope stability analysis will be enhanced by including surface geometry into numerical models.

With the several decades of research in photogrammetry the applicability of the technique is increasing in engineering geological studies. This paper discusses the photogrammetry technique in detail for landslide studies and slope stability investigations. Addressing the basic principle of photogrammetry, followed by workflow and their applicability in examining road cut slopes or catastrophic landslides. Further, a photogrammetry derived point cloud of a Himalayan Road cut slope was used to demonstrate the applicability of the method in engineering geological practices.

## 2 Principles of Photogrammetry

Photogrammetry is a three-dimensional coordinate measuring technique which gathers data about an object by analysing its positions using photographs, captured at different locations and angles as the fundamental medium (Wester-Ebbinghaus 1986; Westaway et al. 2000; Bennett et al. 2012; Wolf et al. 2014; Singh et al. 2022). Basically photogrammetric measurements comprise of mathematical and geometrical reconstruction of light rays from the object to the sensor during acquisition of the image. Triangulation is the fundamental principle used in photogrammetry; it involves mathematical integration of line of sights (lead from camera to specific points on the object being photographed) to produce a 3D coordinate of specified points. Capturing two photographs of an object from different angles will form a single point triangulation (Fig. 1a) whereas multiple photographs captured from multiple locations results in multipoint triangulations (Fig. 1b) (Fryer et al. 2007; Rothermel et al. 2012; Stumpf et al. 2015). The range and the quality of the data acquired is mainly dependent on focal length of the camera, field of view, focus depth and exposure of the sensor (Fig. 2a). Acquisition of photographs for planimetric and topographic features is done aerially where the focal length of the camera and flying height are the deciding factors for the scale of the photograph. The flying path and acquisition technique needs to be decided in such a way that the objective area under consideration should be covered with desired overlap. Different image capturing techniques such as independent convergent, strip and fan method can be followed for acquisition (Fig. 2) (Francioni et al. 2019). Structure from motion (SfM) is the extraction of 3D structure from the sequences of overlapping 2D images without prior knowledge of camera position. Combined multiview stereo (MVS) and SfM helps in generation of the dense point clouds (Westoby et al. 2012; Javernick et al. 2014; Micheletti et al. 2015; Carrivick et al. 2016; Ferreira et al. 2017).

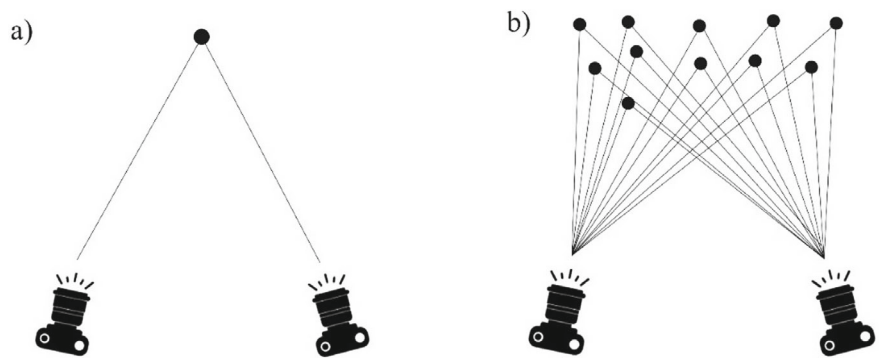


**Fig. 1** a Single point triangulation b multi-point triangulation

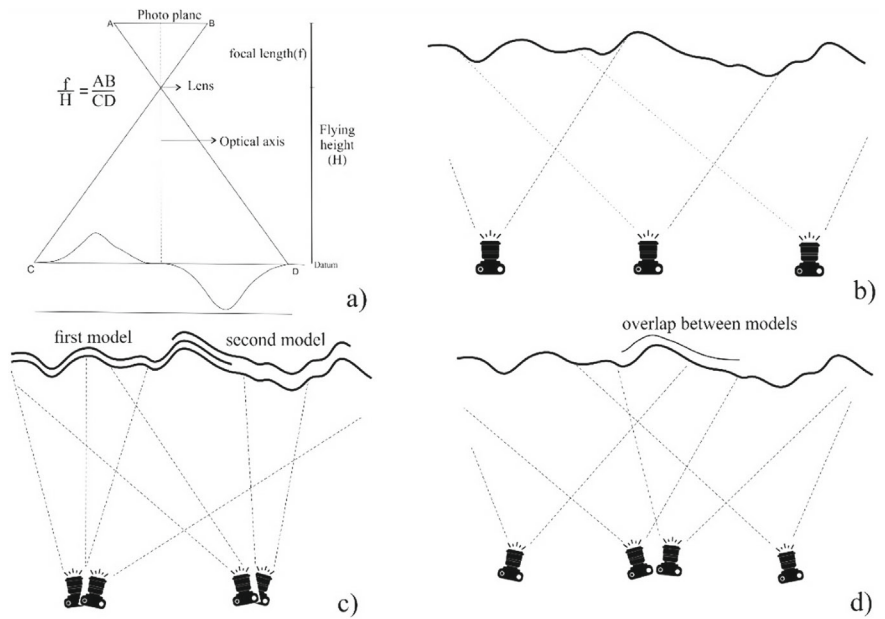


**Fig. 2** a The formula associated with the calculation of image width and overlapping distances; different photo acquisition methods b strip method c Fan method d independent convergent method

### 3 Workflow

Photogrammetry analysis requires multiple phases of processing to generate the final 3D output model. The flow chart in Fig. 3 depicts the steps from photo acquisition to final DEM generation. Scaling or georeferencing the point cloud is one of the necessary steps for measurement accuracy. To scale the photogrammetry models, at least three ground control points (GCP) are required. The position data of the GCPs is

generally found using total station or other accurate GPS systems. But in the case of unavailability of the total station for the small-scale outcrops, an alternative method can be opted to find the coordinates of the GCPs. If trend, plunge and length of a line in space is known, then its endpoint coordinates can be easily calculated with respect to the other using trigonometric calculations. Figure 4 shows the lines marked in different direction over the rock mass using a red thread. Knowing the length and trend of the lines marked over the slope, multiple GCP data can be gathered to scale or georeference the model. Different georeferencing methods and the errors associated with them were extensively studied by Francioni et al. (2019). Two-point clouds developed for the road cut slopes using photogrammetry are shown in Fig. 5. The list of software available for processing and analysing the point clouds are tabulated in Table 1.

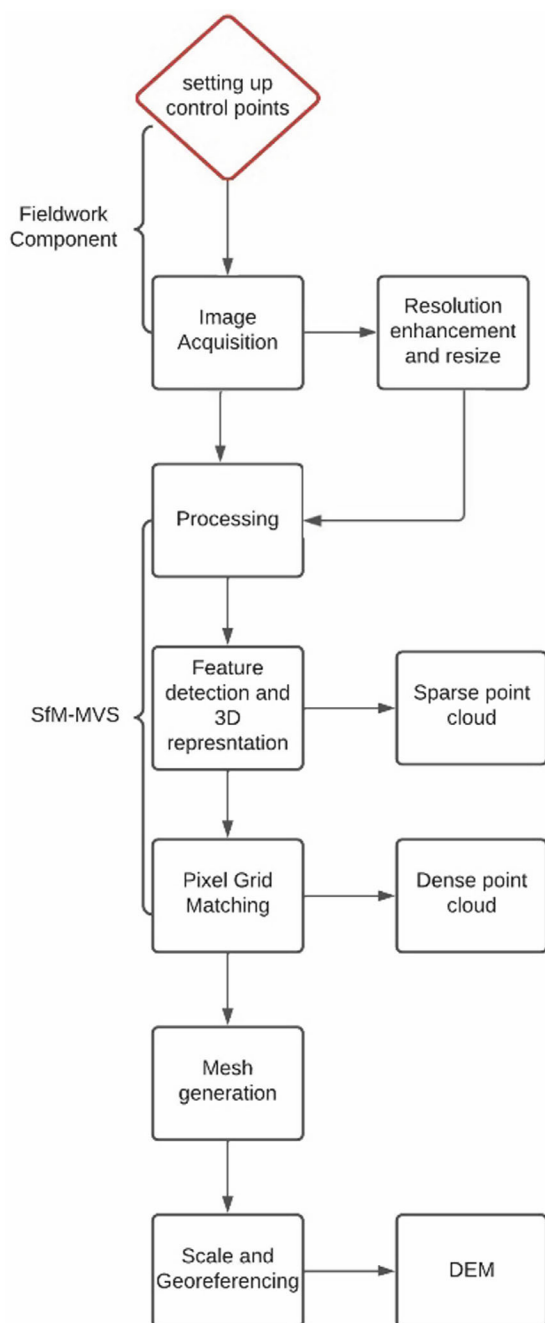
## 4 Different Applications of the Photogrammetry Model

### 4.1 Engineering Geological Data Collection

To examine an outcrop, preliminary work is to collect geological data. The structural geological data includes the detailed analysis related to the joint or fractures present in the rock mass. Traditional field methods are time consuming and require high physical work to acquire the data in the field using Brunton compass, scanline survey or window mapping. The 3D models developed from photogrammetry or high-resolution photographs have a series of applications in relation to gathering useful structural geological data. The rock mass is composed of planar fractures or discontinuities that intersects the rock mass in numerous small blocks. Studying disposition of these discontinuities including orientation and spacing have become easy using the point clouds (Havaej et al. 2015). The free open-source software Cloud compare provides a plugin to fit the planes manually or automatically in the georeferenced point cloud for determining the orientation and orientation distribution of joint sets present in it (Fig. 6) (GPL Software 2018). Based upon the joint orientation data and slope face, preliminary kinematic analysis can be conducted to find the possible mode of failure in the slope (Singh and Thakur 2019; Lenka et al. 2017). The kinematic analysis results for the outcrop present in Fig. 6 shows that the slope is vulnerable for wedge and direct toppling failures (Fig. 7).

Moreover, the scaled points cloud can be used to perform multiple analysis related to joints, such as measuring joint spacing, window mapping, scanline survey, joint trace length, roughness, fracture densities ( $P_{21}$ ,  $P_{10}$ ) (Fig. 8). Riquelme et al. (2015) provided a noble methodology to estimate the normal spacing of persistence and non-persistence discontinuities using 3D point clouds. Persistence indicates the extent or continuity of the discontinuities, the presence of intact rock bridges addons the shear strength to the rock mass. Consequently, randomly distributed rock bridges within the fractured rock profoundly increases the slope stability. Tuckey and Stead (2016)

**Fig. 3** Schematic workflow for photogrammetry study



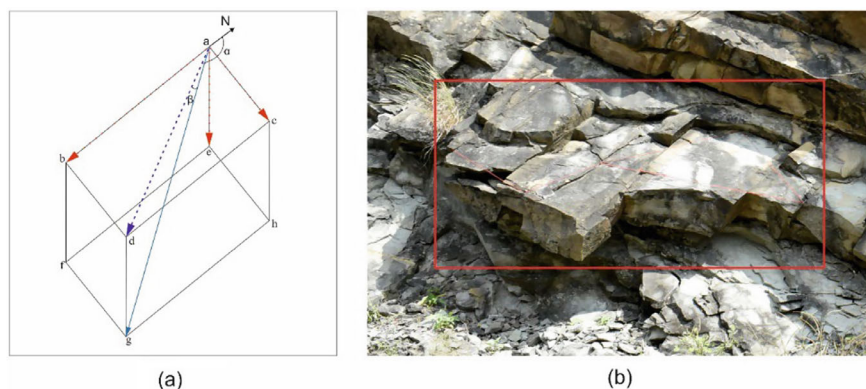


**Fig. 4** **a** Different component of a vector ( $ag$ ) in 3D. Where  $\alpha$  is the trend of a line and  $\beta$  is plunge. 'a' is known point; **b** the box showing lines marked over the rock slope using thread to georeference the point cloud

discussed the new intensity factors to describe intact rock bridge trace intensity  $R_{21}$  and blast-induced fracture intensity  $B_{21}$  measured using high resolution photogrammetry (Fig. 8). Joint roughness profiles and roughness parameters influence the shear strength of the rock joint and are commonly obtained by comparing the manually determined surface geometry with established standard profiles (Barton and Choubey 1977; ISRM 1978). With the advancement in close range photogrammetry, it become possible to measure the surface/joint roughness at different scales (An et al. 2022; Paixão et al. 2022; Francioni et al. 2019; Kim et al. 2016; Unal et al. 2004; Bistacchi et al. 2011; Sturzenegger and Stead 2009). Kim et al. (2016) found that the focal lengths and camera-to-object distance influences the JRC measurement accuracy.

## 4.2 Numerical Modelling

Numerical modelling is often undertaken for conducting the stability analysis of the slope. Different numerical methods such as limit equilibrium, discontinuum, continuum and hybrid codes are used for modelling the slope (Stead and Wolter 2015; Singh et al. 2022; Pradhan et al. 2019; Mitelman and Elmo 2014). The photogrammetry point clouds are commonly used to construct the 3D geometry or 2D profile of the slope and can be later imported into the codes for examining the influence of the geometry (Fig. 9a). The discontinuity related data, such as orientation and trace length found using point cloud/high resolution photographs (Fig. 8) can be used for developing discrete fracture networks to mimic the 3D fracture network in the rock mass (Singh et al. 2023). The developed fracture network can be later imported in numerical simulation codes for analyzing the stability of the fractured rock mass. As observed in the point cloud of the slope outcrop in Fig. 6a, the slope shows the



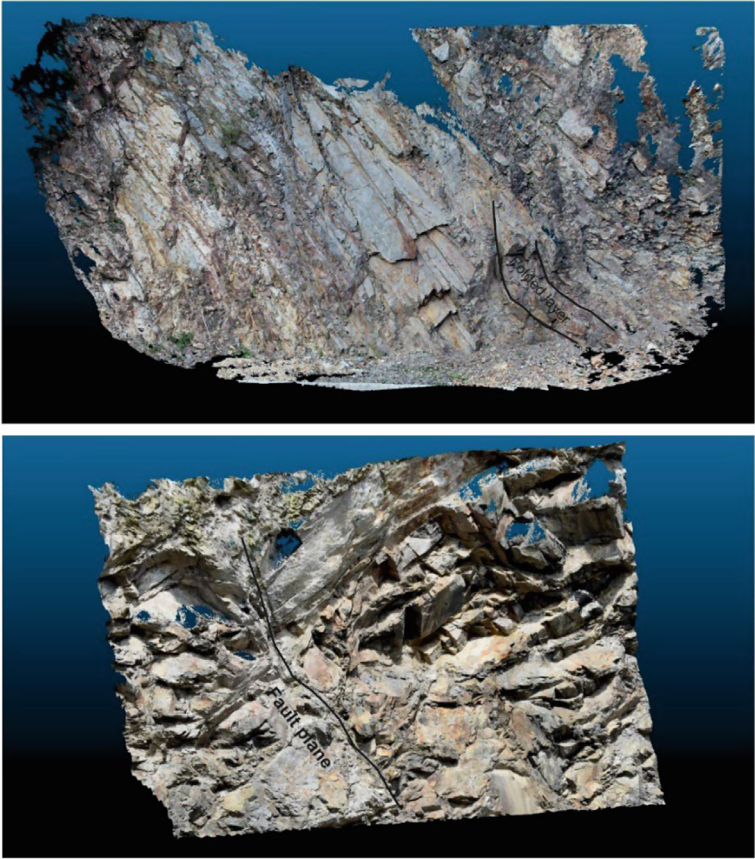


**Fig. 5** Point clouds of the two outcrop slopes developed using terrestrial photogrammetry and marked with identified structural features (fault and fold)

**Table 1** List of software available for processing and analysing the point clouds

Processing software	Point cloud analysing software
Meshroom (open source)	Cloud compare (open source)
Agisoft PhotoScan (requires subscription)	SplitFx (requires subscription)
VisualSFM (open source)	ArcGIS (requires subscription)
PIX4D (requires subscription)	Discontinuity set extractor (open source)
ADAM technology (requires subscription)	ADAM technology (requires subscription)

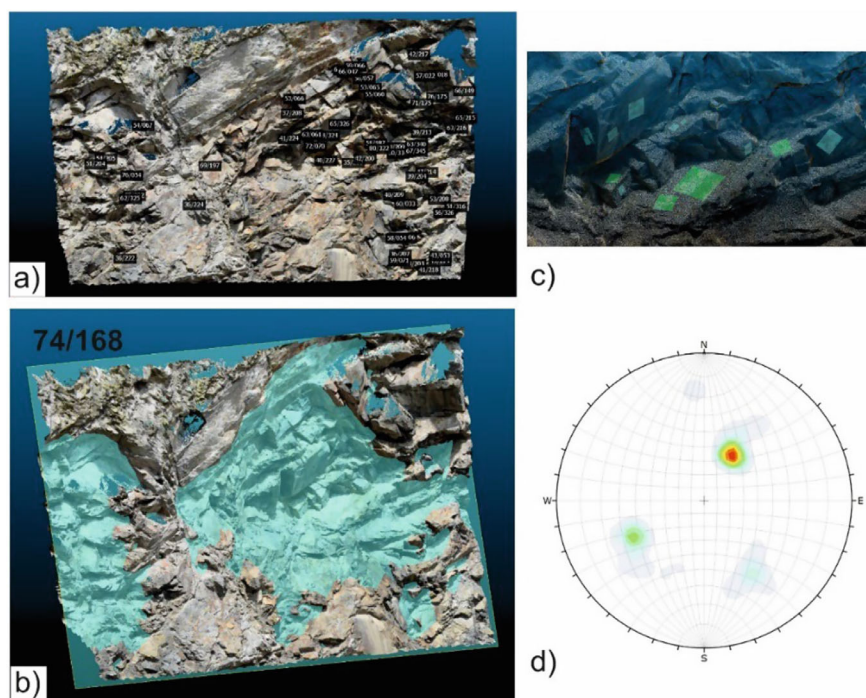


**Fig. 6** **a** Showing orientation of different joint sets found using manual plane fitting in the point cloud. **b** Plane fitted in the point cloud to estimate the orientation of outcrop slope. **c** Zoomed image depicting planes fitted in different joint sets to find the orientation. **d** Stereonet showing the presence of three joint sets in the outcrop

signatures of the block failure, which is also confirmed by the kinematic analysis (Fig. 7) showing the possibility of the wedge failure. The recent versions of wedge stability analysis programs (e.g., Swedge (Rocscience 2022)) allow for performing limit equilibrium (LE) analysis. The LE analysis conducted for the wedge failure in slope using Rocscience Swedge software is shown in Fig. 9b.

### 4.3 Rockfall Detection

Rock fall are frequent events and are serious matter of concerns causing road accidents and infrastructural damage. The three-dimensional photogrammetry models can mark the rockfall origin detection and identification of vulnerable zones within the slope. The photogrammetry technique allows the users to generate 3D point cloud or mesh models of the slope for gathering the information related to rock fall. Dunham et al. (2017) had proposed the Rockfall Activity Index (RAI), which is a morphology-based index, derived from the LiDAR-derived point clouds. RAI

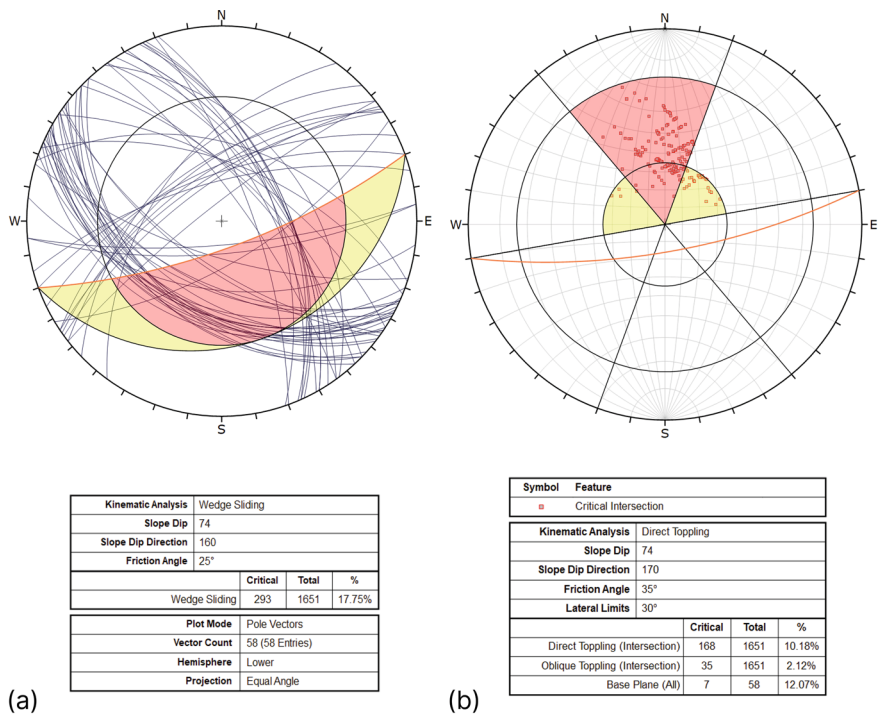


**Fig. 7** Kinematic analysis conducted using the joint data showing two different modes of failure in the slope. **a** Wedge failure **b** direct toppling

provides information on the increasing vulnerability of rockfall activity at cm-scale accuracy. Similarly, based upon the LiDAR technique, Matasci et al. (2017) have tried to quantify the susceptibility of the rockfall covering an area of thousands of square meters at a local to a sub-regional scale. Depending upon the types of failure, locations of the rockfall susceptible areas, and overhanging parts of the slope, the point cloud had been classified for the analysis. However, to overcome the extension of the problem of the overhang in the digital photogrammetry technique for rockfall, Albarelli et al. (2021) has proposed an advanced methodology to relocate and visualize the potential rockfall sources of a vulnerable rock slope by using the point cloud derived from the images taken by UAV. The suggested methodology follows four steps: (a) Generation of the 3D point cloud from image UAV imagery, (b) Characterized the discontinuity sets on generated point cloud, (c) Slope stability analysis based on SMR index, (d) Estimation of Rockfall Susceptibility Index on the 3D point cloud. The methodology, proposed by Albarelli et al. (2021), provides the information to visualize persistence, slope mass rating index and normal spacing using point cloud. Thus, the making of a realistic 3D model as well as rockfall stability analysis would be done very precisely through the photogrammetry method.

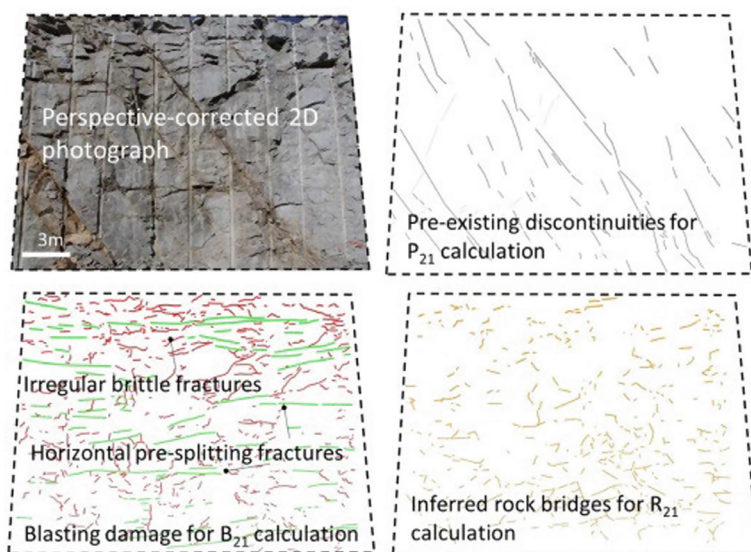


**Fig. 8** Digital fracture trace mapping window marked on the outcrop at the mine site (Tuckey and Stead 2016)

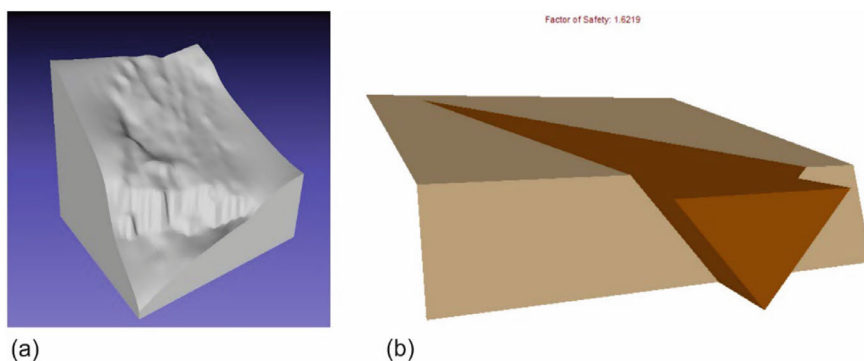


**Fig. 9** **a** 3D closed geometry of the slope **b** limit equilibrium analysis conducted using Swedge software for the wedge formed by the intersection of two joints

#### 4.4 Monitoring Deformation

Among different objectives, the maintenance of the safety conditions of any natural structure as well as artificial civil engineering structures is emerging as one of the important topics for concern. It requires sufficient information of deformation for analysis and prediction purposes. For this aspect, the digital photogrammetric technique has evolved as the best solution for structural deformation monitoring. The

methodologies used in the monitoring of deformation are broadly divided into two types, Surface-point Tracking (SPT) and comparison of 3D surfaces (Scaioni et al. 2015). The main objective of SPT is to reconstruct the 2D or 3D surface displacement model from the images captured from fixed cameras or multi-station fixed cameras. Digital Image Correlation (DIC) or image matching techniques are the concepts that are based on the SPT principle. Based on the user, “seed” points or nodes of grids are taken for the image matching technique from the master image (Le Moigne et al. 2011; Baker et al. 2011; Grün 2012). Area-based matching (ABM) and Feature-based matching (FBM) are the basic concepts in the SPT technique (Grün 2012). When the deformation is a homogeneous shift, then the Normalized Cross-correlation (NCC) algorithms are generally used to trace the deformation pattern between the master and slave images. However, for the case of other geometric deformation, Least-squares Matching (LMC) is adopted for the SPT image matching technique. Feature-based matching is considered for the extraction of two sets of candidate homologous points. The preferred algorithms used for feature-based matching are SIFT and SURF (Lowe 2004; Bay et al. 2008). When the deformation is quick, then the FBM is preferred over ABM due to the robustness and repeatability factor in the identification of similar points within the images (Barazzetti et al. 2010).

Comparison of digital surface models or 3D surfaces is marked as the precise and faithful description of the slope topography. The point cloud-based dense image matching algorithms are used to derive the digital surface model for the purpose of analysing the deformation pattern. The main challenges for dense image matching are the reconstruction of a surface under sharp edges or low-texture portion and robustness against outliers for different causative reasons (Scaioni et al. 2015). Point-to-point, point-to-surface and surface-to-surface fitting of local regular surfaces analysis are the tools used to compare the two DSMs by establishing the Exterior Orientation (EO) of the photogrammetric blocks (Xue et al. 2014). Conditions like the direction of displacements, noise, point density, surface roughness, sharp break lines, gaps, or holes in the data sets are also carefully handled during the comparison process. Nowadays, advanced computer programs are used for better and error-free comparison or image matching processes to monitor the deformation pattern.

## 4.5 *Detection of Landslides*

The photogrammetry analysis does not provide only the geometry of the slope but also provides information about the qualitative description of the surface (Walstra et al. 2007). The 3D point cloud helps in the reconnaissance survey as well as the stereoscopic view, which identifies the effect of different landscape patterns on slope stability. Photogrammetry can be utilized in various stages of the landslide investigation (Mantovani et al. 1996), together with previously discussed applications, the landslide detection and classification is also one of the important objective in the landslide analysis (Crozier 1984; Van Zuidam 1985). The proper investigation of the 3D model generates from the point cloud helps in diagnostic the surface



feature such as morphology, topography, vegetation cover, soil moisture and drainage pattern. Comparing historical images with the recent photograph will help to detect the temporal deformation or movement in the area. The aerial extension of the landslide, changes of head scar, displacement velocity, deformation of surface topography during a landslide event can be derived from the sequential photogrammetric analysis (Chandler 1989). Apart from these objectives, the landslide hazard mapping, as well as the susceptibility mapping are done from the photogrammetric analysis at a local to regional scale. Aerial photogrammetry, satellite high-resolution imagery or optical imagery and close-range photogrammetry are the different applications used to detect ground deformation in photogrammetric analysis for landslides. In aerial photogrammetry, the reconstruction of Digital Terrain Models (DTM) is compared over the period to detect any surficial movement or deformation (Casson et al. 2005). Similarly, the orthoimages are created from aerial photogrammetry to track horizontal movement (Wiegand et al. 2013). In the case of satellite high-resolution imagery, the tracking of surficial movement is done with the help of aerial images (Debella-Gilo and Käab 2012). However, the accuracy of this application depends upon the temporal resolution of the DTMs used for the analysis. A single-camera system, stereo-camera and multi-station networks are the option present in the close-range photogrammetry. Multiple DTMs are created from the point cloud generated by the close-range photogrammetry to compare and detect the volumetric changes within a landslide as well as the deformation pattern (Roncella et al. 2004; Feng et al. 2012). For shallow landslide monitoring, the multi-station networks give a better outcome (Akca 2013). Different characterization methods like feature, pixel and object-based techniques can be executed for delineating landslide boundaries using remotely sensed photographs (Lu et al. 2020; Su et al. 2021). The recent advancement in AI, particularly Convolutional Neural Networks (CNNs) lead to successful implementation for object detection and image segmentation (Ghorbanzadeh et al. 2020; Shi et al. 2020). The studies consider different topographical factors such as elevation along with its derivatives like slope, aspect, and curvature for improved landslide detection (Sameen and Pradhan 2019; Liu et al. 2020; Prakash et al. 2020).

## 5 Limitations

Photogrammetry makes visual analysis much easier and simpler in the various fields of science. Therefore, it has been identified as the most effective non-contact analysis method. However, some limitations are there in the study. These are:

- a. The equipment used for the photogrammetry should be very sensitive to capture each moment very precisely with a very high pixel quality.
- b. The image matching algorithm is very complex and difficult to operate.
- c. Photogrammetry does not have penetration ability.
- d. The photography skill of the operator is also very important for terrestrial photogrammetry.

- e. The environmental condition (fog, snowfall, rainfall) while capturing the image is also responsible for an error.
- f. Proper light source is required to take the photographs for better resolution.

## 6 Concluding Remarks

The photogrammetry technique possesses wider applicability in engineering geology for examining slope stability and landslides. It is an economical and reliable technique compared to LiDAR or other laser techniques for 3D point cloud generation. The point clouds developed using photogrammetry can not only be used for collecting basic engineering geological data, but also to monitor and detect the landslides, hence implying its versatility. Further, integrating thermal and multispectral imaging with photogrammetry has numerous advantages for detecting rock bridges, open fractures, lithology contrast and seepage conditions. However, it requires sophisticated cameras for photography and high precision navigation devices for marking GCPs. Further, the environment and climatic conditions influence the intensity of each pixel and accuracy of navigational systems. Handling data and processing point clouds needs specifically designed software and hardware devices. Merging the point clouds with other remote sensing data sets such as thermal increases additional cost, data complexity and equipment. Overcoming its limitations, photogrammetry is an effective medium in surveying and mapping the risk possessing slopes for hazard mitigation and risk assessment by remotely sensing the target without any physical contact.

**Acknowledgements** We thank Department of Earth sciences, IIT Roorkee for providing facilities and support. We are grateful to anonymous reviewers and editor for their useful suggestions.

**Declarations** The authors declare no competing interests.

## References

- Akca D (2013) Photogrammetric monitoring of an artificially generated shallow landslide. *Photogramm Rec* 28(142):178–195
- Albarelli DSNA, Mavrouli OC, Nyktas P (2021) Identification of potential rockfall sources using UAV-derived point cloud. *Bull Eng Geol Environ* 80:6539–6561. <https://doi.org/10.1007/s10064-021-02306-2>
- An P, Fang K, Zhang Y, Jiang Y, Yang Y (2022) Assessment of the trueness and precision of smartphone photogrammetry for rock joint roughness measurement. *Measurement* 188:110598. <https://doi.org/10.1016/j.measurement.2021.110598>
- Baker S, Scharstein D, Lewis JP, Roth S, Black MJ, Szeliski R (2011) A database and evaluation methodology for optical flow. *Int J Comput vis* 92(1):1–31
- Barazzetti L, Remondino F, Scaioni M (2010) Orientation and 3D modelling from markerless terrestrial images: combining accuracy with automation. *Photogramm Rec* 25:356–381



- Barton N, Choubey V (1977) The shear strength of rock joints in theory and practice. *Rock Mech* 10:1–54
- Bay H, Ess A, Tuytelaars T, Van Gool L (2008) Speeded-up robust features (SURF). *Comput vis Image Underst* 110(3):346–359
- Bennett GL, Molnar P, Eisenbeiss H, McArdell BW (2012) Erosional power in the Swiss Alps: characterization of slope failure in the Illgraben. *Earth Surf Process Landf* 37:1627–1640
- Bistacchi A, Griffith WA, Smith SAF, Di Toro G, Jones R, Nielsen S (2011) Fault roughness at seismogenic depths from LIDAR and photogrammetric analysis. *Pure Appl Geophys* 168:2345–2363
- Carrivick JL, Smith MW, Quincey DJ (2016) Structure from motion in the geosciences (analytical methods in earth and environmental science). Wiley Kindle Edition
- Casson B, Delacourt C, Baratoux D, Allemand P (2003) Seventeen years of the ‘La Clapière’ landslide evolution analysed from orthorectified aerial photographs. *Eng Geol* 68:123–139
- Casson B, Delacourt C, Allemand P (2005) Contribution of multi-temporal sensing images to characterize landslide slip surface application to the La Clapière landslide (France). *Nat Hazards Earth Syst Sci* 5(3):425–437
- Cenni N, Fiaschi S, Fabris M (2021) Integrated use of archival aerial photogrammetry, GNSS, and InSAR data for the monitoring of the Patigno landslide (Northern Apennines, Italy). *Landslides* 18:2247–2263. <https://doi.org/10.1007/s10346-021-01635-3>
- Chandler JH (1989) The acquisition of spatial data from archival photographs and their application to geomorphology. Ph.D. thesis. The City University, London
- Cigna F, Bianchini S, Casagli N (2013) How to assess landslide activity and intensity with persistent Scatterer interferometry (PSI): the PSI-based matrix approach. *Landslides* 10(3):267–283. <https://doi.org/10.1007/s10346-012-0335-7>
- Crozier MJ (1984) Field assessment of slope instability. In: Brunsdon D, Prior DB (eds) *Slope instability*. Wiley, Chichester, pp 103–142
- Debella-Gilo M, Käab A (2012) Measurement of surface displacement and deformation of mass movements using least squares matching of repeat high resolution satellite and aerial images. *Remote Sens* 4:43–67
- Demoulin A (2006) Monitoring and mapping landslide displacements: a combined DGPS-stereophotogrammetric approach for detailed short and long-term rate estimates. *Terra Nova* 18(4):290–298. <https://doi.org/10.1111/j.1365-3121.2006.00692.x>
- Donati D, Stead D, Onsel E (2018) New approaches to characterize brittle fracture and damage in fracture rock masses. In: 10th Asian rock mechanics symposium (ARMS10), Singapore—the 2018 ISRM international symposium
- Donati D, Stead D, Lato M, Gaib S (2020) Spatio-temporal characterization of slope damage: insights from the Ten Mile Slide, British Columbia, Canada. *Landslides* 17:1037–1049. <https://doi.org/10.1007/s10346-020-01352-3>
- Dunham L, Wartman J, Olsen MJ, O'Banion M, Cunningham K (2017) Rockfall activity index (RAI): a lidar-derived, morphology-based method for hazard assessment. *Eng Geol* 221:184–192. <https://doi.org/10.1016/j.enggeo.2017.03.009>
- Feng T, Liu X, Scaioni M, Lin X, Li R (2012) Real-time landslide monitoring using close-range stereo image sequences analysis. In: 2012 international conference on systems and informatics (ICSAI), (ICSAI 2012), Yantai, P. R. China, 19–21 May 2012, pp 249–253
- Francioni M, Simone M, Stead D, Sciarra N, Mataloni G, Calamita FA (2019) New fast and low-cost photogrammetry method for the engineering characterization of rock slopes. *Remote Sens* 11:1267
- Ferreira E, Chandler J, Wackrow R, Shiono K (2017) Automated extraction of free surface topography using SfM-MVS photogrammetry. *Flow Meas and Instrum* 54:243–249
- Fobert M-A, Singhroy V, Spray JG (2021) InSAR monitoring of landslide activity in Dominica. *Remote Sens*. <https://doi.org/10.3390/rs13040815>
- Fryer J, Mitchell H, Chandler JH (2007) Applications of 3D measurement from images. Whittles Publishing

- Ghorbanzadeh O, Tiede D, Wendt L, Sudmanns M, Lang S (2020) Transferable instance segmentation of dwellings in a refugee camp—integrating CNN and OBIA European. *J Remote Sens* 1–14. <https://doi.org/10.1080/22797254.2020.1759456>
- GPL Software (2018) Cloud compare V.2.9. <http://www.cloudcompare.org>
- Gordon S, Licht D, Stewart M (2001) Application of a high-resolution, ground-based laser scanner for deformation measurements. In: *Proceedings of the 10th international FIG symposium on deformation measurements*. Orange, California, USA, 19–22 Mar 2001, pp 23–32
- Grün A (2012) Development and status of image matching in photogrammetry. *Photogramm Rec* 27:36–57
- Haneberg WC (2008) Using close range terrestrial digital photogrammetry for 3-D rock slope modeling and discontinuity mapping in the United States. *Bull Eng Geol Environ* 67:457–469. <https://doi.org/10.1007/s10064-008-0157-y>
- Havaej M, Coggan J, Stead D, Elmo D (2015) A combined remote sensing–numerical modeling approach to the stability analysis of Delabole Slate Quarry. *Cornwall UK Rock Mech Rock Eng* 178:1–19
- ISRM (1978) Suggested methods for the quantitative description of discontinuities in rock masses. *Int J Rock Mech Min Sci Geomech Abstr* 15:319–336
- Jaboyedoff M, Oppikofer T, Abellán A, Derron M-H, Loye A, Metzger R, Pedrainsi A (2012) Use of LIDAR in landslide investigations: a review. *Nat Hazards* 61:5–28. <https://doi.org/10.1007/s11069-010-9634-2>
- Javernick L, Brasington J, Caruso B (2014) Modeling the topography of shallow braided rivers using Structure-from-Motion photogrammetry. *Geomorphology* 213:166–182
- Kim DH, Poropat G, Gratchev I, Balasubramaniam A (2016) Assessment of the accuracy of close distance photogrammetric JRC data. *Rock Mech Rock Eng* 49:4285–4301. <https://doi.org/10.1007/s00603-016-1042-9>
- Lato M, Hutchinson DJ, Gauthier D, Edwards T, Ondercin M (2015a) Comparison of ALS, TLS and terrestrial photogrammetry for mapping differential slope change in mountainous terrain. *Can Geotech J* 52(2):129–140. <https://doi.org/10.1139/cgj-2014-0051>
- Lato M, Gauthier D, Hutchinson DJ (2015b) Selecting the optimal 3D remote sensing technology for the mapping, monitoring and management of steep rock slopes along transportation corridors. *Transp Res Rec J Transp Res Board* 2510:7–14. <https://doi.org/10.3141/2510-02>
- Lenka SK, Panda SD, Kanungo DP, Anbalagan R (2017) Slope mass assessment of road cut rock slopes along Karnprayag to Narainbagarh highway in Garhwal Himalayas, India. In: *Advancing culture of living with landslides, vol 5. Landslides in different environments, 4th world landslide forum*, Ljubljana, Slovenia, pp 407–413. <https://doi.org/10.1007/978-3-319-53483-1>
- Le Moigne J, Netanyahu NS, Eastman RD (2011) *Image registration for remote sensing*. Cambridge University Press, UK, p 484
- Lowe DG (2004) Distinctive image features from scale-invariant keypoints. *Int J Comput vis* 60(2):91–110
- Lissak C, Bartsch A, De Michele M, Gomez C, Maquaire O, Raucoules D, Roulland T (2020) Remote sensing for assessing landslides and associated hazards. *Surv Geophys* 41:1391–1435. <https://doi.org/10.1007/s10712-020-09609-1>
- Liu P, Wei YM, Wang QJ, Chen Y, Xie JJ (2020) Research on post-earthquake landslide extraction algorithm based on improved U-Net model. *Remote Sens* 12. <https://doi.org/10.3390/rs12050894>
- Lu H, Ma L, Fu X, Liu C, Wang Z, Tang M, Li NW (2020) Landslides information extraction using object-oriented image analysis paradigm based on deep learning and transfer learning. *Remote Sens* 12(5):752. <https://doi.org/10.3390/rs1205075>
- Mantovani F, Soeters R, Van Westen CJ (1996) Remote sensing techniques for landslide studies and hazard zonation in Europe. *Geomorphology* 15:213–225
- Matasci B, Stock GM, Jaboyedof M, Carrea D, Collins BD, Guérin A, Matasci G, Raveland L (2017) Assessing rockfall susceptibility in steep and overhanging slopes using three-dimensional

- analysis of failure mechanisms. *Landslides* 15:859–878. <https://doi.org/10.1007/s10346-017-0911-y>
- Mateos RM, Azañón JM, Roldán FJ, Notti D, Perez-Pena V, Galve JP, Perez-Garcia JL, Colomo CM, Gomez-Lopez JM, Montserrat O, Devantery N, Lamas-Fernandez F, Fernandez-Chacon F (2017) The combined use of PSInSAR and UAV photogrammetry techniques for the analysis of the kinematics of a coastal landslide affecting an urban area (SE Spain). *Landslides* 14:743–754. <https://doi.org/10.1007/s10346-016-0723-5>
- Melanie JF, David NP (2018) Global fatal landslide occurrence from 2004 to 2016. *Nat Hazards Earth Syst Sci* 18:2161–2218
- Micheletti N, Chandler JH, Lane SN (2015) Structure from motion (SfM) photogrammetry. *Br Soc Geomorphol* 33
- Mitelman A, Elmo D (2014) Modelling of blast-induced damage in tunnels using a hybrid finite-discrete numerical approach. *J Rock Mech Geotech* 6:565–573
- Paixão A, Muralha J, Resende R, Fortunato E (2022) Close-range photogrammetry for 3D rock joint roughness evaluation. *Rock Mech Rock Eng* 55:3213–3233. <https://doi.org/10.1007/s00603-022-02789-9>
- Peternel T, Kumelj Š, Oštir K, Komac M (2017) Monitoring the Potoška planina landslide (NW Slovenia) using UAV photogrammetry and tachymetric measurements. *Landslides* 14:395–406. <https://doi.org/10.1007/s10346-016-0759-6>
- Pradhan SP, Panda SD, Roul AR, Thakur M (2019) Insights into the recent Kotropi landslide of August 2017, India: a geological investigation and slope stability analysis. *Landslides* 16:1529–1537. <https://doi.org/10.1007/s10346-019-01186-8>
- Prakash N, Manconi A, Loew S (2020) Mapping landslides on EO data: performance of deep learning models vs. traditional machine learning models. *Remote Sens* 12(3). <https://doi.org/10.3390/rs1203>
- Riquelme AJ, Abellan A, Tomas R (2015) Discontinuity spacing analysis in rock masses using 3D point clouds. *Eng Geo* 195:85–195. <https://doi.org/10.1016/j.enggeo.2015.06.009>
- Roncella R, Scaioni M, Forlani G (2004) Application of digital photogrammetry in geotechnics. *Int Arch Photogram Remote Sens Spat Inf Sci* 35(1):93–98
- Rothermel M, Wenzel K, Fritsch D, Haala N (2012) SURE: photogrammetry surface reconstruction from imagery. In: *LC3D Workshop*: Berlin, Germany, p 9
- Salvini R, Mastrorocco G, Seddaiu M, Rossi D, Vanneschi C (2016) The use of an unmanned aerial vehicle for fracture mapping within a marble quarry (Carrara, Italy): photogrammetry and discrete fracture network modelling. *Geomat Nat Haz Risk*. <https://doi.org/10.1080/19475705.2016.1199053>
- Sameen MI, Pradhan B (2019) Landslide detection using residual networks and the fusion of spectral and topographic information. *IEEE Access* 7:114363–114373. <https://doi.org/10.1109/access.2019.2935761>
- Sarro R, Riquelme A, García-Davalillo JC, Mateos RM, Tomás R, Pastor JL, Cano M, Herrera G (2018) Rockfall simulation based on UAV photogrammetry data obtained during an emergency declaration: application at a cultural heritage site. *Remote Sens* 10(12):1923. <https://doi.org/10.3390/rs10121923>
- Scaioni M, Feng T, Barazzetti L, Previtali M, Roncella R (2014) Image-based deformation measurement. *Appl Geomat* 7:75–90. <https://doi.org/10.1007/s12518-014-0152-x>
- Scaioni M, Feng T, Lu P, Qiao G, Tong X, Li R, Barazzetti L, Previtali M, Roncella R (2015) Close-range photogrammetric techniques for deformation measurement: applications to landslides. In: *Modern technologies for landslide monitoring and prediction*, pp 13–41
- Shi W, Zhang M, Ke H, Fang X, Zhan Z, Chen S (2020) Landslide recognition by deep convolutional neural network and change detection. *IEEE Trans Geosci Remote Sens* 59(6):1–19. <https://doi.org/10.1109/TGRS.2020.3015826>
- Singh J, Thakur M (2019) Landslide stability assessment along Panchkula-Morni Road, Nahan salient, NW Himalaya, India. *J Earth Syst Sci* 128:148

- Singh J, Pradhan SP, Singh M, Hruaikima L (2022) Control of structural damage on the rock mass characteristics and its influence on the rock slope stability along National Highway-07, Garhwal Himalaya, India: an ensemble of discrete fracture network (DFN) and distinct element method (DEM). *Bull Eng Geol Environ* 81:96
- Singh J, Pradhan SP, Vishal V, Singh M (2023) Characterization of a fractured rock mass using geological strength index: a discrete fracture network approach. *Transp Geotech* 40:100984. <https://doi.org/10.1016/j.tgeo.2023.100984>
- Stead D, Wolter A (2015) A critical review of rock slope failure mechanisms: The importance of structural geology. *J Struct Geol* 74:1–23. <https://doi.org/10.1016/j.jsg.2015.02.002>
- Stumpf A, Malet JP, Allemand P, Pierrot-Deseilligny M, Skupinski G (2015) Groundbased multi-view photogrammetry for the monitoring of landslide deformation and erosion. *Geomorphology* 231:130–145
- Sturzenegger M, Stead D (2009) Quantifying discontinuity orientation and persistence on high mountain rock slopes and large landslides using terrestrial remote sensing techniques. *Nat Hazards Earth Syst Sci* 9:267–287. <https://doi.org/10.5194/nhess-9-267-2009>
- Su Z, Chow JK, Tan PS, Wu J, Ho YK, Wang Y-H (2021) Deep convolutional neural network-based pixel-wise landslide inventory mapping. *Landslides* 18:1421–1443. <https://doi.org/10.1007/s10346-020-01557>
- Tannant DD (2015) Review of photogrammetry-based techniques for characterization and hazard assessment of rock faces. *Int J Geohazards Environ* 1(2):76–87
- Tuckey Z, Stead D (2016) Improvements to field and remote sensing methods for mapping discontinuity persistence and intact rock bridges in rock slopes. *Eng Geol*. <https://doi.org/10.1016/j.enggeo.2016.05.001>
- Unal M, Yakar M, Yildiz F (2004) Discontinuity surface roughness measurement techniques and the evaluation of digital photogrammetric method. In: *Proceedings of the 20th international congress for photogrammetry and remote sensing, ISPRS*, pp 1103–1108
- Van Zuidam RA (1985) Aerial photo-interpretation in terrain analysis and geomorphological mapping. Smits, The Hague
- Walstra J, Chandler JH, Dixon N, Dijkstra TA (2007) Aerial photography and digital photogrammetry for landslide monitoring. *Geol Soc Lon Spec Publ* 283:53–63
- Warrick JA, Ritchie AC, Schmidt KM, Logan JB (2019) Characterizing the catastrophic 2017 Mud Creek landslide, California, using repeat structure-from-motion (SfM) photogrammetry. *Landslides* 16:1201–1219. <https://doi.org/10.1007/s10346-019-01160-4>
- Wester-Ebbinghaus W (1986) Analytical camera calibration. *Int Arch Photogram Remote Sens* 26:77–84
- Westaway RM, Lane SN, Hicks DM (2000) The development of an automated correction procedure for digital photogrammetry for the study of wide, shallow, gravel-bed rivers. *Earth Surf Process Landf* 25:209–226
- Westoby MJ, Brasington J, Glasser NF, Hambrey MJ, Reynolds JM (2012) “Structure-from-motion” photogrammetry: a low-cost, effective tool for geoscience applications. *Geomorphology* 179:300–314
- Wiegand C, Rutzinger M, Heinrich K, Geitner C (2013) Automated extraction of shallow erosion areas based on multi-temporal ortho-imagery. *Remote Sens* 5:2292–2307
- Wolf P, Dewitt B, Wilkinson B (2014) Elements of photogrammetry with application in GIS, 4th edn. McGraw-Hill Education, Maidenhead
- Xu Q, Li WL, Ju Yz, Dong Xj, Peng D (2020) Multitemporal UAV-based photogrammetry for landslide detection and monitoring in a large area: a case study in the Heifangtai terrace in the Loess Plateau of China. *J Mt Sci* 17:1826–1839. <https://doi.org/10.1007/s11629-020-6064-9>
- Xue Q, Zhang M, Zhu L, Cheng X, Pei Y, Bi J (2014) Quantitative deformation analysis of landslides based on multi-period DEM data. In: Sassa K, Canuti P, Yin Y (eds) 2014. *Landslide science for a safer geoenvironment*, vol 2. Springer, Heidelberg, pp 201–207

**Dr. Jaspreet Singh** received his Ph.D. in Engineering Geology from IIT Roorkee, India and Masters in Geology from Panjab University Chadigarh. He is currently working as a Postdoctoral fellow at Simon Fraser University, Canada. His expertise is in using remote sensing, numerical modeling, geotechnical and geophysical methods for landslide investigation. His Ph.D. research was focused on understanding slope stability and rock mass characterization of Himalayan Road cut slopes using numerical modeling and discrete fracture network. He works on 2D and 3D computationally based modelling for complex rock slope stability assessment/ landslide modelling by coupling remote sensing (LiDAR, Photogrammetry, InSAR) derived datasets. He is recipient of Dr. Shyama Prasad Mukherjee Fellowship by CSIR, Government of India.

**Dr. Amulya Ratna Roul** is a post-doctoral fellow at the Department of Earth Sciences, IIT Bombay, India. He received his Ph.D. in 2021 from IIT Roorkee, specializing in landslide and slope stability analysis, with his thesis focused on the Stability Analysis of Slopes in Eastern Ghats, Odisha, India. Dr. Roul has published extensively in leading international journals and conferences, with research interests spanning landslides, slope stability, numerical modeling, and rock and soil mechanics. In addition to his research publications, Dr. Roul has contributed as a research person to several R&D projects related to landslide studies in the Himalayas and Ghats regions of India. He completed his M.Sc. in Applied Geology from IIT Roorkee in 2015 and his B.Sc. (Hons) in Geology from North Orissa University in 2013. In 2014, he was awarded the Summer Research Fellowship by the Indian Academy of Sciences (IASc).

**Mr. Saurabh Prakash Aher** is a research scholar specializing in slope stability at Department of Earth Sciences, Indian Institute of Technology, Roorkee. He has done B.Sc. (Geology) from Fergusson College, Pune and M.Sc. (Geology) from Savitribai Phule Pune University. His research focuses on the stability of reactivating large-scale landslides in the Northwestern Himalayas. His research interest includes multidimensional slope stability analysis using different numerical simulation methods, designing of suitable mitigation measures to arrest the slope failures and engineering geological and geotechnical behavior of geomaterial. Prior to this, he has previously conducted research on the issues of slope stability and rockfall in the Western Ghats.

**Dr. Sarada Prasad Pradhan** is currently working as an Associate Professor in Indian Institute of Technology (IIT) Roorkee, India in the Department of Earth Sciences. He obtained his M. Sc. (Applied Geology) and Ph.D. from IIT Bombay (India). He worked as a Reservoir Engineer in Oil and Natural Gas Corporation Ltd. (ONGC) for around 5 years where he was associated with many projects of national importance. He was recipient of outstanding young faculty award by IIT Roorkee, Melpadom Attumalil Georgekutty Young Scientist Award, Young Scientist Award from CAFET INNOVA Technical Society and Award of excellence from ONGC Ltd. His research findings have been well received by the scientific community and published in leading national and international journals, book chapters and conference proceedings. He is investigating three major research projects on slope stability. His major research interests are Rock Mechanics, Engineering Geology, Slope Stability, Reservoir Geo-mechanics, Petroleum Geo-science and Carbon Dioxide Sequestration.

**Dr. Vikram Vishal** is a Professor in the Department of Earth Sciences, IIT Bombay, Mumbai. He completed his bachelor's degree at Presidency College, Kolkata and his Master's degree at IIT Bombay. After a brief stint as a geologist in Tata Steel, he pursued his Ph.D. degree during 2010–2012, jointly at IIT Bombay and Monash University (Australia). He worked as DST Inspire Faculty in the Department of Earth Sciences, Indian Institute of Technology (IIT) Roorkee during 2013–2015. He went on to pursue further research as a Fulbright-Nehru Postdoctoral fellow at Stanford University, California, USA in 2015. He is a recipient of the National Geosciences Award—Young Researcher by the Government of India, the Young Scientist Award by the Indian Science Congress Association, the Excellence in Ph.D. Thesis Award by IIT Bombay and Monash

University, and the Best Undergraduate Gold Medal by Presidency College, Kolkata. He holds to his credit over 40 publications on different domains of geomechanics, engineering geology and unconventional petrophysics in various journals, book chapters and conference proceedings of repute. Recently, he co-edited the book titled “Geologic Carbon Sequestration: Understanding Reservoir Concepts” by Springer. He also serves as an Associate Editor for the Journal of Natural Gas Science and Engineering by Elsevier. He is investigating three research projects funded by the Ministry of Science and Technology by the Govt. of India.

# Empirical Method Based Geotechnical Assessment of Engineered Slopes Along National Highway-58, Rajasthan, India



Tariq Siddique, Aquib Shamshad, Tuba Fatima, Pirzada Mohammad Haris, and Md. Erfan Ali Mondal

**Abstract** The study encompasses geotechnical evaluation in the Aravalli-Delhi fold belt. Slope mass rating (SMR) technique and Continuous slope mass rating (CoSMR) have been applied to assess the stability of road cut slopes along NH-58 from Ajmer to Pushkar. The studied five slopes are vulnerable to planar failure, which is further validated by kinematic analysis. Subsequently, the SMR values indicate three slopes are in unstable condition. In addition, to assure more robustness in results, the stability of all slopes was further evaluated by employing a design chart-based technique, Slope stability rating (SSR). As per SSR outcomes, stable slope angles range between  $50^\circ$  and  $70^\circ$  to achieve 1.5 factor of safety. Kinematic analysis-based factor of safety was also determined using pertinent geotechnical parameters. Findings obtained from different methods shows good agreement with each other.

**Keywords** Slope mass rating · Slope stability rating · Kinematic analysis · Factor of safety

## 1 Introduction

In mountainous areas, steep road-cut slopes are vulnerable to landslide due to adverse geological and geotechnical conditions of the rock mass and other factors induced by the environment, including seismicity and water condition of the slope (Pantelidis 2009). The material of the slope i.e. rock type, height and extent of the slope, slope angle, and rock discontinuity orientations govern stability of slopes. In addition to these, increased anthropogenic intervention is a matter of great concern. Infrastructure development such as highways and railways located in river valleys may be located below such slopes, or cut into the toe, which may be detrimental to stability (Hoek and Bray 1981). In India, the geodynamically active Himalayan range, eastern and western ghats are the focus for majority of landslide studies. Geologically, the presence of young, active fold mountains and rejuvenated faults,

---

T. Siddique (✉) · A. Shamshad · T. Fatima · P. M. Haris · Md. E. A. Mondal  
Department of Geology, Aligarh Muslim University, Aligarh 202002, India  
e-mail: [tsiddique@myamu.ac.in](mailto:tsiddique@myamu.ac.in)



combined with anthropogenic factors such as unplanned urbanization in high-risk areas, road widening along cut slopes, environmental degradation, and population expansion, significantly contribute to the occurrence of these geohazards (Pradhan et al. 2015). The assessment of slope stability is a critical task in the tectonically deformed and fragile rock masses, where climatic conditions are unpredictable (Sarkar et al. 2021). The highway corridors along the Western Ghats are experiencing a significant threat from the crumbling of unstable geomaterials, posing risks to the surrounding ecosystem and properties (Niyogi et al. 2020). Recently, intense monsoon rainfall and cyclonic disturbances have induced severe landslides in the eastern ghats. Generally, it has been witnessed that failure events predominantly occur during and post-precipitation events in the region (Roul et al. 2021). From the perspective of landslide studies, Rajasthan has not received as much attention yet. Research on landslides and instability issues along the highways is necessary. On October 4, 2019, multiple areas within Rajasthan experienced extensive detrimental impact to human life, infrastructure, and natural resources as a result of a catastrophic landslide event. A landslip occurred in the Umaid Bhawan Formation (UBF) of the Jodhpur Group (JG) near Masuriya Hill in Jodhpur (Mathur et al. 2020). The 2015 floods around Jalore, Rajasthan, caused a landslide disaster with few recorded casualties (NDTV 2015). The road to Mount Abu was blocked due to a reported landslide incident in the vicinity of Harna Hanuman Road (The Economic Times 2015). These are a few instances of the destruction that occurred in Rajasthan that resulted in infrastructure failure, human casualties, and other environmental risks.

The study includes the geotechnical assessment of road cut slopes in the Ajmer district of Rajasthan. Field investigations were conducted in order to examine the stability, likelihood of failure and support required in road cut slopes between Ajmer and Pushkar along National highway-58 (NH-58). Five vulnerable locations were selected for detailed geotechnical study. The concerned route is heavily loaded with vehicular traffic. Thus, even a small failure may cause lots of inconvenience and may cause fatal accidents. NH-58 cuts the northeast-southwest trending ridge of Aravalli-Delhi fold belt with keen bends and sharp hairpin turns. This reduces the decision sight distance and thereby increasing probability of accidents due to occasional rock-falls and slope failures. Similar geotechnical work has been done in nearby area, along NH-48 (NH-8 erstwhile) from Udaipur to Ahmadabad (Bhardwaj and Salvi 2011). The study concluded that more stability analysis needs to be conducted along road cut slopes within vulnerable sections of the Aravalli mountains. The present study is attempted to characterize vulnerable road cut slopes along NH-58 from Ajmer to Pushkar by using rock mass classification tools. A detailed input of geotechnical factors was used in the present geotechnical investigation, which included laboratory tests and field surveys. Stability was evaluated using different rock mass classification methods, including Rock Mass Rating (RMR), Slope Mass Rating (SMR and CoSMR), Slope Stability Rating (SSR). Furthermore, using the concepts of kinematic analysis, structurally governed failures due to adversely oriented discontinuities were examined and FS was determined. A correlation was found between the outcomes of different rock mass classification techniques.

2 Study Area

The present geotechnical investigation was conducted in the section of NH-58 which joins Pushkar with Ajmer. The investigated section is running through NE-SW trending Aravalli-Delhi fold belt (Fig. 1).

Stratigraphically the studied sites lie in the South Delhi Fold Belt (Fig. 2). Four of the studied slopes (1–4) lie in Quartzite and slope S5 is Granitic Gneiss, which is an emplacement body known as Anasagar Gneiss (Mukhopadhyay et al. 2023). The investigated route is very significant due to pilgrimage activities and tourism.

Fig. 1 DEM of the study area

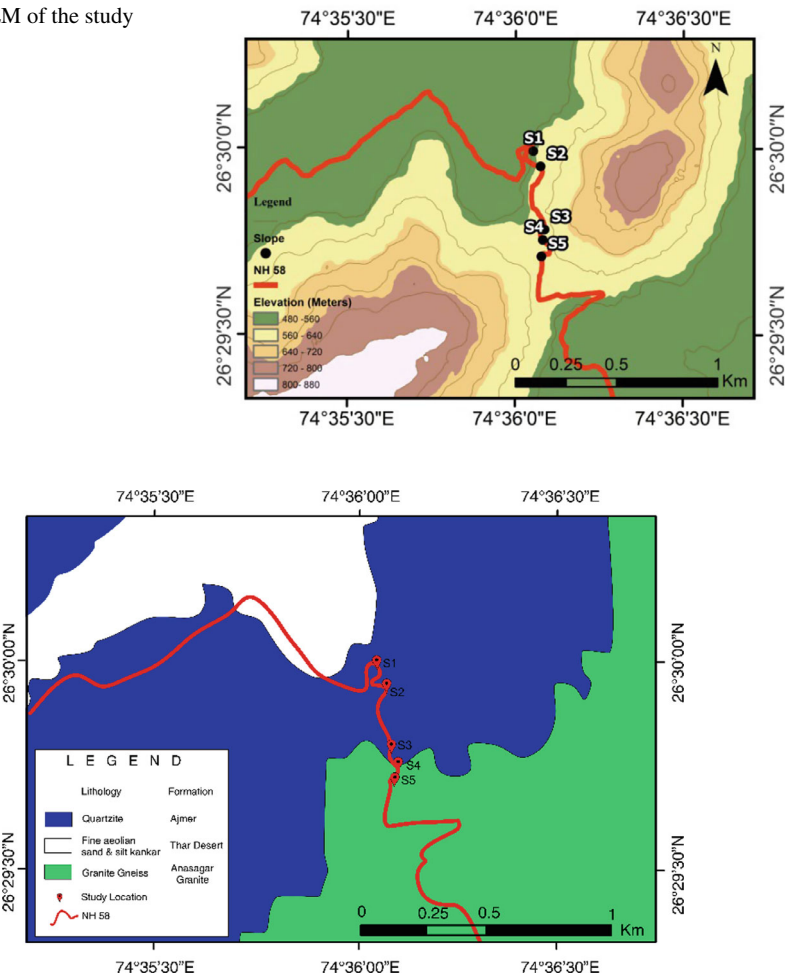


Fig. 2 Stratigraphy of the area depicting investigated slopes. Source District resource map Ajmer, Geological Survey of India, Western Region, Jaipur

### 3 Slope Stability Assessment Along NH-58

In Assessment of geological characteristics and structural attributes in the rock mass is an integral component of geotechnical evaluation. During the field survey along NH-58, five such zones were chosen due to their visual inspection-based vulnerability in the field. Slopes are intersected by multiple sets of discontinuities resulting in fractured and blocky rock masses with minor overhangs. The route is marked with instances of non-scientific roadside planning, very narrow passage and some sharp turns are littered with debris. In studied slopes, minor tension cracks over cut slopes can be witnessed. Additionally, a significant fraction of the studied section is devoid of some common geotechnical safeguards like wire mesh, gabion walls, retaining walls and suitable ditches. The detailed geotechnical data was generated during field survey (Table 1). The adopted methodology for carrying out this work is illustrated via a flowchart (Fig. 3). Observed geotechnical conditions of studied slopes have been shown by field photographs (Fig. 4).

#### 3.1 Rock Mass Rating (RMR)

Rock Mass Rating (RMR) system, a geomechanical classification of rock mass is being extensively utilized in various geo-engineering disciplines including mining, civil construction projects such as tunnelling, roadway development in hilly terrains, dam engineering and hydropower projects. RMR includes six parameters which is ascertained for structural unit, it includes (i) Uniaxial compressive strength (UCS) of intact rock material; which measures the upper most axial load a rock mass can withstand, (ii) rock quality designation (RQD); it's a measure of rock quality, jointing fracturing and shearing, (iii) joint or discontinuity spacing, (iv) discontinuity condition (v) groundwater condition, and discontinuity orientation (Singh and Goel 1999). The compressive strength of rock mass is the evaluation of highest load bearing capacity of the rock mass (Hoek and Bray 1981). In rock mass with joints and fractures, compressive resistance to the load is appreciably affected by the presence of discontinuities (Li and Villaescusa 2005). The compressive strength of rock mass controls its overall quality and plays a critical role in governing the stability. Higher uniaxial compressive strength correlates with greater stability grades. UCS is determined by in-situ Schmidt hammer tests and UCS values are determined using an empirical equation (Yagiz 2009).

$$UCS = 0.0028 \times (Hr)^{2.58} \quad (1)$$

where, Hr is mean Schmidt hammer rebound (SHR) value.

From these UCS values calculated for each slope, the ratings are assigned a per RMR89 by Bieniawski (Table 2).

**Table 1** Geotechnical field data of five cut slopes along NH-58

Location	Orientation		Discontinuity conditions					Groundwater conditions	
	Slope face	Discontinuity sets	Spacing (m)	Persistence (m)	Roughness (JRC)	Aperture (mm)	Weathering	Infilling	
S1 26° 29' 59.54" N 74° 36' 02.93" E	73°/	J1	34°/345°	0.24	–	10–12	< 1	S-M	N
	350°	J2	84°/332°	0.40	5.12	8–10	~ 1	S-M	N
		J3	53°/245°	0.70	1.75	10–12	2–4	S-M	N
		J4	24°/110°	0.18	1.25	–	2–3	S-M	N
S2 26° 29' 57" N 74° 34' 44" E	75°/	J1	15°/275°	0.17	> 20	10–12	< 0.1	S-M	N
	250°	J2	41°/272°	0.22	15	12–14	–	S-M	N
		J3	85°/212°	0.33	7	10–12	–	S-M	N
S3 26° 29' 46.97" N 74° 36' 05.26" E	50°/	J1	46°/070°	0.08	> 20	6–8	< 0.1	S-M	N
	325°	J2	44°/205°	0.83	4–4.5	6–8	2–4	S-M	N
S4 26° 29' 45" N 74° 36' 05" E	51°/	J1	35°/217°	0.41	> 20	4–6	1–2	S-M	N
	220°	J2	72°/210°	0.75	3.45	6–8	3–4	S-M	N
		J3	87°/092°	0.72	3.57	10–12	1–1.5	S-M	N
		J4	70°/010°	0.1	1.37	6–8	1–3	S-M	N
S5 26° 29' 43.82" N 74° 36' 03.62" E	60°/	J1	34°/345°	0.19	20	5	0.1–0.3	S-M	N
	355°	J2	68°/090°	0.55	9	3	1	S-M	N
		J3	57°/172°	0.5	3	5	0.1–1	S-M	N
Location	SHR values		φ in degree				Method of excavation		
S1	41, 41.5, 40.5, 43, 39.5, 49, 43.5, 52, 54.5, 56.5, 52.5		26				SB		
S2	74.5, 78, 76, 73.8		27				SB		
S3	63, 66, 65.5, 74.5, 72.5, 72.5, 70.5, 68.5, 66, 74		26				SB		

(continued)

Table 1 (continued)

Location	SHR values	$\phi$ in degree	Method of excavation
S4	65.5, 57, 59.5, 67, 60, 57, 61, 57.5, 72, 55	25	SB
S5	52.5, 52.5, 48, 46, 58, 59.5, 49, 58.5, 54.5, 53.5, 51.5, 46	28	SB

Abbreviations SHR Schmidt Hammer rebound;  $\phi$  friction angle by tilt test; UCS unconfined compressive strength; JRC joint roughness coefficient; U weathered; S slightly, M moderately; D decomposed; N none; SB smooth blasting

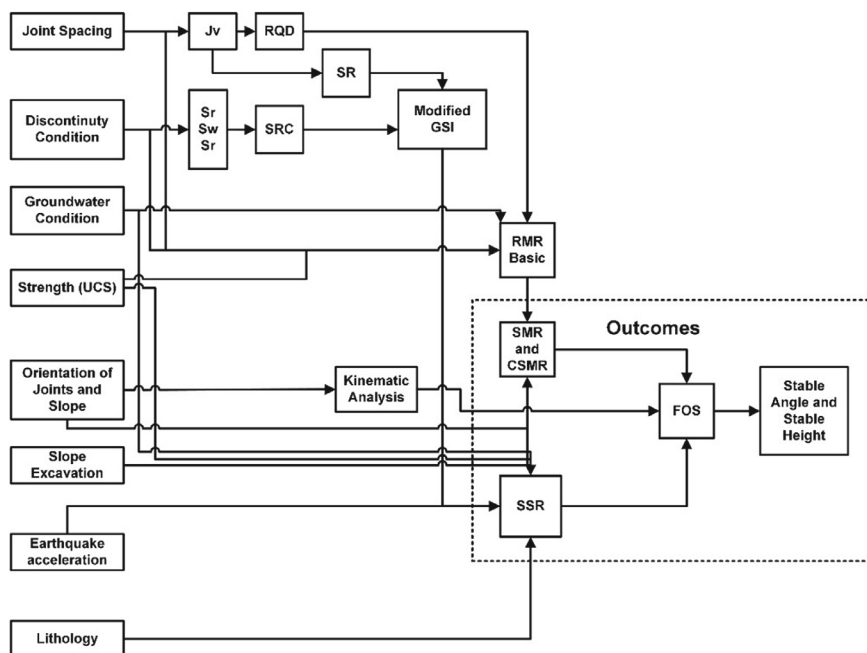


**Fig. 3** Flow chart depicting adopted methodology

Numerous geotechnical parameters influencing the quality of the rockmass comprising the slope are either directly or indirectly affected by the extent of joints, fracture or other discontinuities. Degree of fracture in a rock mass can be gauged by use rock quality designation (RQD), which is second important parameter in the RMR. Since drill cores were unattainable, RQD have been determined using volumetric joint count technique (Palmstrom 2005) and based upon the derived RQD values, ratings were given to studied slopes. Volumetric joint count was calculated by mean joint spacing which is measured as the perpendicular distance within a set of discontinuity. Discontinuity condition which includes extent of discontinuities, joint's roughness, aperture of the joints, weathering conditions, filling in the discontinuity (Siddique et al. 2021), were all measured as the input data for basic RMR. All the parameters were assessed in accordance with the BIS (1987). In the study parameter of RMR is used to determine  $RMR_{basic}$  of the chosen five locations.

### 3.2 Kinematic Analysis

Kinematic analysis enables user to assess the probability of different forms of rock mass failure, i.e., planar, wedge or topple failure. Structurally controlled failures are predominantly caused by the discontinuities that are unfavorably oriented in the rock



**Fig. 4** Field photographs depicting condition of rock mass: (S1) blocky mass prone to rockfall; (S2) soil cover and patchy vegetation on shattered and disintegrated rockmass; (S3) failed blocky mass along cut slope; (S4) adversely oriented discontinuities forming Planar failure and few wedges; (S5) discontinuity sets prone to Planar as well as wedge failure

**Table 2** Ratings for all the parameters of  $RMR_{basic}$

Slope	UCS	RQD	Discontinuity spacing	Groundwater conditions	Conditions of discontinuities	$RMR_{basic}$
S1	5.7	14.5	11.2	15	22.5	68.8
S2	13	16.5	9.5	15	25.0	78.9
S3	11.2	14.1	11.9	15	25.0	77.2
S4	9.1	13.5	12.3	15	15.0	64.9
S5	7	17.2	11.5	15	22.5	73.3

mass. Subsequently, the possibility of such structurally controlled failures also relies upon the friction angle along the joint surface, and relative relation between slope angle and discontinuity orientation (Siddique et al. 2020). Using Markland’s test, kinematic analysis was conducted which uses friction angle of rock along discontinuity surfaces, determined using tilt test (Jang et al. 2018) and orientation of slope face and the prevalent discontinuities measured in the field by using Brunton compass (Table 1). Kinematic analysis for all slopes was done to identify the failure mode using InnStereo software (Fig. 5).



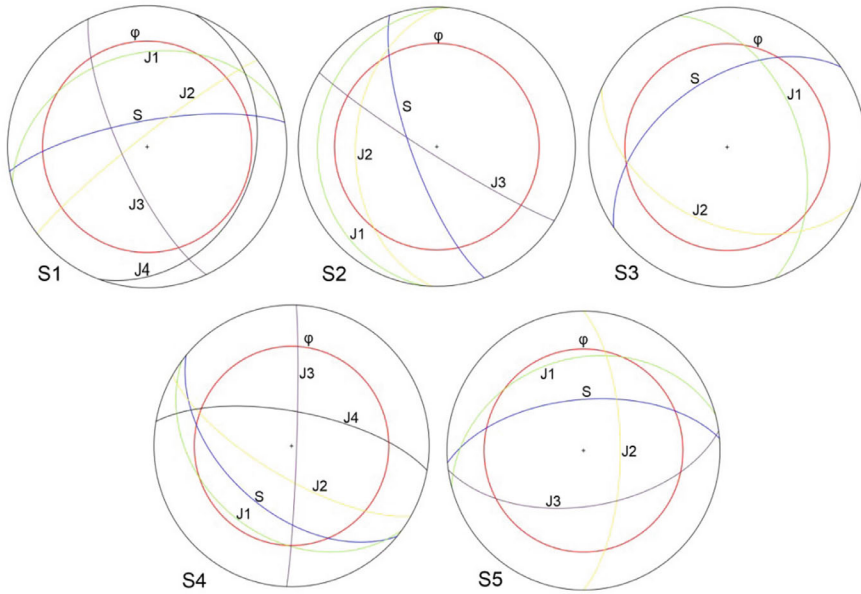


**Fig. 5** Stereographic projection of studied slopes; (S1) prone to planar failure due to joint (J1); (S2) planar failure due to joint set J2 and J1 also; (S3) relative less adverse orientation conditions indicating structural stability; (S4) planar failure with joint J1; (S5) planar failure due to Joint J1 and wedge failure due to intersection J1 and J2

### 3.3 Slope Mass Rating and Its Extension

Slope mass rating is an extension of Rock mass rating (RMR) system with adjustment factors (Romana 1985). It can be computed by accounting three adjustment factors (F1, F2, and F3) from  $RMR_{basic}$ , which depends upon the dip-strike relationship of slope and discontinuity with an addition of fourth correction factor (F4) that accounts for the method, which has been employed to excavate the slope.

$$SMR = RMR_{Basic} + (F1 \times F2 \times F3) + F4 \quad (2)$$

Continuous SMR (CoSMR) is an extension of discrete SMR (Romana 1985) which utilizes continuous function ratings for the three correction factors (Tomás et al. 2007). The continuous expression for F1, F2, and F3 are:

$$F1 = \frac{16}{25} - \frac{3}{500} \arctan \left[ \frac{1}{10} (|A| - 17) \right] \quad (3)$$

$$F2 = \frac{9}{16} - \frac{1}{195} \arctan \left( \frac{17}{1000} B - 5 \right) \quad (4)$$

**Table 3** SMR and CoSMR of investigated slopes along NH-58

S	FT	F	RMR <sub>b</sub>	F1	F2	F3	F1 × F2 × F3	F4	SMR/CSMR	Stability class
S1	P	D	68.8	0.85	0.7	− 60	− 35.7	8	41	III
		C	68.8	0.94	0.76	− 59.5	− 42.5	8	34	IV
S2	P	D	78.9	0.4	0.85	− 60	− 20.4	8	67	II
		C	78.9	0.48	0.89	− 59.4	− 25.4	8	62	II
S3	P	D	77.2	0.15	1	− 50	− 7.5	8	78	II
		C	77.2	0.23	0.92	− 55.3	− 11.7	8	73	II
S4	P	D	64.9	1	0.7	− 60	− 42	8	31	IV
		C	64.9	0.97	0.79	− 58.8	− 45	8	28	IV
S5	P	D	73.3	0.7	0.7	− 60	− 29.4	8	52	III
		C	73.3	0.85	0.76	− 59.3	− 38.3	8	43	III
	W	D	73.3	0.7	0.4	− 60	− 16.8	8	65	II
		C	73.3	0.6	0.6	− 59.5	− 21.4	8	60	III

Note S slope; FT failure type; P planar failure; W wedge failure; F functions; D discrete functions; C continuous functions

$$F3 = -30 + \frac{1}{3} \arctan(C - 120) \quad (\text{For Planar Failure}) \quad (5)$$

$$F4 = -13 + \frac{1}{7} \arctan(C - 120) \quad (\text{For Topple}) \quad (6)$$

where A, B and C correspond to F1, F2 and F3 denotes the auxiliary angles which can be calculated based on the type of failure.

Results of SMR and CoSMR of investigated slopes were calculated by adding basic RMR and the product of adjustment factors along with F4 correction factor (Table 3). Investigated slopes have undergone smooth blasting (SB) for the alignment of road. The method of excavation is evident from blasting holes observed during the field investigation and it takes the rating values same in both SMR and CoSMR.

CoSMR values are found to be lower than SMR values. It is inferred from the results that the SMR value ranges from 31 to 78. The stability class depicts that S1 and S5 falling in class III, S2 and S3 in II class and S4 in class IV as per Romana's classification of (1985). From CoSMR the value ranges from 28 to 73 with a same class as that of SMR, excluding S1 where the class differs.

### 3.4 Slope Stability Rating (SSR)

The SSR classification system was introduced by Taheri and Tani (2006), which was amended by Taheri and Tani (2007). Initially, it was applied for slope stability analysis in Iran and Australia. It considers five other parameters along with the modified geological strength index (GSI) values as follows:

$$SSR = \text{Modified GSI} + P1 + P2 + P3 + P4 + P5 \quad (7)$$

where P1, P2, P3, P4 and P5 are ratings for the parameters: (i) P1: UCS whose rating ranges from 0 to 43 (ii) P2: Rock type (lithology), rating ranges from 0 to 25 (iii) P3: Slope excavation method, whose rating ranges from – 11 to 24 (iv) P4: Groundwater condition whose rating ranges from 0 to – 18 and (v) P5: Earthquake force (horizontal acceleration) rating ranges from 0 to – 26 respectively (Table 4).

SSR is based upon modified Geological Strength Index (GSI) developed by Sonmez and Ulusay (1999), as modification that incorporate quantitative analysis rather than visual estimation of rock masses as proposed by Hoek and Brown (1997). Modified GSI relies on two parameters, namely ‘Structure rating (SR)’ calculated using volumetric joint count ( $J_v$ ) and ‘Surface condition rating (SCR)’ based on three i.e. roughness rating (Rr), weathering rating (Rw) and infilling rating (Rf). In this study, GSI chart proposed by Sonmez and Ulusay (2002) is followed (Fig. 6).

$$SR = -17.5 \ln(J_v) + 79.8 \quad (8)$$

Volumetric joint count ( $J_v$ ) is estimated from the following equation:

$$J_v = \sum_{i=1}^j \frac{1}{S_i} + \frac{Nr}{5\sqrt{A}} \quad (9)$$

where,  $S_i$  is the average perpendicular space between joints for the  $i$ th joint set,  $j$  is the number of joint sets present in the exposure,  $Nr$  represents the number of random sets of joints and  $A$  is the area in  $m^2$ . Using these formulae, values of SR and SCR

**Table 4** Range and corresponding rating table for SSR method (Taheri and Tani 2006)

Parameters	Range/ratings					
P1 (UCS)	0–10	10–25	25–50	50–100	100–150	150–200
Ratings	0	7	18	28	37	43
P2 (rock type)	Group 1	Group 2	Group 3	Group 4	Group 5	Group 6
Ratings	0	4	9	17	20	25
P3 (excavation method)	Waste dump	Poor blasting	Normal blasting	Smooth blasting	Pre-splitting	Natural slope
Ratings	– 11	– 4	0	6	10	24
P4 (ground water)	Dry	0–20%	20–40%	40–60%	60–80%	80–100%
Ratings	0	– 1	– 3	– 6	– 14	– 18
P5 (earthquake force)	0	0.15 g	0.20	0.25 g	0.30 g	0.35
Ratings	0	– 11	– 15	– 19	– 22	– 26

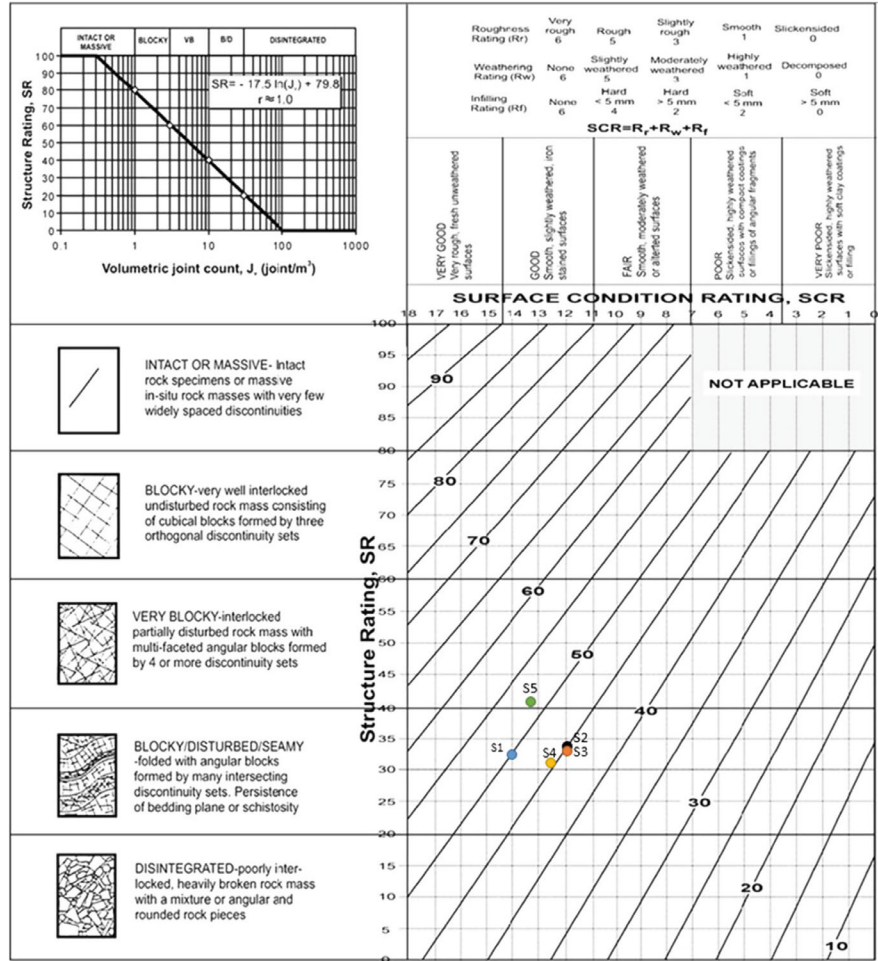


Fig. 6 GSI chart of studied slopes along NH-58

are calculated and plotted on Modified GSI chart (Fig. 6), and the outcomes are in the range of 45–51 (Table 5).

Compressive strength is the most basic geotechnical parameter that governs the overall quality of rock mass and in turn stability. Higher strength of compression correlates with greater stability. UCS is determined using formula (1) (Yagiz 2009) from SHR values and graphically values were plotted as box and whisker plot (Fig. 7). To eliminate any outlier values and represent the data statistically for visualizing data variability, this plot is adopted here. Mean SHR values were taken to calculate the UCS of the whole rock mass.

Rock types were categorized into different groups on the basis of unit weight and friction angle of the intact rock (Taheri and Tani 2007) which is estimated and

**Table 5** Quantified geological strength index of studied cut slopes along NH-58

Slope	Jv	SR	SCR	Modified GSI
S1	13.6	34.0	14	51
S2	13.4	34.3	12	45
S3	14.2	33.3	12	44
S4	15.2	32.1	12.5	45
S5	9.1	41.1	13.3	51

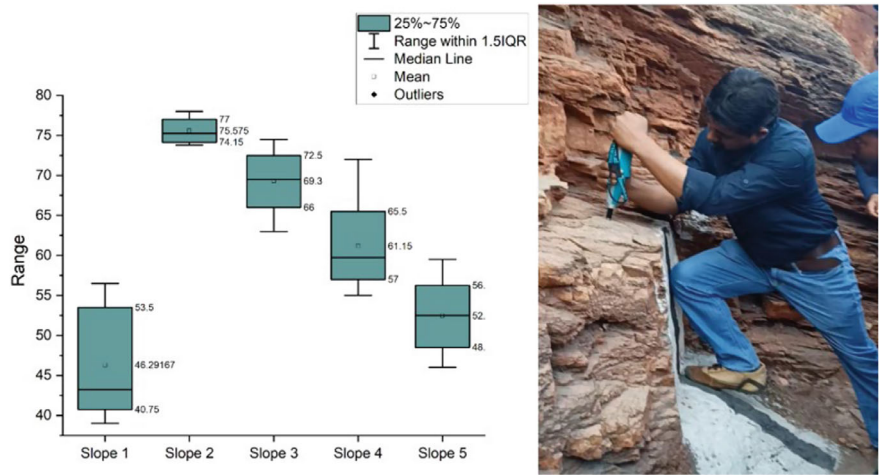


**Fig. 7** Box and whisker plot of SHR values and recording SHR values during field survey

grouped accordingly on the basis of lithology for getting a value of P2. Quality of rock improves with increased rock group number (Taheri and Tani 2010). Rocks in the study area were classified on the basis of mineralogical and textural attributes observed through macroscopic examination and hand lens analysis in the field. These classifications were subsequently validated by thin-section preparation and analysis using petrographic microscope in the laboratory (Fig. 8). Rocks at slopes S1, S2, S3 and S4 were coarse-grained type of rock, with color ranging from grey to pale yellow. Rock at slope 5 is also coarse-grained rock but with certain laminar fabric and assemblage of micaceous minerals and with schistosity and lensoid structure having coarse-grained quartz in the core.

Sample 1 was found to be monomineralic with only quartz grains as abundant constituent and along with highly interlocking texture. Sample 3 was similar to that of sample 1, but it had some muscovite inclusions within the quartz grains. Based on field assessment and thin-section studies, both the samples (1 and 3) are Quartzite. Sample 5 (Granite) contains quartz, K-Feldspar, plagioclase muscovite and biotite. Lithology related ratings have been assigned accordingly.

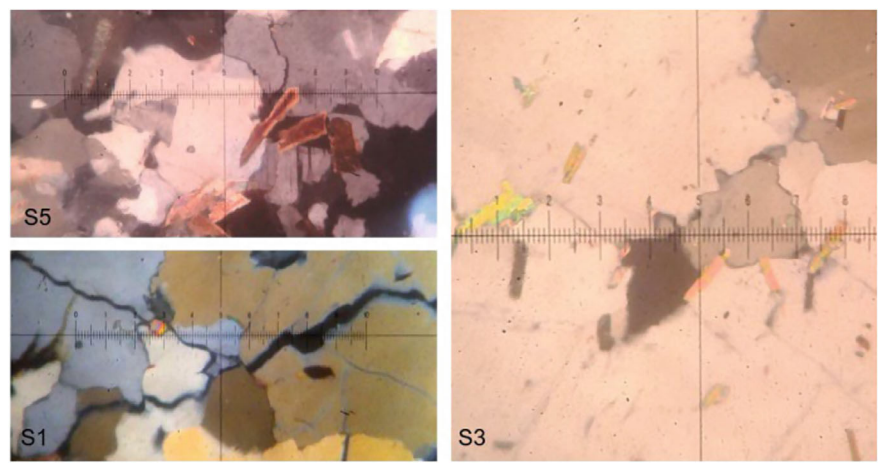


**Fig. 8** Photomicrographs of S5: granite; S1 and S3: quartzites showing highly interlocking texture (magnification: 10× and 5×)

Rock slope stability is strongly affected by the water condition of the slope. Increase in the water pressure in the discontinuity reduces strength thus decreasing the stability of the slope. Rock bursts are small earthquakes caused by mining, excavation, and other activities (Srinivasan et al. 2010). Seismicity has negative effects on the slope stability; therefore, a negative value is used in earthquake force rating. The seismic hazard map of having peak ground acceleration (PGA) with a 10% chance of exceedance in 50 years is used to determine PGA values of the study area. The area under investigation has PGA value of around  $0.4 \text{ m/s}^2$  (Ayala 2003) and accordingly ratings for all slopes are assigned using the following formula:

$$Rating_{(Earthquake\ Force)} = -74.27(PGA) - 0.027 \tag{10}$$

The algebraic sum of ratings of all six parameters is SSR value (Table 6).

**Table 6** Slope stability rating values of investigated slopes along NH-58, from Ajmer to Pushkar

Slope	Ratings of parameters						
	GSI	UCS (P1)	Rock type (P2)	Excavation method (P3)	Groundwater (P4)	Earthquake force (P5)	SSR
S1	51	22.3	20	6	0	− 29.7	69.6
S2	45	42.2	20	6	0	− 29.7	83.5
S3	44	42.0	20	6	0	− 29.7	82.3
S4	45	36.7	20	6	0	− 29.7	78
S5	51	28.6	25	6	0	− 29.7	80.9

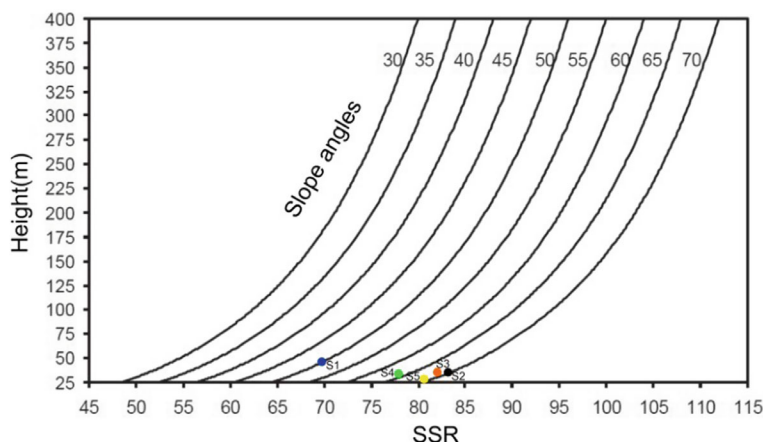


**Fig. 9** SSR design chart for FS 1.5

SSR values, slope height and existing slope angle were plotted on SSR design chart for factor of safety 1.5 (Fig. 9). Stable slope angle for slope analyzed ranges from 50° to 70°. Slope 3, 4 and 5 are stable according to SSR design chart, while Slope 1 and 2 needs reduction in slope angle by 23° and 5°, respectively (Table 9). The advantage of SSR over SMR is that it takes effect of seismicity (earthquake force) as one of the input factors.

### 3.5 Factor of Safety (FS)

Stability is quantified by the factor of safety that is the ratio of the resisting forces to driving forces, termed as limit equilibrium of the slope, which is stable if  $FS > 1$  (Wyllie 2018). Slope stability analysis through FS was determined by applying principles of Kinematic analysis (Hoek and Bray 1981) and it was calculated for all five slopes. Since all the slopes were found to be of dry condition, a modified formula was used, which eliminates the uplift water pressure in the discontinuity plane (U) and water pressure in tension cracks (V).

For planar type of failure, modified formula is:

$$FS = \frac{CA + (W \cdot \cos \Psi_p) \tan \phi}{W \cdot \sin \Psi_p} \quad (11)$$

Here, C is the cohesion, A refers to the area of the sliding plane, W is the weight of the block,  $\Psi_p$  refers to the dip of the joint plane causing failure,  $\Phi$  is the angle of internal friction and H is the height of the studied slope. Internal friction and Cohesion were estimated using RMR values. Area (A) and Weight of the block is calculated by following formulae.



$$\frac{Z}{H} = 1 - \sqrt{\cot \Psi_f \cdot \cot \Psi_p} \quad (12)$$

$$A = (H - Z) \operatorname{Cosec} \Psi_p \quad (13)$$

$$W = \frac{1}{2} \gamma * H^2 \left[ \left( 1 - \left( \frac{Z}{H} \right)^2 \right) \cot \Psi_p - \cot \Psi_f \right] \quad (14)$$

(when tension cracks on the upper slope surface)

$$W = \frac{1}{2} \gamma * H^2 \left[ \left( 1 - \left( \frac{Z}{H} \right)^2 \right) \cot \Psi_p \cdot (\cot \Psi_p \tan \Psi_f - 1) \right] \quad (15)$$

(when tension cracks on the slope face).

Here,  $\Psi_f$  refers to the dip of the slope face,  $H$  is the height of the slope and  $\gamma$  is the unit weight of the rock mass.

Several geotechnical parameters along with some dimensions and geometry related parameters were utilized (Table 7). Slope S1, S2 and S4 are found to be unstable by FS calculation, S5 is critically unstable and slope S3 is stable. For slope S5, the wedge failure was assessed along the line of intersection following equations of kinematic analysis (Hoek and Bray 1981). The equations for the determination of FS for wedge failure are given as follows:

$$FS = \frac{3}{\gamma r \cdot H} (c)A \cdot x + cb \cdot y + \left( A - \frac{\gamma w}{2\gamma r} \cdot X \right) \cdot \tan \phi A + \left( B - \frac{\gamma w}{2\gamma r} \cdot Y \right) \cdot \tan \phi B \quad (16)$$

where  $cA$  and  $cb$  are cohesive strengths and  $\phi A$  and  $\phi B$  are the angles of friction, respectively, on planes  $A$  and  $B$ ;  $\gamma r$  is the unit weight of the rock,  $\gamma w$  the unit weight of the water and  $H$  the total height of the wedge measured along the line of intersection 5. The dimensionless factors  $X$ ,  $Y$ ,  $A$  and  $B$  depend upon the geometry of the wedge, given by the following equation:

**Table 7** Input parameters for FS determination of investigated planar slopes

Slope	$\Phi$	H	$\Psi_p$	$\Psi_f$	A	C	$\gamma$	W	FS
S1	24	47	34	73	56.6	194.2	26.5	97,563.6	0.8
S2	29	38	41	75	32.2	244.6	26.5	46,794.6	0.8
S3	41	37	44	50	49.6	361.2	26.5	4148.2	6.3
S4	22	33	35	51	62.5	235	26.5	8715.3	0.6
S5	22	23	34	60	38.1	166.4	26.0	10,689.4	1.0

$$X = \frac{\sin \theta_{24}}{\sin \theta_{45} \cdot \cos \theta_{2.na}} \quad (17)$$

$$Y = \frac{\sin \theta_{13}}{\sin \theta_{35} \cdot \cos \theta_{1.na}} \quad (18)$$

$$A = \frac{\cos \Psi_a - \cos \Psi_b \cdot \cos \theta_{na.nb}}{\sin \Psi_5 \cdot \sin \theta_{na.nb} \cdot \sin \theta_{na.nb}} \quad (19)$$

$$B = \frac{\cos \Psi_b - \cos \Psi_a \cdot \cos \theta_{na.nb}}{\sin \Psi_5 \cdot \sin \theta_{na.nb} \cdot \sin \theta_{na.nb}} \quad (20)$$

where,  $\Psi_a$ : dip amount of J1,  $\Psi_b$ : dip amount of J2,  $\theta_{na}$  and  $\theta_{nb}$  are the poles of J1 and J2,  $\theta_{nanb}$ : angle between poles,  $\theta_{13}$ ,  $\theta_{35}$ ,  $\theta_{24}$ ,  $\theta_{45}$  represent angles between different intersection points of slope and joints.

The input parameters for FS determination are calculated through principles of kinematic analysis by calculating the angles between different intersection points in a stereonet. From the calculation, the FS for wedge failure of S5 comes out to be 1.11, which is critically stable (Table 8). The planar and wedge failure results of S5 indicate that for Wedge failure, the SMR and FS are comparatively higher than Planar failure which correlates well.

Stable angle for the slopes has been calculated using SSR design chart for FS 1 and 1.5, and by using limit equilibrium (Table 9). Disparities are in the range of  $10^\circ$ , whereas angle by SMR seems too conservative.

RMR<sub>basic</sub>, SMR, CoSMR and SSR methods were compared by correlation line graph (Fig. 10). SMR and CoSMR follow same trend with slight variability in values. The graph demonstrates higher values for SSR among all methods across all slopes because SSR does not account for discontinuity orientation related factors. The empirical methods are in agreement with each other to some extent, as they all show similar trends. This suggests that the applied methods are in good correlation but differ in sensitivity and conservativeness. The peak at S3 for RMR<sub>basic</sub>, SMR, and CoSMR indicates this slope might have the highest overall stability among the five evaluated. In this study, slopes with adversely oriented discontinuities exhibit lower SMR values. The decline in peak at slope S4 (Fig. 10) corresponds to good quality rock having good RMR<sub>basic</sub> value but due to adverse orientation of causative joint, the overall SMR/CoSMR values show low values. This depicts the importance

**Table 8** Input parameters for FS calculation of wedge failure (S5)

Parameter	Value	Parameter	Value (°)	Parameter	Value (°)	Parameter	Value
CA = CB	166	$\theta_{na.nb}$	79	$\theta_{13}$	157	X	0.86
$\Psi_a$	$34^\circ$	1Na	12	$\theta_{35}$	62	Y	1.93
$\Psi_b$	$68^\circ$	2Nb	64	$\theta_{24}$	59	A	1.57
$\Psi_5$	$30^\circ$	$\phi$	28	$\theta_{45}$	32	B	0.47
						FS	1.11

**Table 9** Stable slope angle calculated using different methods

Slope	Existing slope angle (°)	Stability (for FS 1.5) using SSR chart	Stable slope angle for FS 1.5 using SSR chart (°)	Stable slope angle (BIS 1997) (°)	Stable slope angle for FS 1 (limit equilibrium) (°)	Stable slope angle for FS 1.5 (limit equilibrium) (°)
S1	73	Unstable	50	33	60	44
S2	75	Unstable	70	–	69	59
S3	50	Unstable	68	–	–	–
S4	51	Stable	63	–	–	44
S5	60	Stable	67	34	–	49

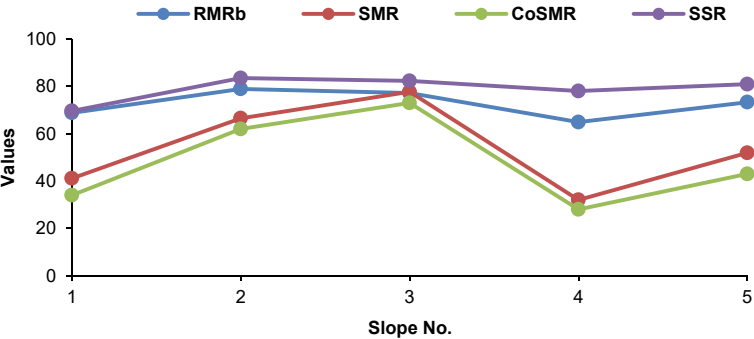


**Fig. 10** Graph showing correlation among different empirical methods

of structurally controlled failure for a rock mass to fall under unstable category. RMR<sub>basic</sub> correlates well with SSR method.

**4 Conclusions**

The present geotechnical evaluation emphasized on stability appraisal of road cut slopes along NH-58, a passage through Aravalli-Delhi fold belt. Slopes were found to be safe from large failures, but chances of smaller slope failures cannot be ruled out. RMR<sub>basic</sub> values of studied slopes ranges from 64.9 to 78.9, indicating a good quality rock mass. Due to adverse orientation of discontinuities, SMR and CoSMR have categorized S1, S5 as partially stable, and S4 as unstable. SSR values of studied slopes range from 69.6 to 83.5, showing analogous outcomes. Based on SSR design chart slope angle should be reduced by few degrees to attain stability. The calculated FS values suggest that three slopes are unstable (S1, S2 and S4), one critically stable (S5) and one as stable (S3). The comparative study of all methods applied depicts that there is compatibility in values for RMR and SSR because these methods do not rely

on orientation factors and lesser values by SMR and CoSMR differ due to adverse orientation of discontinuities in the rock mass. The study will enhance the understanding of critical zones, which can serve as a baseline and way forward towards much detailed rockfall hazard assessment and simulation studies. Such geotechnical appraisal must be undertaken to ensure better safety along the route.

**Declarations** There is no Conflict of interest.

## References

- Ayala D (2003) Seismic vulnerability and strengthening of historic buildings, in Lalitpur, Nepal. Earthquake Hazard Centre Newsletter. Earthquake Hazard Centre, pp 1–5
- Bhardwaj GC, Salvi BL (2011) Slope stability aspects: a case study of the road side hill cuts nh-8, between Udaipur-Ahemdabad, Rajasthan, India. In: International conference on environmental technology and construction engineering for sustainable development. Shahjalal University of Science and Technology, Bangladesh, pp 109–115
- BIS (1987) Indian Standard Code 11315: methods for the quantitative description of discontinuities in rock mass. Bureau of Indian Standards, The National Standards Body of India, India
- BIS (1997) Quantitative classification system of rock mass-guidelines, part 3: determination of slope mass rating. Bureau of Indian Standards, The National Standards Body of India, India
- Hoek E, Bray J (1981) Rock slope engineering. Institute of Mining and Metallurgy, London
- Hoek E, Brown ET (1997) Practical estimates of rock mass strength. *Int J Rock Mech Min Sci* 34:1165–1186. [https://doi.org/10.1016/S1365-1609\(97\)80069-X](https://doi.org/10.1016/S1365-1609(97)80069-X)
- Jang HS, Zhang QZ, Kang SS, Jang BA (2018) Determination of the basic friction angle of rock surfaces by tilt tests. *Rock Mech Rock Eng* 51:989–1004. <https://link.springer.com/article/10.1007/s00603-017-1388-7>
- Li J, Villaescusa E (2005) Determination of rock mass compressive strength using critical strain theory. In: Proceedings of the 40th US symposium on rock mechanics. Anchorage, Alaska
- Mathur S, Singh SK, Khichi CP, Mathur SC (2020) Landslide in rocks of Jodhpur group at Masuria Hill in Jodhpur, Western Rajasthan, India: its causes and threat to significant georesources. *J Earth Syst Sci* 129:1–15. <https://doi.org/10.21203/rs.3.rs-40149/v1>
- Mukhopadhyay D, Bhattacharyya T, Chattopadhyay N, Lopez R, Tobisch OT (2023) Anasagar gneiss: a folded granitoid pluton in the phanerozoic South Delhi Fold Belt, central Rajasthan. *Proc Indian Acad Sci (Earth Planet Sci)* 109:21–37
- NDTV (2015) Rescue teams roped in as heavy rains lash Rajasthan. NDTV India. <https://www.ndtv.com/india-news/rescue-teams-rope-in-as-heavy-rains-lash-rajasthan-1201452>
- Niyogi A, Sarkar K, Singh AK, Singh TN (2020) Geo-engineering classification with deterioration assessment of basalt hill cut slopes along NH 66, near Ratnagiri, Maharashtra, India. *J Earth Syst Sci* 129:1–19. <https://doi.org/10.1007/s12040-020-1378-0>
- Palmstrom A (2005) Measurements of and correlations between block size and rock quality designation (RQD). *Tunn Undergr Space Tech* 20:362–377. <https://doi.org/10.1016/j.tust.2005.01.005>
- Pantelidis L (2009) Rock slope stability assessment through rock mass classification systems. *Int J Rock Mech Min Sci* 46:315–325. <https://doi.org/10.1016/j.ijrmms.2008.06.003>
- Pradhan SP, Vishal V, Singh TN (2015) Study of slopes along River Teesta in Darjeeling Himalayan region. In: Engineering geology for society and territory, vol 1. Climate change and engineering geology. Springer International, pp 517–520

- Romana M (1985) New adjustment ratings for application of Bieniawski classification to slopes. In: Proceedings of the international symposium on role of rock mechanics. Zacatecas, Mexico, pp 49–53
- Roul AR, Pradhan SP, Mohanty DP (2021) Investigation to slope instability along railway cut slopes in Eastern Ghats mountain range, India: a comparative study based on slope mass rating, finite element modelling and probabilistic methods. *J Earth Syst Sci* 130:1–25. <https://doi.org/10.1007/s12040-021-01711-1>
- Sarkar S, Pandit K, Dahiya N, Chandna P (2021) Quantified landslide hazard assessment based on finite element slope stability analysis for Uttarkashi–Gangnani highway in Indian Himalayas. *Nat Haz* 106:1895–1914. <https://link.springer.com/article/10.1007/s11069-021-04518-x>
- Siddique T, Mondal MEA, Pradhan SP, Salman M, Sohel M (2020) Geotechnical assessment of cut slopes in the landslide-prone Himalayas: rock mass characterization and simulation approach. *Nat Haz* 104:413–435. <https://link.springer.com/article/10.1007/s11069-020-04175-6>
- Siddique T, Sazid M, Khandelwal M, Varshney H, Irshad S (2021) Application of slope mass rating and kinematic analysis along road cut slopes in the Himalayan Terrain. In: International conference on geotechnical challenges in mining, tunnelling and underground infrastructures. Springer Nature Singapore, Singapore, pp 697–708. [https://doi.org/10.1007/978-981-16-9770-8\\_47](https://doi.org/10.1007/978-981-16-9770-8_47)
- Singh B, Goel RK (1999) Rock mass classification: a practical approach in civil engineering. Elsevier Science
- Sonmez H, Ulusay R (1999) Modifications to the geological strength index (GSI) and their applicability to stability of slopes. *Int J Rock Mech Min Sci* 36:743–760. [https://doi.org/10.1016/S0148-9062\(99\)00043-1](https://doi.org/10.1016/S0148-9062(99)00043-1)
- Sonmez H, Ulusay R (2002) A discussion on the Hoek-Brown failure criterion and suggested modification to the criterion verified by slope stability case studies. *Yerbilim Earth Sci* 26:77–99
- Srinivasan C, Willy YA, Gupta ID (2010) Estimation of local magnitude of rock-bursts using strong motion accelerograms in the mines of Kolar gold fields. *Acta Geophys* 58:300–316. <https://doi.org/10.2478/s11600-009-00456>
- Taheri A, Tani K (2006) Modified rock mass classification system for preliminary design of rock slopes. In: Proceedings of the international symposium on rock mechanics. ARMA-06
- Taheri A, Tani K (2007) Rock slope design using slope stability rating (SSR)—application and field verifications. In: ARMA Canada-US rock mechanics symposium. ARMA, pp 1–7
- Taheri A, Tani K (2010) Assessment of the slope stability of rock slopes by Slope stability rating classification system. *Rock Mech Rock Eng* 43:321–333. <https://doi.org/10.1007/s00603-009-0104-8>
- The Economic Times (2015) Rajasthan: incessant rainfall triggers flood-like situation. In: The economic times, English edn. <https://economictimes.indiatimes.com/nation-world/rajasthan-incessant-rainfall-triggers-flood-like-situation/slideshow/48260498.cms>
- Tomás R, Delgado J, Serón JB (2007) Modification of slope mass rating (SMR) by continuous functions. *Int J Rock Mech Min Sci* 44:1062–1069. <https://doi.org/10.1016/j.ijrmms.2007.02.004>
- Wyllie DC (2018) Rock slope engineering civil application, 5th edn. CRC Press. <https://doi.org/10.4324/9781315154039>
- Yagiz S (2009) Predicting uniaxial compressive strength, modulus of elasticity and index properties of rocks using the Schmidt hammer. *Bull Eng Geol Env* 68:55–63. <https://doi.org/10.1007/s10064-008-0172-z>

**Dr. Tariq Siddique** works as an Assistant Professor in the Department of Geology, Aligarh Muslim University, Aligarh, India. He is recipient of University Gold Medal and Dr. H.S. Pareek Medal for securing first position in his post-graduation. He is a life member of reputed scientific learned bodies like Indian Geotechnical Society, Delhi Chapter, India and Indian Association of Sedimentologists, India. His research interest includes slope stability appraisal and aligned

aspects of geotechnical engineering. His research is mainly focused on rock mass characterization, kinematic analysis and numerical simulation using Generalized Hoek–Brown Criterion and Mohr–Coulomb Criterion. Dr. Siddique has proposed new guidelines for Q-Slope method and modified adjustment factor in Slope mass rating method for toppling failure. He has published 18 research articles in several peer-reviewed International and National Journals published by Elsevier, Springer and Wiley. He has contributed 5 chapters in various books published by Springer. He has 16 publications in conference/seminar/workshop proceedings. He is a regular reviewer of many reputed journals like Bulletin of Engineering Geology and the Environment, Geological Journal, Geotechnical and Geological Engineering, Indian Geotechnical Journal, Journal of Earth System Science, Journal of Mountain Science, Journal of the Geological Society of India, Modeling Earth Systems and Environment, Natural Hazards, Rock Mechanics and Rock Engineering, Scientific Reports, etc. Dr. Siddique is currently mentoring 4 Ph.D. students and had supervised 16 post-graduate and 32 undergraduate project/dissertation students.

**Aquib Shamshad** completed his Bachelor of Science in Geology, Master of Science in Applied Geology and Post-Graduate Diploma in Hydrogeology from Aligarh Muslim University, Aligarh. He has completed his master's dissertation project in Engineering Geology, focusing on slope stability appraisal using Slope mass rating and kinematic analysis. He is also working on applications of remote sensing and GIS in climate change sensitivity and its effects. He presented an article entitled 'Impacts of climate change on landslides in India: A review' in an International Conference on Climate Change, Disaster Management, and Environmental Sustainability organized by Jamia Millia Islamia, New Delhi. He has attended several workshops, training programs and webinars on various themes like Geotechnics for Disaster Mitigation, Advances in Earth and Environmental Geosciences, Geospatial tool for water resources and natural Hazards monitoring, Application of remote sensing and GIS in mineral exploration, etc.

**Tuba Fatima** completed her Master of Science degree in Applied Geology and Postgraduate Diploma in Hydrogeology from Aligarh Muslim University. Tuba published a review article in Journal of Failure Analysis and Prevention, Springer and presented three articles in national and international conferences. She has an experience as a Geotechnical Engineering Intern at the Zakir Husain College of Engineering and Technology, Department of Civil Engineering, Aligarh Muslim University. Her research interest includes various aspects of Geotechnical Engineering, with a particular emphasis on numerical modeling of tunnels and slope stability assessment. Tuba has also participated in various short-term courses and workshops, focusing on landslide mitigation, disaster management, environmental management systems and environmental geomechanics.

**Pirzada Mohammad Haris** is a research scholar in the Department of Geology, Aligarh Muslim University, Aligarh. He obtained his Master's degree in Applied Geology from the University of Kashmir, Srinagar, Jammu and Kashmir. He has worked in the field of geochemistry of syringothyris limestones during his M.Sc. dissertation project. He is presently working in Engineering Geology, focusing on slope stability studies of road-cut slopes in the Lesser Himalayan terrain using empirical, analytical, numerical and geospatial techniques. He has published two research papers in international journals and one conference article in a national conference. Mr. Haris actively participated in various professional development activities, including national and international conferences, workshops and webinars. He has also gained teaching experience at the college level as a guest lecturer.

**Dr. Md. Erfan Ali Mondal** works as Professor in the Department of Geology, Aligarh Muslim University, Aligarh, India. Research interests of Prof. Mondal include magmatic and tectonic processes of Precambrian crustal evolution, hard rock and clastic rock geochemistry. He is particularly interested in understanding the geodynamic evolution of Indian continental lithosphere, viz. Bundelkhand craton, Bastar craton and Aravalli craton through multi-disciplinary approach

involving field studies, petrology, geochronology and geochemistry. His interest also includes rock mass characterization and slope stability studies. He has supervised 09 doctoral theses. He has published 98 research papers in peer-reviewed journals. He has completed 10 research projects sponsored by DST, Ministry of Mines, UGC & SERB, Govt of India, and at present carrying out 01 research project sponsored by ANRF-SERB Govt of India. He is a fellow and life member of many learned bodies and has been a member of National Working Group for International Geological Correlation Programme (IGCP) on A-type granites and related rocks (IGCP 510), and International Geological Correlation Programme (IGCP) on The Changing Early Earth (IGCP 599). He was member of Science Program Committee of the 36th International Geological Congress 2020, and Coordinator of the theme: Hadean to Archaean. He is recipient of National Geoscience Award 2017 of Govt of India. He was awarded Outstanding Researcher Award 2018, and Gold Medal in 1990 by Aligarh Muslim University. He has Edited a Book titled “Geological Evolution of the Precambrian Indian Shield” published by Springer.



# Slope Stability Evaluation Through Slope Mass Rating and Its Extension



Amit Jaiswal, Md Shayan Sabri, Amit Kumar Verma,  
Ashutosh Pratap Shastri, Komal Kumari, and T. N. Singh

**Abstract** Slope stability plays a significant role in the planning and execution of many infrastructure projects located on sloping terrains, including dams, highways, and urban expansions. The current study is a comprehensive investigation of slope stability using empirical technique. Slope Mass Rating (SMR) approach commonly used empirical method for determining the stability of rock slopes, as well as its extensions, such as Chinese Slope Mass Rating (CSMR) and Continuous Slope Mass Rating (CoSMR) systems. The investigation focuses on the Ramban district of Jammu and Kashmir, which is known for frequent landslides along National Highway NH-44. To assess the efficacy of these approaches they were applied to fourteen susceptible slopes along the NH portion and their stability was thoroughly compared. The results show that except for one slope (SL-4) SMR values are generally greater than CoSMR values and less than CSMR. The majority of the slopes are categorized as having poor stability (Class IV) by Romana's classification, with SMR values ranging from 11 to 59, CoSMR values ranging from 3.39 to 74.56, and CSMR values ranging from 16.36 to 54.25. Unstable slopes are largely made of slate and phyllite, whereas moderately stable slopes are made of granitic gneiss. The study emphasizes the importance of specific adjustment factors on slope stability assessments, suggesting that CoSMR is a more sensible and less biased evaluation than SMR and CSMR.

---

A. Jaiswal · Md Shayan Sabri · A. K. Verma (✉) · A. P. Shastri · K. Kumari · T. N. Singh  
Department of Civil and Environmental Engineering, Indian Institute of Technology Patna, Bihta,  
Patna, Bihar, India  
e-mail: [akv@iitp.ac.in](mailto:akv@iitp.ac.in)

Md Shayan Sabri  
e-mail: [shayan\\_2321ce12@iitp.ac.in](mailto:shayan_2321ce12@iitp.ac.in)

A. P. Shastri  
e-mail: [ashutosh\\_2311ce12@iitp.ac.in](mailto:ashutosh_2311ce12@iitp.ac.in)

K. Kumari  
e-mail: [komal\\_2311ce32@iitp.ac.in](mailto:komal_2311ce32@iitp.ac.in)

T. N. Singh  
e-mail: [tnsingh@iitb.ac.in](mailto:tnsingh@iitb.ac.in)

**Keywords** Himalayan slope stability · Slope mass rating · CoSMR · CSMR

## 1 Introduction

Slope stability is a critical consideration in the planning and execution of infrastructure projects located on sloping terrains, such as dams, roads, and urban expansions. It has a direct impact on the safety and durability of these structures. The Himalayan region, in particular, experiences significant slope failures due to its ongoing tectonic activity and heavy rainfall (Paul and Mahajan 1999; Ghosh et al. 2012). These slope failures are responsible for approximately 30% of all losses worldwide in the Himalayan region (Li 1990; Dahal et al. 2009). To ensure the structural integrity of projects constructed on sloping surfaces and evaluate the condition of slope engineers utilize empirical techniques like the Slope Mass Rating (SMR). This method evaluates the stability of rock slopes by considering geological and geotechnical parameters, such as rock strength, discontinuity spacing, groundwater conditions, and slope geometry (Panthi 2023). The method also incorporates the orientation of both slope and discontinuities, the method of excavation, and the condition of discontinuities, providing a more comprehensive assessment of slope stability. The inclusion of these additional factors enhances the precision and reliability of slope stability assessments, enabling engineers to gain a more thorough understanding of the potential risks and hazards associated with slopes. The quantitative evaluation of slope stability is achieved by rating the rock mass based on these parameters. Furthermore, the SMR method has been expanded to encompass additional factors influencing slope stability, such as seismic activity, weathering, and vegetation cover. The introduction of the modified Slope Mass Rating method, which integrates parameters like slope angle weighting factor and seismic weighting factor, has significantly improved the accuracy of slope stability assessments (Sun et al. 2020).

In the preliminary stages of engineering projects, geomechanical classification systems that rely on empirical data have traditionally been utilized for the evaluation of rock slopes (Pastor et al. 2019). These classification systems provide a foundation for the more detailed and comprehensive slope stability assessments. Numerous classification techniques have been formulated, including the natural slope methodology (NSM) (Shuk 1994), Chinese slope mass rating (CSMR) (Chen 1995), rock mass rating (RMR) (Bieniawski 1979, 1989), rock mass strength (RMS) (Selby 1980; 1982), slope mass rating (SMR) (Romana 1985, 1993), slope rock mass rating (SRMR) (Robertson 1988), and the Q-slope method (Barton and Bar 2015; Bar and Barton 2017). Among these, the CSIR classification system (RMR) developed by (Bieniawski 1973, 1984, 1989) and the NGI index (Q system) introduced by (Barton et al. 1974) are widely recognized and utilized. Despite the existence of these established systems, suggestions for modifications have been put forth to enhance their applicability, such as the latest iterations of Q and RMR proposed by Bieniawski (1989). In the realm of rock slope stability, (Romana 1985) introduced the Slope Mass Rating (SMR) technique, which is based on the RMR system and serves as an

initial method to distinguish stable rock slopes. Additionally Hoek and Brown (1997) brought out the Geological Strength Index (GSI) to tackle the challenges associated with categorizing weak rock masses. The GSI chart was further refined by Sönmez and Ulusay (2002) incorporating quantifiable joint parameters.

This chapter presents a comprehensive overview of the Slope Mass Rating (SMR) method and its extensions, in the assessment of stability of fourteen critical slopes. Several SMR extension results have been compared and empirical correlations among these modified versions of SMR have been established.

## 2 Study Area

The geographical location under investigation is situated in the Ramban district of the Northwestern Himalayas, positioned at a midpoint between Seri and Ramsoo. The spatial extent of the study area covers approximately 21 km, along the stretch of road between the coordinates  $33^{\circ} 14.5' \text{ N}$  and  $33^{\circ} 20.62' \text{ N}$ , and  $75^{\circ} 12' \text{ E}$  and  $75^{\circ} 13.65' \text{ E}$  as illustrated in Fig. 1a. The segment of National Highway NH-44 aligns with the left bank of the Bichleri River, a tributary of the Chenab River.

Geologically, the study area is positioned between a segment of the central crystalline formation and the two thrust zones of regional significance within the Himalayan geological framework (from MBT to MCT). According to earlier researchers, the most common rock types in the study region include limestone, phyllite, quartzite, slate, and granitic gneiss (Bhat et al. 1999) (Fig. 1b). The regional orientation of rock formations within the study area exhibits a strike ranging from NW-SE to WNW-ESE, while the dip angle varies from extremely steep to notably severe in either the northern or southern direction. The rocks in this region are characterized by the presence of two to three prominently inclined joint sets along with a bedding or foliation (Jaiswal et al. 2024).

## 3 Methodology

### 3.1 Rock Mass Classification

Rock mass classification plays a crucial role in assessing slope stability and understanding the geological characteristics of rock masses, providing valuable insights for engineering decisions and risk management. Field investigations for rock mass classification study of rock slopes are the most essential study of these classifications. The field studies for this research work were conducted in the Ramban district of Jammu & Kashmir where frequent landslides along National Highway NH-44 have been witnessed in recent past. Three classification techniques Slope Mass Rating

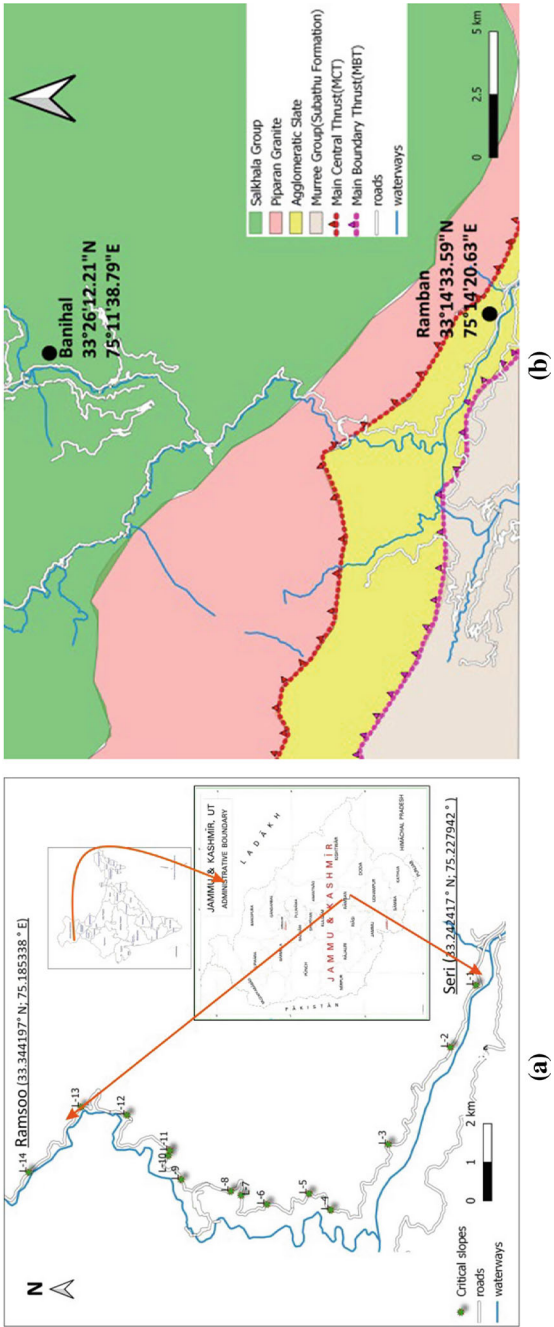


**Fig. 1** a Studied slope along NH44 of Ramban district (J&K); b geological of the study area

(SMR), Chinese Slope Mass Rating (CSMR), and Continuous Slope Mass Rating (CoSMR) have been applied on fourteen susceptible slopes in the area.

### 3.1.1 Slope Mass Rating

Slope mass rating (SMR) technique is used to evaluate the stability of rock slopes, considering joint orientation concerning slope orientation to determine the stability of individual rock masses (Romana 1985). This method based on the fundamental RMR index, incorporates four adjustment factors, as described by Romana (1985, 1993). These adjustment factors are distinct and rely heavily on decision-making processes. SMR proves to be a valuable tool for the assessment of slope stability in scenarios involving heavily jointed rock masses. Initially, the technique only addressed planar and toppling failures, however (Anbalagan et al. 1992) expanded it to include wedge failure. Romana 1985 emphasized the importance of quantifying the relative orientation of slopes in relation to discontinuities within the rock mass. By quantifying orientation parameters, Romana developed the SMR system to provide a detailed evaluation of stability grades for slopes. Over time, various modifications have been made to the SMR system by (Anbalagan et al. 1992; Romana 1993, 1995; Romana Ruiz et al. 2001; Romana et al. 2003) due to extensive experiences and wealth of data. The widespread use of SMR in rocky slopes is attributed to its simplicity and comprehensive, well-established, and quantitative approach to correction factors as highlighted by Tomás et al. (2007) and Siddique et al. (2017). The geomechanical index SMR, introduced by Romana, involves the addition of four correction factors to the basic RMR. These correction factors are determined based on the geometric relationship between discontinuities affecting the rock mass the slope, and the method of slope excavation. The calculation of SMR is expressed as follows:

$$SMR = RMR_{basic} + (F_1 \times F_2 \times F_3) + F_4 \quad (1)$$

where RMR represents the RMR index derived from Bieniawski's Rock Mass Classification without adjustments, in accordance with (Tomás et al. 2007). The first correction factor  $F_1$  focuses on the parallelism between joint dip direction ( $\alpha_j$ ) for planar or toppling failure  $\alpha_i$  for wedge failure and slope dip direction ( $\alpha_s$ ) and is computed using a specific formula involving the angle  $A$  between joint and slope dip direction.

$$F_1 = (1 - \sin A)^2 \quad (2)$$

The second factor,  $F_2$ , pertains to the likelihood of joint shear strength and is influenced by joint dip ( $\beta_j$ ) for planar failure or  $\beta_i$  for wedge failure with a fixed value for toppling failure. It can be empirically determined through a designated equation.

$$F_2 = \tan \beta_j \quad (3)$$

Factor  $F_3$  accounts for the relationship between joint dip ( $\beta_j$ ) for planar or toppling failure  $\beta_i$  for wedge failure) and slope dip ( $\beta_s$ ). The fourth factor,  $F_4$ , is determined based on the excavation method used as discussed by Goel and Singh (2011) and Sardana et al. (2019). This comprehensive framework of SMR provides a systematic and thorough method for evaluating slope stability in rocky terrains by considering various geological and geotechnical parameters.

### 3.1.2 Chinese Slope Mass Rating System (CSMR)

The adaptation of the Slope Mass Rating (SMR) system to rock slope conditions in China was introduced by Chen (1995). This adaptation incorporates two additional factors into the SMR system, which are the height of the slope, denoted as  $\xi$  when exceeding 80 m, and the conditions of discontinuity, represented by  $\lambda$ . These factors,  $\xi$  and  $\lambda$ , are integrated into the modified slope mass rating (SMR) formula as presented below. The Continuous Slope Mass Rating (CSMR) is calculated as follows:

$$\text{CSMR} = \xi(\text{RMR}_{\text{basic}}) + \lambda(F_1 \times F_2 \times F_3) + F_4 \quad (4)$$

The formula accounts for  $\xi$  as the slope height factor, where  $\xi = 0.57 + 0.43(80/H)$  for slopes taller than 80 m and  $\xi = 1$  for slopes with a height less than or equal to 80 m. The factor  $\xi$  represents the slope height factor in the classification system. On the other hand,  $\lambda$  is determined as 1 for faults of long weak seams filled with clay, 0.8–0.9 for bedding planes of large-scale joints with gouge, and 0.7 for joints of tightly interlocked bedding planes, serving as the discontinuity factor in the classification. Both  $\xi$  and  $\lambda$  play crucial roles in enhancing the SMR classification system due to the limited ability of SMR to predict certain slope failures accurately. Therefore, the inclusion of these two factors aims to refine the classification system while keeping other parameters constant. Notably, the factor  $\xi$  is only applicable for slope heights exceeding 80 m. Despite being an accepted classification system in China, its application outside China necessitates various adjustments and adaptations to ensure its effectiveness in different geological settings, as highlighted by Qadri et al. (2021).

### 3.1.3 Continuous Slope Mass Rating (CoSMR)

CoSMR, a modification of the original slope mass rating (SMR) proposed by Romana, is rooted in the well-established rock mass rating (RMR) technique. The concept of continuous slope mass rating was introduced by (Tomás et al. 2007) through the incorporation of continuous functions into Romana's SMR method. This adjustment aimed to enhance the precision of stability grade evaluations. It has been observed in various cases that SMR values exhibit slight deviations from actual field conditions, particularly when values fall on the boundaries of predefined class intervals during the computation of adjustment factors. The integration of continuous functions effectively addresses this issue, making the CSMR method notably robust

for slope stability assessments, as emphasized by (Siddique et al. 2017). The calculation of CoSMR follows the same equation used for SMR computation, with the key distinction lying in the determination of adjustment factors ( $F_1$ ,  $F_2$ , and  $F_3$ ), while factor  $F_4$  remains consistent with SMR, according to the findings of Sardana et al. (2019). Unlike SMR, which is characterized by its discrete nature, CoSMR is characterized by its continuous nature, reflecting a more refined approach to slope stability assessment. The continuous functions integrated into the CoSMR methodology play a pivotal role in mitigating the challenges associated with SMR assessments, particularly in scenarios where values verge on the boundaries of predefined class intervals. Consequently, the utilization of continuous functions in CoSMR not only enhances the accuracy of stability grade evaluations but also ensures a more comprehensive and reliable analysis of slope stability conditions. Overall, the evolution from SMR to CoSMR represents a significant advancement in the field of geotechnical engineering, offering a more sophisticated and nuanced approach to assessing the stability of slopes in various geological settings. The factors  $F_1$ ,  $F_2$  and  $F_3$  for CoSMR are calculated using Eqs. (5)–(8).

$$F_1 = \left(\frac{16}{25}\right) - \left(\frac{3}{500}\right) \arctan\left(\frac{1}{10}|A| - 17\right) \quad (5)$$

$$F_2 = \left(\frac{9}{16}\right) + \left(\frac{1}{195}\right) \arctan\left(\frac{17}{100}B - 5\right) \quad (6)$$

$$F_3 = -30 + \frac{1}{3} \arctan C \quad (7)$$

$$F_3 = -13 - \frac{1}{7} \arctan(C - 120) \quad (8)$$

The arctan functions, as well as parameters A, B, and C, are measured in degrees. These parameters are employed to calculate  $F_1$ ,  $F_2$ , and  $F_3$ . The values of A, B, and C are derived based on the particular mode of failure (Romana 1985).

Factor  $F_3$  is calculated using Eq. (6) for planar or wedge failure and Eq. (7) for toppling failure (Tomás et al. 2007; Sardana et al. 2019).

## 4 Results and Discussion

The calculation summary of SMR, CSMR and CoSMR with help of Eqs. (1)–(8), have been given in Tables 1 and 2. These values for fourteen susceptible slopes were assessed and compared, shown in Fig. 2. The field photographs of these fourteen slopes are given in Fig. 3.

Kinematic analysis plays a crucial role in identifying failure modes by examining the geometric relationships between discontinuities and potential failure surfaces, thereby offering valuable insights into slope stability. The kinematic analysis of these

**Table 1** Summary of CSMR calculation

Slope No.	Slope height (m)	$\xi$	$RMR_{basic}$	$F_1$	$F_2$	$F_3$	$F_4$	$\xi RMR_{basic}$	$\lambda(F_1 \times F_2 \times F_3)$	CSMR
SL-1	151.0	0.7978	39	0.85	1	— 50	15	31.115	— 29.75	16.365
SL-2	100.0	0.9140	51	1.00	1	— 50	15	46.614	— 35.00	26.614
SL-3	205.0	0.7378	58	0.40	1	— 60	8	42.793	— 16.80	33.993
SL-4	110.0	0.8827	65	1.00	1	— 25	10	57.377	— 17.50	49.877
SL-5	75.0	1.0287	40	0.15	0.85	— 60	0	41.147	— 5.36	35.792
SL-6	130.0	0.8346	37	1.00	1	— 6	0	30.881	— 4.20	26.681
SL-7	90.0	0.9522	40	0.15	1	— 50	10	38.089	— 5.25	42.839
SL-8	125.0	0.8452	55	0.85	1	— 50	15	46.486	— 29.75	31.736
SL-9	80.0	1.0000	74	0.85	1	— 50	10	74.000	— 29.75	54.250
SL-10	97.0	0.9246	67	0.70	1	— 50	10	61.951	— 24.50	47.451
SL-11	110.0	0.8827	65	0.70	1	— 50	15	57.377	— 24.50	47.877
SL-12	196.0	0.7455	65	1.00	1	— 6	10	48.458	— 4.20	54.258
SL-13	130.0	0.8346	39	1.00	1	— 6	15	32.550	— 4.20	43.350
SL-14	98.0	0.9210	46	1.00	1	— 50	15	42.367	— 35	22.367

fourteen slopes has been described by Jaiswal et al. (2024). SMR values discussed in the manuscript are essential indicators of slope stability, with lower SMR values suggesting a higher likelihood of failure and instability. The values of SMR suggest slopes (e.g., SL-1, SL-2, SL-8, SL-14) are under completely unstable condition. The estimated values of SMR ranging from 11 to 59 categorize most slopes in unstable condition (Class IV) according to Romana’s classification. The values of CSMR and CoSMR categories only slopes SL-1 under completely unstable condition however both classifications suggest most slopes in unstable condition similar to SMR classification.

It can also be seen from Fig. 2 that the toppling slope (SL-4) the value of CoSMR is significantly higher than the SMR and CSMR value. However, it is evident from



**Table 2** Summary of SMR and CoSMR calculation

Slope number	SMR			CoSMR			F <sub>4</sub>	SMR	CSMR
	F <sub>1</sub>	F <sub>2</sub>	F <sub>3</sub>	F <sub>1</sub>	F <sub>2</sub>	F <sub>3</sub>			
SL-1	0.85	1	− 50	0.91	0.978449	− 56.23	15	12	16.36477
SL-2	1	1	− 50	0.84994	0.975885	− 56.8467	15	16	26.614
SL-3	0.4	1	− 60	0.32542	0.960038	− 58.6367	8	42	33.99268
SL-4	1	1	− 25	0.11494	0.981731	− 3.93857	10	50	49.87727
SL-5	0.15	0.85	− 60	0.29206	0.917987	− 58.5333	0	33	35.79167
SL-6	1	1	− 6	0.91	0.981731	− 6.14667	0	31	26.68077
SL-7	0.15	1	− 50	0.2743	0.969936	− 58.6367	10	43	42.83889
SL-8	0.85	1	− 50	0.94117	0.968192	− 57.2897	15	28	31.736
SL-9	0.85	1	− 50	0.97786	0.968192	− 58.0963	10	45	54.25
SL-10	0.7	1	− 50	0.7402	0.977167	− 51.1433	10	42	47.45082
SL-11	0.7	1	− 50	0.85	0.975885	− 56.8457	15	45	47.87727
SL-12	1	1	− 6	0.871	0.979577	− 15	10	59	54.25816
SL-13	1	1	− 6	0.22624	0.985474	− 4.68	15	48	43.35
SL-14	1	1	− 50	0.988	0.984603	− 51.1433	15	11	22.36694

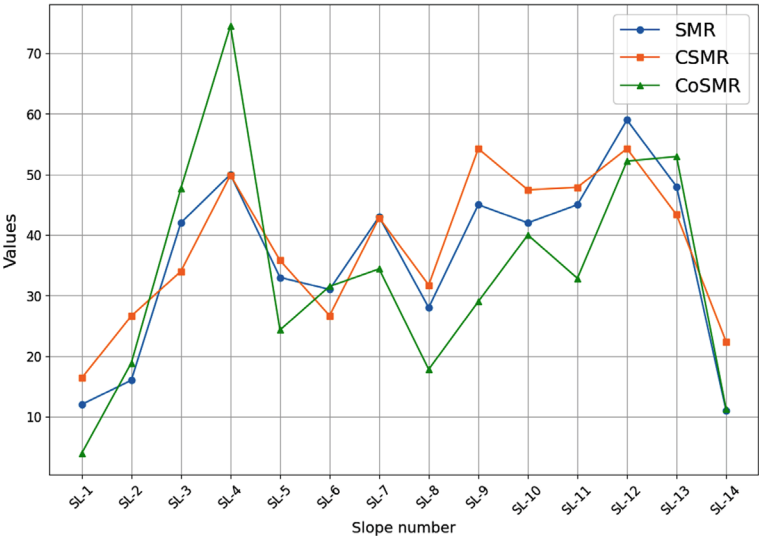


**Fig. 2** Comparative analysis of SMR, CSMR and CoSMR values of fourteen susceptible slopes

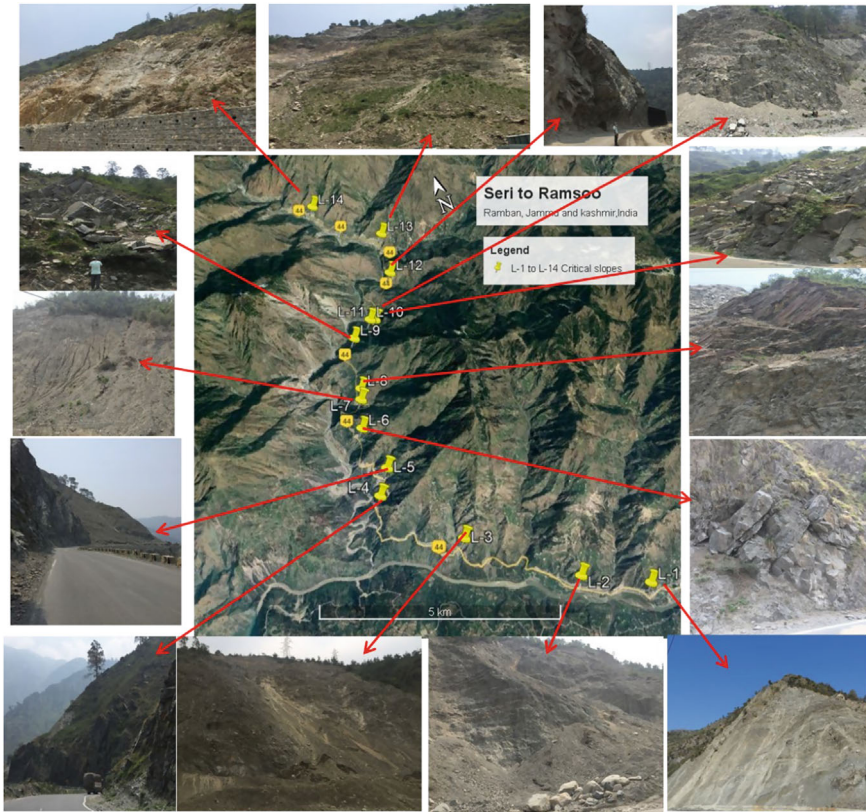


**Fig. 3** Field photograph of studied fourteen rock slopes

Fig. 2 that the CoSMR value is the lowest among all the proposed methods. It can also be deduced that SMR and CSMR have and have an approximately remarkably close value and for most of the slopes their value is more than CoSMR. The results of all the methods are given in Table 3 for each of these slopes.

The discrete and continuous functions were used to calculate the slope mass rating for each slope considered. One or two planes were found to have the most effect on these slopes' stability. Slope stability analysis based on SMR values showed that eight slopes (SL-3, SL-4, SL-7, SL-9, SL-10, SL-11, SL-12 and SL-13) were under partially stable state, three slopes (SL-1, SL-2, and SL-14) were in completely unstable state, and three additional slopes (SL-5, SL-6, and SL-8) were in unstable state. Four slopes (SL1, SL-2, SL-8, and SL-14) were found to be in completely unstable, five (SL-5, SL-6, SL-7, SL-9, and SL10) to be unstable state and four (SL-3, SL-10, SL-12, and SL-13) to be partially stable and one (SL-4) to be stable state according to the CoSMR value. The CSMR classified SL-1 as completely unstable state, six slopes (SL-2, SL-3, SL-5, SL-6, SL-8, and SL-14) in unstable state while seven slopes (SL-4, SL-7, SL-9, SL-10, SL-11, SL-12 and SL-13) are under partially stable state.

**Table 3** Results of all the used method

Slope number	SMR	CSMR	CoSMR
SL-1	12	16.365	3.933
SL-2	16	26.614	18.849
SL-3	42	33.993	47.681
SL-4	50	49.877	74.556
SL-5	33	35.792	24.307
SL-6	31	26.681	31.509
SL-7	43	42.839	34.400
SL-8	28	31.736	17.796
SL-9	45	54.250	28.997
SL-10	42	47.451	40.008
SL-11	45	47.877	32.846
SL-12	59	54.258	52.202
SL-13	48	43.350	52.957
SL-14	11	22.367	11.248

It is observed that majority of the unstable slopes lies in slate and phyllite rocks while granitic gneiss rocks form the partially stable slopes. This is because according to Jaiswal et al. (2024) granitic gneiss often has greater RMR value than slate and phyllite in the study area, and the instability is primarily governed by structural deformation in granitic gneiss. It is important to note that due to their structural deformation, partially stable (granitic gneiss) slopes may be susceptible to failure under external forces like earthquakes, intense rains, or human structures.

When CoSMR and SMR values for all the slopes under consideration are compared, it is shown that for eight slopes (SL-1, SL-5, SL-7, SL-8, SL-9, SL-10, SL-11, and SL-12), but SMR values for six slopes (SL-2, SL-3, SL-4, SL-6, SL-13, and SL-14) are lower than CoSMR. Because the  $F_3$  value, which is based on the angle difference between the slope dip and discontinuity dip, is bigger for CoSMR (dip of the discontinuity is smaller than the dip of the slope), the SMR values for the eight slopes were larger. The product of  $F_1$ ,  $F_2$ , and  $F_3$  has larger negative values as a result, and the CoSMR value is determined to be lower than the SMR value.

Due to the larger value of  $F_1$ , which indicates a parallel relationship between the slope and discontinuity strike direction (the slope and discontinuity are almost parallel to one another), the SMR values for six slopes were lower than the CoSMR values. The SMR's value spans 11–59, whereas the CoSMR spans 3.39–74.56. Romana's SMR is demonstrated to be less conservative than CoSMR. One benefit of CoSMR is that it reduces subjectivity by assigning a unique value to each SMR adjustment factor. SMR, CSMR and CoSMR are three techniques that may be used to assess the state of structurally controlled rock slopes; however, they may not work well on rock slopes with discontinuities that are tightly spaced apart.

#### 4.1 Relationship Between SMR, CSMR, and CoSMR

The relationships between SMR, CSMR, and CoSMR are investigated and compared during this study. Linear relationships between SMR and CSMR, CoSMR and SMR, and CSMR and CoSMR are plotted, and their correlation are analyzed. Figure 4 illustrates the relationship between SMR and CSMR, indicating a coefficient of determination ( $R^2 = 0.84$ ). Additionally, a mathematical relationship between CSMR and SMR is derived [see Eq. (9)]. Similarly, the relationships between CoSMR and SMR, and CSMR and CoSMR are presented in Figs. 5 and 6, respectively. The coefficients of correlation for these relationships are  $R^2 = 0.71$  and  $R^2 = 0.50$ , respectively. Furthermore, derived mathematical expression has been proposed in Eqs. (10) and (11). It should be noted that the analysis was conducted using only 14 slope rock slopes. This analysis indicates that the correlation between SMR and CSMR is stronger than the other proposed relationships with  $R^2 = 0.84$ .

$$CSMR = 0.76 \times SMR + 10.81 \quad (9)$$

$$CoSMR = 1.07 \times SMR - 4.86 \quad (10)$$

$$CoSMR = 1.09 \times CSMR - 8.01 \quad (11)$$

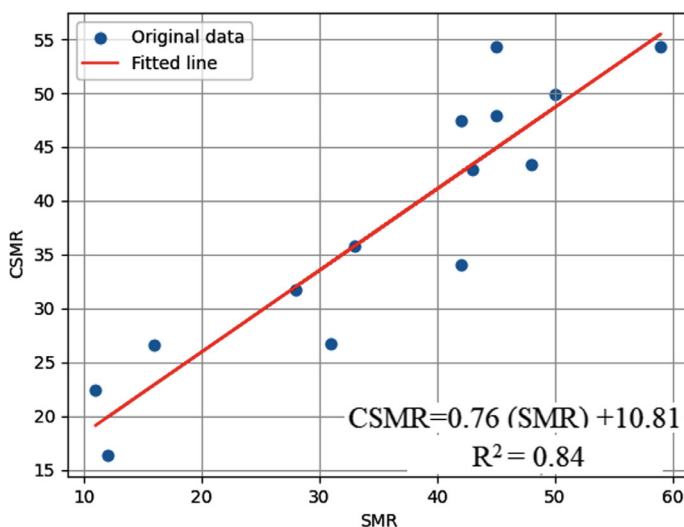


Fig. 4 Relationship between SMR and CSMR

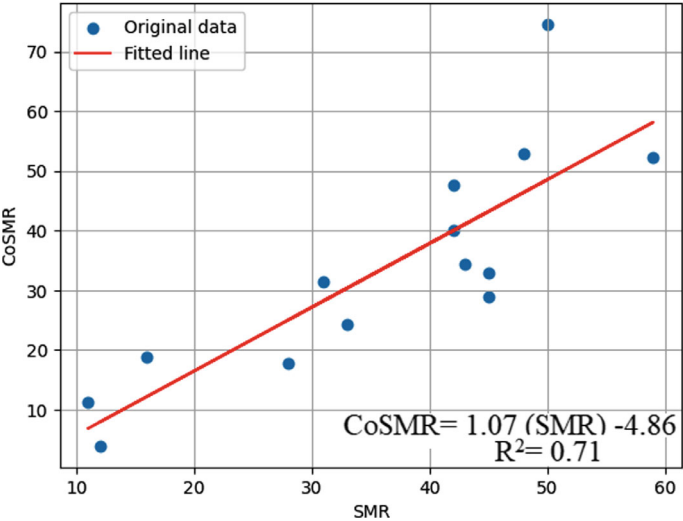


Fig. 5 Relationship between CoSMR and SMR

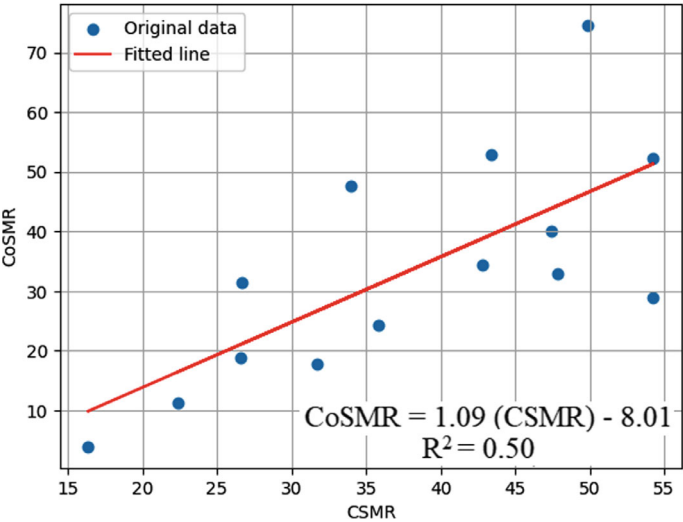


Fig. 6 Relationship between CoSMR and CSMR

## 5 Conclusion

In this work slope stability assessment of fourteen vulnerable slopes have been done using the Slope Mass Rating (SMR), Chinese Slope Mass Rating (CSMR), and Continuous Slope Mass Rating (CoSMR) methodologies. The outcomes suggest that, except for the collapsing slope (SL-4), the SMR and CSMR values generally surpass the CoSMR values. Through different investigations, it was discovered that the most unstable slopes are comprised of slate and phyllite, while the partially stable ones are predominantly made up of granitic gneiss. This is because of the higher strength of granitic gneiss than slate and phyllite and also because of one major plane of weakness presence in case of slate and phyllite i.e. foliation plane.

The findings highlight the effectiveness of CoSMR in delivering a more cautious and less biased evaluation of slope stability when compared to SMR and CSMR. Nonetheless, all three methodologies prove to be efficient in delineating the stability of slopes controlled by structures, with CoSMR standing out for its ability to reduce subjectivity by assigning distinct values to each adjustment factor.

The correlation among these three different classifications systems SMR and CSMR, CoSMR and SMR, and CSMR and CoSMR have been established based on fourteen case studies. It is found that good linear correlation between SMR and CSMR with correlation of coefficient ( $R^2$ ) value of 0.81.

## References

- Anbalagan R, Sharma S, Raghuvanshi TK (1992) Rock mass stability evaluation using modified SMR approach. In: Rock mechanics proceedings of the sixth national symposium on rock mechanics. pp 258–268
- Bar N, Barton N (2017) The Q-slope method for rock slope engineering. *Rock Mech Rock Eng* 50:3307–3322
- Barton N, Bar N (2015) Introducing the Q-slope method and its intended use within civil and mining engineering projects. In: ISRM Eurock. ISRM, p ISRM-EUROCK
- Barton N, Lien R, Lunde J (1974) Engineering classification of rock masses for the design of tunnel support. *Rock Mech* 6:189–236
- Bhat GM, Pandita SK, Singh R et al (1999) Northwest Himalayan successions along Jammu–Srinagar Transect (field guide). *Indian Assoc Sedimentol Aligarh* 1–141
- Bieniawski ZT (1973) Engineering classification of jointed rock masses. *Civ Eng Siviele Ingenieurswese* 1973:335–343
- Bieniawski ZT (1979) The geomechanics classification in rock engineering applications. In: ISRM congress. ISRM, p ISRM-4CONGRESS
- Bieniawski ZT (1984) *Rock mechanics design in mining and tunneling*
- Bieniawski ZT (1989) *Engineering rock mass classifications: a complete manual for engineers and geologists in mining, civil, and petroleum engineering*. Wiley
- Chen Z (1995) Recent developments in slope stability analysis. In: ISRM congress. ISRM, p ISRM-8CONGRESS
- Dahal RK, Hasegawa S, Yamanaka M, Dhakal S, Bhandary NP, Yatabe R (2009) Comparative analysis of contributing parameters for rainfall-triggered landslides in the Lesser Himalaya of Nepal. *Environ Geol* 58(3):567–586

- Ghosh S, van Westen CJ, Carranza EJM, Jetten VG, Cardinali M, Rossi M, Guzzetti F (2012) Generating event-based landslide maps in a data-scarce Himalayan environment for estimating temporal and magnitude probabilities. *Eng Geol* 128:49–62
- Goel RK, Singh B (2011) Engineering rock mass classification: tunnelling, foundations and landslides. Elsevier
- Hoek E, Brown ET (1997) Practical estimates of rock mass strength. *Int J Rock Mech Min Sci* 34:1165–1186
- Jaiswal A, Verma AK, Singh TN (2024) Evaluation of slope stability through rock mass classification and kinematic analysis of some major slopes along NH-1A from Ramban to Banihal, North Western Himalayas. *J Rock Mech Geotech Eng* 16(1):167–182
- Li TC (1990) Landslide management in the mountain area of China. *ICIMOD Kathmandu Occas* 15:50
- Panthi KK (2023) Methods applied for the stability assessment in rock engineering. *J Nepal Geol Soc* 65:29–34
- Paul SK, Mahajan AK (1999) Malpa rockfall disaster, Kali valley, Kumaun Himalaya. *Curr Sci* 76(4):485–487
- Pastor JL, Riquelme AJ, Tomás R, Cano M (2019) Clarification of the slope mass rating parameters assisted by SMRTTool, an open-source software. *Bull Eng Geol Environ* 78:6131–6142
- Qadri J, Alam MM, Sadique MR (2021) Comparison of slope mass ratings classification systems: a review
- Robertson AM (1988) Estimating weak rock strength. In: *Proceedings of the SME annual meeting, Phoenix*. pp 1–5
- Romana M (1985) New adjustment ratings for application of Bieniawski classification to slopes. In: *Proceedings of the international symposium on role of rock mechanics, Zacatecas, Mexico*. pp 49–53
- Romana MR (1993) A geomechanical classification for slopes: slope mass rating. In: *Rock testing and site characterization*. Elsevier, pp 575–600
- Romana M (1995) The geomechanical classification SMR for slope correction. In: *ISRM Congress. ISRM, p ISRM-8CONGRESS*
- Romana Ruiz M, Serón Gáñez JB, Montalar Yago E (2001) La clasificación geomecánica SMR: aplicación, experiencias y validación. In: *V Simposio Nacional sobre Taludes y Laderas Inestables*. Madrid, Spain
- Romana M, Serón JB, Montalar E (2003) SMR geomechanics classification: application, experience and validation. In: *ISRM congress. ISRM, p ISRM-10CONGRESS*
- Sardana S, Verma AK, Verma R, Singh TN (2019) Rock slope stability along road cut of Kulikawn to Saikhamakawn of Aizawl, Mizoram, India. *Nat Hazards* 99:753–767
- Selby MJ (1980) A rock mass strength classification for geomorphic purpose: with tests from Antarctica and New Zealand. *Zeit Geomorph NF* 24:31–51
- Selby MJ (1982) Rock mass strength and the form of some inselbergs in the central Namib Desert. *Earth Surf Process Landforms* 7:489–497
- Shuk T (1994) Key elements and applications of the natural slope methodology (NSM) with some emphasis on slope stability aspects. In: *Proceedings of the 4th South American congress on rock mechanics*. pp 955–960
- Siddique T, Pradhan SP, Vishal V et al (2017) Stability assessment of Himalayan road cut slopes along National Highway 58, India. *Environ Earth Sci* 76:1–18
- Sónmez H, Ulusay R (2002) A discussion on the Hoek-Brown failure criterion and suggested modifications to the criterion verified by slope stability case studies. *Yerbilimleri* 77–99
- Sun C, Chai J, Luo T et al (2020) Stability charts for pseudostatic stability analysis of rock slopes using the nonlinear Hoek-Brown strength reduction technique. *Adv Civ Eng* 2020:1–16
- Tomás R, Delgado J, Serón JB (2007) Modification of slope mass rating (SMR) by continuous functions. *Int J Rock Mech Min Sci* 44:1062–1069

**Amit Jaiswal** is currently a Ph.D. scholar in the Department of Civil and Environmental Engineering, Indian Institute of Technology Patna, India. Presently, he is working on the slope stability assessment of road cut slopes along the national highway of Jammu and Kashmir. He has developed a novel classification for rock slope stability assessment published in nature scientific reports. He has more than nine publications in field of engineering geology and rock mechanic. He has two book chapters and four conference proceedings of international conference. He has completed B.Sc. (Hons.) and M.Sc. in Geology from Department of Geology, Banaras Hindu University, India.

**Md Shayan Sabri** Ph.D. scholar in the Department of Civil and Environmental Engineering, Indian Institute of Technology Patna. Currently, He is working on Tunnelling, Slope Stability, and Artificial Intelligence applications in Civil Engineering. He has published five articles in top-tier journals and presented 3 conference proceeding papers in the field of Geotechnical Engineering and Rock Engineering. Additionally, He has contributed to a book chapter, showcasing his commitment to advancing knowledge in his field. He has completed his bachelor's degree in civil engineering from Heritage Institute of Technology Kolkata and Master of Technology from National Institute of Technology Patna in Geotechnical engineering.

**Dr. Amit Kumar Verma** is currently an associate professor and the Head of Department of Civil and Environmental Engineering, Indian Institute of Technology Patna. He has obtained his Ph.D. degree from Indian Institute of Technology Bombay and worked at several renowned institute across the world like 3S laboratory, Grenoble, France and University of California Davis, USA. He was visiting faculty at Clausthal University of Technology, Germany and Endeavour Executive fellowship at Monash University, Australia. He is recipient of prestigious awards like Institute of Engineers Young fellowship by 2014 and 2015. Dr. Verma has published more than 120 papers in the field of Rock mechanics and Rock engineering. He is a member of the reviewer board of several reputed Journal.

**Ashutosh Pratap Shastri** Master of Technology, in Geotechnical Engineering at the Indian Institute of Technology Patna. His research area focuses on slope stability analysis and the numerical modelling of rock and soil slope. Additionally, He has contributed to a book chapter, reflecting his dedication to advancing knowledge in this field. He has completed his bachelor's degree in civil engineering from Madan Mohan Malaviya University of technology Gorakhpur.

**Komal Kumari** is a master's student at Indian Institute of Technology Patna, where she is pursuing her research interests in Slope Stability Analysis and Geotechnical Engineering. She has already made a significant start by contributing to a book chapter on Slope Stability Analysis, marking the beginning of her academic endeavours. In addition to her academic pursuits, she has received client appreciation twice for proposing latest and cost-efficient solutions to problems and delivering high-quality work. Komal holds a Diploma in Electronics and a B.Tech. in Civil Engineering from Nalanda college of engineering Chandi, showcasing her strong educational foundation in both electronics and civil engineering.

**T. N. Singh** is currently working as Director IIT Patna and the Institute Geoscience Chair Professor in the Department of Earth Sciences, IIT Bombay, Mumbai, and is an expert in the field of rock mechanics, mining geology, and clean energy. He received his Ph.D. degree from the Institute of Technology BHU, Varanasi, in 1991 and subsequently served the institute until 2003. He is a recipient of many prestigious awards such as the National Mineral Award, the first P. N. Bose Mineral Award, the SEAGATE Excellence Award for Geo-Engineering, and the GSI Sesquicentennial Commemorative Award. He has nearly 28 years of experience in research and teaching with 16 doctoral theses completed under his supervision and has authored more than 350 publications in various journals and conferences of national and international repute. He



is currently leading projects of immense scientific and industrial importance related to coalbed methane, carbon sequestration, shale gas, nuclear waste repositories, and mine slope stability, to name a few. He is on the governing and advisory councils of several national institutes and universities.

# **Simulation of Slope Mass Movements Including Numerical Methods**

# Assessment of Progressive Behaviour of Deep-Seated Kotropi Landslides (Himachal Pradesh) Using the 3D Limit Equilibrium Method



Saurabh Kumar, Saurabh Prakash Aher, Sarada Prasad Pradhan,  
and B. D. Patni

**Abstract** Large or deep-seated progressive landslides pose significant challenges due to the complex failure mechanism and the potential for recurring failures. Progressive landslides are characterized by a gradual and continuous downslope movement of soil and rock material over an extended period. Analysing the evolution of deformation within a large landslide can provide valuable insights about the location and direction of progressive sliding events which may lead to severe instability. Identification of the progressive failure in large and deep-seated landslides is essential for risk assessment, timely adopting mitigation strategies, and ensuring public safety. The August 2017 Kotropi landslide in the Mandi district of Himachal Pradesh is an example of a deep-seated progressive landslide. The landslide has experienced continuous sliding events since its initiation and become a threat to local community. This research aimed to analyse the evolution of progressive deformation in Kotropi Landslides (Himachal Pradesh) using the 3D limit equilibrium method. This study uses field data of different time intervals, back analysis, and 3-Dimensional numerical modeling to estimate the stability of the Kotropi landslide. Two 3D models were constructed using the field data conducted in two phases: Phase 1 (year 2017–20) and Phase 2 (year 2021–23) to determine the probability of failure in different time period. The stability analysis examines the evaluation of instabilities in the Kotropi landslide for a period of year 2017–20 and year 2021–23, taking into account factors like changes in surface geometry, pore water pressure, ground deformation, and so on. The results obtained were combined with satellite imagery to check the location and direction of progressive failure with in Kotropi landslide. The results indicate that the progressive failures are concentrated in right flank near to the crown area. Contrary to initial failure which occurred in NE-SW direction, the progressive failures are taking place in N-NW direction.

---

S. Kumar (✉) · S. P. Aher · S. P. Pradhan  
Department of Earth Sciences, IIT Roorkee, Roorkee 246667, India  
e-mail: [saurabh\\_k@es.iitr.ac.in](mailto:saurabh_k@es.iitr.ac.in)

B. D. Patni  
NHPC Limited, Faridabad, India

**Keywords** Progressive landslide · Indian Himalayas · 3D limit equilibrium modeling · Stability analysis

## 1 Introduction

Landslides pose a significant global threat to infrastructure and communities, resulting in deaths, property damage, and environmental degradation (Petley 2012). Landslides not only responsible for loss of life and property, but they also disrupt agricultural operations, transportation networks, and livelihoods (Sarkar et al. 2015; Roul et al. 2022). According to global fatal landslide data, India contributes highest to non-seismically triggered landslide occurrences (Froude and Petley 2018). Landslides are common in hilly and mountainous terrain of India, where steep slopes, weak rock mass and heavy rainfall create favourable conditions for slope instability (Anand and Pradhan 2019; Dikshit et al. 2019; Pradhan and Siddique 2020; Komadja et al. 2020, 2021; Siddique et al. 2022). Landslides in India are especially common in the North-West and North-East Indian Himalayan regions, as well as the Western and Eastern Ghats (NRSC). Landslides in India have become more frequent and intense in recent years due to deforestation, unplanned development, and climate change-induced extreme weather events.

Progressive landslides are distinguished by the continuous downslope movement of soil and rock material over time (Damiano et al. 2021; Bernander et al. 2016; Leshchinsky et al. 2015, 2019). In some cases, these landslides may exhibit recurrent cycles of sliding, with periods of inactivity followed by reactivation as a result of changing environmental conditions or stresses. This type of landslides is characterized by presence of discontinuities such as bedding planes, faults, or shear zones that provides pathway for material movement, as well as formation of deep-seated failure surfaces within the slope (Darban et al. 2019). The key factors that drive the progressive landslides includes gravity, slope geometry, soil characteristics, ground-water conditions, and external loads. Large or deep-seated progressive landslides are influenced by various parameters, including material properties, slope geometry, and environmental conditions (Pei et al. 2022). Understanding the mechanisms and behaviour of such landslides is critical for assessing the associated risks and reducing the potential impacts on communities and infrastructure in landslide-prone areas (Deng et al. 2019). Large progressive landslides require a multidisciplinary approach to comprehend the complicated relationships of geological, hydrological, and environmental elements that cause slope instability (Tandon et al. 2021). Field investigations usually begin with a mapping of the landslide area to record the extent of movement, identify potential failure surfaces, and assess the geological properties of the slope (Baroň and Supper 2013; Fanos and Pradhan 2018; Panda et al. 2023). Geotechnical investigations involve collecting soil or rock samples for laboratory testing to evaluate their physical and mechanical characteristics. Total station data is useful for assessing terrain morphology, detecting land surface changes, and monitoring landslides over time (Baroň et al. 2012; Giussani and Scaioni 2004). Many

researchers (Afeni and Cawood 2014; Tsai et al. 2012; Artese and Perrelli 2018) have employed total stations for landslide monitoring. In addition, stability analysis can be used to evaluate potential failure mechanisms and forecast possible trends and patterns of future sliding. To reduce the damage on communities and infrastructure, a comprehensive understanding of large progressive landslides can be achieved by combining field observations, laboratory testing or back analysis, and numerical modeling.

Stability analysis is a fundamental approach in landslide related studies to evaluate the safety and possibility of slope failure of natural and man-made slopes (Congress and Puppala 2021; Congress et al. 2021; Pradhan and Siddique 2020). The results of stability analysis are greatly influenced by soil parameter; therefore, estimation of accurate soil parameter is essential in slope stability analysis. Determining soil parameters is typically accomplished through in situ or laboratory testing, but this process introduces uncertainties related to testing, modeling, and measurement (Berti et al. 2017; Rana and Sivakumar Babu 2022). Back analysis, also known as inverse analysis, offers a practical approach to determining soil parameters based on observed data (Tang et al. 1999; Harris et al. 2012; Spreafico et al. 2016; Pandit et al. 2021). Back analysis can be adopted to address the inherent uncertainty in soil parameter estimation to account for variations and uncertainties (Wang et al. 2013; Ering and Babu 2016; Li et al. 2016; Zuo et al. 2022). The process of back analysis involves adjustment of parameters such as soil properties, groundwater levels, or slope geometry, to match observed field data by imposing a condition of near instability (Jiang et al. 2020; Li et al. 2021). The stability analysis can be performed using a deterministic or probabilistic approach (Queiroz 2016; Budetta 2020; Kundu et al. 2018). In a deterministic approach, the soil strength parameters and other variables that influence slope stability are assumed to have definite and constant values. On the other hand, the probabilistic analysis considers the uncertainty and variability in the inputs and uses statistical methods to compute the likelihood of failure (Park and West 2001; El-Ramly et al. 2002; Roul et al. 2021; Shafiee et al. 2022; Siddique and Pradhan 2018). This method offers a variety of potential outcomes, and the findings can be expressed in terms of the expected factor of safety or the failure probability. The Finite Element Method (FEM), Finite Difference Method (FDM), Discrete Element Method (DEM), and Limit Equilibrium Method (LEM) are among the numerical modeling techniques that can be used for stability analysis (Abderahmane 1996; Duncan et al. 2014; Wyllie and Mah 2017; Bahsan and Fakhriyyanti 2018; Singh et al. 2022a, b; Singh et al. 2023). Limit Equilibrium Method (LEM) is a conventional technique that only identifies the onset of failure and provides exact solutions. Whereas the Numerical Methods (FEM, FDM, DEM or hybrid methods) have the ability to solve complex problems including the effect of stress redistribution and progressive failure after failure has been initiated. These numerical techniques provide approximate solutions to complex problems, however, have sufficient accuracy for engineering purposes. These techniques model the behaviour of slope material under various conditions, including seismic forces, water pressure, and gravity. The LEM is an extensively used and well-established approach for assessing slope stability (Bishop 1955; Spencer 1967; Reyes and Parra 2014; Johari

et al. 2015; Zhang et al. 2015). 3D model-based stability analysis has gained popularity among researchers due to its significant advantages over 2D models (Wang et al. 2017; Bovolenta and Bianchi 2020; Yeh et al. 2020; Ma et al. 2021). 3D models provide a more accurate representation of complex three-dimensional terrain features (Stark and Eid 1998; Panda et al. 2023). It allows the incorporation of irregularities in slope geometry, which may significantly influence stability conditions. Additionally, 3D models permit the inclusion of spatial variation in soil properties and geological features, providing a more improved and realistic visualization of slope (Zhu et al. 2011; Xiang et al. 2013; Zabuski 2019; Yang et al. 2021). Therefore, 3D limit equilibrium based stability analysis was chosen to complete this study.

The stability of a progressive landslide evolves with progression of failure. It became crucial to check the instabilities arises over a period to understand the ongoing failure pattern. Multi-temporal stability analysis of a landslide involves the assessment of slope stability conditions over multiple time periods to assess the evolution of instability and identify potential trends or patterns (Koca 2021). The comparison of the conditions before, during, and after landslide events, can provide valuable insights about the driving mechanism and factors influencing stability of a landslide. Multi-temporal stability analysis allows for the identification of precursory signs of instability, the monitoring of ongoing slope movements, and the evaluation of post-event recovery and stabilization efforts. Therefore, this study uses the idea of multi-temporal stability analysis to assess the mechanism and ongoing failure pattern of deep-seated Kotropi landslide. The Kotropi landslide have a history of reactivation since 1977 and its last major reactivation was seen in Aug 2017, which have killed more than 45 people. However, apart from 3 major reactivation since 1977, the landslide continuously experiences local failures due to its weak lithology and heavy rainfall conditions. The slide poses a continuous threat to the local community and vehicles passing though the NH-154 (Mandi-Pathankot Highway). Hence, this study aims to evaluate the mechanism and behaviour of failure pattern of Kotropi landslide using the 3D models based on limit equilibrium method.

## 2 Study Area and Geology

Mandi district of Himachal Pradesh is notorious for the occurrence of several landslide events every year because of presence of weak/fragile lithology, regional structural discontinuities, and rainfall in the area. A massive slide event took place near Kotropi, Mandi on 13th August 2017 (third reactivation) which has resulted into the demise of 40 people and 10 were missing, while some of the private vehicles along with two HRTC (Himachal Road Transport Corporation) buses were hit by the failed material from the slide and got buried under it. The Kotropi landslide ( $N31^{\circ} 54' 39.4''$  and  $E76^{\circ} 53' 27.4''$ ) which is located near Kotropi village of Mandi district, on Mandi-Joginder Nagar-Pathankot National Highway (NH)-154, fall in Survey of India Toposheet no 53A/13. The nearby residents have confirmed that the slide has undergone multiple episodes of failure since 1977 with a reactivation

interval of 20 years. A total of 133,674 m<sup>2</sup> area was affected due to the landslide, with width, height, and runout distance of 380 m, 350 m, and 1500 m, respectively (Pradhan et al. 2019; Singh et al. 2020). It is categorized as deep-seated debris slide; it was possibly triggered due to the intense rainfall and presence of highly deformed lithological units in the study area. The past sliding events has exposed pre-existing scars on the slope faces which may result into the progressive failure indicating the threat for the human settlements residing in the adjoining areas. The major rocks found in the nearby area includes Shale, Slate, Quartzite, Cherty Dolomite of Makri Formation, Salt Grit or Purple Grit (locally known as Lokhan) of Guma Formation along with pink-grey limestone, sporadic shale of Sorgharwari Formation and micaceous sandstone, purple clay, and mudstone of Shiwalik group of rocks (Roy et al. 2018; Sharma et al. 2019). The rock mass present in the slide area is highly fragile as it has been subjected to intense deformation due to the thrusting activity. Major discontinuities in slide area include Shali thrust passing through the slide and the Gairu thrust situated just above the crown of the slide (Fig. 1). The unreachable area above crown portion consists of purple mudstone, greenish shale of Dharamshala Group is present (Thakur et al. 2019).

Figure 2 indicates the monthly rainfall data from the year 2013 to 2023 (Guhathakurta et al. 2020). The annual average rainfall of the study area is found to be 1157.74 mm per year. Majority of the rainfall is received in July and August months. The complex geological setup of the study area and current condition of the slope mass is very vulnerable. In addition to that, rainfall event leads to the ingress of the water in the slope mass through cracks and scars present in the slope mass, which leads to the increase in the pore pressure in the material present and subsequently deteriorates the strength of the material present. As the slope mass has a reactivation history hence considering such risks, the progressive failure is meant to happen in the near future.

### 3 Methodology

As previously stated, multi-temporal stability analysis enables a more complete understanding of the process and behaviour of progressive landslides. It can also provide vital insights into the progression of movement in a progressive landslide. As a result, this work employs the idea of multi-temporal stability analysis to investigate the process and behaviour of deep-seated Kotropi landslides, as well as uncover probable trends or patterns. The study uses a combination of geotechnical methodologies, including field investigation, back analysis, and 3D limit equilibrium-based stability analysis, to examine the evolution of instability in the Kotropi landslide. Multiple field surveys were carried out in this study to assess the geological, hydrological, and geotechnical features of the Kotropi landslide. The field surveys involve a total station survey to determine the geometry of the landslide. Back analysis was conducted to determine the shear strength parameters of failed mass at the time of failure. Laboratory testing was performed to obtain the base values of strength





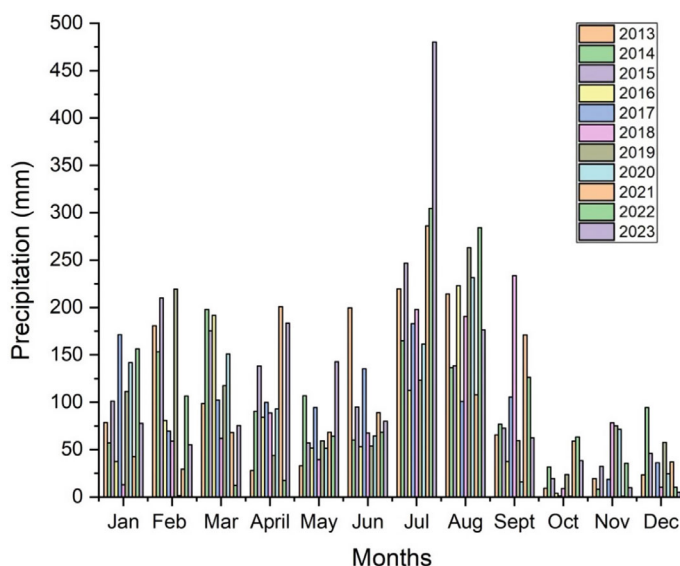


**Fig. 2** Rainfall data of the study area from 2013 to 2023

parameters needed for back analysis. Then results of field surveys, as well as back analysis were incorporated into the 3D models of the slide to check the stability. The multi-temporal stability analysis was performed using Rocscience's SLIDE 3D software.

For the ease of understanding, the field data collected through multiple field investigations were divided into two phases; (1) Phase 1: Field data collected between a period of year 2017–20 (2) Phase 2: Field data collected between a period of 2021–23. Based on this geometric and field data, two 3D models of Kotropi landslide were constructed in SLIDE 3D software to analyse the stability for two different time periods. Model 1 was built using the surface geometry from year 2018 and field data from the phase 1 field investigation, which took place between years 2017 and 2020. On the other hand, Model 2 was constructed using the surface geometry from year 2022 and field data from the phase 2 field investigation, which took place between years 2021 and 2023. The stability result obtained from Model 1 were compared with Model 2 to examine the ongoing failure pattern and behaviour. The findings from the field investigation, including the identification and mapping of tensional cracks and groundwater seepage, were correlated with failure probabilities. The methodology of the current research is described in detail below.

### 3.1 Field Investigation

The Kotropi landslide was categorized as deep-seated debris type slide which re-initiated in Aug 2017. The landslide has been experiencing progressive failures since its re-initiation in different parts. To record the ongoing changes multiple field investigations were carried out on the deep-seated Kotropi landslide between a period of 2017–2022. The field investigation allows to collect geological, and geotechnical data of the slide area. Three distinct lithological layers were found in the slide area. The top layer was primarily composed of crushed grey shale and Makri formation detritus, the middle layer of extensively crushed salt grit (Lokhan) and grey limestone, and the lowest layer of purple clay and mudstone. The rock crushing in the slide is caused by the Shali thrust passing across it. In this study, the top, middle, and bottom layers are labelled as KL1, KL2, and KL3, respectively. Figure 3 depicts images of the Kotropi landslide taken during the 2018 and 2022 field visits. Several tensional cracks were found at various places. The extent and location of these cracks were recorded carefully. Figure 4 shows the failure event and tensional cracks observed during the 2022 field visit. Apart from that, a flowing stream was also encountered below the crown of the landslide, indicating the higher groundwater level in the slide region. Additionally, tacheometric survey was conducted to obtain the geometry of the slide.



**Fig. 3** a Field photograph of showing critically stable right flank during year 2018 field visit and b field photograph of showing failed right flank during year 2022 field visit

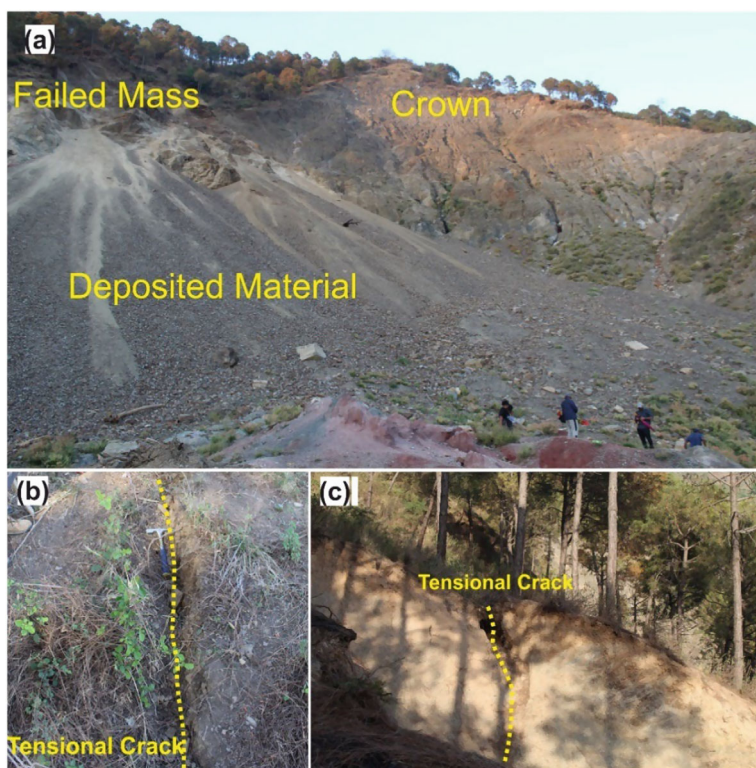


**Fig. 4** Failure signatures observed in right flank during 2022 field visit

### 3.2 Tacheometric Surveying

Tacheometric surveying is commonly used to map and measure surface features with high precision and efficiency. It makes it easier to monitor landslide movements and discover early signatures of slope instability. Tacheometric surveying provides precise data that aid in the construction of numerical models for analysing stability of a slope. Tacheometric surveying is a reliable method for monitoring the progression of a landslide over time by conducting repeated surveys at consistent intervals (Giussani and Scaioni 2004). It can also yield valuable data regarding the direction and speed of movement, which can enhance our understanding of landslide processes and aid in predicting future behaviour (Baroň and Supper 2013). Thus, in order to determine the geometry of the slide over two distinct time periods, a multi-temporal tacheometric survey was conducted utilizing Leica's total station. Two field surveys produced two set of point cloud data with thousands of points each containing the latitude, longitude, and elevation information for the slide. The first point cloud was captured during the 2018 field visit and represents the slide's geometry after the initial landslide occurred. In contrast, the second point cloud was acquired during the 2022 field visit

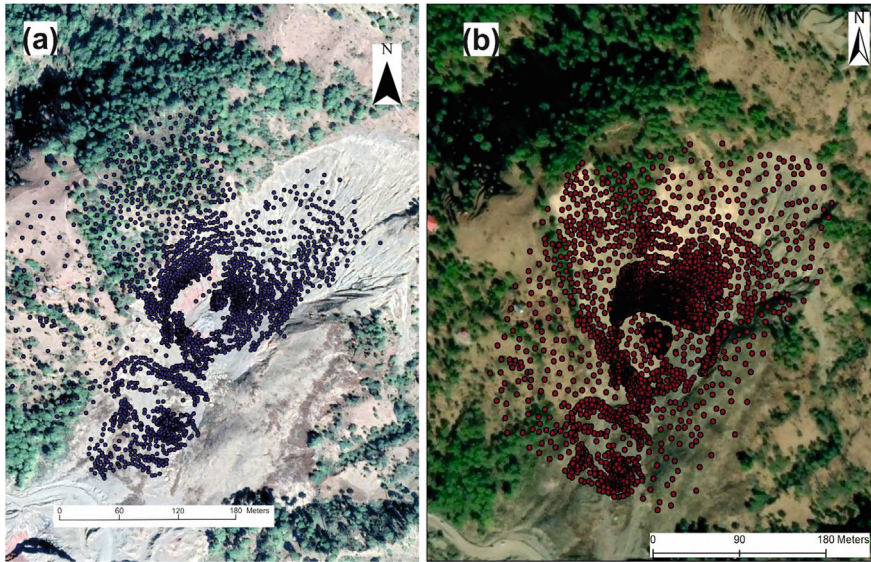


**Fig. 5** Point cloud acquired **a** year 2018, **b** year 2022 field investigation

and captures the slide's current geometry following minor progressive failures and surface alterations (Fig. 5).

### 3.3 *Geometry Reconstruction*

Geometry reconstruction involves accurately collecting landslide topographic data and processing recorded data to construct the geometry by removing noise or distortion. The geometric data of the Kotropi landslide was collected during field survey for year 2018 and 2022 using Leica's total station. The point clouds consisting of thousands of points were processed to remove the noise and distortion present in the recorded data. Cloud Compare software was used for the post-processing of the point cloud. Two different 3D surface geometries representing the landslide's initial (year 2018) and recent topography (year 2022) were generated using multi-temporal point cloud data. Figure 6 show the surface geometry constructed for Kotropi landslide for year 2018 and 2022.

### 3.4 *Back Analysis of Shear Strength Parameters*

Back analysis is the retroactive assessment of a landslide occurrence based on observable field data and numerical or analytical modeling approaches (Chandler 1977).



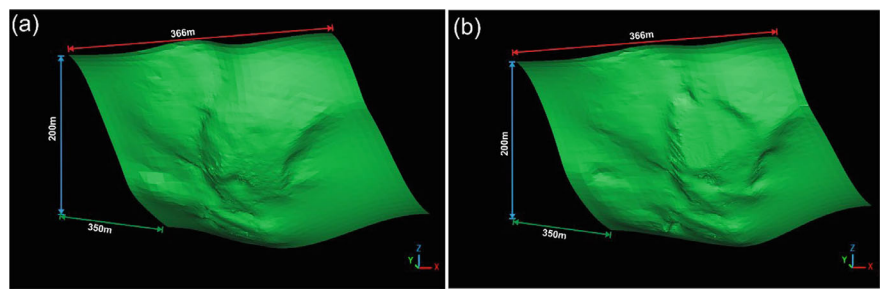


**Fig. 6** Surface geometry of Kotropi landslide during **a** year 2018 **b** year 2022

**Table 1** Back analysed properties of slide material

Parameter		KL1	KL2	KL3
Cohesion (kPa)	Mean	29.3	23.1	19.3
	Standard deviation	5.3	2.3	3.4
Angle of friction (°)	Mean	37.4	35.5	33.4
	Standard deviation	2.6	1.2	2.1
Unit weight (kN/m <sup>3</sup> )	Mean	24.1	21.3	19.6

Back analysis may be used to estimate a variety of uncertain factors that lead to slope failure (Wang et al. 2013; Ering and Babu 2016). The back analysis was performed to account for the uncertainties associated with the limited available data and achieve more exact parameter values (Siddque and Pradhan 2018). For the back analysis, a typical cross-section of the Kotropi landslide characterized by the steepest slope was chosen. Both the cohesion and the internal friction angle were considered random variables. The back analysis was carried out by comparing the numerical modeling findings with the observed failure behaviour, such as displacement or failure surface shape. Through laboratory testing, the initial values of the shear strength parameters were established. After that, these values were changed iteratively until the safety factor reached 1 and the simulated behaviour closely matched the slide’s observed behaviour. Table 1 presents the back-calculated properties obtained from this investigation. These properties were then utilized in numerical simulations to analyse the stability of the slide.

**3.5 3D Limit Equilibrium Based Probabilistic Stability Analysis**

Numerical modeling is critical for understanding how landslides behave under different situations. When analyzing simulation results, it is critical to use appropriate numerical models and be aware of their limits. The LEM is the most widely

used and reliable method for slope stability analysis (Abramson et al. 2001; Xu et al. 2012; Deng et al. 2017). Probabilistic analysis, which takes into account uncertainties and variations in input parameters, uses statistical methods to estimate the probability of slope failure (El-Ramly et al. 2006; Falamaki et al. 2021). For the current study, limit equilibrium-based SLIDE 3D software from Rocscience (Rocscience 2021) was used to analyse the stability of Kotropi landslide under different conditions. The probabilistic analysis was executed on two 3D models (Model 1 and Model 2) of Kotropi landslide belonging to two different time periods. Based on the field observation three different lithological layers of different geo-mechanical properties were incorporated into these models. The back-calculated values of cohesion and angle of internal friction were used in these models. The cohesion and internal friction angle of each layer were taken as random variables which follow a normal distribution while the Latin Hyperloop method was used as sampling method. Spencer's method, a well-known limit equilibrium method (Spencer 1967), was used for determining the probability of failure for both models. The spencer's method can satisfy both force and moment equilibrium, which ensures a more accurate and reliable determination of the factor of safety. Both models were simulated in two different conditions: dry and saturated. In the dry condition, the pre-monsoon state was modelled by taking the pore water pressure ratio ( $R_u$ ) zero. This was done so to model the conditions before the onset of the rainy season. To replicate the saturated situation that exists during the monsoon season, based on the literature and field observation the pore water pressure ratio ( $R_u$ ) was taken 0.2 (Sharma et al. 2019; Prakasam et al. 2022). Results obtained from stability analysis were compared to visualize the evolution of stability in different parts of the Kotropi landslide.

## 4 Results and Discussion

The stability of the Kotropi landslide was assessed using two three-dimensional models that employed the limit equilibrium approach. Model 1 of the Kotropi landslide was constructed using field data collected during the initial phase 1 field surveys conducted between 2017 and 2020. On the other hand, Model 2 was developed using field data obtained during the subsequent phase 2 field surveys carried out between 2021 and 2023. The stability of both models was examined under both dry and saturated conditions. The stability analysis was initially done on Model 1. In totally dry conditions, the factor of safety was 0.99, with a failure probability of 73.52%. Figure 7a depicts the distribution of failure surfaces in dry conditions with values less than 1. The yellow lines indicate the global minimum failure surface whereas red lines are failure surfaces with a value of less than 1. It can be seen that the failure surfaces with a value less than 1 (red colour) are concentrated in right flank near to the right crown of the slide indicating the unstable zone in right crown part. The saturated condition was achieved by incorporating the pore water pressure ratio. The overall stability of the landslide reduces as we incorporated the pore water pressure ratio. The safety factor reduced to 0.65 whereas the probability of failure reaches to

100%. Figure 7b shows the distribution of failure surface in saturated condition. It can be seen that failure surfaces with  $FoS < 1$  are mainly concentrated in the right crown part and some of the failure surfaces are scattered over the whole crown area indicating the instability in crown region of the landslide. The results indicates that the slope mass has the potential of future sliding in dry as well as saturated conditions.

A surface safety map of the whole slide was generated to visualize the distribution of factor of safety in different parts of the slide. The surface safety map was generated for dry as well as saturated condition. This map provides valuable insights to identify the extent of unstable region within the landslide. The region of the landslide with a safety factor  $< 1$  are highlighted in red colour whereas region of the slide with safety factor  $> 1$  are highlighted in yellow to blue colour indicating increasing factor of safety. The red zone in the slide area indicates unstable zone which have the potential of sliding whereas yellow to blue zone indicates the gradual increase in stability of the slope mass. In Fig. 8, it can be seen that in dry condition the unstable region of the slide is concentrated in right crown of the landslide whereas in saturated condition the extent of unstable region become larger which covers the whole crown area.

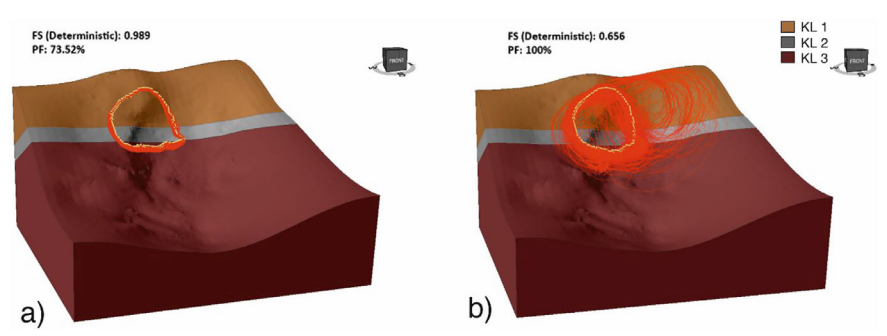


**Fig. 7** Distribution of failure surfaces ( $FoS < 1$ ) in Model 1 in **a** dry condition **b** saturated condition

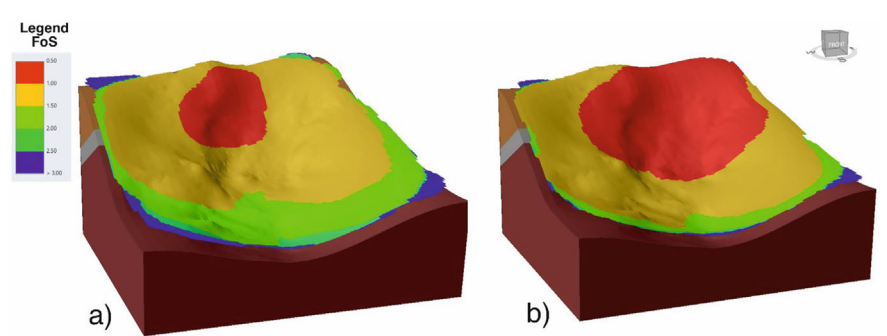


**Fig. 8** Surface safety map showing the extent of unstable region (red colour) for model 1 in **a** dry condition **b** saturated condition

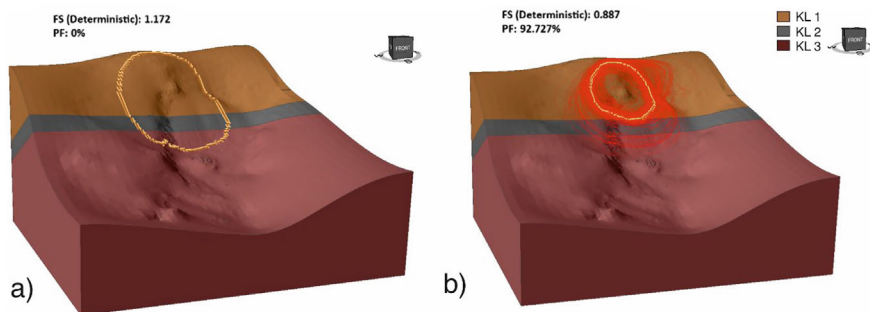


**Fig. 9** Distribution of failure surfaces (FoS < 1) in Model 2 in **a** dry condition **b** saturated condition

Model 2 of the Kotropi landslide was constructed using the surface geometry of year 2022 and field data from Phase 2 field surveys. This model was also simulated in both dry as well as saturated condition. The results indicates that with progression of time the overall safety factor of the slide in dry as well as saturated condition have increased. The factor of safety in dry condition reaches to 1.172 and probability of failure become zero whereas in saturated condition the factor of safety comes out to be 0.887 and probability of failure was 92.72%. Figure 9a shows the location of global minimum failure surface in dry condition having a value of 1.172. The extent of global minimum failure surface has become larger compared to the previous surfaces. Figure 9b shows failure surfaces in saturated condition having a value of less than 1 are spread in the crown region of the slide. The results indicate the slope mass is relatively stable in dry condition but still have the potential of failure during rainy season.

After completing the stability analysis, a surface safety map was generated using Model 2 for the whole slide for dry as well as saturated condition. The red colour in Fig. 10 indicates the unstable region of the landslide. Since the safety factor in dry condition was greater than 1, therefore a major part of the landslide is highlighted in the yellow colour indicating relatively stable region of the landslide (Fig. 10a). In saturated condition the unstable region having a safety factor less than 1 is highlighted in red colour whereas stable region of the landslide is highlighted in yellow to blue colour with increasing factor of safety (Fig. 10b).

Once the 3D stability analysis was finished, the results of all the models were compared to visualize the evolution of instability and mark the location and direction of the progressive failures. During Phase 1 field investigations between 2017 and 2020, minor failure events were observed in right flank near to the crown region of the landslide. Model 1 which was build using the field data of 2017–2018 also predicts instability in right flank and crown of the landslide. The surface safety map generated from Model 1 indicates unstable region in the right flank of the landslide. Failure events observed in right flank during year 2022 field visit also validates the results obtained from Model 1. The failed slope mass from the top of the right flank and crown was deposited at the toe of the right flank. Tensional cracks observed in right flank of



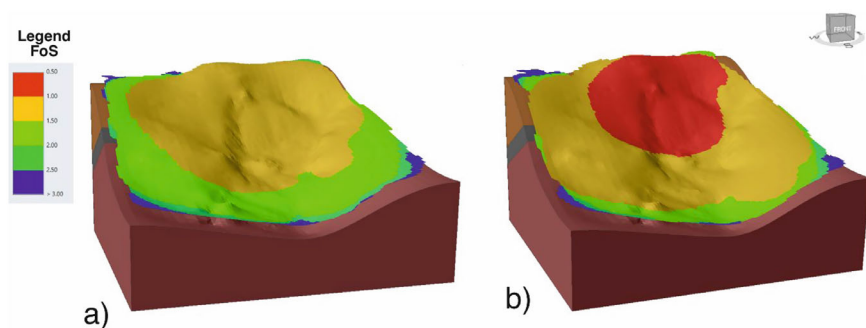


**Fig. 10** Surface safety map showing the extent of unstable region (red colour) for model 2 in **a** dry condition **b** saturated condition

the landslide indicates the potential for future instability (Fig. 11). The results from Model 2 indicate that the right flank have the higher probability of progressive failure in saturated conditions. This indicates that while the landslide is relatively stable in dry conditions, it has the potential for future failures during rainfall due to increased pore pressure. A comparison between Models 1 and 2 reveals a higher safety factor in dry conditions, mostly because to the altered landslide geometry. Due to the earlier sliding events, slope material from the right flank's top was removed and dumped close to the flank's toe, creating a comparatively gentle slope. Therefore, compared to model 2, the right flank of model 1 is significantly steeper resulting in a lower safety factor. The comparison indicates that the overall stability of the landslide is highly sensitive to moisture content and landslide geometry. The field data indicates that while the slope is relatively stable under dry conditions, the presence of tension cracks and heavily crushed rock mass make it susceptible to failure during the rainy season when pore pressure increases.

Google earth images were also used to analyse the evolution of instability in the Kotropi landslide since its initiation. Yellow line in Fig. 12 indicated the initial periphery of the landslide whereas red line marks the boundary of progressive failure taken place after its initiation. It can be seen in satellite image of Dec 2021 that after the initiation in Aug 2017, major failure occurred in right flank near to the crown area, as predicted by our first 3D model (Model 1). The failure was observed after the rainy season of 2021. Our second 3D model (Model 2) which was build using Phase 2 field data suggest further instability in right flank and crown region. Satellite image of Dec 2023 confirms that the further failure has been taken place in right flank near to the crown region.

Combing the results of numerical modeling, field investigation and satellite images, it can be interpreted that the Kotropi landslide has experienced progressive failure since its initiation. The progressive failures are confined in right flank near to the crown region of the landslide. Numerical modeling results suggests the high probability of future sliding in right flank. Contrary to initial re-activation which occurred in NE-SW direction, the progressive failure is taking place in N to NW

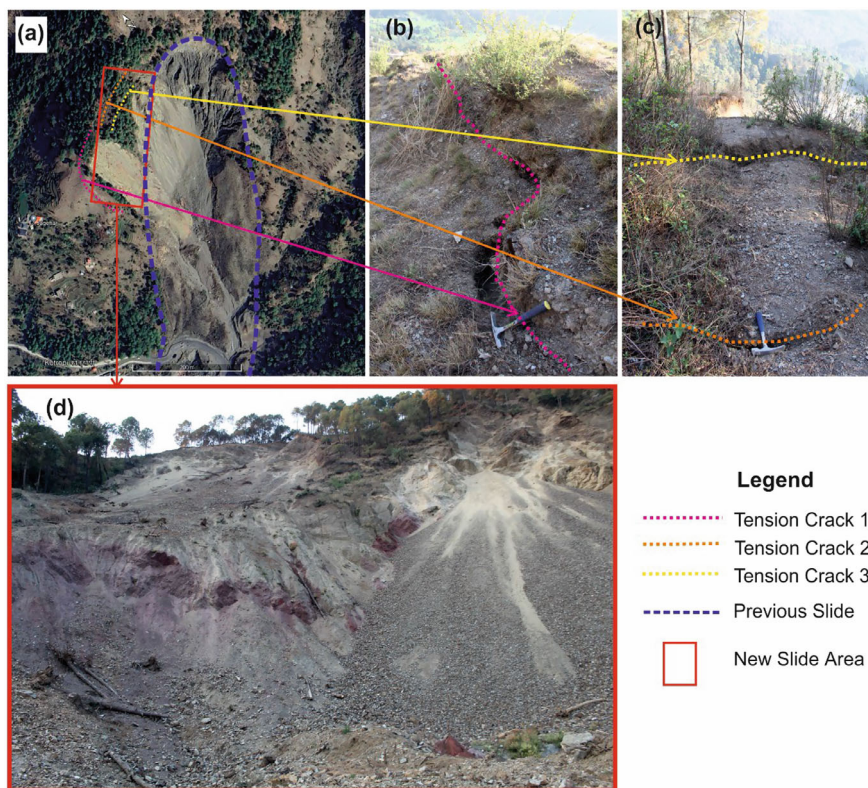


**Fig. 11** Tensional cracks and sliding events observed during Phase 2 field investigation

direction. These failure events pose a significant threat to locals living on right flank and crown of the landslide.

## 5 Conclusion

The progressive failure in a landslide poses a significant threat to local community. Analysing the stability of a landslide with progression of time can provide valuable insights about the location and direction of progressive sliding events which may lead to severe instability. The study of evolution of stability can be helpful in minimizing the impact and damage caused by progressive landslides. The current research was aimed to analyse the evolution of instability in Kotropi landslide and determine the unstable region which have the potential of progressive failures. The key findings of this study are summarized below:

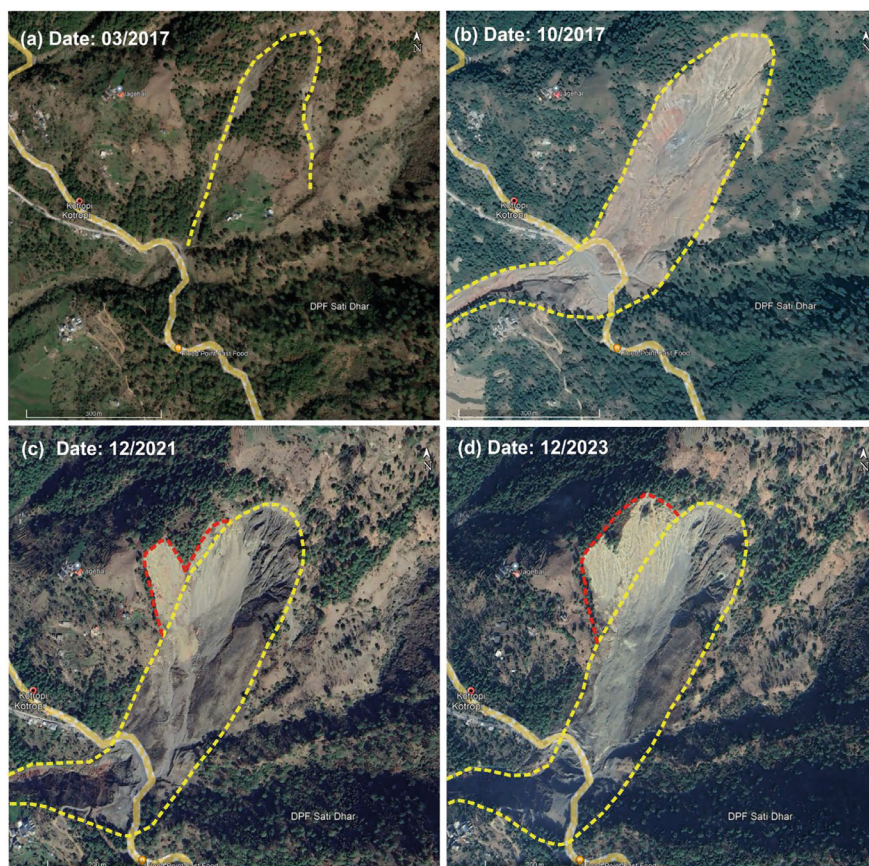


**Fig. 12** Google earth imagery showing progression of failure in Kotropi landslide since its initiation

- (1) The Kotropi landslide which occurred in Aug 2017 have experienced several sliding events since its initiation.
- (2) The results from Model 1 based on the surface geometry of 2018 indicates higher probability of sliding events in right flank of the landslide. The sliding events observed during year 2022 field visit validated the results and indicate the correctness of the 3D model.
- (3) The second 3D model which is based on the surface geometry of 2022 indicate the increased stability of right flank, however it still has the potential of failure in saturated condition.
- (4) The satellite images also confirm the location and direction of progressive failure in right flank.



- (5) Our findings indicates that the instability in right flank is due to the steeper slope and presence of thick layer of highly crushed grey shale and debris of Makri formation. The ingress of rainwater can lead to increased pore pressure during rainy season, which may further lead to instability.

**Declarations** The authors declare that they have no known competing financial interests or personal relationships that could have appeared to influence the work reported in this study.

## References

- Abderrahmane TH (1996) State of the art: limit equilibrium and finite element analysis of slopes. *J Geotech Eng* 577–596
- Abramson LW, Lee TS, Sharma S, Boyce GM (2001) Slope stability and stabilization methods. Wiley
- Afeni T, Cawood F (2014) Slope monitoring using total station: what are the challenges and how should these be mitigated? *S Afr J Geomat* 2:41–53
- Anand AK, Pradhan SP (2019) Assessment of active tectonics from geomorphic indices and morphometric parameters in part of Ganga basin. *J Mt Sci* 16:1943–1961. <https://doi.org/10.1007/s11629-018-5172-2>
- Artese S, Perrelli M (2018) Monitoring a landslide with high accuracy by total station: a DTM-based model to correct for the atmospheric effects. *Geoscience* 8. <https://doi.org/10.3390/geosciences8020046>
- Bahsan E, Fakhriyanti R (2018) Comparison of 2D and 3D stability analyses for natural slope. *Int J Eng Technol* 7:662–667. <https://doi.org/10.14419/ijet.v7i4.35.23085>
- Baroň I, Supper R (2013) Application and reliability of techniques for landslide site investigation, monitoring and early warning—outcomes from a questionnaire study. *Nat Hazards Earth Syst Sci* 13:3157–3168. <https://doi.org/10.5194/nhess-13-3157-2013>
- Baroň I, Supper R, Ottowitz D (2012) SafeLand deliverable 4.6.: report on evaluation of mass movement indicators. European project SafeLand, Grant Agreement No. 226479, 382 pp. Available at: <http://www.safeland-fp7.eu> (ClimChAlp 2008)
- Bernander S, Kullingsjö A, Gylland AS et al (2016) Downhill progressive landslides in long natural slopes: triggering agents and landslide phases modeled with a finite difference method. *Can Geotech J* 53:1565–1582. <https://doi.org/10.1139/cgj-2015-0651>
- Berti M, Bertello L, Bernardi AR, Caputo G (2017) Back analysis of a large landslide in a flysch rock mass. *Landslides* 14:2041–2058. <https://doi.org/10.1007/s10346-017-0852-5>
- Bishop AW (1955) The use of the slip circle in the stability analysis of slope. *Geotechnique* 10:129–150. <https://doi.org/10.1680/geot.1955.5.1.7>
- Bovolenta R, Bianchi D (2020) Geotechnical analysis and 3d FEM modeling of ville san Pietro (Italy). *Geoscience* 10:1–23. <https://doi.org/10.3390/geosciences10110473>
- Budetta P (2020) Some remarks on the use of deterministic and probabilistic approaches in the evaluation of rock slope stability. *Geosciences* 10. <https://doi.org/10.3390/geosciences10050163>
- Chandler RJ (1977) Back analysis techniques for slope stabilization works: a case record. *Geotechnique* 27:479–495. <https://doi.org/10.1680/geot.1977.27.4.479>
- Congress SSC, Puppala AJ (2021) Geotechnical slope stability and rockfall debris related safety assessments of rock cuts adjacent to a rail track using aerial photogrammetry data analysis. *Transp Geotech* 30:100595. <https://doi.org/10.1016/j.trgeo.2021.100595>
- Congress SSC, Puppala AJ, Kumar P et al (2021) Methodology for resloping of rock slope using 3D models from UAV-CRP technology. *J Geotech Geoenvironmental Eng* 147:1–13. [https://doi.org/10.1061/\(asce\)gt.1943-5606.0002591](https://doi.org/10.1061/(asce)gt.1943-5606.0002591)

- Damiano E, Darban R, Olivares L, Picarelli L (2021) An investigation on progressive failure in granular slopes leading to flow-like landslides. In: 13th landslides and engineered slopes. Experience, theory and practice, ISL
- Darban R, Damiano E, Minardo A et al (2019) An experimental investigation on the progressive failure of unsaturated granular slopes. *Geosci* 9. <https://doi.org/10.3390/geosciences9020063>
- Deng DP, Li L, Zhao LH (2017) Limit equilibrium method (LEM) of slope stability and calculation of comprehensive factor of safety with double strength-reduction technique. *J Mt Sci* 14:2311–2324
- Deng L, Yuan H, Chen J et al (2019) Experimental investigation on progressive deformation of soil slope using acoustic emission monitoring. *Eng Geol* 261:105295. <https://doi.org/10.1016/j.enggeo.2019.105295>
- Dikshit A, Satyam N, Pradhan B (2019) Estimation of rainfall-induced landslides using the TRIGRS model. *Earth Syst Environ* 3:575–584. <https://doi.org/10.1007/s41748-019-00125-w>
- Duncan JM, Wright SG, Brandon TL (2014) Soil strength and slope stability. Wiley, New Jersey
- El-Ramly H, Morgenstern NR, Cruden DM (2002) Probabilistic slope stability analysis for practice. *Can Geotech J* 39:665–683. <https://doi.org/10.1139/t02-034>
- El-Ramly H, Morgenstern NR, Cruden DM (2006) Lodalén slide: a probabilistic assessment. *Can Geotech J* 43:956–968. <https://doi.org/10.1139/T06-050>
- Ering P, Babu GLS (2016) Probabilistic back analysis of rainfall induced landslide—a case study of Malin landslide, India. *Eng Geol* 208:154–164. <https://doi.org/10.1016/j.enggeo.2016.05.002>
- Falamaki A, Shafiee A, Shafiee AH (2021) Under and post-construction probabilistic static and seismic slope stability analysis of Barmshour Landfill, Shiraz City, Iran. *Bull Eng Geol Environ* 80:5451–5465. <https://doi.org/10.1007/s10064-021-02277-4>
- Fanos AM, Pradhan B (2018) Laser scanning systems and techniques in Rockfall source identification and risk assessment: a critical review. *Earth Syst Environ* 2:163–182. <https://doi.org/10.1007/s41748-018-0046-x>
- Froude MJ, Petley DN (2018) Global fatal landslide occurrence from 2004 to 2016. *Nat Hazards Earth Syst Sci* 18:2161–2181. <https://doi.org/10.5194/nhess-18-2161-2018>
- Giussani A, Scaioni M (2004) Application of TLS to support landslides study: survey planning, operational issues and data processing. *Int Arch Photogramm Remote Sens Spat Inf* 36:318–323
- Guhathakurta P, Khedekar S, Menon P, Prasad AK, Sangwan N (2020) Observed rainfall variability and changes over Himachal Pradesh state. *IMD Annu Rep* 16:28
- Harris SJ, Orense RP, Itoh K (2012) Back analyses of rainfall-induced slope failure in Northland Allochthon formation. *Landslides* 9:349–356. <https://doi.org/10.1007/s10346-011-0309-1>
- Jiang SH, Huang J, Qi XH, Zhou CB (2020) Efficient probabilistic back analysis of spatially varying soil parameters for slope reliability assessment. *Eng Geol* 271:105597. <https://doi.org/10.1016/j.enggeo.2020.105597>
- Johari A, Mousavi S, Hooshmand Nejad A (2015) A seismic slope stability probabilistic model based on Bishop's method using analytical approach. *Sci Iran* 22:728–741
- Koca TK (2021) Multi-temporal stability investigation of landslides in Çağlayan Dam Reservoir Area
- Komadja GC, Pradhan SP, Roul AR et al (2020) Assessment of stability of a Himalayan road cut slope with varying degrees of weathering: a finite-element-model-based approach. *Heliyon* 6. <https://doi.org/10.1016/j.heliyon.2020.e05297>
- Komadja GC, Pradhan SP, Oluwasegun AD et al (2021) Geotechnical and geological investigation of slope stability of a section of road cut debris-slopes along NH-7, Uttarakhand, India. *Res Eng* 10. <https://doi.org/10.1016/j.rineng.2021.100227>
- Kundu J, Sarkar K, Singh PK, Singh TN (2018) Deterministic and probabilistic stability analysis of soil slope—a case study. *J Geol Soc India* 91:418–424. <https://doi.org/10.1007/s12594-018-0874-1>
- Leshchinsky B, Vahedifard F, Koo HB, Kim SH (2015) Yumokjeong landslide: an investigation of progressive failure of a hillslope using the finite element method. *Landslides* 12:997–1005. <https://doi.org/10.1007/s10346-015-0610-5>

- Leshchinsky B, Olsen MJ, Mohnhey C et al (2019) Quantifying the sensitivity of progressive landslide movements to failure geometry, undercutting processes and hydrological changes. *J Geophys Res Earth Surf* 124:616–638. <https://doi.org/10.1029/2018JF004833>
- Li S, Zhao H, Ru Z, Sun Q (2016) Probabilistic back analysis based on Bayesian and multi-output support vector machine for a high cut rock slope. *Eng Geol* 203:178–190. <https://doi.org/10.1016/j.enggeo.2015.11.004>
- Li Z, Gong W, Li T et al (2021) Probabilistic back analysis for improved reliability of geotechnical predictions considering parameters uncertainty, model bias, and observation error. *Tunn Undergr Sp Technol* 115:104051. <https://doi.org/10.1016/j.tust.2021.104051>
- Ma Z, Zhu C, Yao X, Dang F (2021) Slope stability analysis under complex stress state with saturated and unsaturated seepage flow. *Geofluids*. <https://doi.org/10.1155/2021/6637098>
- Panda SD, Kumar S, Pradhan SP et al (2023) Effect of groundwater table fluctuation on slope instability: a comprehensive 3D simulation approach for Kotropi landslide, India. *Landslides* 20:663–682. <https://doi.org/10.1007/s10346-022-01993-6>
- Pandit K, Singh M, Sharma S et al (2021) Back-analysis of a debris slope through numerical methods and field observations of slope displacements. *Indian Geotech J* 51:811–828. <https://doi.org/10.1007/s40098-021-00553-4>
- Park H, West TR (2001) Development of a probabilistic approach for rock wedge failure. *Eng Geol* 59:233–251. [https://doi.org/10.1016/S0013-7952\(00\)00076-4](https://doi.org/10.1016/S0013-7952(00)00076-4)
- Pei X, Cui S, Zhu L et al (2022) Sanxicun landslide: an investigation of progressive failure of a gentle bedding slope. *Nat Hazards* 111:51–78. <https://doi.org/10.1007/s11069-021-05044-6>
- Petley D (2012) Global patterns of loss of life from landslides. *Geology* 40:927–930. <https://doi.org/10.1130/G33217.1>
- Pradhan SP, Siddique T (2020) Stability assessment of landslide-prone road cut rock slopes in Himalayan terrain: a finite element method-based approach. *J Rock Mech Geotech Eng* 12:59–73. <https://doi.org/10.1016/j.jrmge.2018.12.018>
- Pradhan SP, Panda SD, Roul AR, Thakur M (2019) Insights into the recent Kotropi landslide of August 2017, India: a geological investigation and slope stability analysis. *Landslides* 16:1529–1537. <https://doi.org/10.1007/s10346-019-01186-8>
- Prakasam C, Aravindh R, Nagarajan Visiting B, Kuili S (2022) Stability analysis and control measures of a Debris Landslide—a study along National Highway of Himalayan Region C. *ISER J Earthq Technol Pap* 570:27–45
- Queiroz IM (2016) Comparison between deterministic and probabilistic stability analysis, featuring a consequent risk assessment. In: *ISRM VII Brazilian Symposium on Rock Mechanics—SBMR 2016*, vol 10, pp 636–643. <https://doi.org/10.20906/cps/sbmr-03-0004>
- Rana H, Sivakumar Babu GL (2022) Probabilistic back analysis for rainfall-induced slope failure using MLS-SVR and Bayesian analysis. *Georisk* 0:1–14. <https://doi.org/10.1080/17499518.2022.2084555>
- Reyes A, Parra D (2014) 3D slope stability analysis by the using limit equilibrium method analysis of a mine waste dump. In: *Proceedings tailings and mine waste 2014*. Keystone, Color USA, 5–8 Oct 2014, pp 127–139
- Rocscience (2021) Slide 2 2D limit equilibrium slope stability for soil and rock slopes. Rocscience, Toronto
- Roul AR, Pradhan SP, Mohanty DP (2021) Investigation to slope instability along railway cut slopes in Eastern Ghats mountain range, India: a comparative study based on slope mass rating, finite element modelling and probabilistic methods. *J Earth Syst Sci* 130. <https://doi.org/10.1007/s12040-021-01711-1>
- Roul AR, Pradhan SP, Sahoo KC (2022) Mass movement and initiation of Landslide Dam Burst in the Eastern Ghats, India during the Titli Cyclone. *J Geol Soc India* 98:538–544
- Roy P, Martha TR, Jain N, Vinod Kumar K (2018) Reactivation of minor scars to major landslides—a satellite-based analysis of Kotropi landslide (13 Aug 2017) in Himachal Pradesh, India. *Curr Sci* 115:395–398. <https://doi.org/10.18520/cs/v115/i3/395-398>

- Sarkar S, Kanungo DP, Sharma S (2015) Landslide hazard assessment in the upper Alaknanda valley of Indian Himalayas. *Geomat Nat Hazards Risk* 6:308–325. <https://doi.org/10.1080/19475705.2013.847501>
- Shafiee AH, Falamaki A, Shafiee A, Arjmand F (2022) Probabilistic analysis of an 80,000 m<sup>2</sup> landslide in Shiraz, Iran. *Landslides* 19:659–671. <https://doi.org/10.1007/s10346-021-01792-5>
- Sharma P, Rawat S, Gupta AK (2019) Study and Remedy of Kotropi landslide in Himachal Pradesh, India. *Indian Geotech J* 49:603–619. <https://doi.org/10.1007/s40098-018-0343-1>
- Siddique T, Pradhan SP (2018) Stability and sensitivity analysis of Himalayan road cut debris slopes: an investigation along NH-58, India. *Nat Hazards* 93:577–600. <https://doi.org/10.1007/s11069-018-3317-9>
- Siddique T, Haris PM, Pradhan SP (2022) Unraveling the geological and meteorological interplay during the 2021 Chamoli disaster, India. *Nat Hazards Res* 2:75–83. <https://doi.org/10.1016/j.nhres.2022.04.003>
- Singh N, Gupta SK, Shukla DP (2020) Analysis of landslide reactivation using satellite data: a case study of Kotrupi landslide, Mandi, Himachal Pradesh, India. *Int Arch Photogramm Remote Sens Spat Inf Sci ISPRS Arch* 42:137–142. <https://doi.org/10.5194/isprs-archives-XLII-3-W11-137-2020>
- Singh J, Pradhan SP, Singh M, Hruaikima L (2022a) Control of structural damage on the rock mass characteristics and its influence on the rock slope stability along National Highway-07, Garhwal Himalaya, India: an ensemble of discrete fracture network (DFN) and distinct element method (DEM). *Bull Eng Geol Environ* 81. <https://doi.org/10.1007/s10064-022-02575-5>
- Singh J, Pradhan SP, Singh M, Yuan B (2022b) Modified block shape characterization method for classification of fractured rock: a python-based GUI tool. *Comput Geosci* 164:105125. <https://doi.org/10.1016/j.cageo.2022.105125>
- Singh J, Pradhan SP, Vishal V, Singh M (2023) Characterization of a fractured rock mass using geological strength index: a discrete fracture network approach. *Transp Geotech* 40:100984. <https://doi.org/10.1016/j.tgeo.2023.100984>
- Spencer EA (1967) A method of analysis of the stability of embankments assuming parallel inter-slice forces. *Geotechnique* 17:11–26
- Sprefaco MC, Francioni M, Cervi F et al (2016) Back analysis of the 2014 san leo landslide using combined terrestrial laser scanning and 3D distinct element modelling. *Rock Mech Rock Eng* 49:2235–2251. <https://doi.org/10.1007/s00603-015-0763-5>
- Stark TD, Eid HT (1998) Performance of three-dimensional slope stability methods in practice. *J Geotech Geoenviron* 124(11):1049–1060
- Tandon RS, Gupta V, Venkateshwarlu B (2021) Geological, geotechnical, and GPR investigations along the Mansa Devi hill-bypass (MDHB) Road, Uttarakhand, India. *Landslides* 18:849–863. <https://doi.org/10.1007/s10346-020-01546-9>
- Tang WH, Stark TD, Angulo M (1999) Reliability in back analysis of slope failures. *Soils Found* 39:73–80. [https://doi.org/10.3208/sandf.39.5\\_73](https://doi.org/10.3208/sandf.39.5_73)
- Thakur VC, Jayangondaperumal R, Jeevivek V (2019) Seismotectonics of central and NW Himalaya: plate boundary–wedge thrust earthquakes in thin- and thick-skinned tectonic framework. *Geol Soc Spec Publ* 481:41–63. <https://doi.org/10.1144/SP481.8>
- Tsai ZX, You GJY, Lee HY, Chiu YJ (2012) Use of a total station to monitor post-failure sediment yields in landslide sites of the Shihmen reservoir watershed, Taiwan. *Geomorphology* 139–140:438–451. <https://doi.org/10.1016/j.geomorph.2011.11.008>
- Wang L, Hwang JH, Luo Z et al (2013) Probabilistic back analysis of slope failure—a case study in Taiwan. *Comput Geotech* 51:12–23. <https://doi.org/10.1016/j.compgeo.2013.01.008>
- Wang M, Liu K, Yang G, Xie J (2017) Three-dimensional slope stability analysis using laser scanning and numerical simulation. *Geomat Nat Haz Risk* 8:1–15. <https://doi.org/10.1080/19475705.2017.1290696>
- Wyllie DC, Mah CW (2017) Rock slope engineering: civil and mining. In: *Rock slope engineering*, 4th edn, pp 1–432. <https://doi.org/10.1201/9781315274980>

- Xiang G, Wang CL, Bai MZ, Xu ZY, Yan JJ (2013) Stability analysis of slope under the condition of rainfall infiltration. *Appl Mech Mater* 405–408:256–261. <https://doi.org/10.4028/www.scientific.net/AMM.405-408.256>
- Xu Q, Tolaymat T, Townsend TG (2012) Impact of pressurized liquids addition on landfill slope stability. *J Geotech Geoenviron* 138(4):472–480
- Yang Q, Chen ZQ, Zhang DD, Shi Y (2021) Comprehensive evaluation on the stability of deposit slope from reservoir bank. *IOP Conf Ser Earth Environ Sci* 861. <https://doi.org/10.1088/1755-1315/861/6/062051>
- Yeh PT, Lee KZZ, Chang KT (2020) 3D Effects of permeability and strength anisotropy on the stability of weakly cemented rock slopes subjected to rainfall infiltration. *Eng Geol* 266:105459. <https://doi.org/10.1016/j.enggeo.2019.105459>
- Zabuski L (2019) Three-dimensional analysis of a landslide process on a slope in Carpathian Flysch. *Arch Hydroeng Environ Mech* 66:27–45. <https://doi.org/10.1515/heem-2019-0003>
- Zhang LL, Fredlund MD, Fredlund DG et al (2015) The influence of the unsaturated soil zone on 2-D and 3-D slope stability analyses. *Eng Geol* 193:374–383. <https://doi.org/10.1016/j.enggeo.2015.05.011>
- Zhu D, Yan E, Hu G, Lin Y (2011) Revival deformation mechanism of Hefeng landslide in the three gorges reservoir based on FLAC 3D software. *Proc Eng* 15:2847–2851. <https://doi.org/10.1016/j.proeng.2011.08.536>
- Zuo S, Zhao L, Deng D et al (2022) Back analysis of shear strength parameters for progressive landslides: case study of the Caifengyan landslide, China. *Bull Eng Geol Environ* 81. <https://doi.org/10.1007/s10064-021-02507-9>

**Mr. Saurabh Kumar** is currently pursuing Ph.D. degree in engineering geology in Dept. of Earth Sciences, IIT Roorkee. His research is focused on developing landslide early warning system for debris slide. He received M.Sc. degree in applied geology from IIT Roorkee and B.Sc. degree in geology from Aligarh Muslim University. His research interest includes 2D and 3D slope stability analysis, landslide early warning system, landslide physical modeling, geotechnical and geophysical field investigation, laboratory testing, advance numerical modeling techniques including Finite element modeling, Finite Difference Modeling, Discrete Element Modeling. He has published research papers on method to reduce the cost of a landslide early warning system and numerical modeling of landslides. He has also actively participated and presented his research work in few national and international conferences.

**Mr. Saurabh Prakash Aher** is a research scholar specializing in slope stability at Department of Earth Sciences, Indian Institute of Technology, Roorkee. He has done B.Sc. (Geology) from Fergusson College, Pune and M.Sc. (Geology) from Savitribai Phule Pune University. His research focuses on the stability of reactivating large-scale landslides in the Northwestern Himalayas. His research interest includes multidimensional slope stability analysis using different numerical simulation methods, designing of suitable mitigation measures to arrest the slope failures and engineering geological and geotechnical behavior of geomaterial. Prior to this, he has previously conducted research on the issues of slope stability and rockfall in the Western Ghats.

**Dr. Sarada Prasad Pradhan** is currently working as an Associate Professor in Indian Institute of Technology (IIT) Roorkee, India in the Department of Earth Sciences. He obtained his M. Sc. (Applied Geology) and Ph.D. from IIT Bombay (India). He worked as a Reservoir Engineer in Oil and Natural Gas Corporation Ltd. (ONGC) for around 5 years where he was associated with many projects of national importance. He was recipient of outstanding young faculty award by IIT Roorkee, Melpadom Attumalil Georgekutty Young Scientist Award, Young Scientist Award from CAFET INNOVA Technical Society and Award of excellence from ONGC Ltd. His research findings have been well received by the scientific community and published in leading national and



international journals, book chapters and conference proceedings. He is investigating three major research projects on slope stability. His major research interests are Rock Mechanics, Engineering Geology, Slope Stability, Reservoir Geo-mechanics, Petroleum Geo-science and Carbon Dioxide Sequestration.

**Mr. B. D. Patni** is a renowned geological and geotechnical expert. He is the vice president of Himalayan Society of Geoscientists. He was the Former Chief of Geology Division, NHPC Ltd. India and member expert of Polavaram Project Authority. He has more than 35 years of experiences in hydropower projects, landslide mitigation, geotechnical investigation and instrumentations. Renowned for his expertise in the field of geotechnical engineering, he has played a pivotal role in the planning, design, and execution of numerous hydroelectric power projects, dams, tunnels, and foundations across India, contributing significantly to the country's infrastructure development. He contributed to numerous technical papers, workshops, and conferences, sharing his knowledge and experience with scientific community.

# Simulating Failure Modes in a Jointed Rock Slope Using Distinct Element Modeling—A Case Study from the Himachal Himalayas in India



Avishek Dutta, Kripamoy Sarkar, and T. N. Singh

**Abstract** Landslides have been a perpetual menace for the hilly terrains of the Himachal Himalayas of India. Along the strategic National Highway 05, several incidents of rock slope failures have occurred in the past which have caused tremendous damage to the roads and other infrastructures, apart from claiming the lives of people. This study aims to assess the instability condition of one such unstable jointed rock slope in that area. The modes of failure have been first predicted using kinematic analysis of the slope. Then, distinct element method was applied using the Universal Distinct Element Code (UDEC) program to model the slope and determine the most vulnerable zones in the slope with the maximum probability of failure. The slope has been revealed to be unstable with a factor of safety less than 0.03 and maximum displacement of 6.51 cm at 100,000 calculation cycles. Both the planar sliding and direct toppling modes of failure predicted in the kinematic analysis have been validated using distinct element modeling with the help of three monitoring stations set up in the UDEC model. A displacement history chart has been constructed to compare the displacements of the three monitoring points in the slope model. The zone revealing toppling failure has shown the maximum horizontal displacement, whereas the zone revealing planar sliding has shown the maximum vertical displacement.

**Keywords** Slope stability · Kinematic analysis · Modes of failure · Distinct element modeling

---

A. Dutta · K. Sarkar (✉)

Indian Institute of Technology (Indian School of Mines), Dhanbad, Jharkhand 826004, India  
e-mail: [kripamoy@iitism.ac.in](mailto:kripamoy@iitism.ac.in)

T. N. Singh

Indian Institute of Technology Patna, Bihta, Patna, Bihar 801106, India

## 1 Introduction

Landslides and related mass movements are very common in the Himalayan states of India. Himachal Pradesh has its share of the mighty western Himalayas. With extreme landscape features, and a notable variation in the climate the hilly terrains of this exquisite state suffer from the incessant problem of landslides every year (Kahlon et al. 2014; Kundu et al. 2017b). The rock slopes along the National Highway 05 connecting various cities in the state are highly vulnerable to failures. Various factors like the lithology, structural orientation, and geo-environmental scenario of the region have been responsible for the significant occurrences of slope failures in this area (Sarkar et al. 2016b; Verma et al. 2018). Loss of lives, infrastructure damage and disruption in transportation have led many researchers to take up the responsibility of studying the unstable slopes in this area.

The most primitive methods of analyzing the instability conditions of road-cut hill slopes involve the classification systems of rock and slope masses. The rock mass rating (RMR), rock structure rating (RSR), slope mass rating (SMR), and geological strength index (GSI) are some of the common classification techniques for the same. Limit equilibrium methods were mostly used for soil or debris slopes (Singh et al. 2017), and they had many assumptions associated with their analyses (for instance, the inter-slice shear forces are neglected). Jointed rock slopes show various modes of failures, like planar sliding, toppling, and wedge failure. Planar failure refers to the sliding of a rock block along a vulnerable joint plane (or any other plane of discontinuity). The plane of discontinuity should have a dip angle less than that of the slope face (should also daylight on the slope face), and more than the average friction angle of the slope material. Generally, the upper end of the sliding plane intersects the upper face of the slope; sometimes it may also end in a tension crack. The strike of the plane of discontinuity should be within  $20^\circ$  of the strike of the slope face; in ideal conditions, both the strikes of the joint plane and the slope face are parallel (Wyllie and Mah 2004). Toppling failure is a type of mass movement involving rotation of rock blocks, and their subsequent fall. Three most common types of toppling failures are observed in jointed rock slopes, viz., block toppling, flexural toppling, and block-flexural toppling. In block toppling, two sets of discontinuities, one steeply dipping into the slope face, and the other one orthogonal, cause breakage of the rock columns, turning them into smaller blocks, followed by their rotation about the base. Flexural toppling involves bending of the continuous rock columns before their subsequent breakage and fall. Block-flexural toppling involves motion of the blocks resembling the earlier two types, mainly due to displacements of the blocks at the cross-joints (Wyllie and Mah 2004). Wedge failure mainly occurs due to the sliding of a rock wedge formed by the intersection of two planes of discontinuity. The sliding occurs along the line of intersection, which should have a plunge more than the friction angle of the rock, and less than the dip of slope face (Wyllie and Mah 2004). Kinematic analysis has been mainly used for jointed rock slopes for determination of the probable modes of failure in them. It uses the geometry and orientation of the slope face and the discontinuities to find out

which modes of failure might occur in the jointed rock slope (Sarkar et al. 2016a; Acharya et al. 2017; Acharya et al. 2020). Though these methods are widely used, their reliability can be sometimes questioned due to the smaller number of input features considered for the analyses. Numerical methods like finite element method (FEM) (Cheng et al. 2007; Sarkar et al. 2012; Pain et al. 2014; You et al. 2018), distinct element method (DEM) (Kainthola et al. 2012, 2014; Lin et al. 2012; Lu et al., 2012; Kundu et al. 2017a; Roslan et al. 2020), and finite difference method (FDM) have been used by many researchers for analyzing the stability of slopes. These techniques involve lesser number of assumptions than the limit equilibrium methods (since a greater number of input parameters are taken into consideration), and yield several other output features, like displacement and stress–strain parameters which are often more important than the factor of safety of the model (Ugai and Leshchinsky 1995; Cheng and Lau 2014; Salih 2021). For jointed rock slopes, the distinct element method stands out to be the best one for simulating the post-failure behaviour, since it focuses on the principles of discontinuum mechanics (Ajalloeian and Dardashti 2013).

In this study, distinct element modeling has been applied with the help of the Universal Distinct Element Code (UDEC) to simulate the behaviour of a vulnerable jointed rock slope lying along the National Highway 05 in Himachal Pradesh. Field investigation and laboratory testing were done initially to obtain the structural orientation and geotechnical parameters for modeling, followed by kinematic analysis to predict the modes of failure occurring in the slope. UDEC has been used to model the slope, and simulate the modes of failures obtained from the kinematic analysis. Three monitoring points have been set up in the model to understand the differences in the vulnerability of the zones, and the maximum magnitudes of displacements at each of them. Using the time-stepping scheme of the distinct element method, the states of the slope model were attempted to be shown at various calculation cycles. The magnitudes of the displacements at the three monitoring stations were also plotted against the maximum feasible number of calculation cycles to give a deeper insight into the vulnerability of the zones surrounding the individual points in the model.

## 2 Study Area

The study area lies between Tranda in the Kinnaur district and Jeori in the Shimla district of Himachal Pradesh in India. The road-cut slope lies along the strategically important National Highway 05, located at the bank of river Sutlej. Mica-schist and gneissic rocks are the major lithological composition of the jointed rock slopes in this region. Well-defined joint-sets are visible which have persistence of nearly 10–20 m. Though, majority of the landslides and rockfall events occur during the monsoons, the structural orientation of the primary discontinuities plays a huge role in initiating these slope failures.

The area lies in the Larji-Rampur-Wangtu window zone of Larji tectonostratigraphic domain (Srikantia and Bhargava 1998). Locally, the area is situated in the

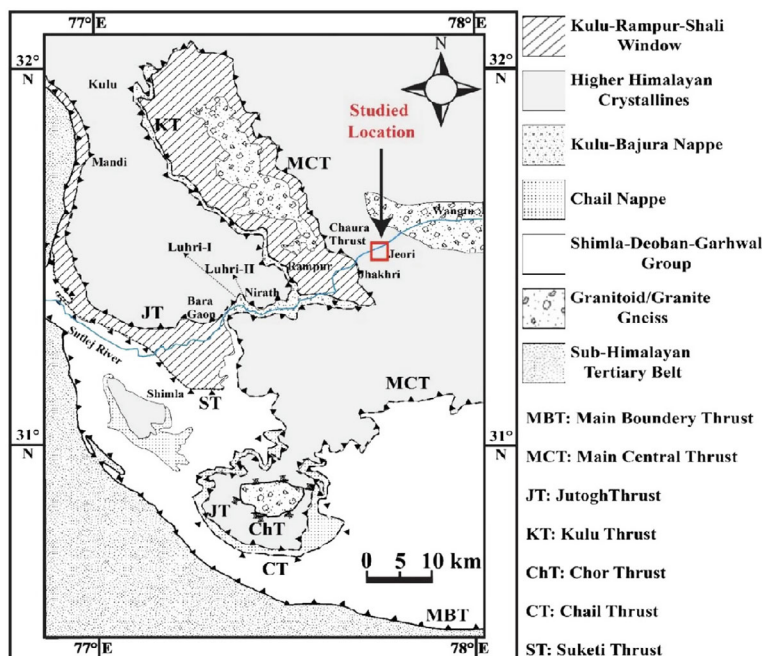


Fig. 1 Location map of the study area (after Singh et al. 2009)

lesser and higher Himalaya region and consists of rocks from the Jutogh group of formations (Singh 1979). This Jutogh nappe tectonically overlies the autochthonous Rampur Group and Wangtu Gneissic Complex (Pandey et al. 2004). The Jutogh group of rocks have undergone tectonic detachment through ductile shearing (Mukhopadhyaya et al. 1997). The average annual rainfall in the district is 816 mm, recorded at lower Kinnaur. Most of the precipitation occurs between June to October (Fig. 1).

### 3 Methodology

#### 3.1 Field Investigation and Laboratory Testing

A detailed field study has been executed to do a preliminary survey on the slope condition. The slope is composed of gneissic rocks. It has been found to be dry in slightly weathered condition. The height of the slope is approximately between 15 and 20 m. The average slope angle is nearly  $90^\circ$  (the slope face is almost vertical), with the face having strike of  $30^\circ$  or  $210^\circ$ . Two distinct joint-sets have been observed in the slope. The orientation of these joint-sets has revealed structural instability of the slope. Figure 2a, b shows the field photographs of the studied slope along

National Highway 05. Rock samples were collected from the slope face for testing to determine their geotechnical parameters. The obtained geotechnical parameters were required to be further used as the input features for distinct element simulation of the jointed rock slope. Direct shear test was done to determine the shear strength parameters, viz., cohesion and angle of internal friction. Apart from this, uniaxial compressive strength test was also performed. All the tests were done following the acceptable standards of testing (ISRM 1978, 1981a, b, c, d).

### 3.2 Kinematic Analysis

Determining the modes of failure is a crucial task for investigation into the instability conditions of jointed rock slopes. The most common modes of failures in jointed rock slopes include planar sliding, wedge failure, and toppling failure (direct and flexural) (Wyllie and Mah 2004). Using the geometry and orientation of the slope and its discontinuities kinematic analysis is generally implemented to find out the modes of failure (Acharya et al. 2020). For this, a stereographic depiction of the structural orientation of the slope face and its discontinuities is carried out (Kundu et al. 2017b; Sardana et al. 2019). The friction angle of the slope material is also an important parameter for the analysis.

In this study, the Dips program from Rocscience Inc. (Rocscience 2022) has been used for kinematic analysis of the slope. As customary, the lateral limit has been set to 20. The structural orientation data in Table 1 along with the friction angle of the slope material in Table 2 have been used as input features for the analysis.

### 3.3 Constitutive Model and Joint Slip Criterion

The constitutive model adopted in the distinct element simulation for both the rock material and the two distinct joint planes is the Mohr–Coulomb failure theory. In Coulomb's hypothesis, the graph plotted between shear strength and the normal stress gives the linear equation as:

$$\tau = c + \sigma \tan \phi \quad (1)$$

where,  $\tau$  is the material shear strength,  $c$  represents the cohesion,  $\sigma$  is the normal stress, and  $\phi$  is the friction angle (or angle of shearing resistance) of the material (Coulomb 1776; Labuz and Zang 2012). The rock material and joint properties used in the distinct element modeling have been given in Table 2.

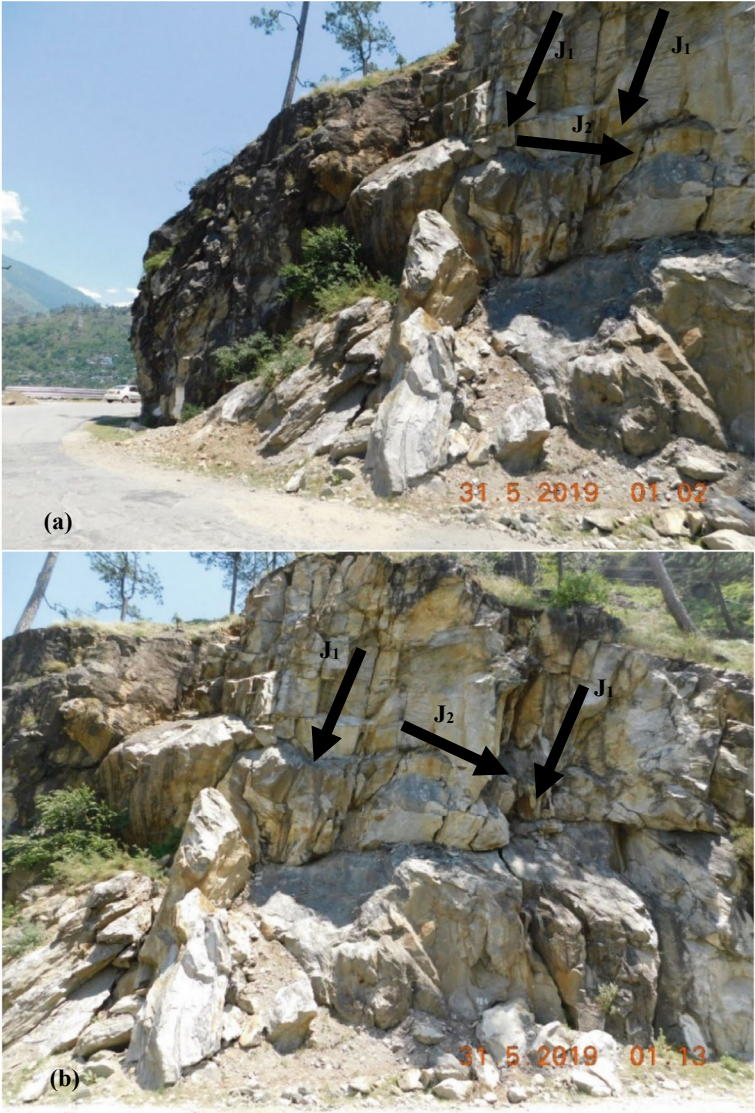


**Fig. 2** Field photographs (a, b) of the studied slope showing two distinct joint sets

**Table 1** Structural orientation data

Joint set (J <sub>1</sub> )		Joint set (J <sub>2</sub> )		Slope (S <sub>L</sub> )	
Dip	Dip direction	Dip	Dip direction	Dip	Dip direction
50°	300°	52°	85°	90°	300°



**Table 2** Geotechnical parameters to be used for numerical simulation

Rock parameters		Values
Unit weight (MN/m <sup>3</sup> )		0.024
Cohesion (MPa)		18.6
Angle of internal friction (°)		36
Young's modulus (MPa)		33,000
Poisson's ratio		0.06
Joint parameters		Values
Friction angle (°)		33
Cohesion (MPa)		17
Normal stiffness (MPa/m)	J <sub>1</sub>	109,000
	J <sub>2</sub>	104,000
Shear stiffness (MPa/m)	J <sub>1</sub>	10,900
	J <sub>2</sub>	10,400

### 3.4 Distinct Element Modeling

The distinct element method (DEM) is a special type of discrete element method. This technique is mainly used for analyzing the behavior of a large number of small particles. This method was first applied to the problems of soil and rock mechanics by Cundall (1971). In its early stages, the distinct element method dealt with the mechanisms of failure of jointed rock masses (Cundall 1971; Maini et al. 1978; Lemos et al. 1985). Eventually, it became evident that the distinct element method could also be potentially useful in developing constitutive relations for granular media (Cundall and Strack 1979). The applicability of the distinct element modeling in this case was based on the fact that any granular medium consists of discrete particles which interact only at the boundaries (or contact points). During the loading phase of any particular system, this discrete feature of the granular medium makes the analysis of its behavior more complicated and time-consuming (Antonelli and Pollard 1995). Following the approach of discontinuum modeling, this method assumes the space to be discontinuous with a large number of particles of different sizes and masses separated by discontinuities. The motions of these particles are defined by the laws of Newtonian mechanics, while interactions between the discontinuities and the elements are defined by contact mechanics (Fig. 3).

The behavior of a rigid block in distinct element method is defined by Newton's second law of motion in the block and force–displacement law at its boundaries. Initially, the self-weight of a block bounded by discontinuities is considered as the known force. As the cycle commences, using Newton's second law of motion.

$$a^{(t)} = \frac{F^{(t)}}{m} \quad (2)$$

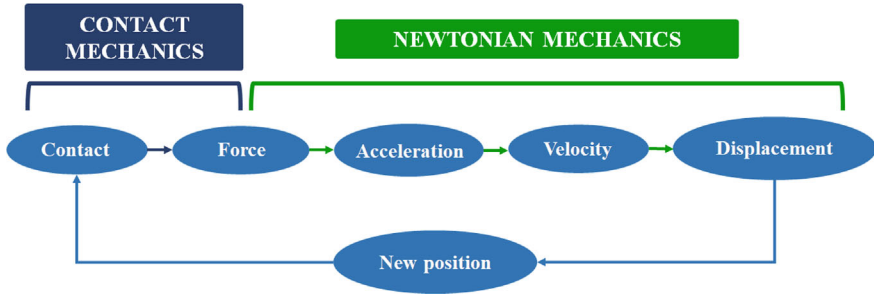


**Fig. 3** Flowchart showing the workflow of DEM

where  $a^{(t)}$  represents the block acceleration at time  $t$ ,  $m$  is the block mass, and  $F^{(t)}$  is the force acting on the block at time  $t$ . The left-hand side of Eq. (2) can be written as

$$a^{(t)} = \frac{v^{(t+0.5dt)} - v^{(t-0.5dt)}}{dt} \quad (3)$$

where,  $v^{(t+0.5dt)}$  is the block velocity halfway along the calculation cycle, and  $dt$  is the cycle length. From Eqs. (2) and (3)

$$v^{(t+0.5dt)} = v^{(t-0.5dt)} + \frac{F^{(t)}}{m} * dt \quad (4)$$

The block displacement can be then determined as follows.

$$S^{(t+dt)} = S^{(t)} + v^{(t+0.5dt)} * dt \quad (5)$$

where  $S$  represents the block displacement. In the first calculation cycle, the values of  $v^{(t-0.5dt)}$  and  $S^{(t)}$  are zero. The displacement is resolved into its corresponding normal and shear components, from which new contact forces are determined using the corresponding normal and shear stiffness values (Fig. 4).

$$F_n^{(t+dt)} = k_n * S_n^{(t+dt)} \quad (6)$$

$$F_s^{(t+dt)} = k_s * S_s^{(t+dt)} \quad (7)$$

where,  $F_n$  and  $F_s$  are the new normal and shear forces on the contact,  $S_n$  and  $S_s$  represent the normal and shear displacement components of the displacement obtained from Eq. (5), and  $k_n$  and  $k_s$  represent the normal and shear stiffness of the contact respectively.

The net resultant force for the second calculation cycle is obtained from its corresponding normal and shear components.

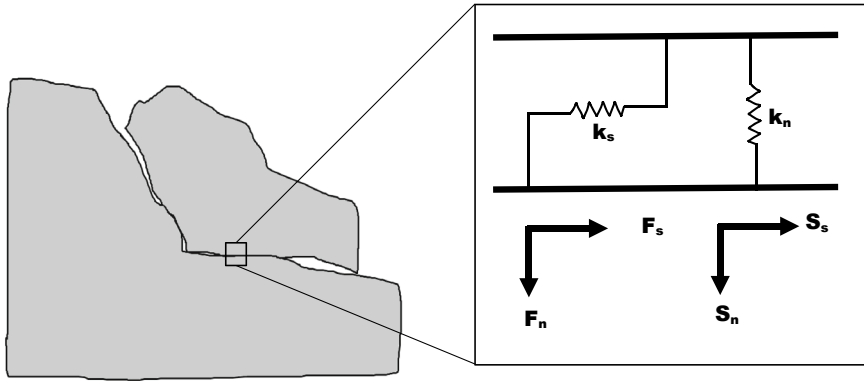


**Fig. 4** Normal ( $F_n$ ) and shear ( $F_s$ ) forces resulting from normal ( $S_n$ ) and shear ( $S_s$ ) displacements (Eqs. 6 and 7) which in turn depends on the normal ( $k_n$ ) and shear ( $k_s$ ) stiffnesses at the contact

$$F^{(t+dt)} = \sqrt{(F_n^{(t+dt)})^2 + (F_s^{(t+dt)})^2} \quad (8)$$

Hence, each calculation cycle gives a displacement which results in a new position of the block, and gives rise to a new contact force (Itasca 2022). Acceleration is calculated from the force, and the velocity and displacement magnitudes are determined by successive integration of the acceleration over the time increment (Fig. 5).

In this study, the Universal Distinct Element Code (UDEC) has been utilized for modeling the jointed rock slope. The FISH scripting language (short for FLAC-ISL, the language of FLAC) has been used for generating the model geometry and

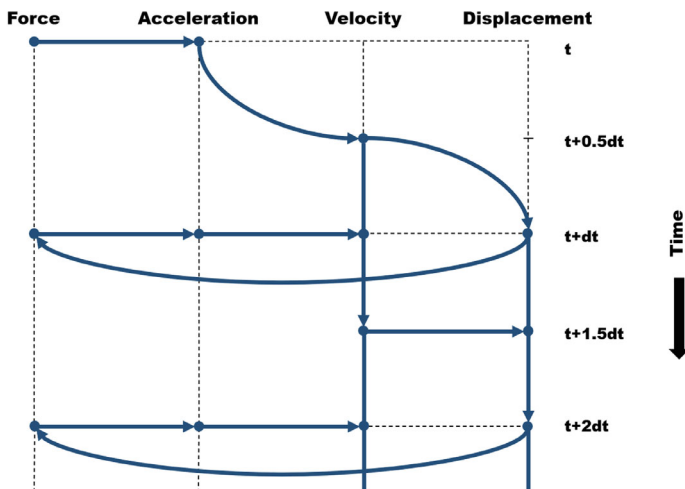


**Fig. 5** Flow of calculation cycle with time (modified after Itasca 2022)

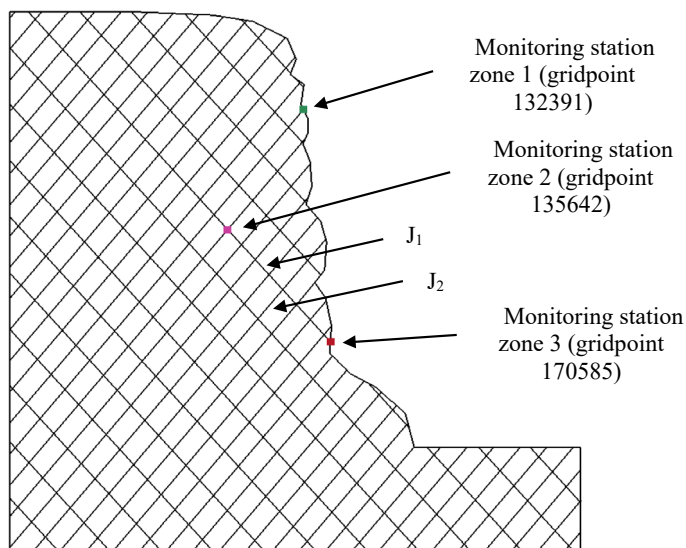


**Fig. 6** Geometry of the slope model created in UDEC

analyzing the same. Though the model has been discretized into a finite number of zones, the primary discontinuities in the model are the continuous lines representing the planes of the two joint sets. The rear side of the slope model and the front of the road section have been restrained in the x-direction (roller supports), and the base of the model has been restrained in both x and y-directions (fixed). Three monitoring stations have been set up in the model that had revealed considerable displacement in the first trial run of the code. Further ahead, the horizontal and vertical displacements at these three points have been plotted with respect to the number of calculation cycles (Fig. 6).

## 4 Results and Discussion

### 4.1 Results of Kinematic Analysis

Figure 7 shows one result of the kinematic analysis of the rock slope. Possibility of planar sliding has been revealed; the percentage of the critical joints matching the criterion has been obtained to be 50%. The planar failure is happening due to the alignment of the plane of joint-set 1 dipping at an angle of  $50^\circ$  towards  $300^\circ$ , i.e., dipping towards the slope face at an angle less than the dip of the slope face and more than the friction angle.

In Fig. 8, a possibility of direct toppling has been revealed. The percentage of the critical joint planes matching the criterion of direct toppling is 50%. The pole of the

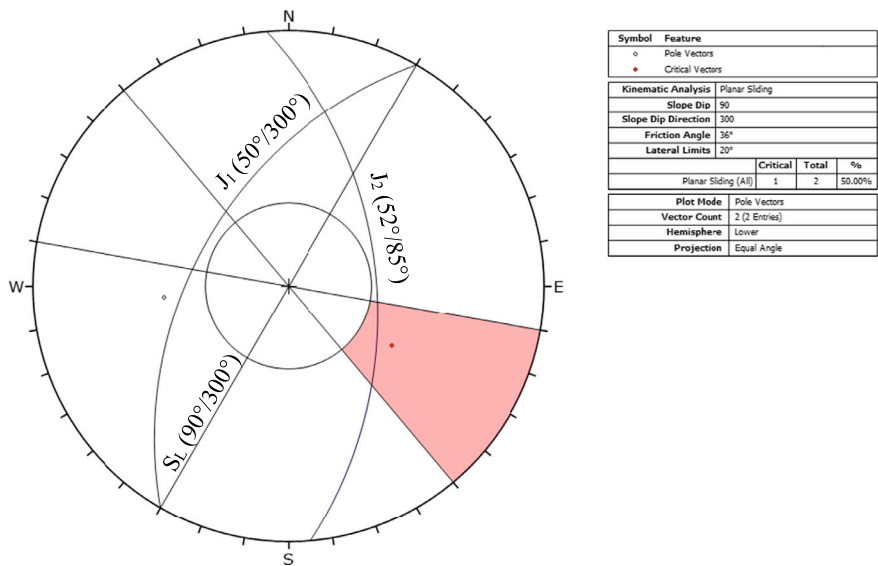


Fig. 7 Kinematic analysis showing planar failure

joint plane of set 1 falls outside the friction circle. Hence, the plane of joint-set 1 acts as a release plane (or sliding plane), indicating a simultaneous occurrence of a combination of sliding and toppling failures.

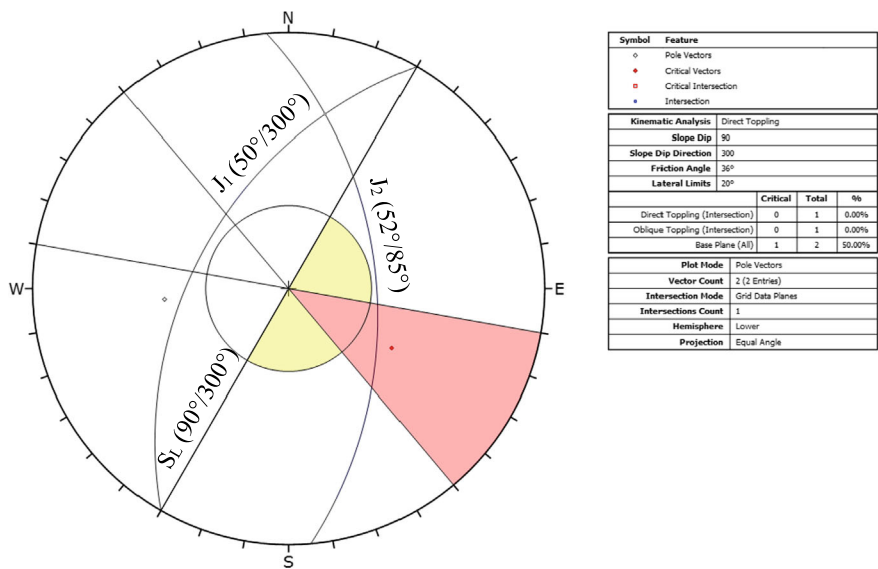
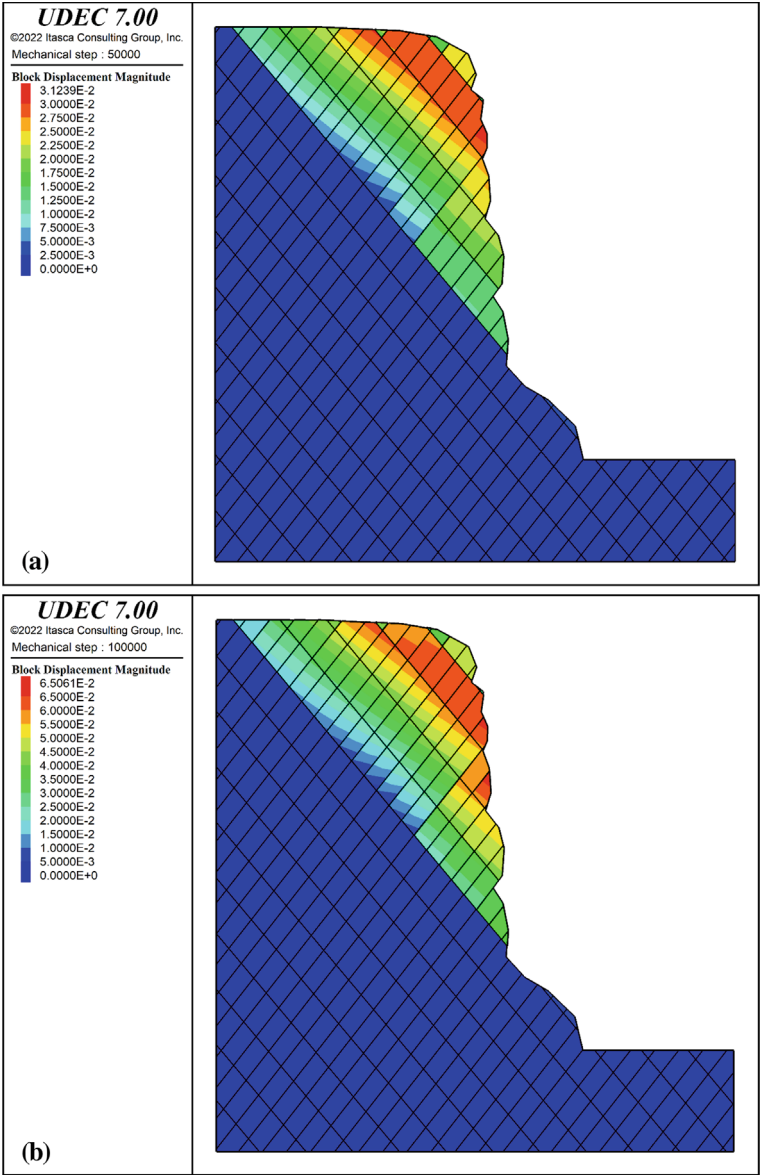


Fig. 8 Kinematic analysis showing direct toppling failure

## 4.2 Results of Distinct Element Modeling

Figure 9a–d shows the states of the model after calculation cycles 50,000, 100,000, 200,000, and 300,000, using the explicit time-stepping scheme of DEM. The calculation could not be proceeded further since the differences among the vulnerable zones marked by the three monitoring points became less distinct. At calculation cycles lower than 50,000, no considerable displacement was observed in the vulnerable zones. The factor of safety value obtained in this analysis is less than 0.03, indicating severe block dislodgement due failed conditions of the model. In UDEC, any value of factor of safety less than 0.5 indicates that considerable displacement of the discrete rock blocks has occurred due to which the model has been rendered to be unstable. When the magnitude of the factor of safety lies between 0.5 and 1, the analysis might indicate presence of highly vulnerable zone(s) in the model, without the possibility of detectable dislodgement of the individual rock blocks. At 50,000 cycles of calculation, the maximum displacement observed in the model is 3.12 cm (Fig. 9a). The zone of the maximum displacement is around the first monitoring point (gridpoint 132,391). Incrementing the calculation further to 100,000 cycles, the vulnerable zones in the model spread out to the lower regions, and slight displacement of blocks can be observed. The maximum displacement observed in this model is 6.51 cm (Fig. 9b). Upon incrementing the calculation to 200,000 cycles, further change in the vulnerable zones of the model has been observed (Fig. 9c). The maximum displacement for 200,000 calculation cycles has been observed to be 13.53 cm. When the calculation reached 300,000 cycles, considerable block dislodgement could be observed in the model (Fig. 9d). The maximum block displacement can be observed at the monitoring station 3 (gridpoint 170,585), the magnitude of which is 24.75 cm. Figure 10a–c shows the block dislodgement at each individual monitoring station set up in the model as shown in Fig. 6 after 300,000 cycles of calculation. Figure 10a shows detachment of zone 1 from the parent rock in toppling mode (direct); forward sliding of the block can also be observed in the same. This validates the direct toppling (base plane) failure mode revealed in the kinematic analysis (Fig. 8). In Fig. 10b, zone 2 reveals forward sliding with the displacement magnitude more at the bottom of the rock blocks than at the top. This might be an indication of the initiation of sliding of the blocks before the occurrence of reverse toppling mode of failure in the slope. Figure 10c shows the displacement of zone 3 in the model. The maximum displacement has been observed in this zone. Sliding of the rock block along the plane of joint-set 1 has been observed, which validates the planar sliding failure mode revealed in kinematic analysis (Fig. 7). The modes of failure obtained in kinematic analysis have been thus validated by distinct element modeling.

Figure 11 shows the displacement history of the three monitoring stations up to 300,000 calculation cycles. Maximum horizontal displacement has been observed at the topmost point (gridpoint 132,391) of a magnitude of 16.4 cm. The third (gridpoint 170,585) monitoring point has yielded the maximum magnitude of vertical



**Fig. 9** States of the analyzed model after (a) 50,000, (b) 100,000, (c) 200,000, and (d) 300,000 cycles of calculation



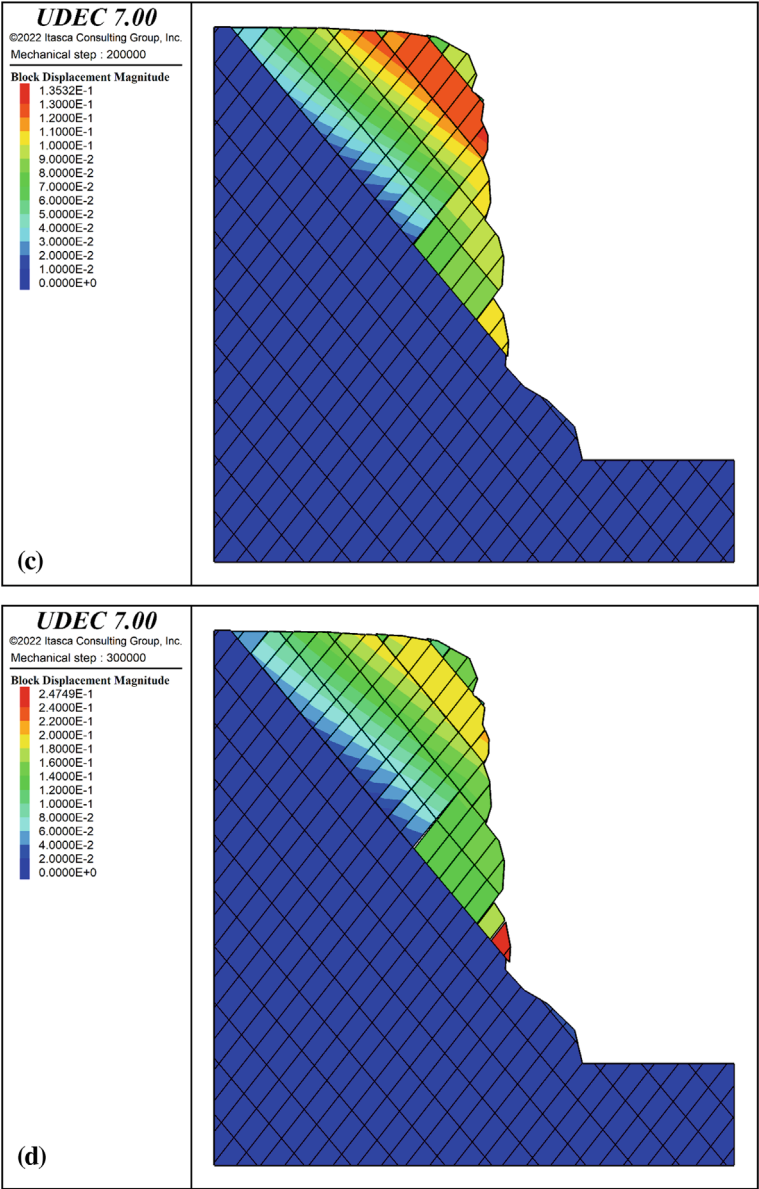
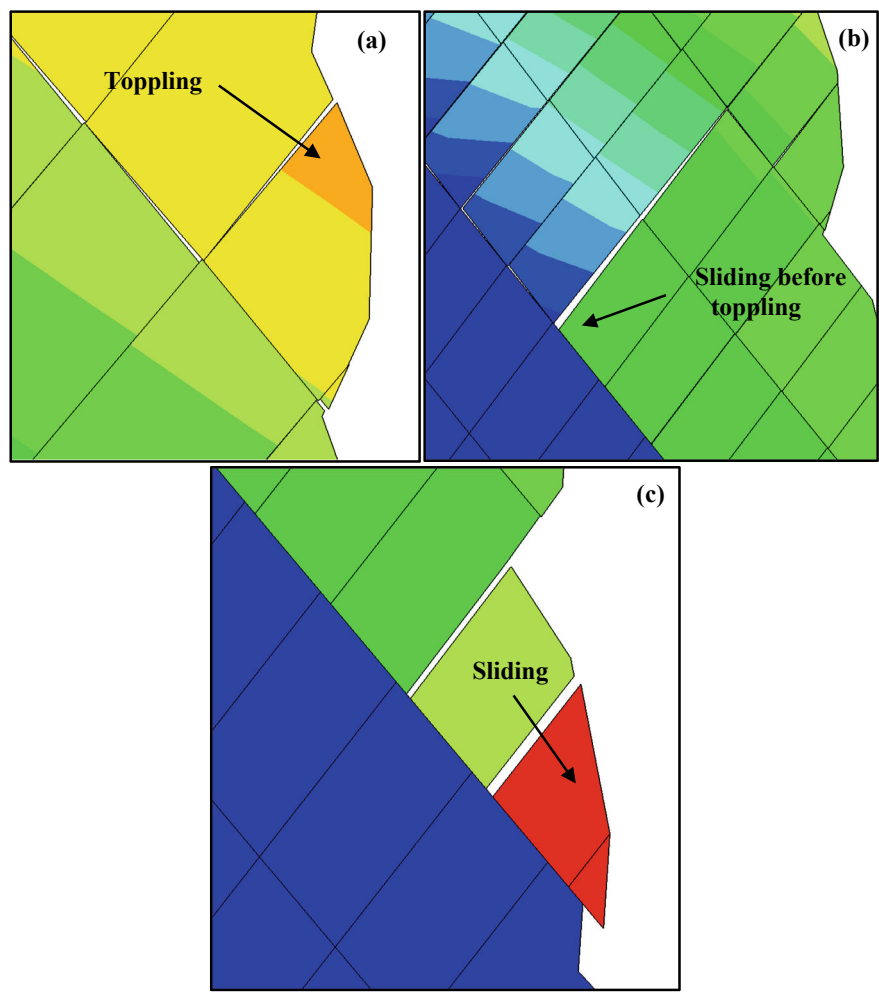
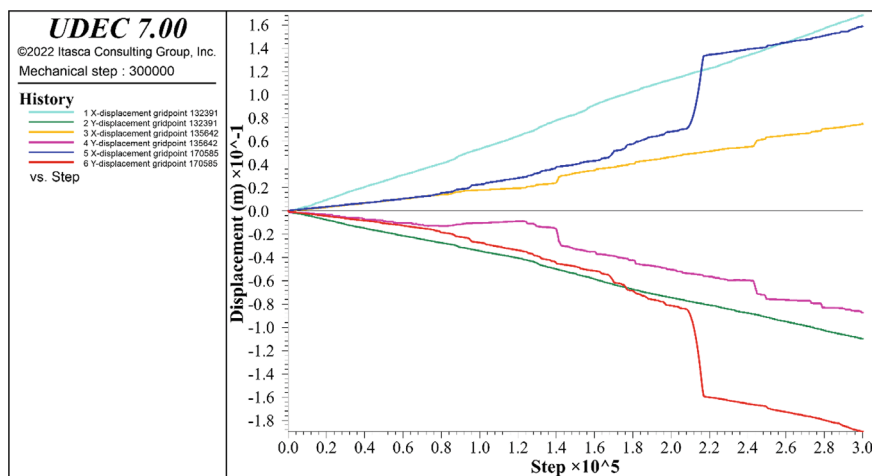


Fig. 9 (continued)



**Fig. 10** Zones of displacement (a) zone 1 showing toppling failure, (b) zone 2 showing sliding before toppling (reverse), (c) zone 3 showing planar sliding

displacement of the order of 18.5 cm. It also has a high value of horizontal displacement (16 cm), making it the most vulnerable zone in the model. The movement of the second monitoring point (gridpoint 135,642) was partly restricted by the surrounding blocks, hence showing comparatively lower magnitudes of both horizontal and vertical displacements.



**Fig. 11** Plot of the displacement history of the three monitoring points in the model

## 5 Conclusions

Using both kinematic analysis and distinct element method, the slope has been inferred to be unstable. Using the time-stepping scheme of the distinct element method, the conditions of the model have been described for 50,000, 100,000, 200,000, and 300,000 cycles of calculations. The major conclusions of this study are as follows:

- The rock slope has revealed kinematic instability with high possibilities of planar sliding along the joint-set 1, and direct toppling. There is a chance of simultaneous occurrence of sliding and toppling of rock blocks in the slope.
- Distinct element modeling has shown that the slope is unstable with fragmentation and detachment of rock blocks—mostly at the slope face—from the parent material. The magnitudes of displacements of the monitoring stations are also quite high, confirming the failed state of the slope model.
- The modes of failures predicted during kinematic analysis have been well validated using the distinct element method. Toppling failure has been observed at the first monitoring point, while the third point revealed planar sliding along a plane of joint-set 1. The second monitoring station has shown a possibility of combined sliding and toppling (reverse).

The unstable slope can be stabilized in the field by using various reinforcement and rock removal methods. However, since the slope face is very steep, resloping or scaling of the face would be recommended before proceeding with the installation of any reinforcements in the form of bolts or dowels.

**Acknowledgements** The authors are immensely grateful to the Engineering Geology Laboratory of the IIT (ISM) Dhanbad for geotechnical testing of samples, and giving access to the Dips, and UDEC programs for carrying out the necessary analysis.

**Declarations** The authors declare no competing interests.

## References

- Acharya B, Kundu J, Sarkar K, Chawla S (2017) Stability assessment of a critical slope near Nathpa Region, Himachal Pradesh, India. In: Indian Geotechnical conference 2017 GeoNEst, IIT Guwahati, Guwahati, India
- Acharya B, Sarkar K, Singh AK, Chawla S (2020) Preliminary slope stability analysis and discontinuities driven susceptibility zonation along a crucial highway corridor in higher Himalaya, India. *J Mount Sci* 17(4):801–823
- Ajalloeian R, Dardashti AF (2013) Evaluation of fluid flow from a Dam Foundation using numerical modeling technique by UDEC software. *Electron J Geotech Eng* 18:1787–1800
- Antonelli MA, Pollard DD (1995) Distinct element modeling of deformation bands in sandstone. *J Struct Geol* 17(8):1165–1182
- Cheng YM, Lau CK (2014) Slope stability analysis and stabilization—new methods and insight, 2nd edn. CRC Press, Boca Raton
- Cheng YM, Lansivaara T, Wei WB (2007) Two-dimensional slope stability analysis by limit equilibrium and strength reduction methods. *Comput Geotech* 34(3):137–150
- Coulomb CA (1776) Essai sur une application des regles des maximis et minimis a quelques problemes de statique relatifs, a la architecture. *Mem Acad Roy Div Sav* 7:343–387
- Cundall PA (1971) A computer model for simulating progressive, large-scale movements in block rock systems. *Proc Symp Int Soc Rock Mech* 1971:128–132
- Cundall PA, Strack ODL (1979) A discrete numerical model for granular assemblies. *Geotechnique* 29:47–65
- ISRM (1978) Suggested methods for determining tensile strength of rock materials. *Int J Rock Mech Min Sci Geomech Abs* 15(3):99–103
- ISRM (1981a). Rock characterization testing and monitoring, ISRM suggested methods. *Int J Rock Mech Min Sci* 211
- ISRM (1981b) Rock characterization testing and monitoring, ISRM suggested methods. International Society for Rock Mechanics, p 211
- ISRM (1981c) Suggested method for determining the uniaxial compressive strength of rock materials, rock characterization, testing and monitoring. *Int J Rock Mech Min Sci Geomech Abs* 113
- ISRM (1981d) Suggested methods for determining shear strength. In: Brown ET (ed) Rock characterization, testing and monitoring. Pergamon Press, Oxford, pp 129–140
- Itasca (2022) UDEC (version 7.00.81). Distinct-element modeling of jointed and blocky material in 2D. Itasca Consulting Group Inc., Minneapolis
- Kahlon S, Chandel VBS, Brar KK (2014) Landslides in Himalayan mountains: a study of Himachal Pradesh, India. *Int J IT Eng Appl Sci Res (IJEASR)* 3(9):28–34
- Kainthola A, Singh PK, Wasnik AB, Singh TN (2012) Distinct element modelling of Mahabaleshwar Road Cut Hill Slope. *Geomaterials* 2(4):105–113
- Kainthola A, Singh PK, Singh TN (2014) Stability investigation of road cut slope in basaltic rockmass, Mahabaleshwar, India. *Geosci Front* 6(6):837–845
- Kundu J, Sarkar K, Singh TN (2017a) Static and dynamic analysis of rock slope—a case study. *Proc Eng* 191:744–749

- Kundu J, Sarkar K, Tripathy A, Singh TN (2017b) Qualitative stability assessment of cut slopes along the National Highway-05 around Jhakri area, Himachal Pradesh, India. *J Earth Syst Sci* 126(8)
- Labuz JF, Zang A (2012) Mohr-Coulomb failure criterion. *Rock Mech Rock Eng* 45:975–979
- Lemos JV, Hart RD, Cundall PA (1985) A generalized distinct element program for modeling jointed rock mass. In: *International symposium on fundamentals of rock joints*, pp 335–343
- Lin Y, Zhu D, Deng Q, He Q (2012) Collapse analysis of jointed rock slope based on UDEC software and practical seismic load. *Proc Eng* 31:441–446
- Lu W, Zhou Z, Liu T, Liu YH (2012) Discrete element simulation analysis of rock slope stability based on UDEC. *Adv Mater Res* 461:384–388
- Maini T, Cundall PA, Marti J, Beresford NL, Asgarian M (1978) Computer modeling of jointed rock masses. Technical report. N-78-8, U.S. Army Waterways Experiment Station
- Mukhopadhyaya DK, Ghosh TK, Bhadra BK, Srivastava DC (1997) Structural and metamorphic evolution of the rocks of the Jutogh Group, Chur half-klippe, Himachal Himalayas: a summary and comparison with the Simla area. *Proc Indian Acad Sci Earth Planet Sci* 197–207
- Pain A, Kanungo DP, Sarkar S (2014) Rock slope stability assessment using finite element based modelling—examples from the Indian Himalayas. *Geomech Geoeng* 9(3):215–230
- Pandey AK, Sachan HK, Virdi NS (2004) Exhumation history of a shear zone constrained by microstructural and fluid inclusion techniques: An example from the Satluj valley, NW Himalaya, India. *J Asian Earth Sci* 23(3):391–406
- Rocscience (2022) Dips (version 8.021). Graphical and statistical analysis of orientation data. Rocscience Inc., Toronto
- Roslan R, Omar RC, Putri RF, Wahab WA, Baharuddin INZ, Jaafar R (2020) Slope stability analysis using Universal Distinct Element Code (UDEC) method. *IOP Conf Ser Earth Environ Sci* 451(1)
- Salih A (2021) Stability analysis of residual soil slope model by numerical modeling using FEM against LEM. *IOP Conf Ser Earth Environ Sci* 856(1)
- Sardana S, Verma AK, Verma R, Singh TN (2019) Rock slope stability along road cut of Kulikawn to Saikhamakawn of Aizawl, Mizoram, India. *Nat Hazards* 99:753–767
- Sarkar K, Singh TN, Verma AK (2012) A numerical simulation of landslide-prone slope in Himalayan region—a case study. *Arab J Geosci* 5:73–81
- Sarkar K, Buragohain B, Singh TN (2016a) Rock slope stability analysis along NH-44 in Sonapur Area, Jaintia Hills District, Meghalaya. *J Geol Soc India* 87:317–322
- Sarkar K, Singh AK, Niyogi A, Behera PK, Verma AK, Singh TN (2016b) The assessment of slope stability along NH-22 in Rampur-Jhakri Area, Himachal Pradesh. *J Geol Soc India* 88(3):387–393
- Singh K (1979) Deformation history of the rocks around Sarahan Bushair, Himachal Pradesh. In: Saklani PS (ed) *Structural geology of the Himalaya. Today and Tomorrow's Printers & Publishers*, pp 163–182
- Singh S, Jain AK, Barley ME (2009) SHRIMP U-Pb c. 1860 Ma anorogenic magmatic signatures from the NW Himalaya: implications for Paleoproterozoic assembly of the Columbia Supercontinent, Geological Society, London, Special Publications, vol 323, pp 283–300
- Singh AK, Kundu J, Sarkar K (2017) Stability analysis of a recurring soil slope failure along NH-5, Himachal Himalaya, India. *Nat Hazards* 90:863–885
- Srikantia SV, Bhargava ON (1998) *Geology of Himachal Pradesh*. Geological Society, India
- Ugai K, Leshchinsky D (1995) Three-dimensional limit equilibrium and finite element analyses: a comparison of results. *Soils Found* 35(4):1–7
- Verma AK, Sardana S, Singh TN, Kumar S (2018) Rockfall analysis and optimized design of Rockfall barrier along a strategic road near Solang Valley, Himachal Pradesh, India. *Indian Geotech J* 48(1):686–699
- Wyllie DC, Mah CW (2004) *Rock slope engineering—civil and mining*. Spon Press, London
- You G, Mandalawi MA, Soliman A, Dowling K, Dahlhaus P (2018) Finite element analysis of rock slope stability using shear strength reduction method. In: *GeoMEast 2017 international conference: soil testing, soil stability and ground improvement*, pp 227–235

**Mr. Avishek Dutta** is a research scholar in the Department of Applied Geology at the Indian Institute of Technology (Indian School of Mines) Dhanbad. Currently in the fourth year of Ph.D. programme, his domain of research includes landslide hazard assessment using numerical simulation and machine learning techniques. He has completed his Bachelor of Technology in Civil Engineering from Netaji Subhash Engineering College, Kolkata, and Master of Technology in Engineering Geology from the Indian Institute of Technology (Indian School of Mines) Dhanbad.

**Kripamoy Sarkar** is an Associate professor in the Department of Applied Geology in the Indian Institute of Technology (Indian School of Mines) Dhanbad. He is an accomplished and trained Engineering Geologist by profession. With a unique blend of industry and academic experience, he has contributed significantly in the field of natural hazard investigations and soft computing applications in landslides. A few noteworthy contributions of Prof. Sarkar include improvements in rock mass characterization systems, and application of numerical modelling techniques to solve slope instability problems in the Indian Himalayas. His list of publications includes 85 scientific papers in various national and international journals and conference proceedings of repute. He has also published 4 edited book chapters that reflect advanced studies on the assessment of the landslide hazards. Prof. Sarkar has been the principal investigator of 5 major projects on landslide vulnerability analysis and rockfall hazard assessment sponsored by the Ministry of Earth Sciences, DST, and IIT (ISM) Dhanbad in the Northern and North-Eastern parts of the Indian Himalayas. He is the recipient of the prestigious Inder Mohan Thapar Research Award (2021 and 2022) from IIT (ISM) Dhanbad. He is an Associate Editor of the Journal of Earth system Science.

**Trilok Nath Singh** is currently working as the Director of IIT Patna and the Institute Geoscience Chair Professor in the Department of Earth Sciences, IIT Bombay, Mumbai, and is an expert in the field of rock mechanics, mining geology, and clean energy. He received his Ph.D. degree from the Institute of Technology BHU, Varanasi, in 1991 and subsequently served the institute until 2003. He is a recipient of many prestigious awards such as the National Mineral Award, the first P. N. Bose Mineral Award, the SEAGATE Excellence Award for Geo-Engineering, and the GSI Sesquicentennial Commemorative Award. He has nearly 28 years of experience in research and teaching with 16 doctoral theses completed under his supervision and has authored more than 350 publications in various journals and conferences of national and international repute. He is currently leading projects of immense scientific and industrial importance related to coalbed methane, carbon sequestration, shale gas, nuclear waste repositories, and mine slope stability, to name a few. He is on the governing and advisory councils of several national institutes and universities.

# Two-Dimensional Finite Element Modelling for an Optimum Engineered Design for Portal Slopes



Ravi Kumar Umrao, Rajesh Singh, L. K. Sharma, and T. N. Singh

**Abstract** The construction of tunnels in hilly terrains poses significant challenges, particularly in ensuring the stability of the portal slopes. This study focuses on proposing an optimum design for the portal slopes of a twin traffic tunnel in a part of the National Highway (NH-13) near Hospet town, Karnataka, India. The geotechnical investigation revealed that the tunnel primarily passes through litho-units of the Sandur schist belt, viz. metabasic, phyllite and banded iron formation. The phyllite rock exposed at the tunnel portal faces exhibits close-spaced joints and bedding joints as major weak structural features. The stability of the slopes was analysed using two-dimensional finite element modelling (FEM), which allows for a detailed analysis of stress and strain distribution within the rock mass. Various slope heights ranging from 12 to 26 m were considered with different permutations and combinations of stripping ratios (1:2 and 1:3). The FEM analysis indicated that slopes with a 1:3 ratio and 20 m height showed a factor of safety less than unity, requiring support measures such as wire meshing, shotcreting, and bolting. Lower heights, such as an 18 m bench provided a safety factor above unity. The study also proposed designs for the portal slopes based on field investigation, geo-mechanical characterisation, and numerical simulation. These designs included support measures such as rock bolting, shotcreting, and wire meshing. Overall, the study highlights the importance of employing advanced numerical methods like FEM for designing stable and safe portal slopes in tunnel construction projects.

---

R. K. Umrao (✉)

School of Environmental Sciences, Jawaharlal Nehru University, New Delhi 110067, India  
e-mail: [ravikumrao@jnu.ac.in](mailto:ravikumrao@jnu.ac.in)

R. Singh

Department of Geology, University of Lucknow, Lucknow 226007, India

L. K. Sharma

Geological Survey of India, Eastern Region, State Unit: Jharkhand, Ranchi 834002, India

R. K. Umrao · R. Singh · L. K. Sharma · T. N. Singh

Indian Institute of Technology Bombay, Powai, Mumbai 400076, India

T. N. Singh

Indian Institute of Technology Patna, Bihta, Bihar 801106, India



**Keywords** FEM · Slope stability · Tunnel portal · Highway

## 1 Introduction

The stability of rock cut slopes is a critical consideration in various geotechnical engineering projects, including road construction, tunnelling, quarrying, and railway cuttings (Sarkar et al. 2012; Umrao et al. 2016, 2017; Singh et al. 2020). Ensuring rock slope stability during the design and construction stages is essential for safe and efficient infrastructure development (Verma and Singh 2010; Sharma et al. 2016). The selection of excavation techniques for rock masses depends on the strength of the intact rock and the characteristics of pre-existing discontinuities/weak surfaces, such as fractures, faults, joints, folds and bedding planes. The properties of these discontinuities, including their spacing, aperture, and infilling, significantly influence the overall strength and stability of the rock mass.

The design of slopes presents significant challenges at all planning and operation stages, playing a crucial role in the safety and economy of civil works. Effective slope design must balance safety and economy, achieving the most efficient compromise between these often conflicting requirements. Flat slopes are generally recommended for safety and stability, whereas steep slopes minimise excess excavation of waste rock (Hoek and Pentz 1969). This requires specialised geological knowledge, including understanding rock structure, material properties, and the practical aspects of design implications. Therefore, the primary aim of slope stability analysis is to design a stable, economical slope with minimal possibility of failure (Monjezi and Singh 2000).

Hill rock cut slope stability assessments necessitate a comprehensive evaluation of rock structures, as failures typically initiate and propagate along pre-existing discontinuities/weaker surfaces (Maerz 2000). The orientation of these discontinuities can lead to various types of failures, including planar, wedge, and toppling failures (Umrao et al. 2011, 2015). Consequently, loose or unstable rock masses must be removed or controlled to ensure safe commuting. The design of slopes depends on the physico-mechanical properties of the geo-materials involved. Geotechnical data is used to assess rock mass quality and estimate rock mass properties, which in turn are utilised to evaluate slope stability through empirical, analytical, and numerical techniques (Umrao et al. 2011, 2012; Sarkar et al. 2012; Ahmad et al. 2013; Singh et al. 2013, 2014). The limit equilibrium and finite element methods are the most widely used modelling techniques for slope stability analyses (Singh et al. 2008; Behera et al. 2016; Sharma et al. 2017; Kumar et al. 2018; Pradhan and Siddique 2020).

This study focuses on proposing an engineered slope design for construction of a twin traffic tunnel for NH-13 at the bank of the Pampa Sagar reservoir of the Tungbhadra dam near Hospet in the Ballary District of Karnataka (Fig. 1). The tunnel was proposed to mitigate the steep gradient, sharp curve, and traffic congestion at the railway crossing near the bank of the Tungbhadra reservoir (Umrao et al.

2015). The twin tunnel, trending nearly N-S, has a proposed diameter of 9.4 m and a width of 14.5 m, passing below a low-cover railway track (Figs. 1 and 2a). This study assesses the stability of the cut slope faces on the sides of the tunnel portals, which were a concern during the tunnel's construction. Figure 1 presents the details of the investigation area. A geotechnical investigation was conducted to determine the engineering properties of the hill slope strata and assess the cut slope design and stabilisation. The investigation included field studies and laboratory testing of selected rock/soil samples to estimate the underlying rock mass strength. The typical design arrangement for slope protection measures was prepared based on the strength of the rock mass and slope stability analyses of slopes under excavation. In this study, stability assessment was carried out to determine the optimum design for the portal faces at both sides of the tunnel using a two-dimensional finite element modelling method.

## 2 Geology of Hospet Area

The Hospet region is characterised by rock formations from the Sandur Schist Belt, part of the Dharwar Supergroup. This schist belt, situated within the Dharwar craton in Karnataka, stretches in a northwest-southeast direction for approximately 60 km, reaching a maximum width of 18 km at its center. Metasedimentary belts flank the schist belt on both the eastern and western sides, separated by a substantial band of metabasic rock. The twin traffic tunnels along NH-13 are located in the northwestern segment of the Sandur Schist Belt, passing beneath a hill range on the right bank of the Pampa Sagar reservoir near Hospet town, Karnataka. These tunnels traverse three primary litho-units within the Sandur Schist Belt: phyllite, metabasic rock, and banded iron formation (BIF) (Umrao et al. 2015), with additional occurrences of weathered, detrital, and colluvial deposits. Notably, the tunnel portal face predominantly exposes phyllite rock.

Initially, the regional structure of the Sandur Schist Belt was interpreted as a syncline or synclinorium by Bruce Foote (1895) and later by Roy and Biswas (1983). However, Mukhopadhyay and Matin (1993) later contested this view, demonstrating that the sedimentary assemblages in the eastern and western belts do not correspond to the same stratigraphic level. The eastern metasedimentary belt exhibits a broad eastward convexity, a feature not observed in the western belt. Bedding in the eastern belt dips steeply, with regional strikes between  $115^{\circ}$  and  $150^{\circ}$ . Conversely, the western flank shows tightly folded pairs with an average bedding strike of  $135^{\circ}$  on the longer limb and  $90^{\circ}$  on the shorter limb. The NNW-SSE trending ridge of BIF near Deogiri displays an isoclinal fold with a basal decollement (Mukhopadhyay and Matin 1993).

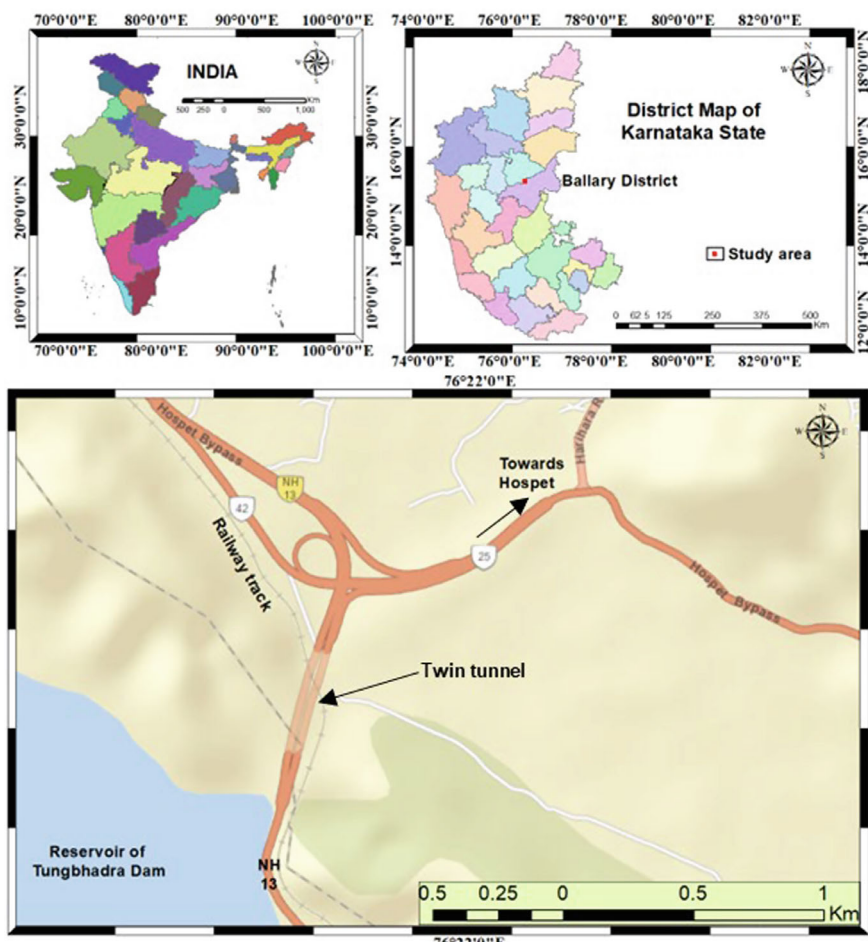


**Fig. 1** Location map of the study area with twin tunnel along National Highway-13 with the existing railway line

### 3 Materials and Methods

A geotechnical investigation was carried out to determine the engineering properties of the underground strata in the study area. This investigation comprised fieldwork to collect geological data, site assessments, and laboratory testing of rock samples to estimate rock mass strength. The primary objective of the study was to propose an optimal design for the slope of the tunnel portal faces. Different slope heights, ranging from 12 to 26 m, were analysed using various permutations and combinations of striping ratios (1:2 and 1:3) and a bench height of 6 m.

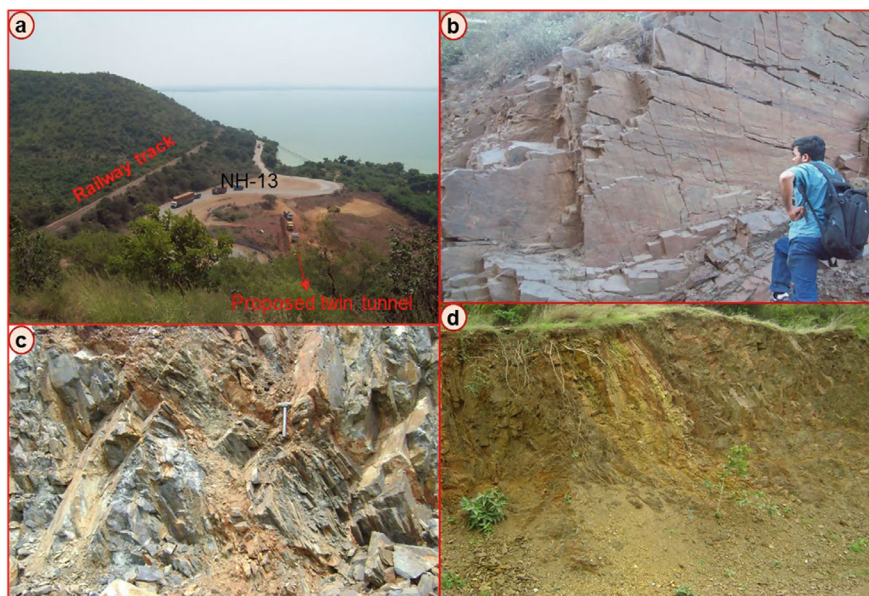


**Fig. 2** **a** A view of the twin tunnel site (southern portal) with the existing NH-13 and railway track. The Pampa Sagar reservoir of the Tungbhadra dam can be seen in the background. This side of NH-13 has a steep slope gradient and sharp curves due to the hill ridge, **b** phyllite rock mass with sub-vertical bedding planes and three sets of joints, **c** weathered phyllite rock layers in crystalline metabasic rock mass in the left wall of the proposed east side tunnel, **d** moderate to highly weathered phyllite exposed at the southern portal face

The slope stability was analysed using a numerical approach with a finite element method. The finite element method (FEM) is an effective approach for analyzing complex shapes, stress distribution, and material responses. In FEM, the structural continuum is modelled by a series of finite elements linked at specific points known as nodes. These elements possess key physical and elastic properties, such as thickness, density, shear modulus, Young's modulus, and Poisson's ratio. They connect only at their boundary nodes, which collectively represent the full domain with high accuracy. Each node exhibits degrees of freedom or nodal displacements, which may include translations, rotations, and, in certain cases, higher-order displacement derivatives. When nodes move, the associated elements shift accordingly based on the element's formulation, allowing displacement within any point of an element to be approximated from nodal displacements. For this study, a uniform mesh composed of 6-node triangular elements was employed to facilitate the analysis.

The stability analysis employed the shear strength reduction (SSR) technique proposed by Matsui and Sam (1992). This technique involves iteratively reducing the shear strengths of the slope-forming material until failure occurs, as indicated by the non-convergence of the finite element model solution (Singh et al. 2014). For Mohr–Coulomb material, the factor of safety (F) can be determined from the Eq. (1).

**Table 1** Geotechnical properties of phyllite samples used for the modelling

Unit weight (kN/m <sup>3</sup> )	Youngs modulus (kPa)	Poissons ratio	Tensile strength (kPa)	Friction angle (°)	Cohesion (kPa)
26	5000	0.11	4.158	18.394	55.196

$$\frac{\tau}{F} = \frac{c'}{F} + \frac{\tan \phi'}{F} \quad (1)$$

where  $\tau$  is the shear strength of the material, and  $F$  is the strength reduction factor (SRF) or the factor of safety (FoS).

Following the conceptual design and based on the ground conditions at the site, a two-dimensional finite element method was chosen over the conventional manual slip surface calculation method (Singh et al. 2014). The stability of the portal slope was investigated for phyllite rock, which is inherently weak and contains three sets of joints within the rock mass. Vertical joints along the foliation in the phyllite rock further weakened the rock mass. The necessary input material properties of phyllite were derived from laboratory test results. Two types of slopes were generated for stability analysis, with different heights and berm ratios (1:3 and 1:2). In each slope type, three cases were analysed concerning different numbers of benches. Slope stability was analysed using the finite element method. The input parameters required for numerical simulation included unit weight, cohesion, angle of friction, Young's modulus, Poisson's ratio, and tensile strength. The geomechanical properties of intact phyllite samples were obtained from laboratory geotechnical investigations. The details of intact rock strength parameters, kinematic analysis, rock mass rating, and continuous slope mass rating for the east and west sides of tunnel sites may be obtained from Umrao et al. (2015). The rock mass properties of phyllite incorporating field observations have been obtained using rocLab software, as suggested by Singh et al. (2013). The input parameters for slope modelling have been presented in Table 1. The assumptions for the FEM modelling included field stress and body force as initial element loading, isotropic elasticity, and Mohr–Coulomb failure criteria. The slopes were analysed using Phase<sup>2</sup> software from Rocscience.

## 4 Field Investigation

The study area is located at the bank of Pampa Sagar reservoir of Tungbhadra dam near the town of Hospet in Bellary district, Karnataka, India (Fig. 2a). A comprehensive investigation was conducted to examine the area where twin tunnels were being proposed. This region has experienced significant geological deformation and metamorphism. The predominant rocks observed include phyllite, crystalline metabasic rock, banded iron formation (BIF), and schist. Phyllite is the most abundantly exposed rock on the north and south sides of the proposed tunnel (Fig. 2b, d). Crystalline metabasic rock appears as intrusive formations within the phyllite

exposures (Fig. 2c). The BIF and schist are not prominently exposed on the surface. The phyllite rock mass exhibits varying degrees of weathering, ranging from slight to moderate to highly weathered conditions. At the bottom of the hillock, the phyllite beds show a vertical to sub-vertical orientation at both the north and south ends (Fig. 2b–d), whereas, at the top, the beds exhibit a gentle dip. Typically, phyllite has three sets of joints and displays bedding joints (Umrao et al. 2015).

## 5 Results and Discussions

Geotechnical investigations encompassing field- and laboratory-based were carried out to evaluate the stability of hill-cut slopes around the tunnel portal areas. The geotechnical investigation revealed that the tunnel primarily passes through lithounits of the Sandur schist belt viz. phyllite, metabasic and banded iron formation (Umrao et al. 2015). The phyllite rock exposed at the tunnel portal faces has closely spaced joints and bedding joints, which are major weak structural features. Phyllite is also weathered to different degrees due to its structural weaknesses from tectonic deformations in the Sandur Schist Belt. On the southern side of the tunnel, the phyllite is highly weathered and chloritized, appearing as scree material, while on the northern portal side, the phyllite is fractured with at least three sets of joints.

Based on detailed field investigations along the proposed twin tunnel and the surrounding hill area, as well as laboratory investigations of surface and core samples, Umrao et al. (2015) assessed the stability of the slope cuttings along the tunnel using kinematic analysis, basic rock mass rating ( $RMR_{basic}$ ), and continuous slope mass rating (CSMR). Various failure modes, including planar, wedge, and toppling, are possible at different site-specific localities. The phyllite rock mass was classified into poor category based on the estimated  $RMR_{basic}$ . The CSMR values for phyllite at the northern side of the tunnel range from 13.58 to 37.78, while on the southern side, only weathered and fragile phyllite is exposed, with CSMR values ranging from 20.06 to 35.61. These CSMR values at both tunnel portals indicate unstable to completely unstable conditions, mainly due to the structural disposition and weathering of the phyllite rock mass. These RMR and CSMR values correlate with the poor rock quality designation (RQD) of phyllite in the boreholes (Umrao et al. 2015).

### 5.1 Stability Analysis of Proposed Slopes

Two-dimensional finite element modeling (FEM) is an effective tool for achieving an optimal design for the slope of a tunnel portal face. This method has emerged as a robust alternative to conventional methods for slope stability analysis (Singh et al. 2014; Sharma et al. 2020). FEM allows for a detailed analysis of stress and strain distribution within the rock mass and can simulate the behaviour of complex geological conditions under various loading scenarios.



Considering that the slope height increases towards the tunnel portal due to excavation, slope heights ranging from 12 to 26 m were analysed with different permutations and combinations of stripping ratios (Berm: Height), i.e., 1:2 and 1:3, with an ideal slope height of 6 m. The stability analysis results, in terms of Factor of Safety (FoS), are tabulated in Table 2 for all analysed slope heights. For slopes with a 1:2 ratio, FoS varies from 1.44 to 0.93 for slope heights from 12 to 26 m, respectively (Table 2). For slopes with a 1:3 ratio, FoS varies from 1.31 to 0.83 for slope heights from 12 to 26 m, respectively (Table 2). For 1:2 slopes, the critical SRF for heights of 24 m and 26 m are below unity, and the critical SRF for heights above 18 m are below 1.2. For 1:3 slopes, the critical SRF for heights of 22 m, 24 m, and 26 m are below unity, and the critical SRF for heights above 14 m are below 1.2 (Table 2). The representative analysed portal slope of 26 m for berm ratios of 1:2 and 1:3 is presented with vectors of shear strain and critical SRF in Fig. 3a, b. The required support for excavated slopes has been recommended based on field observations, laboratory observations, and numerical analysis of all slope heights for both berm: height ratios (Table 2).

A 1:2 ratio slope of 26 m height was analysed using equivalent support in a numerical model to provide optimum support for excavated slopes. Rock bolting and shotcreting were employed to support the slope using Phase<sup>2</sup> software. Bolts of 25 mm diameter and 4 m length were used at 2 m spacing. The strength properties of the steel bolts were assumed to be a bolt modulus of 200 GPa and a tensile capacity of 200 MPa. Rock bolting was applied perpendicular to the slope. Two layers of shotcreting, each 50 mm thick with wire mesh, were added to the analysis, using strength properties such as Young's modulus of 30 MPa, Poisson's ratio of 0.2, compressive strength of 50 MPa, and tensile strength of 5 MPa. The critical SRF using rock bolting and shotcreting with wire mesh was obtained as 1.23 (Fig. 4). Similar rock support may be applied to other slopes depending on the height of the slope. The direction of bolt penetration in the rock will vary once the slope face is exposed. A bolt spacing of 2.5–3 m for lower heights will be sufficient to keep the FoS above 1.2.

## 5.2 Proposed Conceptual Slope Designs

Based on the field assessment and stability analysis of slopes of different heights and berm: height ratios, three designs were proposed along with support measures. The diameter and width of the proposed tunnel are 9.4 m and 14.5 m, respectively.

**Proposed Design 1.** In this case, both side slopes are considered to be 18 m in height, with the slope maintained at 1:3 (Berm: Height) (Fig. 5). The suggested bolt size is 4.5 m with 2.25 m spacing in a staggered pattern, prior to shotcreting and wire meshing. The shotcreting and wire mesh will further strengthen the weak or unstable rock and reinforce the tunnel structure. A number of research studies have



**Table 2** Results of numerical analysis of 1:2 and 1:3 (berm: height) for different slope heights and suggested support

Height (m)	Number of benches	Slope at 1:2		Slope at 1:3	
		FoS	Suggested support	FoS	Suggested support
12	2 (6 m)	1.44	No support	1.31	No support
14	2 (7 m)	1.28	Wire mesh and shotcrete	1.141	Wire mesh and shotcrete
16	3 (6 m, 4 m)	1.23	Wire mesh and shotcrete	1.11	Systematic Rock bolt, wire mesh, shotcrete
18	3 (6 m)	1.14	Systematic Rock bolt, wire mesh, shotcrete	1.02	Systematic Rock bolt, wire mesh, shotcrete
20	3 (7 m, 6 m)	1.05	Systematic Rock bolt, wire mesh, shotcrete	0.94	Systematic Rock bolt, wire mesh, shotcrete
22	4 (6 m, 4 m)	1.04	Systematic rock bolt, wire mesh, shotcrete	0.92	Systematic reinforce shotcrete with systematic rock bolt/toe wall
24	4 (6 m)	0.99	Systematic reinforce shotcrete with systematic rock bolt/toe wall	0.88	Systematic reinforce shotcrete with systematic rock bolt/toe wall
26	4 (7 m, 6 m)	0.93	Systematic reinforce shotcrete with systematic rock bolt/toe wall	0.83	Systematic reinforce shotcrete with systematic rock bolt/toe wall/retaining wall

been performed to model shotcrete using finite element analysis have been followed in this study (Chen et al. 2009; Neuner et al. 2021; Luu 2024).

**Proposed Design 2.** In the second design, the slope was flattened to a ratio of 1:2 (Berm: Height). This design requires more excavation but less support to maintain slope stability (Fig. 6).

**Proposed Design 3 for the southern side tunnel (If overburden will be removed).**

In this case, the top loose material of about 4–6 m may be removed to reduce the height of the slope from 18 to 12 m. Under these conditions, slopes 1:3 and 1:2 indicated better stability than in previous cases (Figs. 7 and 8). This would further reduce the requirements for support design. If the material is loose and bouldery, wire mesh with shotcreting will be adequate to support the slope. The toe wall of the slope may be supported using an M20 grade retaining wall of 1.5 m height and 0.45 m thickness. Above the portal head, wire mesh fencing with pinning should be provided to prevent possible rockfall incidences.

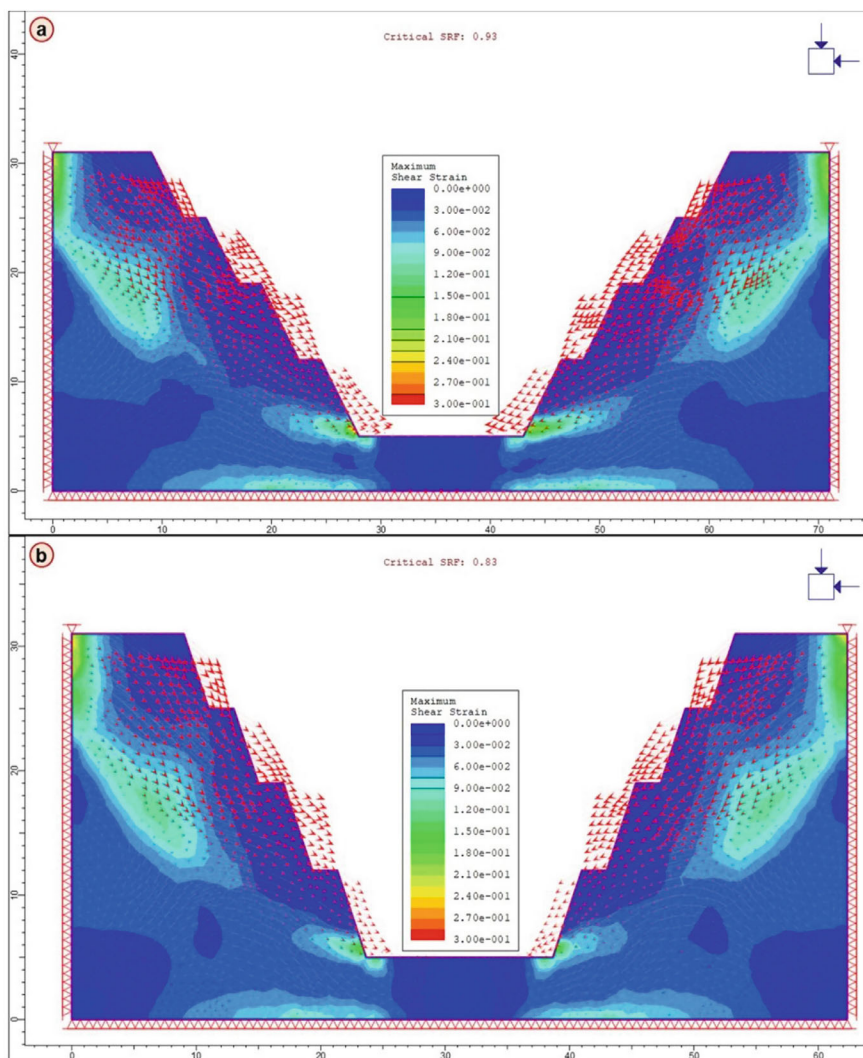


**Fig. 3** Portal slope of 26 m height analysed for berm; height of **a** 1:2 and **b** 1:3

## 6 Conclusions

The stability of the northern and southern portal slopes of the twin tunnel along National Highway 13 near the Pampa Sagar reservoir was systematically evaluated. The analyses indicate that optimal slope stability can be achieved by varying the slope angle, and height and applying necessary support systems based on factor of safety (FoS) values obtained through finite element modelling (FEM). The findings

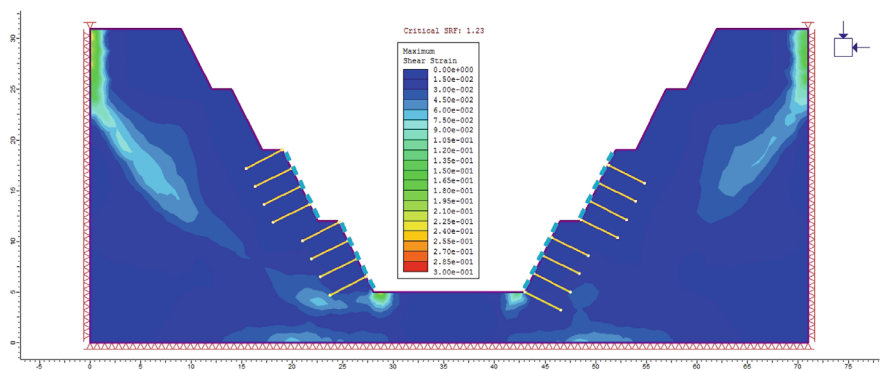


**Fig. 4** 1:2 ratio portal slope of 26 m height analysed by using FEM with support of rock bolting and shotcreting

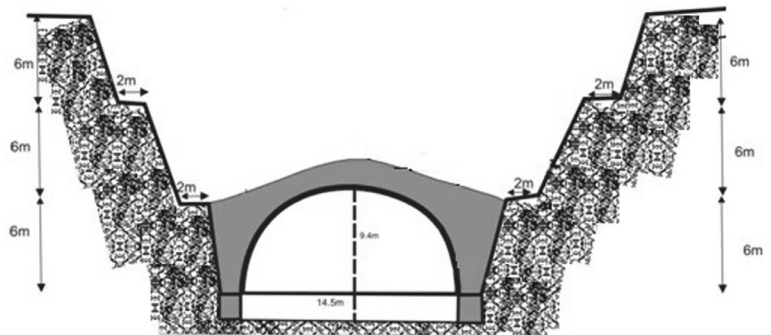


**Fig. 5** East and west side tunnels on northern and southern sides with 2 m berm and 18 m slope height with three benches

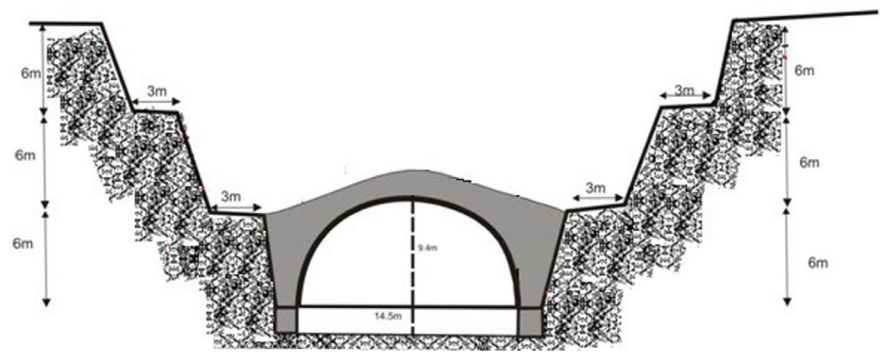


**Fig. 6** East and west side tunnels on northern and southern sides with 3 m berm and 18 m slope height with three benches

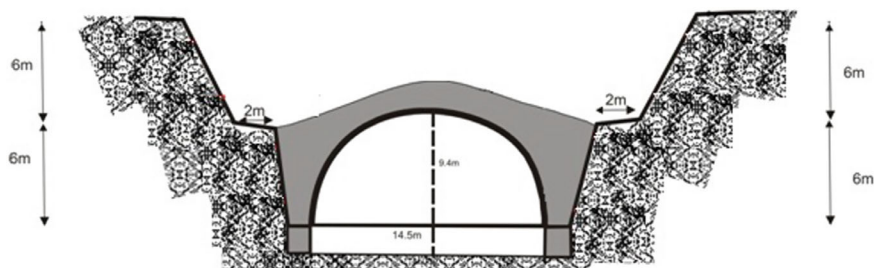


**Fig. 7** East and west side tunnels on the southern side with 2 m berm and 12 m slope height with two benches

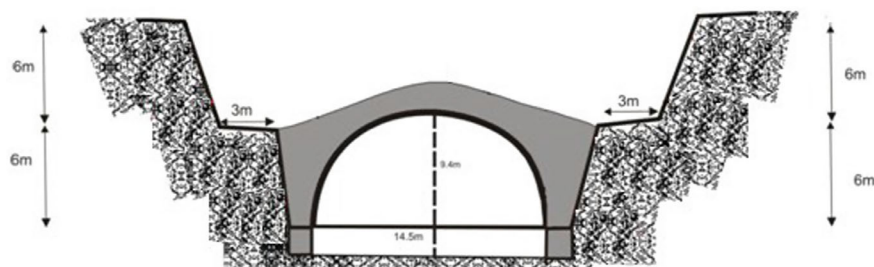


**Fig. 8** East and west side tunnels on the southern side with 3 m berm and 12 m slope height with two benches

highlight the importance of dynamic, adaptable designs that respond to site-specific conditions.

- Slope configurations with a 1:2 berm ratio are generally stable up to a height of 22 m, with a FoS greater than unity, reducing the need for extensive support. However, it is important to aim for higher FoS to ensure durability and stability. In the present study, considering the geology and tectonic setup of the area, the FoS of safety greater than unity has been considered in the proposed conceptual slope designs.
- Slopes with a 1:3 ratio and heights over 20 m show FoS values below unity, necessitating additional support measures such as wire meshing, shotcreting, and bolting.
- Interactive slope design ensures flexibility, allowing modifications during construction based on real-time performance monitoring.
- Reducing the slope height below 16 m minimizes the requirement for heavy support, although the toe wall should be reinforced with an M20 grade retaining wall, and rockfall protection should be installed above the portal head.

These findings contribute to a safe and efficient construction process for the twin tunnel project.

**Acknowledgements** The authors express their sincere gratitude to M/s. Sammon Infracorp and M/s. GMR Group for their valued support and association during the study. The findings and interpretations presented in this paper are based solely on scientific analysis and are in no way influenced by the stated commercial companies.

**Declarations** The authors declare no conflict of interest.

## References

- Ahmad M, Umrao RK, Ansari M, Singh R, Singh TN (2013) Assessment of rockfall hazard along the road cut slopes of state highway-72, Maharashtra, India. *Geomaterials* 3(1):15–23. <https://doi.org/10.4236/gm.2013.31002>
- Behera PK, Sarkar K, Singh AK, Verma AK, Singh TN (2016) Dump slope stability analysis—a case study. *J Geol Soc India* 88:725–735
- Bruce Foote B (1895) The geology of Bellary district, Madras Presidency. *Mem Geol Surv India* 25:1–218
- Chen SH, Fu CH, Isam S (2009) Finite element analysis of jointed rock masses reinforced by fully-grouted bolts and shotcrete lining. *Int J Rock Mech Min Sci* 46(1):19–30
- Hoek E, Pentz DL (1969) Review of the role of rock mechanics research in the design of open-cast mines. In: *Proceedings of the 9th international congress on mining and metallurgy*, London
- Kumar N, Verma AK, Sardana S, Sarkar K, Singh TN (2018) Comparative analysis of limit equilibrium and numerical methods for prediction of a landslide. *Bull Eng Geol Env* 77:595–608
- Luu XB (2024) Finite element modelling of reinforced concrete beam strengthening using ultra-high performance fiber-reinforced shotcrete combined with reinforcing bars. *Structures* 60:105794. <https://doi.org/10.1016/j.istruc.2023.105794>
- Maerz NH (2000) Highway rock cut stability assessment in rock masses not conducive to stability calculations. In: *Proceedings of the 51st annual highway geology symposium*, Seattle, Washington, pp 249–259
- Matsui T, San KC (1992) Finite element slope stability analysis by shear strength reduction technique. *Soils Found* 32(1):59–70
- Monjezi M, Singh TN (2000) Slope instability in an opencast mine. *Coal Int* 145–147
- Mukhopadhyay D, Matin A (1993) The structural anatomy of the Sandur schist belt—a greenstone belt in the Dharwar craton of South India. *J Struct Geol* 15(3–5):309–322
- Neuner M, Dummer A, Schreter M, Gamnitzer P, Hofstetter G, Cordes T (2021) From experimental modeling of shotcrete to numerical simulations of tunneling. *Adv Appl Mech* 54:205–284
- Pradhan SP, Siddique T (2020) Stability assessment of landslide-prone road cut rock slopes in Himalayan terrain: a finite element method based approach. *J Rock Mech Geotech Eng* 12:59–73
- Roy A, Biswas SK (1983) Stratigraphy and structure of the Sandur schist belt, Karnataka. *J Geol Soc India* 24:19–29
- Sarkar K, Singh TN, Verma AK (2012) A numerical simulation of landslide-prone slope in Himalayan region—a case study. *Arab J Geosci* 5:73–81
- Sharma LK, Umrao RK, Singh R, Ahmad M, Singh TN (2016) Geotechnical characterization and stability evaluation of hill cut soil slopes along highway: a case study. In: *Proc. INDOROCK 2016*, Mumbai, pp 824–841
- Sharma LK, Umrao RK, Singh R, Ahmad M, Singh TN (2017) Stability investigation of hill cut slopes along national highway 222 at Malshej Ghat, Maharashtra. *J Geol Soc India* 87(2):165–174
- Sharma LK, Umrao RK, Singh R, Singh TN (2020) Assessment of rockfall hazard of hill slope along Mumbai-Pune expressway, Maharashtra India. *Acta Geodyn Geomater* 17(3):285–296

- Singh TN, Gulati A, Dontha L, Bhardwaj V (2008) Evaluating cut slope failure by numerical analysis—a case study. *Nat Hazards* 47:263–279
- Singh R, Umrao RK, Singh TN (2013) Probabilistic analysis of slope in Amiyani landslide area, Uttarakhand. *Geomat Nat Haz Risk* 4(1):13–29. <https://doi.org/10.1080/19475705.2012.661796>
- Singh R, Umrao RK, Singh TN (2014) Stability evaluation of road-cut slopes in the Lesser Himalaya of Uttarakhand, India: conventional and numerical approaches. *Bull Eng Geol Env* 73(3):845–857. <https://doi.org/10.1007/s10064-013-0532-1>
- Singh HO, Ansari TA, Singh TN, Singh KH (2020) Analytical and numerical stability analysis of road cut slopes in Garhwal Himalaya, India. *Geotech Geol Eng* 38:4811–4829
- Umrao RK, Singh R, Ahmad M, Singh TN (2011) Stability analysis of cut slopes using continuous slope mass rating and kinematic analysis in Rudraprayag District, Uttarakhand. *Geomaterials* 1(3):79–87. <https://doi.org/10.4236/gm.2011.13012>
- Umrao RK, Singh R, Ahmad M, Singh TN (2012) Role of advance numerical simulation in landslide analysis: a case study. In: *Proceedings of national conference on advanced trends in applied sciences & technology (ATAST-2012)*, pp 590–597
- Umrao RK, Singh R, Singh TN (2015) Stability evaluation of hill cut slopes along national highway-13 near Hospet, Karnataka, India. *Georisk* 9(3):158–170. <https://doi.org/10.1080/17499518.2015.1053494>
- Umrao RK, Singh R, Sharma LK, Singh TN (2016) Geotechnical investigation of a rain triggered Sonapur landslide, Meghalaya. In: *Proceedings of the INDOROCK2016*, Mumbai, pp 302–313
- Umrao RK, Singh R, Sharma LK, Singh TN (2017) Soil slope instability along a strategic road corridor in Meghalaya, north-eastern India. *Arab J Geosci* 10:260. <https://doi.org/10.1007/s12517-017-3043-8>
- Verma AK, Singh TN (2010) Assessment of tunnel instability—a numerical approach. *Arab J Geosci* 3:181–192

**Dr. Ravi Kumar Umrao** is an Associate Professor in the School of Environmental Sciences at Jawaharlal Nehru University, New Delhi, India. He holds a Ph.D. degree in the field of Engineering Geology from the Indian Institute of Technology Bombay. Previously, Dr. Umrao served at the Geological Survey of India in various capacities for about 12 years. He has been instrumental in geological mapping and stability assessment of natural and engineered slopes at various geological terrains. His research interests include geomaterial characterization, natural and engineered slope stability analysis, application of soft computing in rock mechanics, geological and geochemical mapping, and mineral exploration for critical metals. He has published over 40 research articles in national and international journals, book chapters and conference proceedings.

**Dr. Rajesh Singh** is an Assistant Professor in the Department of Geology at the University of Lucknow, Lucknow. He holds an M.Sc. in Applied Geology from the University of Allahabad, an M.Tech in Geo-exploration, and a Ph.D. from IIT Bombay, India. His doctoral research earned him the Excellence in Thesis Work (Best Thesis Award) in 2017 from IIT Bombay. Dr. Singh was also honoured with the Young Scientist Award for 2015–2016 by the U.P. Council of Science and Technology, Government of Uttar Pradesh. His research focuses on rock science and engineering, slope stability, and the application of artificial intelligence in rock mechanics. Dr. Singh has published over 60 articles in national and international journals. He has developed tools for slope mass rating, enhanced rock mass characterization systems, and numerical modelling techniques to address slope instability issues in the Indian Himalayas.

**Dr. Lakshmi Kant Sharma** is currently working as a Geologist in the Geological Survey of India. He obtained his M.Sc. (Applied Geology) from the University of Allahabad, M. Tech (Geo-exploration) and Ph.D. in Engineering Geology from the Department of Earth Sciences, IIT

Bombay. His research focuses on soil and rock characterization, slope stability analysis, site selection and stability studies of dams and tunnels and application of soft computing in rock and soil mechanics. So far, Dr. Sharma has published more than 25 research articles in national and international journals and conference proceedings, with more than 1100 citations. Dr. Sharma actively reviews journals such as *Measurement*, *Scientific Reports—Nature*, *Engineering with Computers*, *Geotechnical and Geological Engineering*.

**Prof. Trilok Nath Singh** is currently working as Director IIT Patna and the Institute Geoscience Chair Professor in the Department of Earth Sciences, IIT Bombay, Mumbai, and is an expert in the field of rock mechanics, mining geology, and clean energy. He received his Ph.D. degree from the Institute of Technology BHU, Varanasi, in 1991 and subsequently served the institute until 2003. He is a recipient of many prestigious awards such as the National Mineral Award, the first P. N. Bose Mineral Award, the SEAGATE Excellence Award for Geo-Engineering, and the GSI Sesquicentennial Commemorative Award. He has nearly 28 years of experience in research and teaching with 16 doctoral theses completed under his supervision and has authored more than 350 publications in various journals and conferences of national and international repute. He is currently leading projects of immense scientific and industrial importance related to coalbed methane, carbon sequestration, shale gas, nuclear waste repositories, and mine slope stability, to name a few. He is on the governing and advisory councils of several national institutes and universities.



# Finite Element Modeling for Rock Slope Stability Assessment in North-Eastern India



Kripamoy Sarkar and Avishek Dutta

**Abstract** The unfortunate occurrences of landslides have been a matter of serious concern in the hilly terrains of the north-eastern regions of India. The vulnerable road-cut slopes along the crucial National Highway 06 connecting Assam and Meghalaya witness several such mass movements that endanger the lives of the people apart from detrimental effects on the infrastructures and transportation. In this study, a jointed rock slope in that region composed of sandstone and weathered shale has been analyzed. Kinematic analysis has revealed high chances of wedge sliding between two distinct joint sets. Finite element modeling has been performed, which has revealed the slope to be marginally stable with a critical strength reduction factor (SRF) of 1.02. To visualize the vulnerable zone in the slope model during any probable failure, the shear strength reduction search area (SSR search area) has been used to analyze only a part of the model. The critical SRF obtained then was 0.96, signifying that part of the model to be unstable with the maximum displacement of 1.55 cm.

**Keywords** Slope stability · Kinematic analysis · Finite element modeling · SSR search area

## 1 Introduction

The occurrence of landslides in India is very common, especially in the hilly terrains. Several devastating events of landslides and rockfalls have claimed countless lives, apart from causing damage to various infrastructures and disrupting the environment in general. The transportation facilities are the worst affected as severe downslope mass movements cause rock blocks or debris to block the roads leading to a cessation of vehicle movements. Often, rivers running below these road cut slopes are blocked by the falling rocks or debris material, which leads to the occurrence of floods in the nearby areas. The assessment of the instability conditions in road-cut slopes has

---

K. Sarkar · A. Dutta (✉)

Indian Institute of Technology (Indian School of Mines), Dhanbad, Jharkhand 826004, India  
e-mail: [avishek Dutta@mail@gmail.com](mailto:avishek Dutta@mail@gmail.com)

been a matter of concern for geotechnical engineers. Time and again, researchers have studied the vulnerability of these slopes to failures (Cheng et al. 2007; Singh et al. 2017; Kundu et al. 2017a). If left unidentified, the failures in these slopes lead to mass movements in the forms of landslides, or rockfall hazards.

Although various methods are available to evaluate the stability of the slopes, each individual method has its own advantages and disadvantages. The conventional methods for rock slope stability assessment include the rock mass and slope mass classification systems. Some of the most common rock mass classification systems are the rock mass rating (RMR), the geological strength index (GSI), and the rock structure rating (RSR). The slope mass rating (SMR) classifies rock slopes using some common relationships between joints and slope, and a factor based on excavation method. These methods are mostly empirical involving several assumptions in their calculations which make the results somewhat questionable. Also, there are several parameters related to the outcomes of stability assessment which cannot be determined using these analyses. For soil/debris slopes, the limit equilibrium method is mostly used for determining their stability (Singh et al. 2017). Even for jointed rock slopes, the limit equilibrium method is often used with a limited number of input parameters for evaluating their stability against a particular mode of failure. Among the traditional methods for analyzing stability of jointed rock slopes, the kinematic analysis is mostly resorted to. This is used to find out the most probable modes of failure likely to occur in the slopes (Acharya et al. 2020). However, in this method, only the orientation of the slope face and joints are taken in consideration which do not give a clear idea about the vulnerable zones in the actual rock slope.

Numerical methods for simulating slope models and determining their stability have been used by researchers worldwide. Techniques like the finite element method (FEM), and the distinct element method (DEM) have been previously used by geoscientists and geotechnical engineers for evaluating slope stability. The numerical techniques do not deal with the exact solutions, rather approximate solutions to partial differential equations governing the behavior of structures. These methods have an edge over the conventional methods in that they do not incorporate so many assumptions in their analyses (Ugai and Leshchinsky 1995; Cheng and Lau 2014; Salih 2021). Also, a greater number of input parameters are associated with these techniques. While the finite element method deals with problems related to continuum mechanics (Sarkar et al. 2012; Pain et al. 2014), the distinct element method is more suitable for solving problems of discontinuous media (Kundu et al. 2017a; Roslan et al. 2020). Due to this, the distinct element method often takes a significant amount of computational time in its analysis. The finite element method, on the other hand, is not only faster, but also incorporates the same number of input features as the distinct element method. For jointed rock slopes, both the finite and distinct element methods have been used by geotechnical engineers to study their instability conditions. Apart from calculating the stability of the simulated slope models against failure, these methods can also yield other significant parameters like maximum displacement, stress, and strain in the model. Previously, Cheng et al. (2007) performed a comparative analysis with the limit equilibrium and strength reduction approaches to calculate the critical slip surface of a soil slope. You et al.

(2018) had implemented finite element modeling using the shear strength reduction (SSR) method to examine the stability of an open cut mine slope. Lin et al. (2012) utilized UDEC to study the deformation features of a jointed rock slope with distinct element method. Kainthola et al. (2012) studied a 100 m high jointed basaltic slope by means of the distinct element approach using UDEC to explore its instability conditions under dry and saturated states.

In this study, a jointed rock slope in the north-eastern hilly region of the Jaintia Hill district of India has been studied to determine its instability conditions and vulnerability to failure. For preliminary understanding of the modes of failure, kinematic analysis has been done. Stability analysis has been accomplished by finite element simulation of the jointed rock slope model with the help of the RS2 program by Rocscience. As customary in numerical simulation techniques, continuous joint planes have been incorporated throughout the slope model. The shear strength reduction (SSR) technique used by the finite element program has been utilized to calculate the critical strength reduction factor (SRFc) of the model. Interpretation of the initial results of the analysis has led to the incorporation of the SSR search area in the analysis. Based on the results of the analyses in terms of the magnitude of the obtained critical strength reduction factor and maximum displacement in the model some remedial measures have been suggested at the end that might help in improving the strength of the jointed rock slope and prevent any probable failure.

## 2 Study Area

The Jaintia Hill district in the Indian state of Meghalaya has several road cut slopes alongside the National Highway 06 beside the Lubha river. The study area for this work extends from the Sonapur tunnel situated in Assam to the Malidor bridge in Meghalaya alongside this strategic highway connecting the two states. The region under consideration falls in toposheet no. 83C/8 of the Survey of India between latitudes  $25^{\circ} 01' 30''$  N– $25^{\circ} 7' 0''$  N and longitudes  $92^{\circ} 19' 0''$  E– $92^{\circ} 29' 0''$  E (Fig. 1). On the regional scale, the present area forms a part of the Assam-Arakan tectono-sedimentary basin, which is the largest onshore receptacle of the Palaeogene-Neogene rocks in India. This area is very much prone to landslides and rockfall hazards. There is a lack of proper assessment of the unstable slopes in this region. Every year these unfortunate events of mass movements have severe devastating effects on lives of the people in this region (Sarkar et al. 2016).

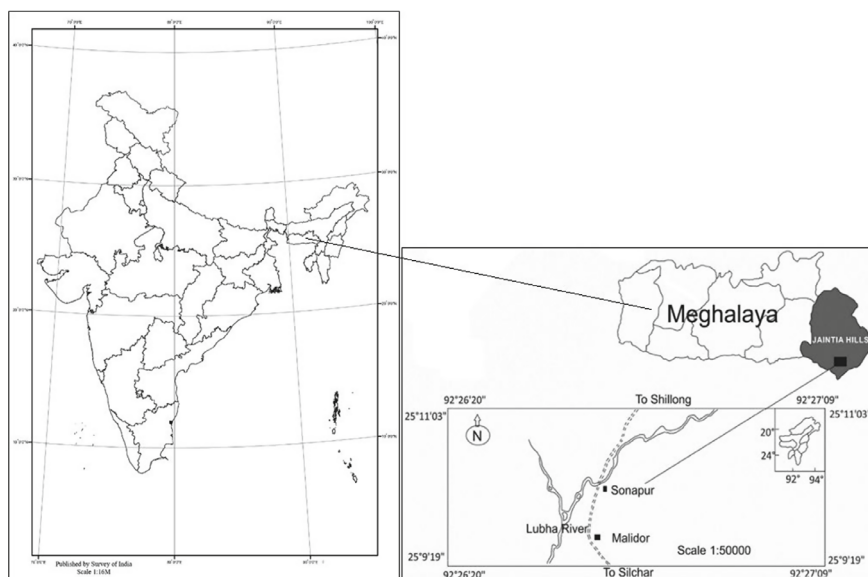


**Fig. 1** Location map of the study area (after Geological Survey of India 1985; Survey of India 2024)

### 3 Methodology

#### 3.1 Field Investigation and Laboratory Testing

The site was visited and the slope was studied to know the lithology, its structural orientation, and the orientation of the discontinuities. The slope is primarily composed of sandstone—belonging to the Barail group of the Oligocene age—on the upper part, with heavily weathered shale in the lower regions. The sandstone has two distinct sets of joints and a bedding plane (Fig. 2). The weathered shale is heavily fractured with the two prominent joint sets extending from the sandstone layer. The average height of the slope ranges from 14.5 to 15 m, with the average dip of the slope being  $66^\circ$ . Table 1 shows the structural orientation data of the slope (mainly the sandstone layer) and the joint planes and the bedding plane.

From the face of the slope, rock samples were collected, and these samples were tested in the laboratory for determining their strength parameters. Direct shear test was performed to evaluate their shear strength parameters, viz., cohesion and the angle of internal friction. Uniaxial compressive strength test was performed to find out the elastic properties, namely, Young's modulus and Poisson's ratio of the rock. The tests were performed following the acceptable standards of testing (ISRM 1978, 1981a, b, c, d). The geotechnical parameters used for simulation of the slope have been given in Table 2.

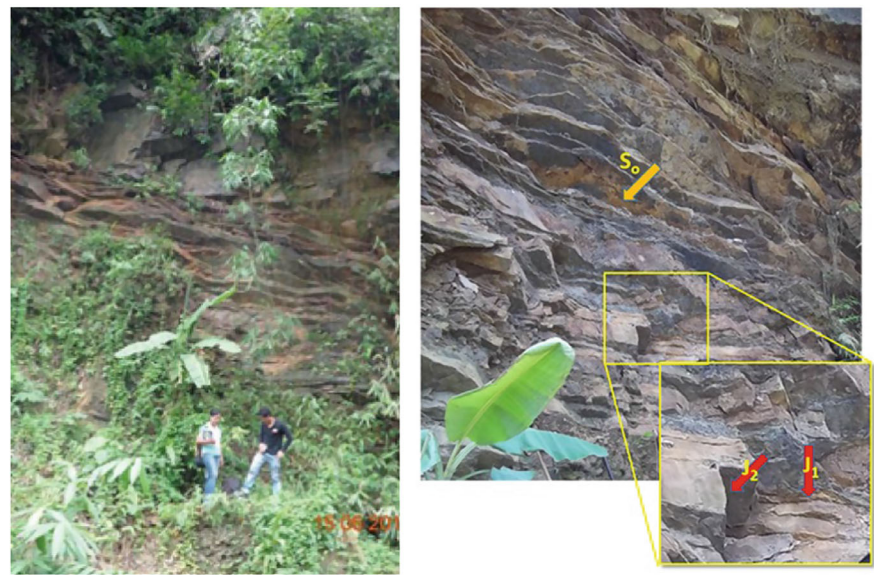


**Fig. 2** Field photographs of the studied slope showing two distinct joint sets ( $J_1$  and  $J_2$ ) and a bedding plane ( $S_0$ )

**Table 1** Structural orientation data

Joint set ( $J_1$ )		Joint set ( $J_2$ )		Bedding plane ( $S_0$ )		Slope ( $S_L$ )	
Dip	DD	Dip	DD	Dip	DD	Dip	DD
45°	25°	75°	255°	58°	165°	66°	280°

\*DD dip direction

### 3.2 Kinematic Analysis

For jointed rock slopes, determining the modes of failures is an important task. Planar, wedge, and toppling (direct and flexural) failures are the most common modes of failures detected in jointed rock slopes (Wyllie and Mah 2004). Kinematic analysis is done to find out the most probable modes of failure with respect to the orientation of the slope face, and its discontinuities (Acharya et al. 2020). A stereographic representation of the slope and the joint sets is incorporated (Kundu et al. 2017b; Sardana et al. 2019). The only material property used in this case is the angle of internal friction of the rock.

Dips program from Rocscience Inc. (Rocscience 2022) has been used in this study for kinematic analysis of the jointed rock slope. The lateral limit for the analyses has been set to 20. The orientation data in Table 1 and the angle of internal friction in Table 2 has been used as the input parameters for the kinematic analysis in this study.

**Table 2** Geotechnical parameters to be used for numerical simulation

		Sandstone	Shale
<i>Rock parameters</i>			
Unit weight (MN/m <sup>3</sup> )		0.024	0.023
Cohesion (MPa)		17.21	12.56
Angle of internal friction (°)		32	29
Young's modulus (MPa)		4400	5620
Poisson's ratio		0.26	0.06
<i>Joint parameters</i>			
Friction angle (°)		30	26
Cohesion (MPa)		16	12
Normal stiffness (MPa/m)	J <sub>1</sub>	42,060	40,040
	J <sub>2</sub>	56,940	51,260
	S <sub>0</sub>	66,420	–
Shear stiffness (MPa/m)	J <sub>1</sub>	4206	4004
	J <sub>2</sub>	5694	5126
	S <sub>0</sub>	6642	–

### 3.3 Finite Element Modeling

Differential equations govern the behavior of any structure. Along with the boundary conditions, these equations form the boundary value problems. Often it becomes difficult to describe the exact behavior of a body using these equations. In many such cases, the finite element method is used as a tool to convert these complicated differential equations into a simple system of linear equations (Fig. 3). The main advantage of this technique is that the approximate solutions to the differential equations are much easier to calculate (Seshu 2003).

In the finite element method, the structure under consideration is separated into a finite number of small elements by a process called discretization. The elements are connected together at nodes, and this collection of the elements and their nodes is called a mesh. The shape of the element varies depending upon the system under consideration. Each shape has a different formulation, and introduces different levels of approximations. The elements used in the study can be of first order (having nodes only at the intersection of edges), or second order (having nodes at mid-point of the edges also). For most engineering problems, the fundamental variable that is calculated from the analysis is the displacement.

#### Constitutive Model and Joint Slip Criterion

The Mohr–Coulomb model has been taken as the constitutive model for the rock material, and also the joint slip criterion for the simulation. From Coulomb's theory, with the help of the graph of shear strength versus normal stress, the linear relationship can be expressed as:

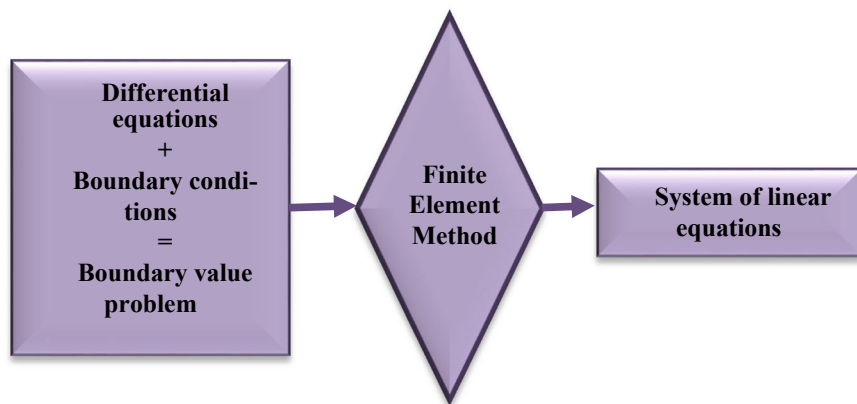


**Fig. 3** FEM as a tool to transform boundary value problems into linear equations

$$\tau = c + \sigma \tan \phi \quad (1)$$

where,  $\tau$  represents the shear strength,  $c$  represents the material cohesion,  $\sigma$  is the normal stress, and  $\phi$  is the angle of shearing resistance (or internal friction) of the material (Labuz and Zang 2012). The material and joint properties used in the finite element simulation have been given in Table 2.

The RS2 program by Rocscience Inc. (Rocscience 2023) analyses the slope model based on finite element method. The main output of the program is the critical strength reduction factor ( $\text{SRF}_c$ ). This parameter is analogous to the factor of safety of the slope. The slope model is discretized into uniform three-node triangular elements, and the primary variable of the calculation—displacement in this case—is estimated based on the given input parameters. The approximations of the underlying differential equations are continued in an iterative manner for calculation of the displacement equations, and simultaneously reducing the strength parameters of the slope material until the point of non-convergence is reached (Acharya et al. 2017). The calculation of the critical strength reduction factor ( $\text{SRF}_c$ ) proceeds as follows.

$$C_r = C / \text{SRF}_c \quad (2)$$

$$\phi_r = \tan^{-1}(\tan \phi / \text{SRF}_c) \quad (3)$$

where  $C_r$  is the reduced magnitude of cohesion, and  $\phi_r$  is the reduced value of the angle of internal friction of the slope material derived from their initial values ( $C$  and  $\phi$  respectively).

Figure 4 shows the geometry of the jointed rock slope model created in the RS2 program. The top yellow region represents the sandstone layer, and the lower grey part shows the weathered shale. Joint-sets 1 and 2 are represented by the red and green continuous lines respectively. The bedding plane in the sandstone layer has



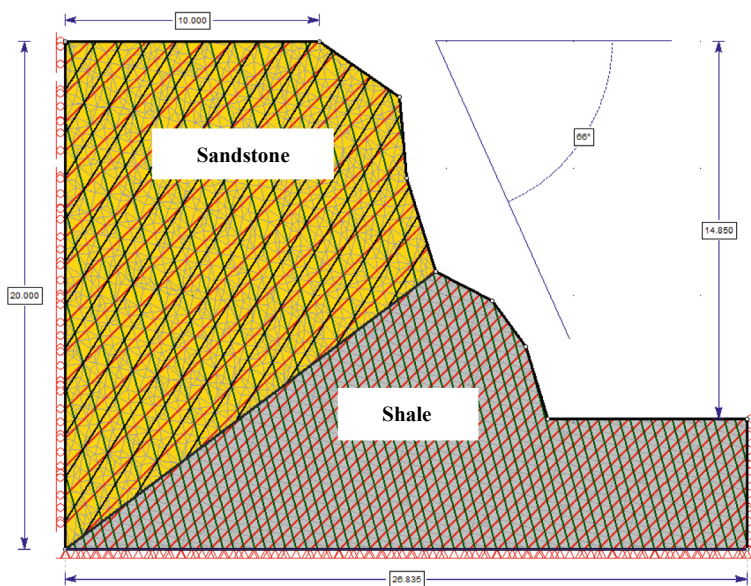


**Fig. 4** Geometry of the slope model created in RS2

been shown using black continuous lines. The back of the slope model and the front portion of the road section have been restrained in the x-direction (roller supports), while the base of the model has been restrained in both x and y-directions (fixed).

## 4 Results and Discussion

### 4.1 Results of Kinematic Analysis

The sandstone layer has two joint planes and one bedding plane. With the friction angle of the sandstone as  $32^\circ$ , wedge sliding mode of failure has been obtained from kinematic analysis. The percentage of critical intersections matching the criterion is 33.33% (Fig. 5). The wedge formation and sliding are occurring due to the unfavorable intersection of joints planes 1 and 2, and the direction of the sliding has been obtained to be  $335^\circ$ .

In the shale layer, the bedding plane is absent. With the angle of internal friction as  $29^\circ$ , again wedge sliding mode of failure is obtained between joint planes 1 and 2, at a direction of  $335^\circ$  (Fig. 6). The percentage of critical intersections matching the criterion is 100%.

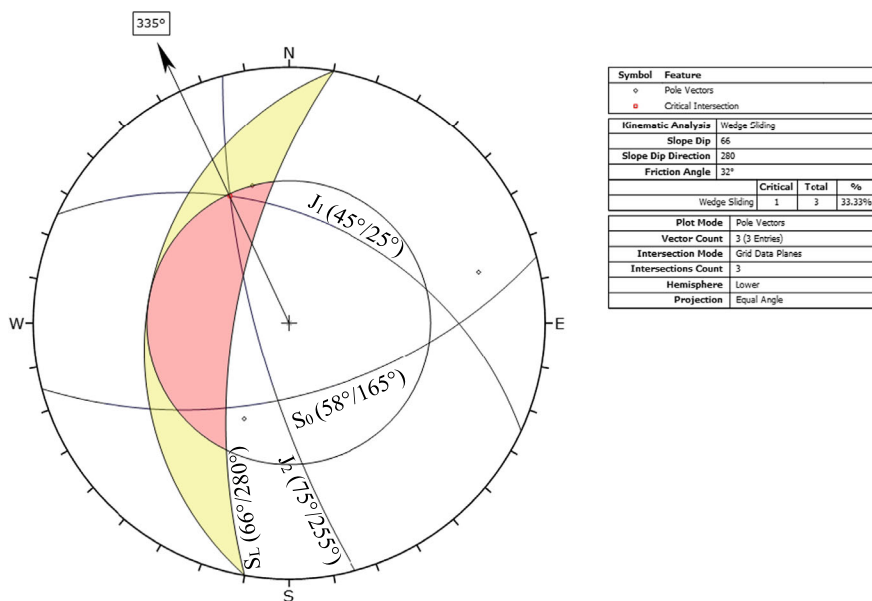


**Fig. 5** Kinematic analysis showing probability of wedge failure in the sandstone layer

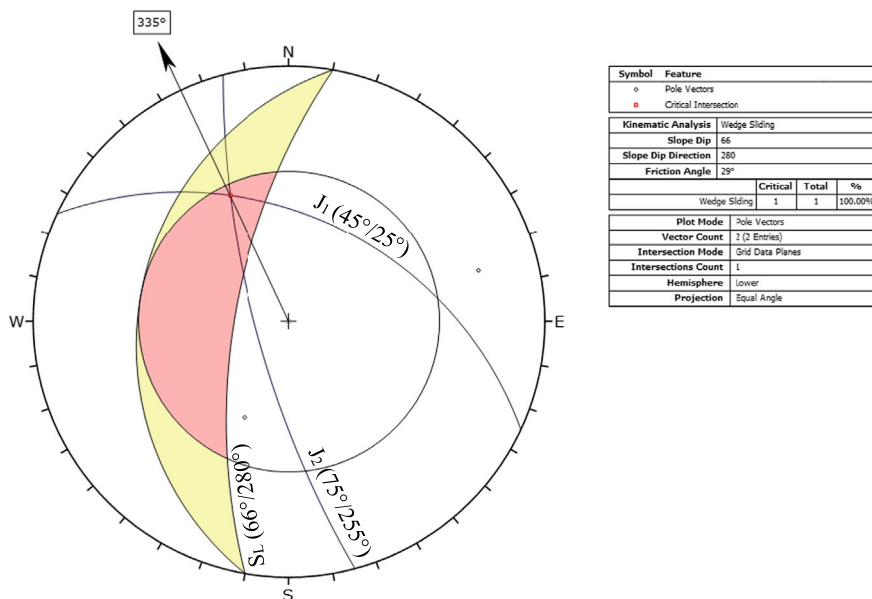


**Fig. 6** Kinematic analysis showing probability of wedge failure in the weathered shale

4.2 Results of Finite Element Modeling

Finite element analysis using the RS2 program has revealed the slope to be just marginally stable against failure (Fig. 7). The critical strength reduction factor of the jointed rock slope model has been estimated to be 1.02. This signifies that the reduced values of the shear strength parameters (cohesion and friction angle) need to be reduced by a factor of 1.02 to make the slope model fail. Since the critical SRF is more than 1, the maximum displacement of the model has been shown to be zero at  $SRF = 1$ . The SRF value as 1 has been taken to show the displacement since it represents the actual field condition. In other words, the reduced values of the shear strength parameters are equal to actual shear strength parameters used in the study.

Upon reducing the shear strength by 1.02, the values of the cohesion and friction angle of the slope model gets reduced. Hence, while viewing the model at the critical SRF, the maximum displacement value is not zero. In this slope model (Fig. 8), the maximum displacement value is 0.225 cm at critical SRF 1.02. However, this representation of the maximum displacement and the most vulnerable zone in the rock slope model might be questionable since the magnitudes of the shear strength parameters have been actually reduced from their original values. The magnitude of the maximum displacement obtained is a result of the reduced shear strength of

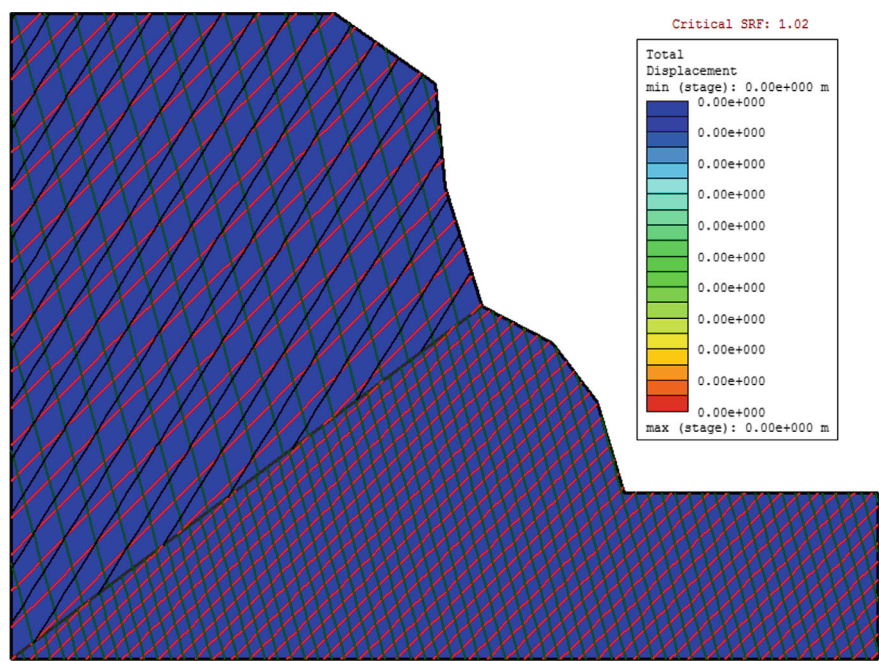
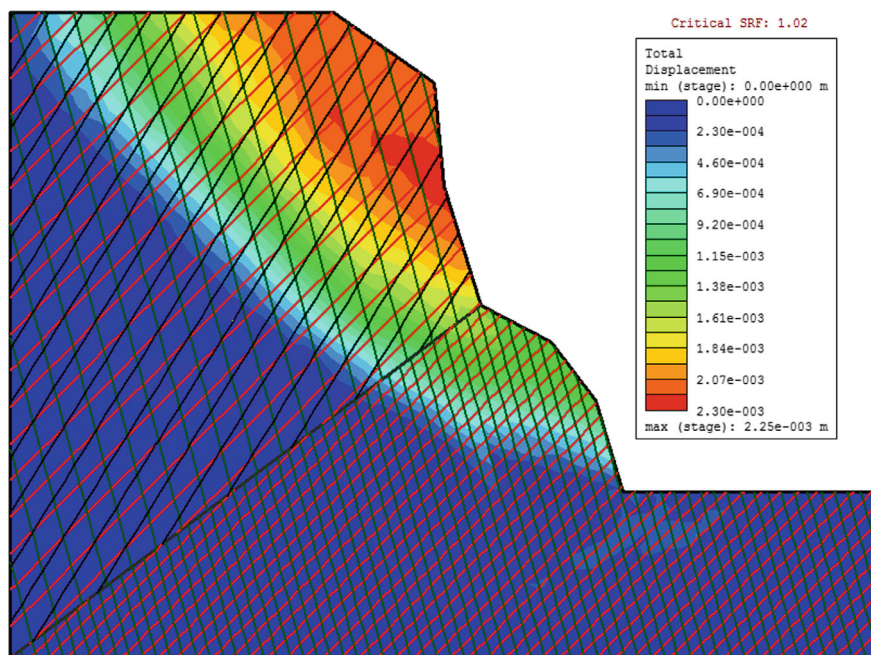


Fig. 7 Analyzed model showing zero displacement at  $SRF = 1$  for critical SRF 1.02



**Fig. 8** Analyzed model at  $\text{SRF} = 1.02$  showing maximum displacement of 0.225 cm

the model; it is not the condition observed in the actual slope with its inherent shear strength parameters.

### Incorporation of SSR Search Area

In the normal shear strength reduction (SSR) analysis using RS2, the entire slope model is being taken into consideration for determining the stability. This implies that the vulnerable zones in the model (or the zone of maximum displacement) can occur in any part of the model. In many cases, like the present study, the critical strength reduction factor obtained is more than 1, revealing the slope under study to be marginally stable or stable. In such cases, the maximum displacement zone cannot be obtained at SRF equal to 1. The discrepancy of showing the vulnerable zones in the slope at the critical SRF has been mentioned in the previous section. Here, an alternative and better option of obtaining vulnerable zones of stable slope models has been explained with the SSR search area method of the RS2 program. The SSR search area in RS2 has been used here to visualize the vulnerable zones of the slope model at the initiation of any probable failure. Using this, only a particular region of the slope can be analyzed with the shear strength reduction technique, and not the entire model. For this study, this technique is useful for segregating the slope from the road-section in the analysis. The SSR search area window has been applied as shown in Fig. 9. The critical SRF of the zone falling under the SSR search area has been computed to be 0.96. This signifies that the slope, when considered separately



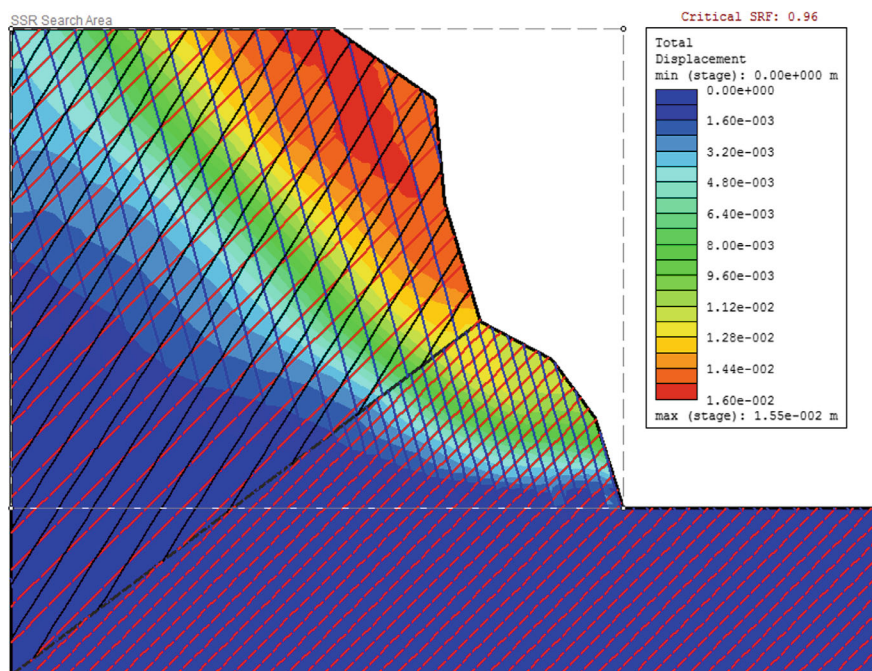


**Fig. 9** Analyzed model at  $SRF = 1$  showing maximum displacement of 1.55 cm for critical SRF 0.96

from the road section, is unstable. In other words, compared to the entire model, the slope is more susceptible to failure. The most vulnerable zone in the model has been obtained at the sandstone layer near the crest of the model. The maximum displacement in the model after analyzing the same with the SSR search area is 1.55 cm. Figure 10 shows the deformation vectors in the SSR search area showing the direction of displacement of the material in the model. Downward displacement has been observed in the sandstone layer, while the weathered shale region shows outward displacement.

## 5 Conclusions

The slope under consideration has been examined first using kinematic analysis, and then with simulation based on the finite element method. The SSR search area of the RS2 has been employed in this study to visualize the vulnerable zones in the slope model and determine the maximum displacement. Following are the major conclusions derived from this study.

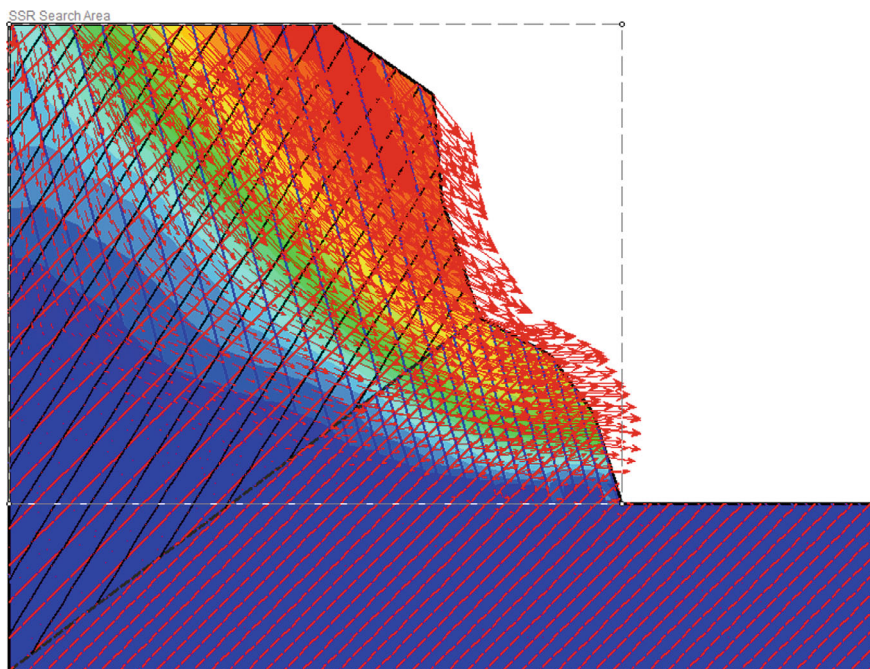


**Fig. 10** Deformation vectors showing downward displacement in sandstone layer and outward displacement in shale

- The slope is kinematically unstable and susceptible to wedge sliding due to the intersection of the two distinct joint planes. The weathered shale has been inferred to be kinematically more vulnerable to failure than the sandstone layer.
- Finite element modeling has revealed the slope to be marginally stable with a critical SRF of 1.02. The vulnerable zone in this case can be obtained showing the model at the critical SRF. However, this state would not represent the actual field condition of the slope.
- A better representation of the probable failure zones in the model has been given by the SSR search area. The slope has been revealed to be unstable with a critical SRF of 0.96. The sandstone layer is highly vulnerable showing downward displacement, whereas outward displacement has been observed in the weathered shale.

Since the critical SRF of the slope (both with and without the SSR search area) is less than 1.5, it needs to be stabilized. Methods like rock-bolting or tied-back walls can be adopted to improve the stability. Rock removal methods which are less costly like resloping or scaling can be implemented to decrease the overall slope angle and/or modify the profile of the slope face; the latter would be also helpful for the smooth installation of rock bolts or dowels.

**Acknowledgements** The authors are immensely grateful to the Engineering Geology Laboratory of the IIT (ISM) Dhanbad for geotechnical testing of samples, and giving access to the Dips, and RS2 programs for carrying out the necessary analysis.

**Declarations** The authors declare no competing interests.

## References

- Acharya B, Kundu J, Sarkar K, Chawla S (2017) Stability assessment of a critical slope near Nathpa Region, Himachal Pradesh, India. In: Indian geotechnical conference 2017 GeoNEst, IIT Guwahati, Guwahati, India
- Acharya B, Sarkar K, Singh AK, Chawla S (2020) Preliminary slope stability analysis and discontinuities driven susceptibility zonation along a crucial highway corridor in higher Himalaya, India. *J Mount Sci* 17(4):801–823
- Cheng YM, Lansivaara T, Wei WB (2007) Two-dimensional slope stability analysis by limit equilibrium and strength reduction methods. *Comput Geotech* 34(3):137–150
- Cheng YM, Lau CK (2014) Slope stability analysis and stabilization—new methods and insight, 2nd edn. CRC Press, Boca Raton
- Geological Survey of India (1985) Key papers presented in group discussion on tertiary stratigraphy of North-Eastern India, vol 23, 43
- ISRM (1978) Suggested methods for determining tensile strength of rock materials. *Int J Rock Mech Min Sci Geomech Abs* 15(3):99–103
- ISRM (1981a) Rock characterization testing and monitoring, ISRM suggested methods. *Int J Rock Mech Min Sci* 211
- ISRM (1981b) Rock characterization testing and monitoring, ISRM suggested methods. In: International society for rock mechanics, p 211
- ISRM (1981c) Suggested method for determining the uniaxial compressive strength of rock materials, rock characterization, testing and monitoring. *Int J Rock Mech Min Sci Geomech Abs* 113
- ISRM (1981d) Suggested methods for determining shear strength. In: Brown ET (ed) Rock characterization, testing and monitoring. Pergamon Press, Oxford, pp 129–140
- Kainthola A, Singh PK, Wasnik AB, Singh TN (2012) Distinct element modelling of Mahabaleshwar road cut hill slope. *Geomaterials* 2(4):105–113
- Kundu J, Sarkar K, Singh TN (2017a) Static and dynamic analysis of rock slope—a case study. *Proc Eng* 191:744–749
- Kundu J, Sarkar K, Tripathy A, Singh TN (2017b) Qualitative stability assessment of cut slopes along the National Highway-05 around Jhakri area, Himachal Pradesh, India. *J Earth Syst Sci* 126(8)
- Labuz JF, Zang A (2012) Mohr-Coulomb failure criterion. *Rock Mech Rock Eng* 45:975–979
- Lin Y, Zhu D, Deng Q, He Q (2012) Collapse analysis of jointed rock slope based on UDEC software and practical seismic load. *Proc Eng* 31:441–446
- Pain A, Kanungo DP, Sarkar S (2014) Rock slope stability assessment using finite element based modelling—examples from the Indian Himalayas. *Geomech Geoeng* 9(3):215–230
- Rocscience (2022) Dips (version 8.021). Graphical and statistical analysis of orientation data. Rocscience Inc., Toronto
- Rocscience (2023) RS2 (version 11.018). 2D finite element analysis. Rocscience Inc., Toronto
- Roslan R, Omar RC, Putri RF, Wahab WA, Baharuddin INZ, Jaafar R (2020) Slope stability analysis using Universal Distinct Element Code (UDEC) method. *IOP Conf Ser Earth Environ Sci* 451(1)
- Salih A (2021) Stability analysis of residual soil slope model by numerical modeling using FEM against LEM. *IOP Conf Ser Earth Environ Sci* 856(1)



- Sardana S, Verma AK, Verma R, Singh TN (2019) Rock slope stability along road cut of Kulikawn to Saikhamakawn of Aizawl, Mizoram, India. *Nat Hazards* 99:753–767
- Sarkar K, Singh TN, Verma AK (2012) A numerical simulation of landslide-prone slope in Himalayan region—a case study. *Arab J Geosci* 5:73–81
- Sarkar K, Buragohain B, Singh TN (2016) Rock slope stability analysis along NH-44 in Sonapur Area, Jaintia Hills District, Meghalaya. *J Geol Soc India* 87:317–322
- Seshu P (2003) Textbook of finite element analysis. PHI Learning Private Limited, New Delhi
- Singh AK, Kundu J, Sarkar K (2017) Stability analysis of a recurring soil slope failure along NH-5, Himachal Himalaya, India. *Nat Hazards* 90:863–885
- Survey of India (2024) Department of Science and Technology. <https://surveyofindia.gov.in/pages/outline-maps-of-india>. Accessed: 07 Aug 2024
- Ugai K, Leshchinsky D (1995) Three-dimensional limit equilibrium and finite element analyses: a comparison of results. *Soils Found* 35(4):1–7
- Wyllie DC, Mah CW (2004) Rock slope engineering—civil and mining. Spon Press, London
- You G, Mandalawi MA, Soliman A, Dowling K, Dahlhaus P (2018) Finite element analysis of rock slope stability using shear strength reduction method. In: *GeoMEast 2017 international conference: soil testing, soil stability and ground improvement*, pp 227–235

**Kripamoy Sarkar** is an Associate professor in the Department of Applied Geology in the Indian Institute of Technology (Indian School of Mines) Dhanbad. He is an accomplished and trained Engineering Geologist by profession with unique blend of industry and academic experience, has contributed significantly in the field of natural hazard investigations and soft computing applications in landslides. A few noteworthy contributions of Prof. Sarkar include improvements in rock mass characterization systems, and application of numerical modelling techniques to solve slope instability problems in the Indian Himalayas. His list of publications includes 85 scientific papers in various national and international journals and conference proceedings of repute. He has also published 4 edited book chapters that reflect advanced studies on the assessment of the landslide hazards. Prof. Sarkar has been the principal investigator of 5 major projects on landslide vulnerability analysis and rockfall hazard assessment sponsored by the Ministry of Earth Sciences, DST, and IIT (ISM) Dhanbad in the Northern and North-Eastern parts of the Indian Himalayas. He is the recipient of the prestigious Inder Mohan Thapar Research Award (2021 and 2022) from IIT (ISM) Dhanbad. He is an Associate Editor of the *Journal of Earth system Science*.

**Mr. Avishek Dutta** is a research scholar in the Department of Applied Geology at the Indian Institute of Technology (Indian School of Mines) Dhanbad. Currently in the fourth year of Ph.D. programme, his domain of research includes landslide hazard assessment using numerical simulation and machine learning techniques. He has completed his Bachelor of Technology in Civil Engineering from Netaji Subhash Engineering College, Kolkata, and Master of Technology in Engineering Geology from the Indian Institute of Technology (Indian School of Mines) Dhanbad.

# Effect of Ditch Design on Rockfall Hazard Using Rigid Body Model



Anurag Niyogi, Kripamoy Sarkar, and T. N. Singh

**Abstract** Rockfalls are landslides characterized by distinct mechanisms with limited understanding. The extensively interconnected fractures and fragmented rock slopes present a significant threat to the possibility of such an event. To evaluate the hazard of rockfall, it is necessary to conduct an assessment to accurately describe the nature and characteristics of the rock slope being examined. This study focuses on analysing kinematically permissible failure from the rock mass that causes rockfall activity in the area. The strategy related to hazard mitigation has been addressed based on field investigation and rockfall modeling. The statistical evaluation of rockfall potential has been performed with Rocfall 5.0 with rigid body modeling. A study on the effectiveness of ditches, using the Ritchie chart with the derivatives from Section Factor has been conducted to determine the optimum approach of remediation. The analysis proposes important ditch design recommendations based on site-specific requirements.

**Keywords** Rockfall simulation · Rockfall mitigation · Ditch design · Western Ghat

---

A. Niyogi (✉) · K. Sarkar  
Department of Applied Geology, Indian Institute of Technology (Indian School of Mines),  
Dhanbad, Jharkhand, India  
e-mail: [tabun111@gmail.com](mailto:tabun111@gmail.com)

A. Niyogi  
Department of Earth and Environmental Sciences, Indian Institute of Science Education and  
Research, Bhopal, Madhya Pradesh, India

T. N. Singh  
Department of Civil and Environmental Engineering, Indian Institute of Technology Patna, Bihta,  
Patna, Bihar, India

## 1 Introduction

The Western Ghats are prone to landslides, occurring quite frequently. Several studies have already existed citing slope stability crisis along highways (Singh et al. 2013; Kainthola et al. 2015; Sharma et al. 2020; Niyogi 2022). The economic impact of rockfall on roads is considerable, because they often lead to disruption or delay, necessitating costly remedial measures (Turner and Schuster 1996). Rockfall, on the other hand, is a failure mechanism that is still quite unfamiliar within India. A rockfall, predominantly, is a detached rock mass from the parent body (Varnes 1978). They move to collide, rotate, bounce, and slide until they cease of energy. The extruded rock mass from the slope face follows a path of movement known as trajectory, that are considered as hazardous. The causative factors involved in triggering rockfall include heavy precipitation, human and nature-induced ground vibrations etc. The hilly cut slopes following NH-66 in Maharashtra are critically affected by rock fall incidences. Rockfall studies have been carried out in nearby areas using variable analysis and modeling techniques (Ansari et al. 2014; Ahmad et al. 2013).

Prediction of hazards possessed by falling rock blocks needs to be thoroughly analysed. There are two ways to achieve it: manual field-based experiments or simulation software to virtually observe the full scenario. In recent years, studies have been conducted to acquire practical field results by dropping rock blocks (Dorren et al. 2005; Gili et al. 2022), monitoring rockfalls with sensors like LiDAR, laser scanners, etc. (Abellán et al. 2006; Lan et al. 2010; Bouali et al. 2017; Yan et al. 2019). The physical simulations are pertinent to deliver more accurate results however, the cost of project operation, complexities related to geographical variabilities, slope vegetation and the iteration with different block shapes and sizes pose a difficult situation. Numerical assessment of rockfall came into existence due to a limited understanding of rock fall mechanics (Pfeiffer and Bowen 1989). In the last two decades, rockfall simulation programs have developed several folds with 2D and 3D techniques (Pfeiffer and Bowen 1989; Guzzetti et al. 2002; Rocscience 2016a, b). To ensure the results are appropriate it is essential to have the best possible understanding of rock properties, slope geometry, structural and mineralogical properties to identify specific problems and implement suitable protection systems in the affected zones. The hazard related to falling blocks remains alarming in hilly regions. The discontinuities in the rock slope form favourable intersections deriving potential rockfall. The kinematic analysis is quick to assess the failure types and helps in marking out potential failure zones in the field (Niyogi et al. 2020). Kinematic analysis and field signatures were used to pinpoint the site of the block detachment, which serves as the commencement point for rockfall. The statistical distribution of post-detachment possibilities defines the design options for corrective interventions. Hazard assessment is important to qualitatively forecast the rockfall trajectories.

The basalt hills alongside the road provide a significant hazard if not properly managed, as they exhibit irregular fractures occurring at different intervals. Since the area is seismically inactive, an understanding of other factors initiating the cause is required. The studied slope is sub-vertical with several failed blocks have been

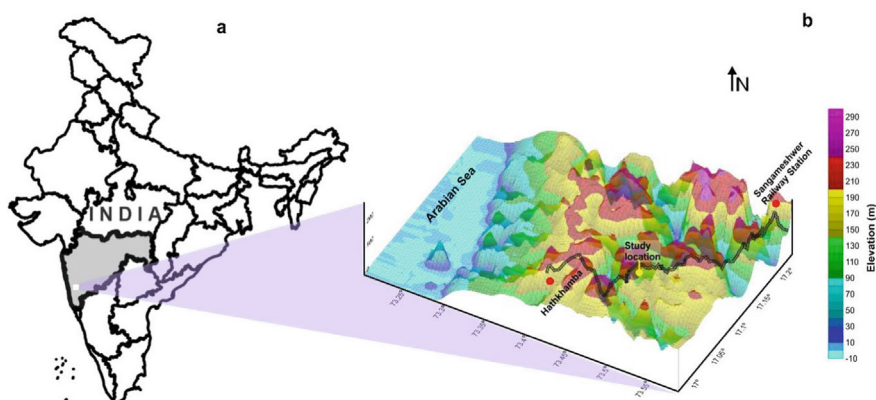


**Fig. 1** **a** The administrative boundary of India marked by the state of Maharashtra (in grey color), **b** the elevation map of the studied location along NH-66 near Sangameshwar

detected as a result of joint contact with the slope face. With this study an attempt was made to solve the problem related to cost-effective and sustainable protective measures.

## 2 Study Area

The study location chosen along NH-66, connecting Mumbai to Goa, near Sangameshwar taluka in Ratnagiri district of Maharashtra (Fig. 1). Running parallel to river Bav the location falls under the Purandargarh formation of Sahyadri group which is dates back to the upper Cretaceous to lower Eocene age. The slope is formed in a single flow formation with steep inclination and table top crown.

## 3 Effect of Ditch Design and Protection System as a Remedial Measure

As a measure for prevention from rockfall, many different mitigation methods are already in use such as barrier fences, dams, mesh wires etc. (Jaccard et al. 2020). These can manage rockfall both actively and passively in the field condition. The employment of the protection techniques needs to be carefully assessed mainly based on topography, cost-effectiveness, and intensity of occurrence of rockfall events. A ditch is a trench created on the edge of a roadway that works as a catchment area for the falling and sliding rock and soil geomaterials and prevents them from reaching highways or settlements.

Ritchie (1963), with the Washington State Department of Transportation (WSDOT), was the pioneer in developing a simple yet efficacious technique to inhibit the blocks from falling and precariously reaching the transportation corridor. This proposed design criterion was the outcome of the experiments performed by rock blocks thrown from variable slope angles and heights. Several authors experimented with real field test conditions and compared the results on the basis of Ritchie's ditch design (Budetta 2004; Maerz et al. 2005). Eliassen and Springston (2007) found out that the ditch dimension and orientation (width, shape and depth) play a significant role in containing the rock fall. Thomas and Eliassen (2012) used this subjective ditch study and gave a comparative result with the Rockfall Hazard Rating System (RHRS). They structured their research around the angle of the slope and its impact on ditch catchment ability.

### 3.1 Section Factor

New York State Department of Transportation (NYSDOT) in the year 1996 came up with a concept of section factor. It is a mathematical value that defines a range of values depending on the percentage of material catchment by a ditch. Section factor is an appraisal for appropriate ditch design for the requisite slope of study. It is the ratio of Ritchie depth-width to the actual field condition depth-width of the catchment ditch. The calculation is as follows Eq. (1)

$$\text{Section Factor} = \frac{\text{Ritchie Depth} + \text{Ritchie Width}}{\text{Actual Depth} + \text{Actual Width}} \quad (1)$$

After assessing the catchment performance set by NYSDOT, Thomas and Eliassen (2012) categorized four catchment classes termed as good, moderate limited and poor with respective ranges of values assigned to them. These recommendations are documented in Table 1.

**Table 1** Recommendation of section factor for ditch design from Ritchie chart (1963)

Thomas and Eliassen (2012)		NYSDOT 1996	
Range	Catchment class	Range	Minimum catchment (%)
0.1–1.00	Good	0.1–1.00	> 85
1.01–2.00	Moderate	1.00	85
2.01–3.00	Limited	> 1.01	< 85
3.01–11.00	Poor		

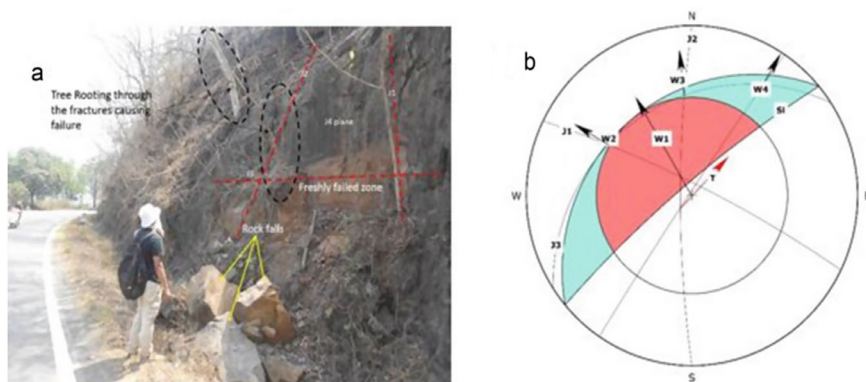


**Fig. 2** Pictorial representation of (a) field photo showing large blocks of Rockfall and structural orientation of slope, (b) kinematic analysis of the observed discontinuities

## 4 Result and Discussion

### 4.1 Kinematic Analysis

The slope steepness and unfavorable joint affinity make it a vulnerable location with persistent rock fall problems (Fig. 2a). Kinematic analysis shows that four major joint sets prevail in the concerned slope. J1 and J2 remain as the predominantly critical joint set producing wedge-type failure (W1). It is followed by the joint association between J1–J3, J2–J3 and J3–J4 which are less critical and may produce wedge-type failures, W2, W3 and W4 respectively. The direction of failure is covered along NNW to NNE. An oblique toppling failure (T) is witnessed in the area and is one of the most critical failure types observed in the location (Fig. 2b).

### 4.2 Rockfall Hazard Assessment

The present slope is 10–11 m high along NH-66. Composed primarily of basalt with fine vesicles, the rock material seems to be affected by weathering. The area under consideration is most prone to rockfall hazards. The hill is around 100 m in stretch with variations in height. Several dislodged rock blocks were observed scattering over the pavement strip. The associated discontinuities and slope orientation account for the formation of rock blocks of varied sizes. The majority of the boulders seen in the site area are different forms of rectangular shape. Rockfall simulation has been conducted using RocFall v5 software (Rocscience 2016a) for the model having three parts i.e. basalt slope, soil pavement and asphalt road. The soil pavement has an

uncompromising width of 0.75 m. The input parameters of the materials have been chosen from the RocFall v5 user guide documented in Table 2.

The other properties were kept at default. The slope surface is where the failing of block occurs formed by rock detachment. It is necessary to mark out the possible zones of detachment to statistically quantify and remediate accordingly. Thus, line seeders are applied based on kinematic assessment and overhangs in field condition. Placement of seeders are kept at a height of 7.8 m for line seeder, S1, and point seeder, S2, at 2.3 m respectively invariably throws rigid mass of 100 rocks each (Fig. 3).

Each seeder has been provided with two block shapes of rhombus and super ellipse (2:3). The density of basalt rock was measured at 2870 (kg/m<sup>3</sup>) and block size observed at the site location had a volume of 0.060 m<sup>3</sup> resulting in a mass of 169.8 kg. The simulation outcomes show out of 200 rock throws 193 units were

**Table 2** Rockfall material properties (Rocscience 2016b)

Material properties	Normal restitution	Tangential restitution	Dynamic friction	Rolling resistance
Basalt slope	0.35 ± 0.04	0.85 ± 0.04	0.5 ± 0.04	0.15 ± 0.04
Soil pavement	0.32 ± 0.04	0.8 ± 0.04	0.5 ± 0.04	0.3 ± 0.04
Asphalt road	0.4 ± 0.04	0.9 ± 0.04	0.6 ± 0.04	0.4 ± 0.04

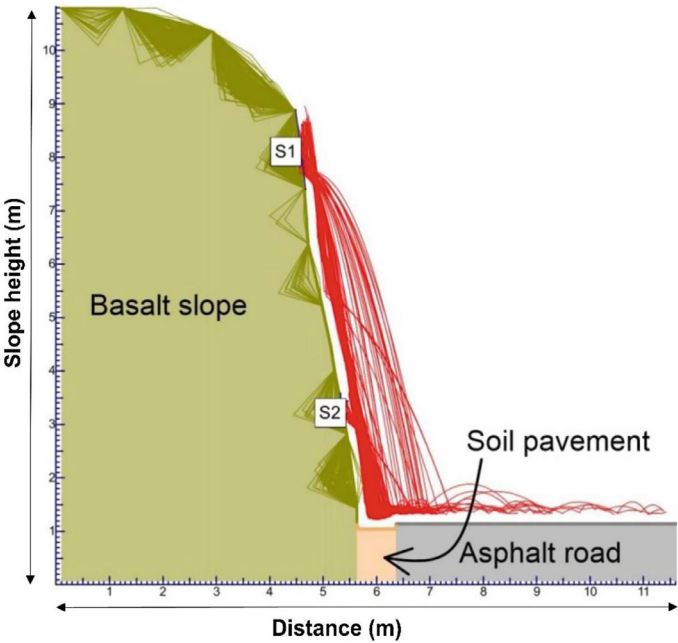


**Fig. 3** Rockfall simulation on present field condition



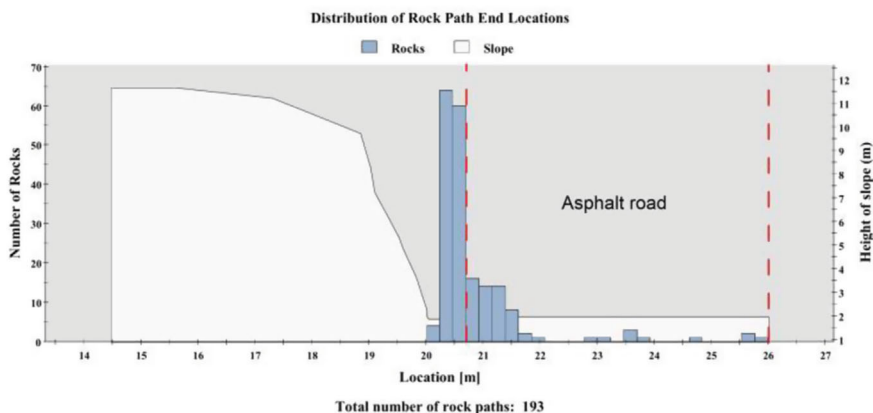


**Fig. 4** Histogram representing the number of rockfalls at the horizontal stretch in the present field condition

initiated. 128 units have been ceased by the ditch comprising of 66% of the total rock fall (Fig. 4). This is still a matter of concern as 34% reaches the highway. Due to this severity, a proper ditch design is needed.

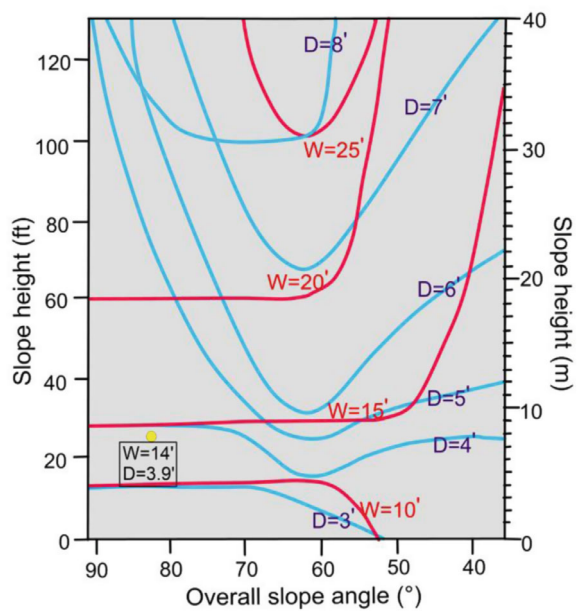
### 4.3 Ditch Effectiveness Study

In this study area the rockfall zones identified, has a height range from 7.8 m and 2.3 m. The slope is sub-vertical with an overall slope angle of  $82^\circ$ . To get the effective ditch dimension Ritchie ditch design chart is used which considers the actual height of block fall and the actual slope angle studied. The highest point of release i.e. 7.8 m from the base of the slope, is taken into consideration, to measure the recommended width and depth dimensions of the ditch for complete safety. The Ritchie width (W) and Ritchie depth (D) are determined to be 14 ft (4.24 m) and 3.9 ft (1.18 m) respectively. Moreover, the actual ditch width was measured to be 2.47 ft (0.75 m) and the actual ditch area was found to have a depth of 0.33 ft (0.1 m) (Fig. 5). Outcome of the section factor calculated using Eq. (1) is 6.37. The result shows the present situation falls under the poor catchment class according to Thomas and Eliassen (2012).

To achieve a good section factor, modification in actual ditch dimensions is required. As it is apparent from the real field situation, the width of the ditch is limited. Hence the majority of alteration is needed in ditch depth. It was seen that  $85^\circ$  as the most favourable ditch shoulder inclination angle for a flat-bottom ditch to holds most rock fall within the ditch space.

The aim is to reach a score of greater than 85% catchment of rockfalls by a ditch (Table 1). Hence, to get a section factor range below 1, ditch should be made to 4.67 m depth. For this purpose, several test runs were conducted of rockfall simulation

**Fig. 5** Ritchie chart depicting recommendation for ditch design



at different section factor with different ditch depths. The optimum ditch design obtained from the simulation results is presented in Table 3 which recommends a minimum of 0.25 m of ditch depth necessary to attain the good catchment.

**Table 3** Ditch design effectiveness for rockfall catchment

Ditch depth (m)	Number of rocks captured	% capture
0.1	128	66.32
0.15	143	74.09
0.2	155	80.31
0.225	161	83.42
0.25	167	86.53
0.5	173	89.64
1	173	89.64
4.67	173	89.64

## 5 Conclusion

The region around NH-66 is vulnerable to rockfall hazards due to slope elevation and orientation. A slope primarily composed of basalt rock with a height of 10–11 m with  $80^{\circ}$ – $82^{\circ}$  mean inclination is experiencing wedge-type failure. Field measurement of fallen blocks and laboratory estimation of material density were used for computerized rockfall simulations. The point of impact and the rock rollout numbers were determined. A ditch design optimization study for managing rockfall events was conducted based on statistical hazard analysis. Ritchie chart for optimal ditch design combined with Section Factor shows an improved site-specific result. The Ritchie chart is efficient in proposing a generalised design but site-specific demand and proper estimation of their influencing factors must be thoroughly understood. The results show that good catchment of  $> 85\%$  can be achieved at a much shallower depth of 0.25 m in comparison to 4.67 m as recommended by Ritchie chart.

**Acknowledgements** The authors sincerely appreciate the Indian Institute of Technology (Indian School of Mines) Dhanbad for providing financial and laboratory assistance and Rock Science and Rock Engineering (RSRE) lab, the Department of Earth Sciences, Indian Institute of Technology Bombay for providing facilities to conduct experiments.

**Declaration** There is no conflict of interest between the authors. This work is a component of the first author's doctoral research.

## References

- Abellán A, Vilaplana JM, Martínez J (2006) Application of a long-range terrestrial laser scanner to a detailed rockfall study at Vall de Núria (Eastern Pyrenees, Spain). *Eng Geol* 88(3–4):136–148
- Ahmad M, Umrao RK, Ansari MK, Singh R, Singh TN (2013) Assessment of rockfall hazard along the road cut slopes of state highway-72. Maharashtra, India
- Ansari MK, Ahmad M, Singh R, Singh TN (2014) Rockfall hazard assessment at Ajanta Cave, Aurangabad, Maharashtra, India. *Arab J Geosci* 7(5):1773–1780
- Bouali EH, Oommen T, Vitton S, Escobar-Wolf R, Brooks C (2017) Rockfall hazard rating system: benefits of utilizing remote sensing. *Environ Eng Geosci* 23(3):165–177
- Budetta P (2004) Assessment of rockfall risk along roads. *Nat Hazard* 4(1):71–81
- Dorren LK, Berger F, Le Hir C, Mermin E, Tardif P (2005) Mechanisms, effects and management implications of rockfall in forests. *For Ecol Manage* 215(1–3):183–195
- Eliassen TD, Springston GE (2007) Rockfall hazard rating of rock cuts on US and state highways in Vermont. Vermont Agency of Transportation, Montpelier
- Gili JA, Ruiz-Carulla R, Matas G, Moya J, Prades A, Corominas J, Lantada N, Núñez-Andrés MA, Buill F, Puig C, Martínez-Bofill J, Saló L, Mavrouli O (2022) Rockfalls: analysis of the block fragmentation through field experiments. *Landslides* 19(5):1009–1029
- Guzzetti F, Crosta G, Detti R, Agliardi F (2002) STONE: a computer program for the three-dimensional simulation of rock-falls. *Comput Geosci* 28(9):1079–1093
- Jaccard CJ, Abbruzzese JM, Howald EP (2020) An evaluation of the performance of rock fall protection measures and their role in hazard zoning. *Nat Hazards* 104(1):459–491
- Kainthola A, Singh PK, Singh TN (2015) Stability investigation of road cut slope in basaltic rockmass, Mahabaleshwar, India. *Geosci Front* 6(6):837–845

- Lan H, Martin CD, Zhou C, Lim CH (2010) Rockfall hazard analysis using LiDAR and spatial modeling. *Geomorphology* 118(1–2):213–223
- Maerz NH, Youssef A, Fennessey TW (2005) New risk–consequence rockfall hazard rating system for Missouri highways using digital image analysis. *Environ Eng Geosci* 11(3):229–249
- Niyogi A (2022) Stability evaluation of road cut slopes along NH 66, Ratnagiri, Maharashtra, India. Ph.D. thesis. <http://hdl.handle.net/10603/441868>
- Niyogi A, Sarkar K, Singh AK, Singh TN (2020) Geo-engineering classification with deterioration assessment of basalt hill cut slopes along NH 66, near Ratnagiri, Maharashtra, India. *J Earth Syst Sci* 129(1):1–19
- Pfeiffer TJ, Bowen TD (1989) Computer simulation of rockfalls. *Bull Assoc Eng Geol* 26(1):135–146
- Ritchie AM (1963) Evaluation of rockfall and its control. *Highw Res Rec* 17
- Rocscience (2016a) RocFall v5.0, computer program for risk analysis of falling rocks on steep slopes. Rocscience Inc., Toronto
- Rocscience (2016b) Rocfall user guide. Documentation
- Sharma LK, Umrao RK, Singh R, Singh TN (2020) Assessment of rockfall hazard of hill slope along Mumbai-Pune expressway, Maharashtra, India. *Acta Geodyn Geomater* 17(3)
- Singh PK, Wasnik AB, Kainthola A, Sazid M, Singh TN (2013) The stability of road cut cliff face along SH-121: a case study. *Nat Hazards* 68:497–507
- Thomas E, Eliassen TD (2012) Rock slope catchment ditch effectiveness: an assessment of methods used for RHRS scoring. In: 63rd highway geology symposium highway geology symposium
- Turner AK, Schuster RL (1996) Landslides: investigation and mitigation. Special report 247. Transportation Research Board, National Academy Press, Washington, DC
- Varnes DJ (1978) Slope movement types and processes. *Spec Rep* 176:11–33
- Yan Y, Li T, Liu J, Wang W, Su Q (2019) Monitoring and early warning method for a rockfall along railways based on vibration signal characteristics. *Sci Rep* 9(1):6606

**Dr. Anurag Niyogi** is working as Scientist B (Project) on Permanent sequestration of gigatons of CO<sub>2</sub> in continental margin basalt deposits at the IISER Bhopal. His research is focused on fracture modeling and reservoir estimation. With a Ph.D. in Engineering Geology from IIT (ISM) Dhanbad, Dr. Niyogi has made contributions to the field of slopes stability, numerical modeling of landslide, and geotechnical engineering through research papers, book chapter and conference presentations.

**Dr. Kripamoy Sarkar** is an Associate professor in the Department of Applied Geology in the Indian Institute of Technology (Indian School of Mines) Dhanbad. He is an accomplished and trained Engineering Geologist by profession with unique blend of industry and academic experience, has contributed significantly in the field of natural hazard investigations and soft computing applications in landslides. A few noteworthy contributions of Prof. Sarkar include improvements in rock mass characterization systems, and application of numerical modelling techniques to solve slope instability problems in the Indian Himalayas. His list of publications includes 85 scientific papers in various national and international journals and conference proceedings of repute. He has also published 4 edited book chapters that reflect advanced studies on the assessment of the landslide hazards. Prof. Sarkar has been the principal investigator of 5 major projects on landslide vulnerability analysis and rockfall hazard assessment sponsored by the Ministry of Earth Sciences, DST, and IIT (ISM) Dhanbad in the Northern and North-Eastern parts of the Indian Himalayas. He is the recipient of the prestigious Inder Mohan Thapar Research Award (2021 and 2022) from IIT (ISM) Dhanbad. He is an Associate Editor of the *Journal of Earth system Science*.

**Prof. Trilok Nath Singh** is currently working as Director IIT Patna and the Institute Geoscience Chair Professor in the Department of Earth Sciences, IIT Bombay, Mumbai, and is an expert

in the field of rock mechanics, mining geology, and clean energy. He received his Ph.D. degree from the Institute of Technology BHU, Varanasi, in 1991 and subsequently served the institute until 2003. He is a recipient of many prestigious awards such as the National Mineral Award, the first P. N. Bose Mineral Award, the SEAGATE Excellence Award for Geo-Engineering, and the GSI Sesquicentennial Commemorative Award. He has nearly 28 years of experience in research and teaching with 16 doctoral theses completed under his supervision and has authored more than 350 publications in various journals and conferences of national and international repute. He is currently leading projects of immense scientific and industrial importance related to coalbed methane, carbon sequestration, shale gas, nuclear waste repositories, and mine slope stability, to name a few. He is on the governing and advisory councils of several national institutes and universities.

# Probabilistic Stability Analysis of Opencast Coal Mine Dump Slopes from Lower Gondwana Region, India: A Case Study



Prasanta Kr. Behera, Ashok Kr. Singh, and Kripamoy Sarkar

**Abstract** The failure characterization of internal or external dump slopes in opencast coal mines is considered to be highly crucial for safe and sustainable mining operations across the globe. As the opencast mining method is contributing majorly in the coal production in India, thus, analyzing the risk in safe mining operations due to possibility of dump slope failure is inevitable. Therefore, the present study intended to quantify the probability of dump slope failure in Ananta Opencast Mine, Lower Gondwana region, India. To achieve the objective of the study, the probabilistic stability analysis is carried out through Limit Equilibrium Method (LEM). In the realm of slope stability analysis, this method leverages conditional probability and employs Monte Carlo Simulation (MCS) to systematically assess the likelihood of failure events occurring in sequence, providing insights into various stability scenarios. Two critical dump slopes at Ananta Opencast Mine, AOCP-1 and AOCP-2 in the Indian Lower Gondwana region, have been analyzed in prevailing geomechanical settings considering saturated condition. The analyzed stability results of AOCP-1 have shown instability under saturated conditions with a Factor of Safety (FOS) of 0.958. The observed failure probability for AOCP-1 is 63.4%, highlighting an unsafe dump design in these conditions. In contrast, the simulated stability of AOCP-2 recommends a safe and stable dump design, with an average FOS of 1.602. Based on the critical stability concerns, potential remedial actions have been proposed to ensure long-term stability for safe mining operations.

**Keywords** LEM stability analysis · Dump stability · Monte Carlo Simulation · Ananta Opencast Mine · Probability of Failure

---

P. Kr. Behera

Geological Survey of India (GSI), Kolkata, West Bengal 700091, India

A. Kr. Singh

CSIR-Central Institute of Mining and Fuel Research, Regional Research Centre, Roorkee, Uttarakhand 247667, India

K. Sarkar (✉)

Department of Applied Geology, Indian Institute of Technology (Indian School of Mines) Dhanbad, Dhanbad, Jharkhand 826004, India

e-mail: [kripamoy@iitism.ac.in](mailto:kripamoy@iitism.ac.in)

# 1 Introduction

Open-cast mining serves a critical function in the global extraction of minerals and resources. In India, this mining technique has significantly contributed to the economic progress of the nation by providing essential raw materials for various sectors. However, this method of extraction is associated with various challenges and risks, particularly concerning the potential for failures in dump slopes (Poulsen et al. 2014; Kasmer et al. 2006; Speck et al. 1993). These failures can lead to significant environmental damage, fatalities, damage to mining equipment and economic setbacks (Mohanty et al. 2022; Dash 2019; Behera et al. 2016; Gupta et al. 2014; Kainthola et al. 2011; Orendorff 2009). Over the past two decades, there have been several notable instances of dump slope failures across the globe, highlighting the need for comprehensive analysis and mitigation strategies for internal as well as external dump slopes.

Generally, dump materials are heterogeneous in nature and mostly consist of coal-bearing rock fragments such as sandstone, shale and gravel of varying sizes, along with loose soil (varying from sand to clay sizes). Therefore, their properties vary spatially within the dump slope (Nayak et al. 2020; Singh 2000). Many uncertainties in the properties of the dump affect the total slope mass and the anticipated failure characteristics. As the properties of overburden material are highly heterogeneous, probabilistic stability analysis methods are considered to be highly suitable to examine the uncertain nature of dump materials. This uncertainty includes errors in measurement and a lack of data to understand the material behaviour (Behera 2018). Consequently, the probabilistic stability analysis of slopes involves consideration of material uncertainties, such as variability in soil and rock properties (Li et al. 2014), which may affect the failure mechanism of a slope.

Considering the above discussion, a probabilistic stability assessment of the dump slopes, namely AOCP-1 and AOCP-2 of Ananta Opencast Mine from Lower Gondwana coalfield region in the state of Odisha is performed to evaluate the hazard associated with dump failure and possible failure characteristics in prevailing geomechanical conditions.

## 1.1 Failures in Open Cast Mines: Global and Indian Perspective

According to the International Council on Mining and Metals (ICMM), dump slope failures have been responsible for a significant number of fatalities and environmental incidents in the past two decades. Between 2000 and 2020, there were over 50 documented cases of dump slope failures worldwide, resulting in hundreds of fatalities and substantial environmental damage. A study conducted by the World Mine Tailings Failures (WMTF) initiative found that the majority of dump slope failures were attributed to factors such as poor waste management practices, inadequate monitoring



systems, and geological instability. Furthermore, the research identified a correlation between rapid expansion in mining activities and an increase in the frequency of dump slope failures. In the recent past worldwide, one of the most significant dump slope failures occurred in 2015 at the Samarco iron ore mine in Brazil. The disaster of the Fundão tailings dam failure resulted in a catastrophic release of mine dump, causing extensive environmental damage and claiming several lives. This incident underscored the importance of proper waste management practices and monitoring systems in open-cast mines. In 2019, the Brumadinho dam collapse, also in Brazil, further emphasized the potential consequences of dump slope failures. The collapse released a torrent of mining waste, leading to significant loss of life and environmental devastation. Investigations into the incident revealed a combination of structural flaws, inadequate monitoring, and regulatory failures as contributing factors. Similarly, in 2020, the failure of a waste dump at the Neryungrinsky coal mine in Russia resulted in the death of several workers and environmental pollution. The incident highlighted the global nature of the issue and the need for stringent safety regulations and enforcement measures across mining operations.

Over the last 20 years, India has witnessed several incidents of dump slope failures in its open-cast mines (Mohanty et al. 2022; Dash 2019; Behera 2018). While comprehensive data on every failure may not be readily available, a review of reported incidents reveals a concerning trend (Dash 2019). The frequency of such failures appears to have increased, possibly due to factors like intensified mining activities, inadequate safety measures, and environmental changes.

## 2 Study Area and Geological Setting

The study region belongs to the Talcher Coalfield Area of the Lower Gondwana Group, (Fig. 1). In India the most important coal-bearing area are mainly covered by the Barakar, Karharbari and Talcher Formation. These Formations are mainly characterized by conglomeratic sandstones along with very coarse to fine-grained sandstones, carbonaceous and grey shales with coal seams. The presence of coal seams has been identified along both the western edge and the northern boundary of the Talcher coalfield (Manjrekar et al. 2006).

## 3 Materials and Methods

### 3.1 Dump Slope Geometries and Geotechnical Investigation

The geotechnical investigation includes the observations and measurement of dump slope geometries of AOCP-1 and AOCP-2 of Ananta Coalfield Mines during field investigation. The field conditions and slope geometries with representative LEM

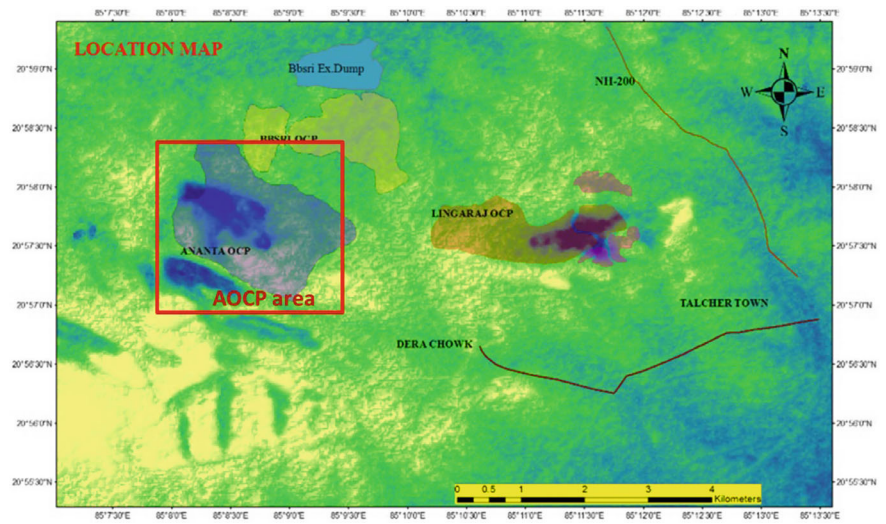


**Fig. 1** Map of the study area of Talcher Coalfield of the Lower Gondwana Group (Behera 2018)

material models of internal dumps of AACP-1 and AACP-2 are given in Figs. 2 and 3. The geotechnical tests for material models were performed as per the specifications of the International Society of Rock Mechanics (ISRM 1981). The representative soil samples were taken for the experiment to know the physico-mechanical characteristics such as unit weight, cohesion and angle of friction. The dump slopes are made up of loose mixtures of rock and soil generated during mining operations. As a result, the tensile strength of dump materials is considered negligible compared to other strength parameters (Rai et al. 2012). Consequently, a tensile strength of 0 kPa has been assumed for the analyses. The geotechnical parameters used in the stability analysis are provided in Table 1.

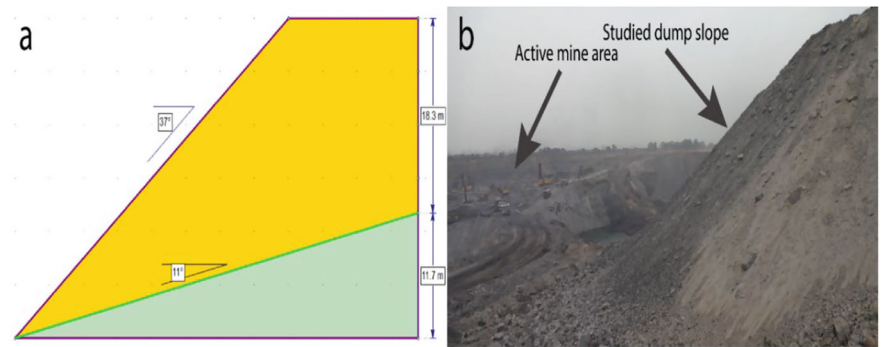


**Fig. 2** Internal dump of AACP-1 (a) LEM material model (b) field view

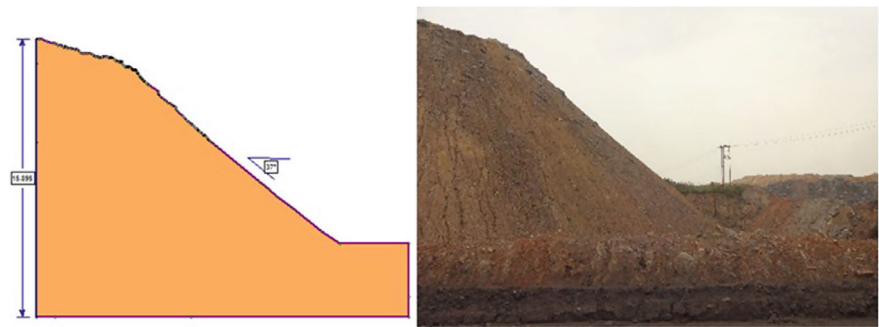


**Fig. 3** Internal dump of AOCP-2 (a) LEM material model (b) field view

**Table 1** Input parameters for the LEM stability analyses for the dump slopes of AOCP-1 and AOCP-2

Parameter	AOCP-1	AOCP-2
Unit weight (kPa)	17.33 ± 2.03	20.00 ± 2.19
Cohesion (C in kPa)	4.14 ± 4.7	2.36 ± 5.2
Angle of internal friction (φ in Degree)	30.0 ± 3.5	45.29 ± 5.8
Slope height (m)	30	20
Slope angle (°)	37	37

3.2 Limit Equilibrium Method

The Limit Equilibrium Methods (LEMs) have been extensively used in slope stability analysis since the 1930s. Over time, various LEMs have been developed by researchers to assess slope stability, with the Method of Slices (MoSs) being the most commonly employed in routine design. Several MoSs techniques have emerged, some focusing solely on force or moment equilibrium, while others satisfy complete equilibrium conditions. The primary output of these methods is the Factor of Safety (FOS), which indicates the stability of the analyzed slope model and identifies potential failure surfaces, including the critical slip surface that corresponds to the minimum FOS and reliability index (Zeng et al. 2015). These methods are known to be statically indeterminate, relying on assumed distributions of interslice forces, which leads to variations in the FOS obtained by different methods due to differing assumptions. Notable MoSs include the Ordinary Method of Slices (OMS), the Simplified Bishop method, Janbu’s Generalized method, Morgenstern-Price’s method, Spencer’s method, Sarma’s method, and the General Limit Equilibrium (GLE) method. Among these, the Bishop Simplified method, Janbu method, GLE, and Morgenstern-Price method are particularly popular for their ability to quickly calculate the FOS for most slip surfaces (Abramson et al. 2002; Behera 2018). Slope

stability analysis also involves various uncertainties, such as the inherent spatial variability of soil properties (Li et al. 2014). The application of deterministic analysis, which focuses on the average soil strength and stiffness, results in non-conservative conclusions, largely due to the variability that characterizes these soil properties (Liu et al. 2018).

### **3.3 Probabilistic Stability Analysis**

In a probabilistic stability analysis of slopes, statistical distributions can be assigned to the model's input parameters to reflect the uncertainty in their values (Vanneschi et al. 2018; Behera 2018). In the LEM, input data samples are generated randomly according to the user-defined statistical distributions. The Monte-Carlo sampling method has been adopted to perform probabilistic analysis to quantify the effect of uncertainty or variability of material parameters on stability of dump. The sampling method utilize random numbers to sample from given input probability distribution data (Rocscience manual). The Probability of Failure (PF) is defined as the number of analyses with FOS less than 1, divided by the total number of samples.

$$\text{or PF} = (\text{No of failed}/\text{No of samples}) \times 100\%$$

The FOS and the PF are shaped by several determinants, including the reliability of the system, the distribution of the input parameters in the analysis, and the analytical approach taken to establish the final probability distribution (Kumar et al. 2023).

## **4 Results and Discussion**

### **4.1 Deterministic Stability Analysis of AOCP-1 and AOCP-2 of Ananta Opencast Mine**

The analyzed result of AOCP-1 has been presented in (Fig. 4a) which shows an unstable slope with a deterministic FOS of 0.958. According to the United States Army Corps of Engineers (USACE), a minimum FOS of 1.5 is recommended for dump and embankment materials. The saturation of materials results in a reduction of the deterministic FOS to as low as 0.958. This reduction is primarily due to a significant decrease in the friction angle and an increase in the unit weight of the dump, which in turn raises the gravity load. The critical failure surface (Fig. 4a) exhibits a circular pattern, with the maximum depth of the critical slip surface reaching 4.5 m from the surface in the saturated slope. In contrast, the line of thrust (indicating the location of the resultant interslice force) is situated at a depth of 2.4 m from the slope surface.

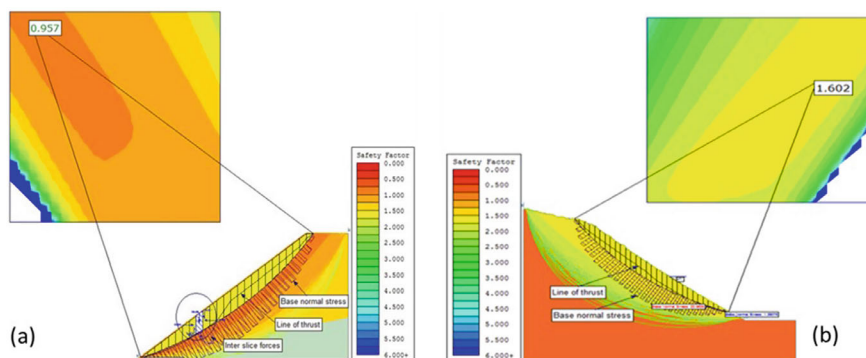


**Fig. 4** Deterministic LEM stability analysis of (a) AOCP-1 and (b) AOCP-2

Conversely, the analyzed result of AOCP-2 has been presented in Fig. 4b. According to the USACE recommendation, the present dump exhibits stable condition with a deterministic FOS of 1.602. Based on the reliability Index, the value is 2.480 which is less than 3, so it is not recommended for safe slope design. In generalized LEM analysis results, the FOS obtained for Bishop, Ordinary, Janbu, GLE/MP methods are 1.605, 1.549, 1.609, and 1.602 respectively. In AOCP 2, critical failure surface (Fig. 4b) follows a semi-circular to circular slip pattern. The line of thrust completely lies within the sliding mass exhibiting no tension cracks at the top of the dump. It also shows that the compressive positive interslice forces, which are dominant within the potential sliding mass, result in a higher FOS even in the presence of loose materials.

## 4.2 Probabilistic Stability Analysis of AOCP-1 and AOCP-2 of Ananta Opencast Mine

LEM technique has been adopted for the probabilistic stability analysis of two dump slopes of the Ananta Opencast Coal Field Area marked as AOCP-1 and AOCP-2. The sampling method utilizes random numbers to sample from given input probability distribution data (Rocscience manual). The analysis was performed using an auto-refined search method combined with a half-sine force function to calculate the Global FOS. According to the USACE, a minimum FOS of 1.5 is considered in this study for the safe design of dump and embankment materials. The probabilistic stability analysis of AOCP-1 has been presented in Fig. 5a which shows an unstable slope with a deterministic FOS of 0.957. The materials saturation reduces the deterministic FOS value to 0.958 and the probabilistic FOS to 0.961, which typically indicates instability with a probability of failure of 63.4% (Fig. 9a). The Reliability Index is  $-0.375$  which is less than 3 and is not recommended for the safe slope design (Table 2). The significant decrease in the friction angle and the increase in

the unit weight of the dump due to saturation, which raises the gravity load, are also the reasons for the reduction in the FOS (Behera 2018).

On the other hand, AOCB-2, presented in Fig. 5b exhibits stable conditions with deterministic and Probabilistic FOS of 1.602 and 1.628 respectively (Table 2). Based on the reliability index, the value is 2.480 which is less than 3. The critical failure surfaces (Fig. 5b) follow a semi-circular to circular slip pattern. The line of thrust completely lies within the sliding mass exhibited no tension cracks shall appear at the top of the dump. It also indicates that the compressive positive interslice forces, which are dominant in the sliding mass, lead to a higher factor of safety (FOS) despite the presence of unconsolidated materials. The observed higher FOS for AOCB might also be attributed to the relatively lower height of the dump, which has a significant impact on the stability of dumps in this area (Behera et al. 2016; Behera 2018). Therefore, the further instability within the dump slope may contributed by the increase in height as well as modification in dump geometry along with intense rainfall and ground vibration due to seismicity.

The highlighted data (yellow bars) in the histogram plot (Fig. 6a) shows the FOS less than 1 and explains the PF for the chosen sample points. The PF is defined as the number of analyses with FOS less than 1, divided by the total number of samples as:

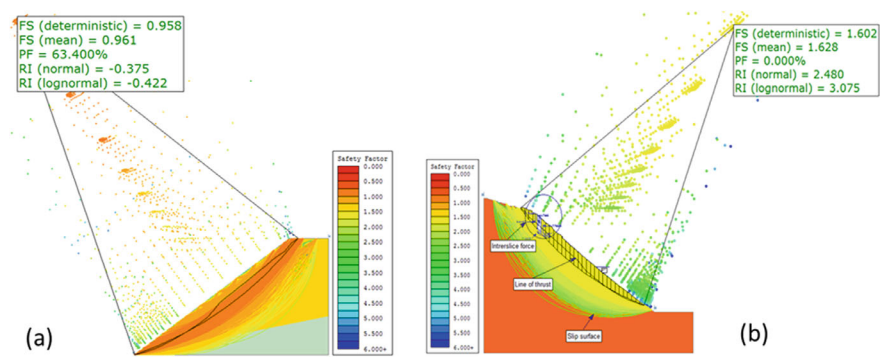


**Fig. 5** Probabilistic stability analyses of (a) AOCB-1 and (b) AOCB-2

**Table 2** Results of deterministic and probabilistic stability analyses of AOCB dumps

Dump locations	Methods of analysis	Morgenstern price method			
		Factor of safety		Probability of failure (%)	Reliability index (Normal)
		Deterministic	Probabilistic		
AOCB-1	Saturated condition	0.958	0.961	63.4	−0.375
AOCB-2	Saturated condition	1.602	1.628	0.00	2.480

$$PF = (\text{No of failed} / \text{No of total samples}) \times 100\%$$

Therefore, 634 sample points out of the selected 1000 samples have a FOS less than 1 which apparently suggests the PF of 63.40%. The statistical distribution of

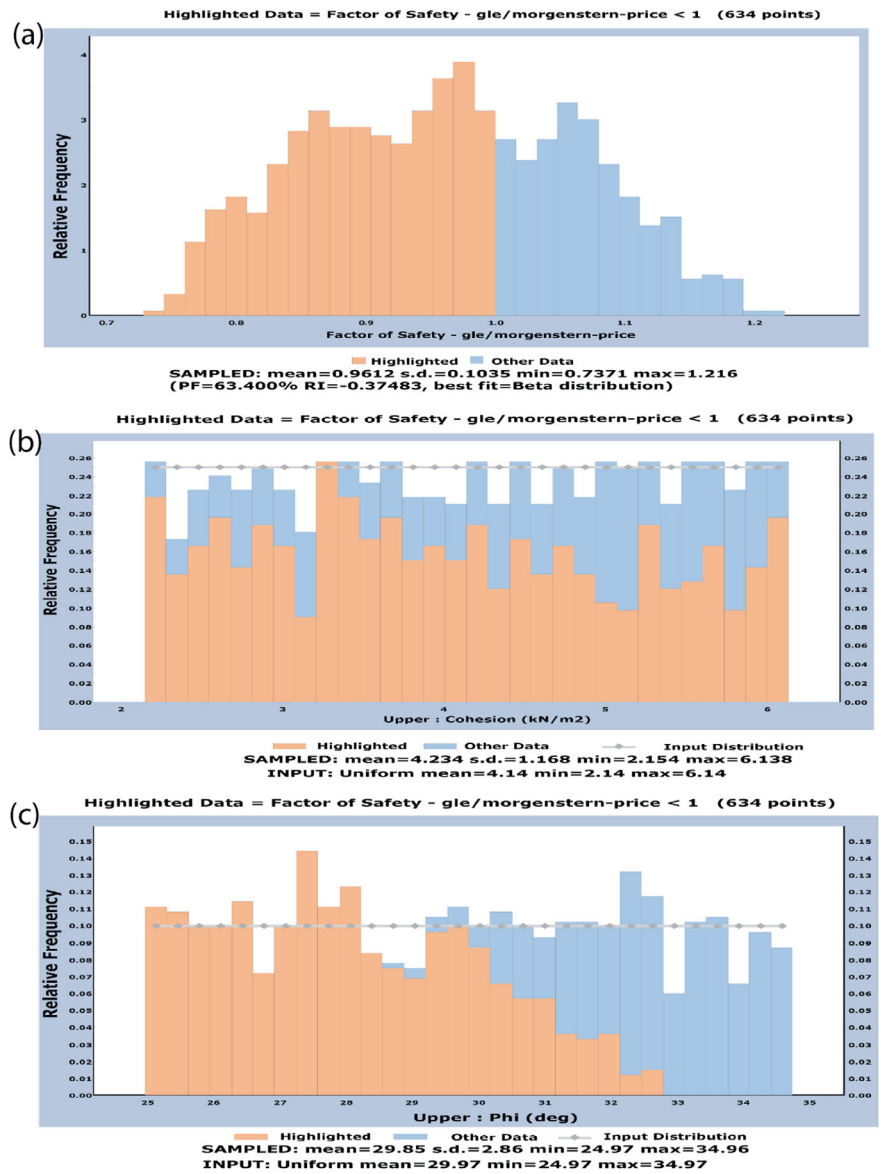


Fig. 6 Histogram plots of **a** FOS (MP) versus relative frequency **b** cohesion versus relative frequency **c** phi versus relative frequency for AOC-P-1



cohesion (Fig. 6b) suggests a random influence on dump stability whereas failure agrees with the lowest friction angle ( $<30^\circ$ ) that is generated by the random sampling (Fig. 6c).

Moreover, the cumulative distribution function (Fig. 7a) represents the probability of unsuccessful performance for a specific FOS value or denotes the cumulative probability when the value of FOS is less than 1 (at failure in this case). The cumulative probability of 0.634 implies 63.4% of PF for the GLE/MP method. The scatter plot has been plotted for the correlation of two independent variables with FOS. A quite good positive correlation has been observed between the friction angle ( $\phi$ ) and FOS with a Correlation Coefficient (CC) of 0.9165 using Beta ( $\beta$ ) best-fit distribution (Fig. 7b). However, best fit linear regression line between cohesion and FOS is found poorly (positive) correlated (CC of 0.35) implies more sensitiveness of cohesion with respect to FOS as compare to friction angle (Fig. 7c).

Conversely, for AOC-P-2, the probabilistic analysis suggested that the highlighted data (yellow bars) shows those FOS whose values are less than 1.5 in the histogram plot (Fig. 8a). The observed PF is 0% due to variation of FOS values greater than 1.5. The statistical distribution of cohesion and friction angle ( $\phi$ ) that is generated by the random sampling (Fig. 8b, c) suggests a wide frequency distribution of samples for FOS  $> 1.5$  that validates the observed PF. Here, the cumulative distribution function (Fig. 9a) of unsuccessful performance at FOS of 1.5 is 0.321. This implies that the cumulative probability of failure is much less i.e. 0.321 even at a stable threshold FOS (1.5). The scatter plot indicates a good positive correlation between friction angle ( $\phi$ ) and FOS with a CC of 0.974 using best-fit beta distribution (Fig. 9b) indicating more sensitivity toward FOS variation. However, the linear regression line between cohesion and FOS is found poorly (positive) correlated (CC of 0.147) implying less sensitivity towards FOS variation as compared to friction angle (Fig. 9c).

### 4.3 Mitigation Strategies for Dump Slopes of AOC-P

In response to the growing concern over dump slope failures, the mining industry has been implementing various mitigation strategies aimed at enhancing safety and minimizing environmental impact. Considering the criticality of internal AOC-P dump slopes in terms of stabilization strategies, the following practices can be employed:

- Improved waste management practices, such as the use of geosynthetic liners and engineered structures to contain mining waste with proper dumping methodologies (Behera 2018).
- Enhanced monitoring and surveillance systems utilizing remote sensing technologies, geophysical surveys, and real-time monitoring of slope stability.
- Implementation of strict regulatory frameworks governing mine safety and environmental protection, including regular inspections and audits.
- Adoption of advanced modelling and risk assessment techniques to predict and prevent dump slope failures.

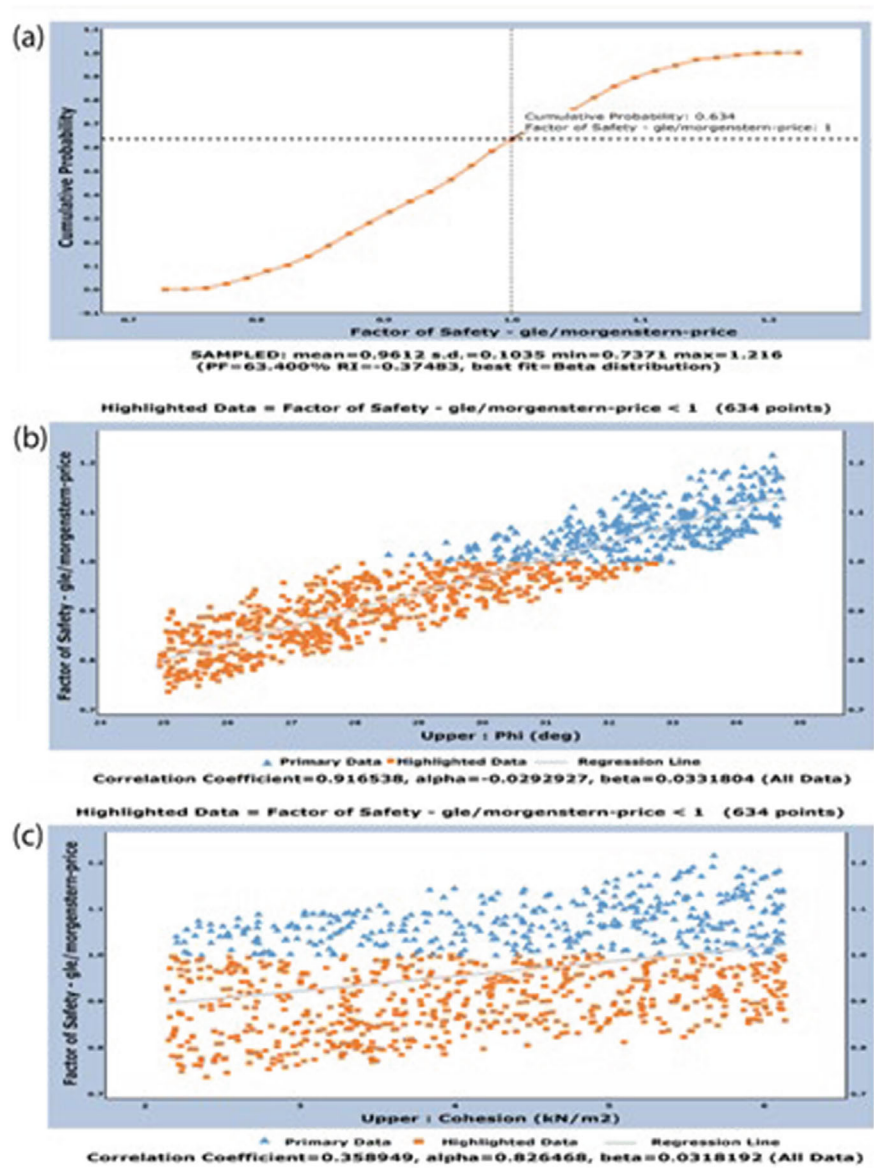


**Fig. 7** (a) Cumulative plot of safety factor (b) scatter plot—friction angle versus FOS (c) scatter plot—FOS versus Cohesion for AOCP-1

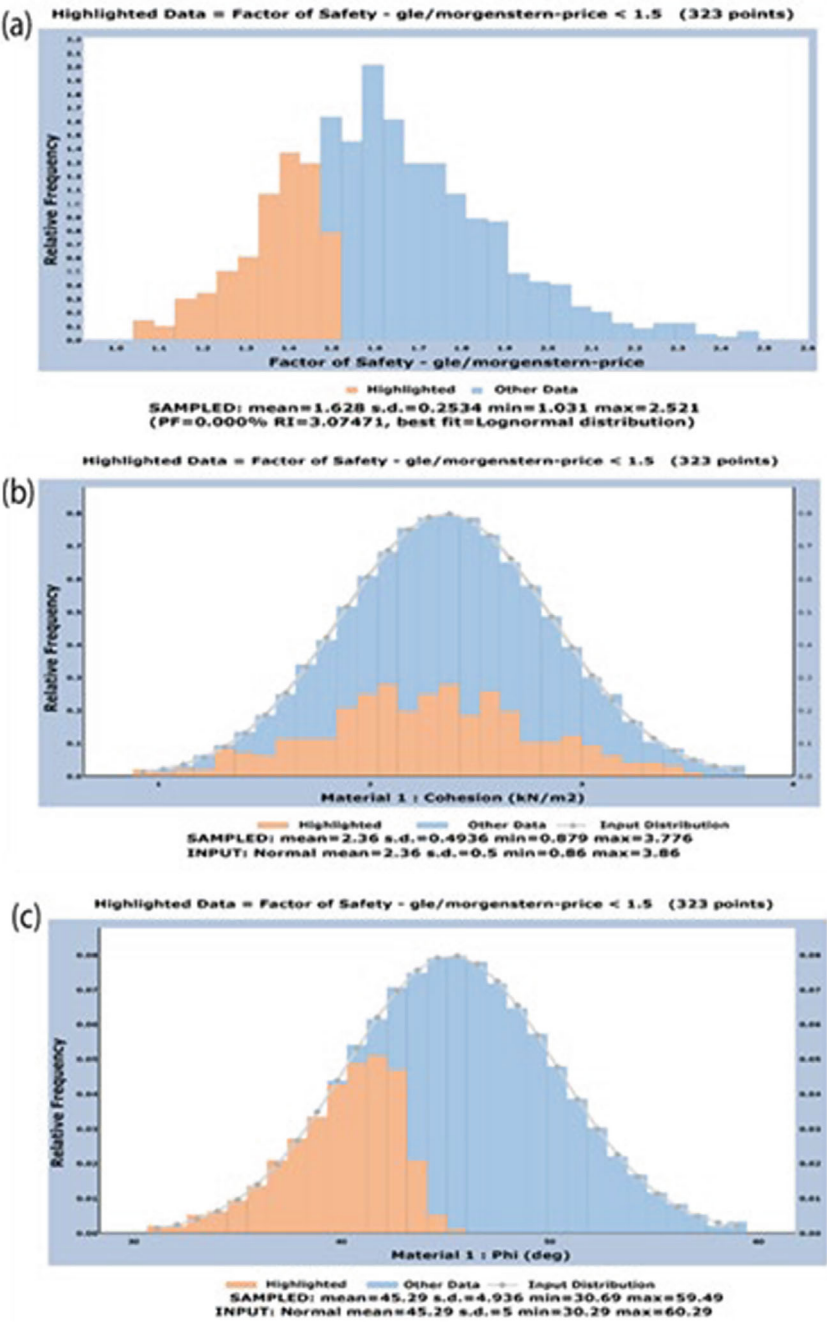
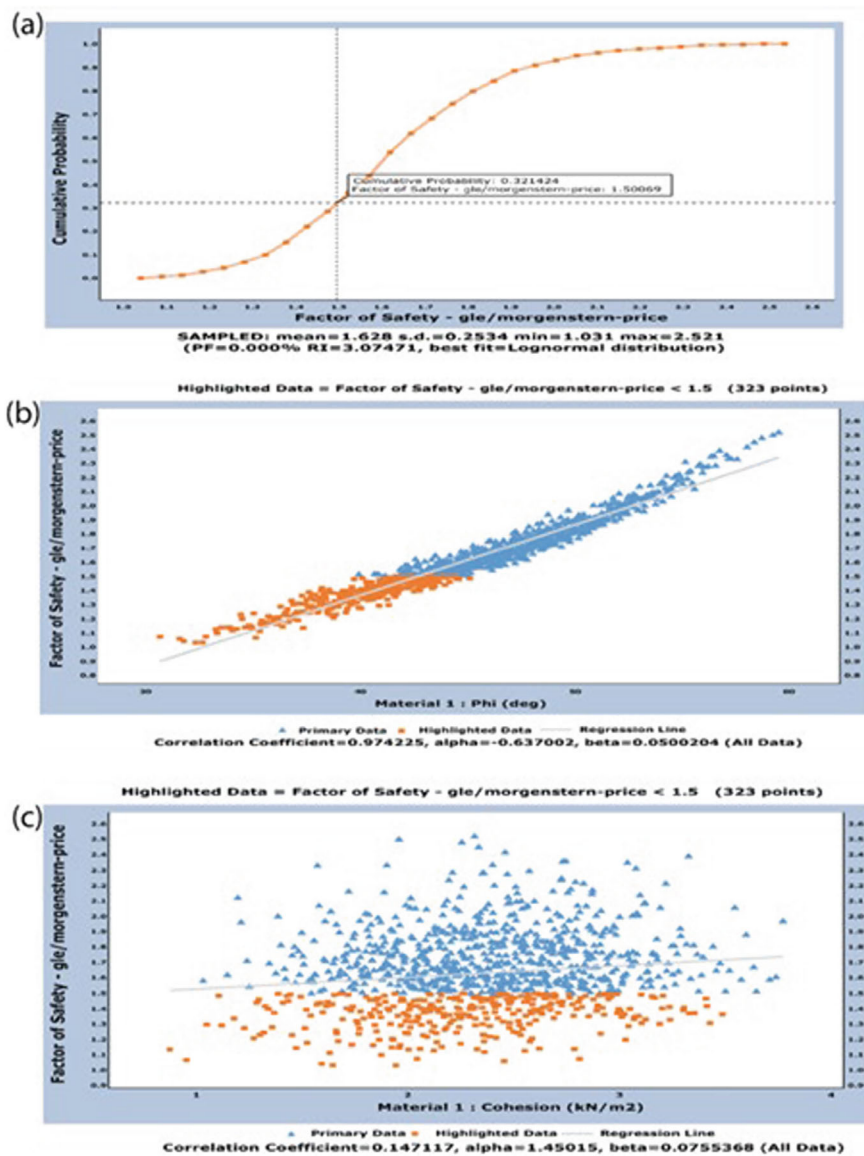


Fig. 8 Histogram plots of **a** FOS (MP) versus relative frequency **b** cohesion versus relative frequency **c** phi versus relative frequency for AOCP-2



**Fig. 9** (a) Cumulative plot of safety factor (b) scatter plot—friction angle versus FOS (c) scatter plot—FOS versus Cohesion for AOCP-2

- Consideration of extreme climate events such as torrential rainfall for designing internal as well as external dump slopes.

## 5 Conclusions

Dump slope failures represent a significant challenge for the mining industry, posing threats to both human life and the environment. Over the past two decades, several high-profile incidents have highlighted the urgent need for comprehensive risk management strategies and regulatory oversight. By implementing proactive measures such as improved waste management practices, enhanced monitoring systems, and strict regulatory frameworks, the mining industry can mitigate the risk of dump slope failures and ensure sustainable and responsible mining practices for the future. The stability investigation of AOCP-1 indicates instability under saturated conditions, with a mean factor of safety of 0.958 using the LEM technique. This corresponds to a 63.4% probability of failure and a reliability index of  $-0.375$ , suggesting that the current slope design is poor and unsafe given the existing physico-mechanical conditions. In contrast, the simulated stability condition of AOCP-2 suggests a stable dump with a mean FOS of 1.602. The analysis reveals that compressive positive inter-slice forces dominate within the sliding mass, resulting in a higher and safer FOS despite the presence of unconsolidated dump mass. To improve dump stability and enhance safety, several practices can be unitized such as geosynthetic liners and engineered structures for effective dump containment along with employing advanced monitoring systems.

**Acknowledgements** The authors would like to thank the management of Mahanadi Coalfields Limited (MCL), India and the officials of Ananta Opencast Mine, Odisha for their cooperation and support during the fieldwork. The authors are grateful to Rock Science and Rock Engineering Laboratory at IIT Bombay for geotechnical analysis.

The authors declare that they have no known competing financial interests or personal relationships that could have appeared to influence the work reported in this paper.

## References

- Abramson LW, Lee TT, Sharma S, Boyce GM (2002) Slope stability concepts. In: Slope stabilisation and stabilisation methods, 2nd edn. Wiley, New York
- Behera PK, Sarkar K, Singh AK, Verma AK, Singh TN (2016) Dump slope stability analysis—a case study. *J Geol Soc India* 88(6):725–735
- Behera PK (2018) Dump slope stability analysis of open cast mines in Talcher Coal Field, Angul District, Odisha. PhD Thesis (Unpublished), IIT(ISM) Dhanbad
- Dash AK (2019) Analysis of accidents due to slope failure in Indian opencast coal mines. *Curr Sci* 117:304–308. <https://doi.org/10.18520/cs/v117/i2/304-308>
- Gupta T, Rai R, Jaiswal A, Shrivastva BK (2014) Sensitivity analysis of coal rib stability for internal mine dump in opencast mine by finite element modelling. *Geotech Geol Eng* 32(3):705–712

- Kainthola A, Verma D, Gupte SS, Singh TN (2011) A coal mines dump stability analysis—a case study. *Geomaterial* 01(01):1–13
- Kasmer O, Ulusay R, Gokceoglu C (2006) Spoil pile instabilities with reference to a strip coal mine in Turkey: mechanisms and assessment of deformations. *Environ Geol* 49:570–585. <https://doi.org/10.1007/s00254-005-0092-1>
- Kumar A, Das SK, Nainegali L, Raviteja KVNS, Reddy KR (2023) Probabilistic slope stability analysis of coal mine waste rock dump. *Geotech Geol Eng* 41:4707–4724
- Li L, Wang Y, Cao Z (2014) Probabilistic slope stability analysis by risk aggregation. *Eng Geol* 176:57–65
- Liu Y, Zhang W, Zhang L, Zhu Z, Hu J, Wei H (2018) Probabilistic stability analyses of undrained slopes by 3D random fields and finite element methods. *Geosci Front* 9:1657–1664
- Manjrekar VD, Choudhury V, Gautam KVV (2006) Coal, geology and mineral resources of Orissa. In: Mahalik NK (ed) *Society of geoscientists and allied technologist*, Bhubaneswar, pp 205–226
- Mohanty M, Sarkar R, Das SK (2022) Probabilistic assessment of effects of heterogeneity on the stability of coal mine overburden dump slopes through discrete element framework. *Bull Eng Geol Environ* 81(6):1–28. <https://doi.org/10.1007/s10064-022-02720-0>
- Nayak PK, Dash AK, Dewangan P (2020) Design considerations for waste dumps in Indian opencast coal mines—a critical appraisal. In: *Proceedings of 2nd international conference on opencast mining technology and sustainability*, pp 19–31
- Orendorf B (2009) An experimental study of embankment dam breaching. Doctoral dissertation, University of Ottawa, Canada
- Poulsen B, Khanal M, Rao AM, Adhikary D, Balusu R (2014) Mine overburden dump failure: a case study. *Geotech Geol Eng* 32(2):297–309
- Rai R, Khandelwal M, Jaiswal A (2012) Application of geogrids in waste dump stability: a numerical modelling approach. *Environ Earth Sci* 66(5):1459–1465
- Singh RS (2000) Revegetation of coal mine overburden dump (OBD) slopes by aromatic grasses. *J Med Aromat Plant Sci* 22(1):506–509
- Speck RC, Huang SL, Kroeger EB (1993) Large-scale slope movements and their effect on spoil-pile stability in interior Alaska. *Int J Surf Min Reclam* 7(4):161–166
- Vanneschi C, Eyre M, Burda J, Žižka L, Francioni M, Coggan JS (2018) Investigation of landslide failure mechanisms adjacent to lignite mining operations in North Bohemia (Czech Republic) through a limit equilibrium/finite element modelling approach. *Geomorph*. <https://doi.org/10.1016/j.geomorph.2018.08.006>
- Zeng P, Jimenez R, Jurado-piña R (2015) System reliability analysis of layered soil slopes using fully specified slip surfaces and genetic algorithms. *Eng Geol* 193:106–117

# **Machine Learning Methods for Landslide and Slope Stability Prediction**



# An Emerging Machine Learning Approach for Predicting Risk and Stability on Susceptible Terrain



Sanjay Singh, Amit Kumar Verma, and Jayraj Singh

**Abstract** Landslides and slope failures are extremely unfavourable occurrences that frequently have disastrous results in many countries. The accurate prediction of slope instability is a crucial concern in geotechnical engineering. However, forecasting the instability of slopes in collapse-prone areas presents considerable challenges due to the involvement of numerous physical and geometric variables. To address this, various artificial intelligence (AI) and machine learning techniques have been employed, although their full potential has yet to be realized due to the limitations of existing algorithms. In this research, we propose an efficient machine learning approach using the Random Forest model, specifically tailored to solve the nonlinear problem discussed. We conducted an investigation, focusing on 221 cases of slopes, to assess the risk and identify its susceptibility. Our analysis revealed that the present machine model outperformed other empirical investigations in terms of the accuracy of the stability prediction. The research can aid professionals in construction and disaster management authorities by swiftly assessing slope stability for site selection in infrastructure projects. This contributes to environmental planning by supplying data for impact assessments and ensuring the safety of vital infrastructure through monitoring adjacent slopes along roads, railways, and pipelines.

**Keywords** Artificial intelligence · Machine learning techniques · Slope stability analysis · Landslides

---

S. Singh (✉) · A. K. Verma

Department of Civil and Environmental Engineering, Indian Institute of Technology, Patna, India  
e-mail: [Singh.sanjay343@gmail.com](mailto:Singh.sanjay343@gmail.com)

J. Singh

CAIRO, Universiti Teknologi Malaysia, Kuala Lumpur, Malaysia

NIIT University, Neemrana, Rajasthan, India

# 1 Introduction

Slope stability analysis is a critical aspect of geotechnical engineering, particularly due to the prevalence of slope failure caused by natural hazards like floods, landslides, and anthropogenic activities (Abramson et al. 2001; Fredlund and Krahn 1977). These occurrences often result in significant damage to public property, the environment, and society. Hence, there is a pressing need for researchers, scientists, and engineers to focus on minimizing and mitigating the risks associated with such events. However, predicting the stability of slopes in collapse-prone areas is exceptionally challenging due to the presence of ambiguous and fluctuating physical and geometric variables (Sah et al. 1994). To address this challenge, engineers have employed various analytical techniques, such as limit equilibrium, limit analysis, and numerical techniques such as finite element, and finite difference. Among these methods, the limit equilibrium approach is commonly used for its efficiency in evaluating slope stability by identifying the critical slip surface associated with the lowest factor of safety value (Sah et al. 1994). The factor of safety (FoS) plays a crucial role in determining slope stability, considering parameters such as slope height, unit weight, internal friction angle, cohesion, slope angle, and pore water pressure. However, determining the critical slip surface can be complex, often involving multi-modal and highly constrained optimization problems (Madani-Isfahani et al. 2014).

To tackle these challenges, researchers have explored stochastic global optimization and simulation-based machine learning techniques, such as dynamic programming, simplex methods, genetic algorithms, particle swarm optimization, and others (Madani-Isfahani et al. 2014; Qi and Tang 2018; Khajehzadeh et al. 2014; Kashani et al. 2016; Singh et al. 2018, 2019a; Pasik and Meij 2017). These methods provide a fast and reliable results despite inherent incompleteness and nonlinearity of various geotechnical parameters. Additionally, there is growing interest in employing machine learning and artificial intelligence (AI) techniques to enhance fault detection and deformation analysis in geotechnical science (Kashani et al. 2016; Singh et al. 2018, 2019a, 2019b; Pasik and Meij 2017; Baker 1980; Bellman 1966; Nguyen 1985; Liu et al. 2021; Chen and Shao 1988; Deng et al. 2021; Nelder and Mead 1965; Bardet and Kapuskar 1989; Greco and Gulla 1985). For instance, studies have utilized artificial neural networks (ANNs), support vector machines (SVMs), and other ML algorithms to assess slope stability and analyse the nonlinear relationship between stability and influencing factors (McCombie and Wilkinson 2002; Bolton et al. 2003; Cheng 2003; Pham and Fredlund 2003; Zolfaghari et al. 2005). However, despite their potential, ML and AI techniques have limitations, including high computational costs, the need for extensive data, and challenges in determining appropriate parameters and architecture (Cheng et al. 2007; Wang and Goh 2021; Li et al. 2022; Liu et al. 2014). Nonetheless, these techniques provide valuable empirical and statistical insights into slope stability analysis, paving the way for more precise and efficient results. In this context, this study aims to comprehensively analyse slope stability using supervised machine learning techniques, specifically focusing on the

**Table 1** Information about the notations

	Terminology		
FoS	Factor of safety	$\theta$	Interslice forces of slice's inclination angle
H	Height (in meter)	$\gamma$	Unit weight (density) of material ( $\text{kN/m}^3$ )
ru	Pore water ratio	$\Phi$	Internal friction angle (in degree)
C	Cohesion (kPa)	$\beta$	Angle of slope (in degree)
PoF	Probability of failure	MAE	Maximum absolute error
DT	Decision tree	ML	Machine learning
RF	Random forest	MLP	Multilayer perceptron
F	Failure	RMSE	Root mean square error
S	Stable	LEM	Limit equilibrium method
$\mu$	Mean	R	Correlation coefficient
CoV	Coefficient of variation	StdDev	Standard deviation

Fellenius method for computing the factor of safety through the limit equilibrium procedure. The simulation design is facilitated by SLIDE, a Rocscience engineering software tool, known for its user-friendly interface and diverse analytical methods for slope analysis and modeling (Zhao et al. 2012).

## 2 Preliminary Notation

The definitions of certain notations, variables, and acronyms from Table 1 are provided in this section. These notations are related to several terminologies that were utilised in the research.

## 3 Dataset and Its Preliminary Analysis

In this study, there are 221 distinct slope records were considered in the dataset. Sixty locations were used to gather the actual slope records, which include 106 failure slope cases and 115 stable slope cases between 1994 and 2011 (Wang and Goh 2021; RocScience 2002; Zhou et al. 2019; Lu and Rosenbaum 2003; Wang et al. 2005; Das et al. 2011; Hoang and Pham 2016; Tien Bui et al. 2019; Xu and Shao 1998; Liangxing et al. 2004). In line with previous research, the circular mode of failure has been modeled here using the six input parameters (RocScience 2002). Examples of parameters that may include slope height (H), unit weight ( $\gamma$ ), internal friction angle ( $\Phi$ ), cohesion (C), slope angle ( $\beta$ ), and coefficient of pore water pressure (ru). These parameters are depicted using a box diagram in Fig. 1 and often dictate the conditions for slope failure.

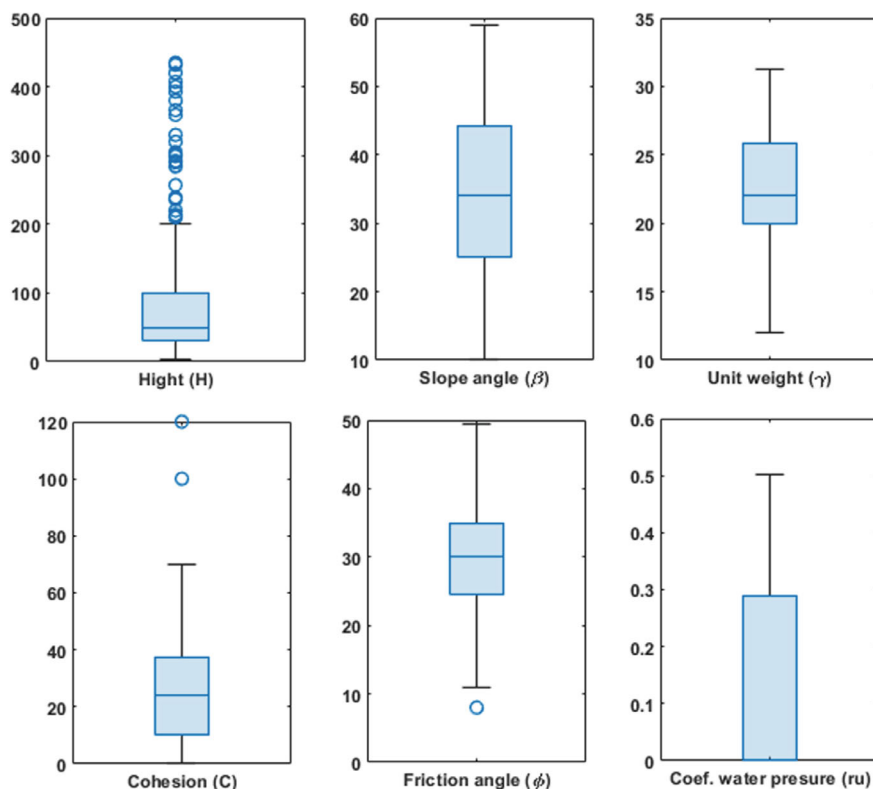


**Fig. 1** Box plots for each variable for slope cases

As can be seen from Fig. 1, most of these parameter medians (with the exception of  $ru$  and cohesion) are not centred, indicating that the parameter distribution for the data is not symmetrical. The correlation between all the parameters is shown in Table 2.

Besides, all input features aside from  $\phi$  and  $\beta$  have several outliers. The machine learning algorithms mentioned above can be greatly impacted by outliers, which are data points with exceptionally small or large values. Even a few outliers can have a significant impact on the model's performance. Several of these outliers are found in conditions like soil slopes, rock slopes with great cohesiveness, and heavily weathered soil that resembles rock, according to studies like (Liu et al. 2014; Li et al. 2006; Chen et al. 2009). A model's prediction performance can be improved by lowering these outliers. Here, the statistical procedure known as the "Z-score" was used to determine the range of variation for the values in the dataset (Feng and Hudson 2004), detect outliers, and minimize them.

**Table 2** Correlation table in consolidated samples

	H	$\beta$	$\gamma$	C	$\Phi$	Ru	Stability value
H	1						
$\beta$	0.282866						
$\gamma$	0.440632	0.343057	1				
C	0.187849	0.395454	0.442552	1			
$\Phi$	0.244352	0.423646	0.464835	0.263419	1		
Ru	− 0.04002	0.006645	− 0.15890	− 0.10753	0.010046	1	
Stability value	0.16280	0.053654	0.368935	0.136613	0.344961	0.001331	1

```
Algorithm 1: Pseudo-code for Z-Score algorithm for outliers reduction
begin Z-Score
  Check no missing values for parameters in data set;
  Set N = No of parameters,;
  Set StdDev = 3 (i.e., data point is deviated more than 3 StdDev);
  for i = 1 to N do
    X = Parameter(i), K = length(X);
    Find  $\mu$  = Mean (X), and  $\sigma$  = StdDev (X);
     $Z_{score} = (X - \mu) / \sigma$ ;
    Consider Output, Temp as a temporal variables array;
    if ( $Z(i) \leq \text{StdDev}$ ) && ( $Z(i) \geq -\text{StdDev}$ ) then
      Output(i) = X(i);
      Temp(i) = 0; (i.e., It reflects, the data point is not an outlier)
    end
    else
      Temp(i) = 1; (i.e., It reflects, the data point is an outlier)
    end
    Results = Output(i);
  end
end
```

The approach described above can be used to determine how distant a data value is from the mean and if it is significant than the mean. The Z-score, for instance, shows how much a data point deviates from the mean in terms of standard deviations. An algorithm 1 is presented to illustrate the procedural steps of the mentioned method through pseudo-code. Using this approach, 21 cases with values outside the range of the data were identified and removed, resulting in the elimination of outliers from the dataset. The remaining dataset comprised of only 200 cases for analysis.

Figure 2 through histograms illustrates the statistical features (mean, standard deviation, maximum and minimum) of the variables in the dataset. Typically, a machine learning model uses data interpolation to make predictions about a variable or variables, and performs better when the training data has a wider range of variation. Therefore, it is important to establish a valid range for independent variables. The dataset discussed in Zhou et al. (2009) shows that, apart from “ru” and “cohesion,” the medians of most parameters are not centrally located, indicating that the data’s parameter distribution is not symmetrical. To enhance algorithm performance, it is important to identify relevant features in the dataset and discard redundant ones (Bolon-Canedo et al. 2011).

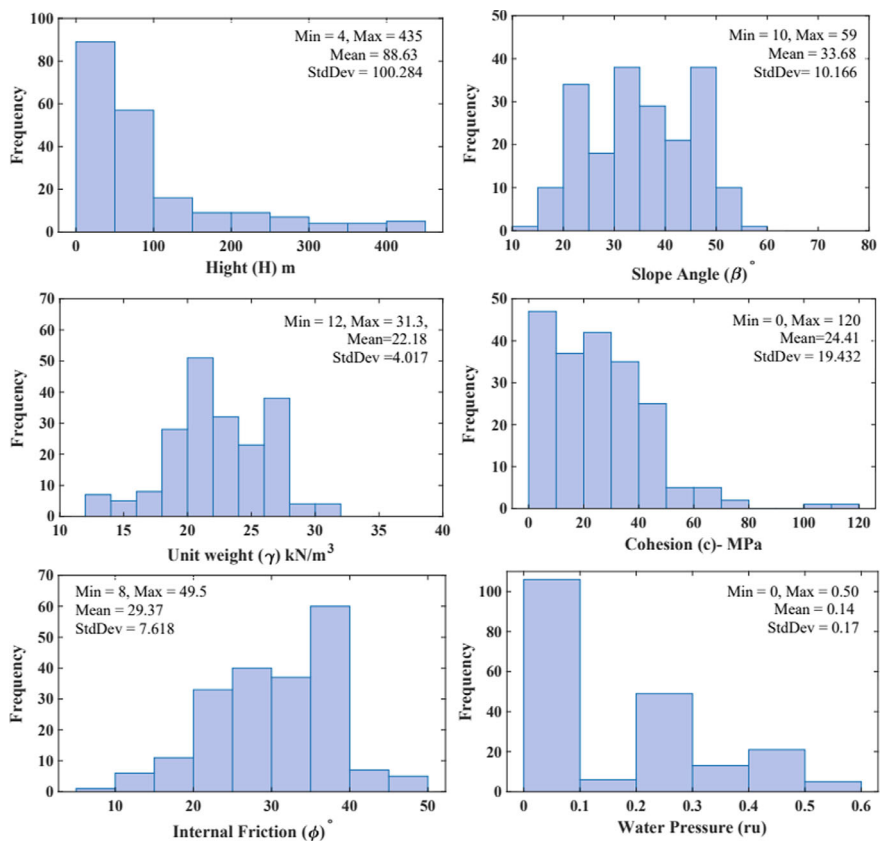


Fig. 2 The visualization of a dataset after the removal of outliers

## 4 Adaptation of the Machine Learning Methods

Predicting slope stability poses a significant challenge due to numerous uncertain factors. Currently, many engineers rely on machine learning (ML) methods that are familiar to them for slope stability assessment, as evidenced by various studies. In this research, an enhanced supervised method known as Random Forest (RF) is employed to efficiently predict slope stability. The initial step involves constructing a predictive classifier to analyse multivariate data related to circular mode slope failures. Four distinct supervised approaches Multilayer perceptron (MLP), Decision tree (DT), AdaBoost, and Random Forest are examined to compare and validate their effectiveness. These techniques are gaining popularity due to their simplicity, effectiveness, and ability to model complex nonlinear interactions. Table 3 provides a concise overview of these algorithms, with further details available in the relevant references. Despite near performance observed among the approaches (MLP, decision tree, and random forest) when applied to the slope stability dataset, the Random Forest exhibits higher prediction accuracy, achieving approximately 97%, compared to 92 and 76% for MLP and Decision tree, respectively. Moreover, the Random Forest method is preferred for its simplicity, versatility, and capability to handle large datasets, high percentages of missing data, and potential overfitting issues. Additionally, consistent with prior research, the Random Forest (RF) method emerged as a more effective approach for multivariate classification tasks. This method combines an instance filter-resample technique with an attribute evaluator, resulting in superior classification accuracy. Its adaptability and user-friendliness contribute to enhanced performance in generating classification outcomes (Zhou et al. 2019; Lu and Rosenbaum 2003; Wang et al. 2005; Das et al. 2011; Hoang and Pham 2016; Tien Bui et al. 2019; Xu and Shao 1998; Liangxing et al. 2004; Li et al. 2006; Chen et al. 2009; Feng and Hudson 2004; He et al. 2004; Bolon-Canedo et al. 2011; Zhang et al. 2014). Therefore, the Random Forest algorithm was chosen for this study based on these considerations. Details regarding the materials and methods employed are described in the following section.

## 5 Materials and Methods

Typically, a machine learning model relies on data interpolation to make predictions. To enhance prediction performance, the dataset was partitioned, considering statistical considerations such as mean, coefficient of variation, and standard deviation for both training and testing datasets. Specifically, for a slope stability classifier, input parameters including height, cohesion, unit weight, pore water pressure, slope angle, and internal friction angle were defined, with the output indicating the slope stability state (Stable or Failed). The study's workflow is depicted in Fig. 3.



**Table 3** A concise explanation of four supervised machine learning methods

ML methods	Definition
MLP	A multilayer perceptron (MLP) is a type of neural network that is utilized to construct a linear algorithm. To form complex resolution boundaries, an MLP comprises three or more layers: an input layer, a hidden layer, and an output layer (Lu and Rosenbaum 2003; Wang et al. 2005; Das et al. 2011; Hoang and Pham 2016; Tien Bui et al. 2019; Xu and Shao 1998; Liangxing et al. 2004; Li et al. 2006; Chen et al. 2009; Feng and Hudson 2004)
J48-decision tree	Implemented in Java, J48 is a method for constructing decision trees in a top-down manner. It employs the C4.5 algorithms, which is a successor of iterative dichotomize 3. By selecting the most informative attribute or one with the least entropy, J48 adopts a greedy approach (Hoang and Pham 2016; Lin et al. 2018; Manouchehrian et al. 2014; Singh and Banka 2021; Hornyák and Iantovics 2023; Ibrahim et al. 2012; Zift 2011; Breiman 2001)
RF	Random forest is an algorithm that creates a “forest” of decision trees through bootstrapping. To grow the trees, RF introduces randomness. Therefore, it only considers a random subset of the features (Pham et al. 2021; Tanyu et al. 2021; Sirikulviriya and Sinthupinyo 2011)
AdaBoost	Adaptive boosting, is a supervised ensemble machine learning algorithm that can be used in a wide variety of classification tasks. AdaBoost classify data by combining multiple weak or base learners (e.g., decision trees) into a strong learner. It works by weighting the instances in the training dataset based on the accuracy of previous classifications (Hornyák and Iantovics 2023; Ibrahim et al. 2012)

To ensure dataset integrity, the Z-score method was utilized to detect and eliminate outliers, while also evaluating the dataset’s variance–covariance structure. Subsequently, the dataset was split into training and testing subsets, with 80% allocated to training and 20% to testing. Notably, the number of stable instances far exceeded that of failure cases in both sets, indicating class imbalances within the dataset. Performance evaluation of the models involved metrics such as precision, accuracy, AUC, F-measure, and recall. The results, presented in Table 5, demonstrated that the Random Forest (RF) model exhibited superior performance compared to other models, achieving success rates of 98% in the training dataset and 97% in the testing dataset.

## 6 Results and Discussion

### 6.1 Calculations of R, RMSE, and MAE

The correlation coefficient and root-mean-square error (R & RMSE) values are used to evaluate the ability of the model to generalize, and they have been calculated for both the training and testing datasets. Similar experiments were conducted to

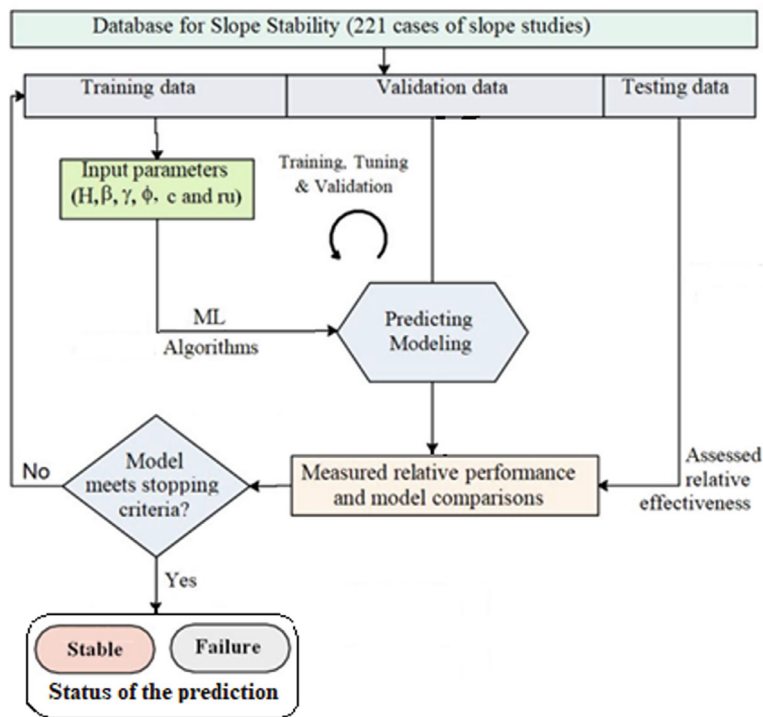


**Fig. 3** A flowchart depiction for the overall procedure to assess slope stability

evaluate the performance of the MLP, DT-J48, AdaBoost, and RF models. The results are shown in Table 4. The training data was used to calculate the maximum absolute error (MAE) for MLP, J48, AdaBoost and RF, which was found to be 0.192, 0.218, 0.176, and 0.172, respectively.

Similarly, the MAE values for the testing data were calculated and found to be 0.119, 0.226, 0.192, and 0.127, respectively. The performance of the models can also be evaluated using RMSE, which was calculated to be 0.304, 0.399, 0.431, and 0.392 for MLP, DT, AdaBoost, and RF, respectively, for the training data. Also, the testing data’s RMSE values were noted and found to be 0.266, 0.437, 0.303, and 0.342,

**Table 4** Comparison of ML-algorithms for classification of slope

Algorithms	Correlation coefficient		Root mean square error (RMSE)	
	Training	Testing	Training	Testing
MLP	0.775	0.797	0.304	0.266
DT	0.613	0.595	0.399	0.437
AdaBoost	0.975	0.950	0.431	0.303
RF	0.651	0.902	0.392	0.342

**Table 5** Performance comparison of different machine learning models

ML algorithms	Data set	Failure			Stable			AUC	Accuracy (%)
		Precision	Recall	F-measure	Precision	Recall	F-measure		
MLP	Training	0.869	0.913	0.890	0.908	0.863	0.885	0.935	88.75
	Testing	0.889	0.889	0.889	0.909	0.909	0.909	0.935	90.00
Decision tree	Training	0.928	0.955	0.941	0.967	0.946	0.957	0.868	80.62
	Testing	0.778	0.778	0.778	0.818	0.818	0.818	0.800	80.00
Adaboost	Training	0.802	0.863	0.831	0.851	0.788	0.818	0.982	95.00
	Testing	1.000	0.947	0.973	0.955	1.000	0.977	0.980	97.50
RF (Random Forest)	Training	0.976	1.000	0.988	1.000	0.975	0.987	0.985	98.75
	Testing	1.000	0.944	0.971	0.957	1.000	0.978	0.980	97.50

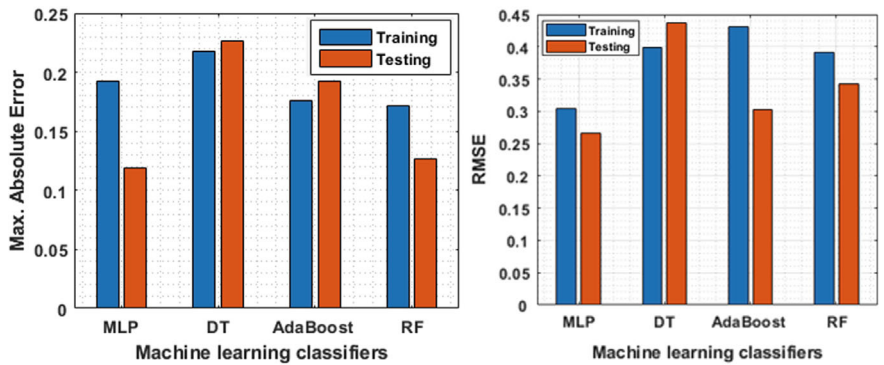


Fig. 4 MAE and RMSE comparison across training and test data

respectively. The results presented in Fig. 4 show that the RF model outperforms the presented models in terms of producing better quality solutions with lower MAE and RMSE faults.

6.2 Performance Measures of Machine Learning Models

Several statistical measures, including accuracy, recall, precision, and F-measure, were used to evaluate the effectiveness of the classification models. To compute these measures, a confusion matrix was utilized as it provides an accurate evaluation of different methods in various ways. As discussed in the previous section, the accuracy rates of almost 90, 80, 97, and 97%, the DT, MLP, AdaBoost, and RF algorithms correctly detected stable and failure cases in the testing dataset. Like this, the models accurately categorized occurrences in the training dataset with success rates of 88%, 80%, 95%, and 98%, respectively. To further illustrate the superiority of the models, Cohen’s Kappa coefficient (Kappa) and mean absolute error (M error) were computed.

The RF model had the highest precision, F-measure, and recall values in both the datasets used for training and testing for these domains. Overall, the RF model outperformed other ML models according to the analysis of the five performance factors. The ROC plot presented in Fig. 5 shows the prediction rates. Furthermore, the RF model showed remarkable performance that is quite acceptable for predicting stability of slope, according to the kappa and F1-score. Therefore, based on the results finding, it is claimed here that, the RF-classification model had a better overall performance than the other three methods (Table 5).

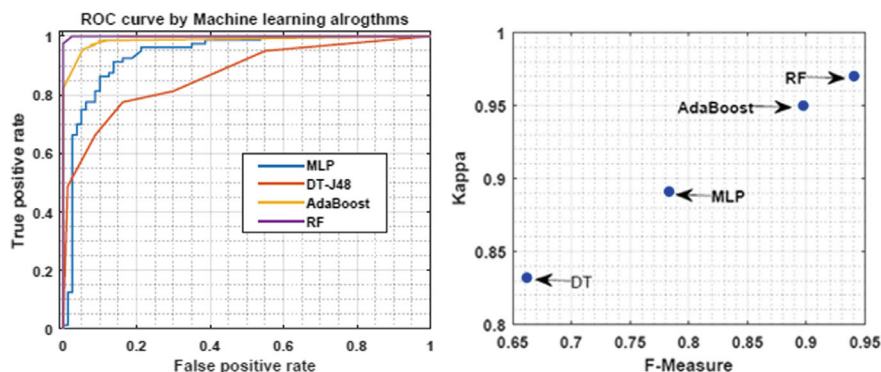


Fig. 5 ROC curve for ML-classifiers and kappa versus F-measure graph on the test set

## 7 Conclusions

This paper focuses on utilizing advanced machine learning techniques to evaluate slope stability. To achieve this, historical data from 221 cases of slope stability sourced from existing literature were utilized to construct a classification model, incorporating input parameters representing material behaviour and slope geometry. Machine learning models underwent training and testing using a dataset comprising 200 cases, with an 80–20% split ratio. The machine learning algorithms' parameters were fine-tuned to minimize absolute error. The resulting model can be employed further to assess the likelihood of slope failure in scenarios where geotechnical parameters such as cohesion and friction-angle are uncertain. Performance metrics including accuracy, precision, recall, and F-measure indicated that the advanced random forest model exhibited statistical significance and surpassed alternative methods. The study offers recommendations for researchers regarding the selection of appropriate machine learning algorithms and the enhancement of predictive capabilities.

## References

- Abramson LW, Thomas SL, Sharma S, Boyce GM (2001) Slope stability and stabilization methods. Wiley, United States
- Baker R (1980) Determination of the critical slip surface in slope stability computations. *Int J Numer Anal Methods Geomech* 4(4):333–359
- Bardet JP, Kapuskar MM (1989) A simplex analysis of slope stability. *Comput Geotech* 8(4):329–348
- Bellman R (1966) Dynamic programming. *Sci Am Assoc Adv Sci* 153(3731):34–37
- Bolon-Canedo V, Sanchez-Marono N, Alonso-Betanzos A (2011) Feature selection and classification in multiple class datasets: an application to KDD Cup 99 dataset. *Expert Syst Appl* 38(5):5947–5957

- Bolton H, Heymann G, Groenwold A (2003) Global search for critical failure surface in slope stability analysis. *Eng Optim* 35(1):51–65
- Breiman L (2001) Random forests. *Mach Learn* 45(1):5–32
- Chen LQ, Peng ZB, Chen W, Peng WX, Wu QH (2009) Artificial neural network simulation on prediction of clay slope stability based on fuzzy controller. *J Central South Univ (Sci Technol)* 40:05
- Chen Z-Y, Shao C-M (1988) Evaluation of minimum factor of safety in slope stability analysis. *Can Geotech J* 25(4):735–748
- Cheng YM (2003) Location of critical failure surface and some further studies on slope stability analysis. *Comput Geotech* 30(3):255–267
- Cheng YM, Li L, Chi SC (2007) Performance studies on six heuristic global optimization methods in the location of critical slip surface. *Comput Geotech* 34(6):462–484
- Das SK, Biswal RK, Sivakugan N, Das B (2011) Classification of slopes and prediction of factor of safety using differential evolution neural networks. *Environ Earth Sci* 64(1):201–210
- Deng L, Smith A, Dixon N, Yuan H (2021) Machine learning prediction of landslide deformation behaviour using acoustic emission and rainfall measurements. *Eng Geol* 293:106315
- Feng XT, Hudson JA (2004) The ways ahead for rock engineering design methodologies. *Int J Rock Mech Min Sci* 41(2):255–273
- Fredlund DG, Krahn J (1977) Comparison of slope stability methods of analysis. *Can Geotech J* 14(3):429–439
- Greco VR, Gulla G (1985) Slip surface search in slope stability analysis. *Riv Ital Geotec* 19(4):189–198
- He F, Wu S, Zhang Y, Bao H (2004) A neural network method for analyzing compass slope stability of the highway. *Acta Geoscientia Sinica* 25(1; ISSU 80):95–98
- Hoang ND, Pham AD (2016) Hybrid artificial intelligence approach based on metaheuristic and machine learning for slope stability assessment: a multinational data analysis. *Expert Syst Appl* 46:60–68
- Hornýák O, Iantovics LB (2023) AdaBoost algorithm could lead to weak results for data with certain characteristics. *Mathematics* 11(8):1801
- Ibrahim HE, Badr SM, Shaheen MA (2012) Adaptive layered approach using machine learning techniques with gain ratio for intrusion detection systems. *arXiv preprint [arXiv:1210.7650](https://arxiv.org/abs/1210.7650)*
- Jin L, Feng W, Zhang J (2004) Maximum likelihood estimation on safety coefficients of rocky slope near dam of Fengtan project. *Chin J Rock Mech Eng* 11
- Kashani AR, Gandomi AH, Mousavi M (2016) Imperialistic competitive algorithm: a metaheuristic algorithm for locating the critical slip surface in 2-dimensional soil slopes. *Geosci Front* 7(1):83–89
- Khajehzadeh M, Taha MR, El-Shafie A, Eslami M (2014) Stability assessment of earth slope using modified particle swarm optimization. *J Chin Inst Eng* 37(1):79–87
- Li Y, Rahardjo H, Satyanaga A, Rangarajan S, Lee DTT (2022) Soil database development with the application of machine learning methods in soil properties prediction. *Eng Geol* 306:106769
- Li WX, Yang SC, Chen EZ, Qiao JL, Dai LF (2006) Neural network method of analysis of natural slope failure due to underground mining in mountainous areas. *Yantu Lixue (Rock Soil Mech)* 27(9):1563–1566
- Lin Y, Zhou K, Li J (2018) Prediction of slope stability using four supervised learning methods. *IEEE Access* 6:31169–31179
- Liu Z, Shao J, Xu W, Chen H, Zhang Y (2014) An extreme learning machine approach for slope stability evaluation and prediction. *Nat Hazards* 73(2):787–804
- Liu Z, Gilbert G, Cepeda JM, Lysdahl AOK, Piciullo L, Hefre H, Lacasse S (2021) Modelling of shallow landslides with machine learning algorithms. *Geosci Front* 12(1):385–393
- Lu P, Rosenbaum MS (2003) Artificial neural networks and grey systems for the prediction of slope stability. *Nat Hazards* 30(3):383–398
- Madani-Isfahani M, Tavakkoli-Moghaddam R, Naderi B (2014) Multiple cross-docks scheduling using two meta-heuristic algorithms. *Comput Ind Eng* 74:129–138

- Manouchehrian A, Gholamnejad J, Sharifzadeh M (2014) Development of a model for analysis of slope stability for circular mode failure using genetic algorithm. *Environ Earth Sci* 71(3):1267–1277
- McCombie P, Wilkinson P (2002) The use of the simple genetic algorithm in finding the critical factor of safety in slope stability analysis. *Comput Geotech* 29(8):699–714
- Nelder JA, Mead R (1965) A simplex method for function minimization. *Comput J* 7(4):308–313
- Nguyen VU (1985) Determination of critical slope failure surfaces. *J Geotech Eng Am Soc Civ Eng* 111(2):238–250
- Pasik T, van der Meij R (2017) Locating critical circular and unconstrained failure surface in slope stability analysis with tailored genetic algorithm. *Stud Geotech Mech* 39(4)
- Pham K, Kim D, Park S, Choi H (2021) Ensemble learning-based classification models for slope stability analysis. *CATENA* 196:104886
- Pham HTV, Fredlund DG (2003) The application of dynamic programming to slope stability analysis. *Can Geotech J* 40(4):830–847
- Qi C, Tang X (2018) Slope stability prediction using integrated metaheuristic and machine learning approaches: a comparative study. *Comput Ind Eng* 118:112–122
- RocScience (2002) 2D limit equilibrium slope stability for soil and rock slopes: sample problems. [https://www.rocsience.com/documents/pdfs/education/Slide\\_Problem\\_Sets](https://www.rocsience.com/documents/pdfs/education/Slide_Problem_Sets). Accessed on 14 Apr 2020
- Sah NK, Sheorey PR, Upadhyaya LN (1994) Maximum likelihood estimation of slope stability. *Int J Rock Mech Min Sci Geo Abstr* 31(1):47–53
- Singh J, Banka H (2021) A meta-heuristic based approach for slope stability analysis to design an optimal soil slope. In: *Machine learning algorithms for industrial applications*, pp 195–207
- Singh J, Verma AK, Banka H (2018) A comparative study for locating critical failure surface in slope stability analysis via meta-heuristic approach. In: *Handbook of research on predictive modeling and optimization methods in science and engineering*. IGI Global, pp 1–18
- Singh J, Banka H, Verma AK (2019a) A BBO-based algorithm for slope stability analysis by locating critical failure surface. *Neural Comput Appl* 31(10):6401–6418
- Singh J, Banka H, Verma AK (2019b) Locating critical failure surface using meta-heuristic approaches: a comparative assessment. *Arab J Geosci* 12:1–20
- Sirikulviriyi N, Sinthupinyo S (2011) Integration of rules from a random forest. In: *International conference on information and electronics engineering*, vol 6, pp 194–198
- Tanyu BF, Abbaspour A, Alimohammadlou Y, Tecuci G (2021) Landslide susceptibility analyses using random forest, C4.5 and C5.0 with balanced and unbalanced datasets. *CATENA* 203:105355
- Tien Bui D, Moayedi H, Gr M, Jaafari A, Foong LK (2019) Predicting slope stability failure through machine learning paradigms. *ISPRS Int J Geo-Inf* 8(9):395
- Wang ZZ, Goh SH (2021) Novel approach to efficient slope reliability analysis in spatially variable soils. *Eng Geol* 281:105989
- Wang HB, Xu WY, Xu RC (2005) Slope stability evaluation using back propagation neural networks. *Eng Geol* 80(3–4):302–315
- Xu W, Shao JF (1998) Artificial neural network analysis for the evaluation of slope stability. In: *Application of numerical methods to geotechnical problems*. Springer, Vienna, pp 665–672
- Zhang Z, Liu Z, Zheng L, Zhang Y (2014) Development of an adaptive relevance vector machine approach for slope stability inference. *Neural Comput Appl* 25(7):2025–2035
- Zhao H, Yin S, Ru Z (2012) Relevance vector machine applied to slope stability analysis. *Int J Numer Anal Meth Geomech* 36(5):643–652
- Zhou J, Li E, Yang S, Wang M, Shi X, Yao S, Mitri HS (2019) Slope stability prediction for circular mode failure using gradient boosting machine approach based on an updated database of case histories. *Saf Sci* 118:505–518



- Zift A (2011) Random forests ensemble classifier trained with data resampling strategy to improve cardiac arrhythmia diagnosis. *Comput Biol Med* 41(5):265–271
- Zolfaghari AR, Heath AC, McCombie PF (2005) Simple genetic algorithm search for critical non-circular failure surface in slope stability analysis. *Comput Geotech* 32(3):139–152

# Comparative Assessment of XGBoost Model and Hyper-Parameter Optimization Techniques in Landslide Susceptibility Mapping—A Case Study of Aglar Watershed, Part of Lesser Himalaya



Dipika Keshri, Kripamoy Sarkar, and Shovan Lal Chattoraj

**Abstract** Aglar watershed, located in the Tehri-Garhwal district of Uttarakhand, is a part of Lesser Himalaya. The diverse geography, highly rugged topography, and continuously changing climatic conditions make the Himalayan region landslide-prone. In the Aglar watershed, landslides occur frequently due to various geological, anthropogenic, and vegetation factors. Reducing landslide risk requires an accurate assessment of landslide susceptibility through mapping. This paper delves into Extreme Gradient Boosting (XGBoost), a well-known machine-learning algorithm for landslide Predictive Modeling. In addition, XGBoost is an ensemble learning algorithm that combines numerous weak predictive models (decision trees) to develop a strong landslide predictive model. However, the effectiveness of algorithms greatly relies on choosing the best Hyperparameter values. This study examines the utilization of hyper-parameter optimization techniques in combination with the XGBoost algorithm to improve the performance of landslide susceptibility Modeling. Sixteen causative factors were utilized in this study based on the topographical and geological conditions of the study area. Including active, old, and stabilized landslides, 375 inventories were created using satellite imagery and validated through field investigation. The inventory map was divided into training (70%) and testing (30%) datasets through a random sampling method and further converted the dataset into dichotomous binary data to construct the XGBoost Landslide prediction model. Higher classification accuracy with an AUC-ROC curve ( $AUC = 0.92$ ) could be

---

D. Keshri (✉)

Department of Civil Engineering, School of Engineering and Technology (SOET), DIT University, Dehradun, Uttarakhand 248001, India  
e-mail: [Dipika.keshri@dituniversity.edu.in](mailto:Dipika.keshri@dituniversity.edu.in)

D. Keshri · K. Sarkar

Department of Applied Geology, Indian Institute of Technology (Indian School of Mines) Dhanbad, Dhanbad 826004, India

S. L. Chattoraj

Geosciences and Disaster Management Studies Group, IIRS, Dehradun, Dehradun 248001, India

obtained from the XGBoost algorithm. The result shows that with the tuning of Hyper-parameter optimization, the XGBoost model gains the 84.73% kappa score and 92.40% accuracy score, which generates the final Landslide Susceptibility Mapping of the study area.

**Keywords** XGBoost · Hyper-parameter optimization · Landslide susceptibility modeling · Accuracy score · Kappa score

## 1 Introduction

The complex geological, topographical, and geomorphological structure of the Himalayan region makes it prone to frequent landslides, especially during short bursts of high-intensity rain (Champati et al., 2016; Ahmed, 2015), seismic activity or any other circumstances suitable for slides. These natural disasters can be incredibly destructive, causing severe economic loss and loss of people's lives (Wang et al., 2021; Chatteraj, 2017). Much research indicates that the Himalayan region experiences annual landslides due to high-intensity rainfall during a short period of time span or continuous low-intensity rainfall with a longer duration (Nayava et al., 2022; Pandey et al., 2021; Chakraborty et al., 2019). However, it was also evident from various research that rainfall is recommended as a triggering factor. Deforestation, ill-planned land use, and infrastructure development in hazardous mountainous regions cause rock falls, debris flows, and soil erosion (Regmi et al., 2014a, b; Regmi et al., 2014a, b). For an effective solution to reduce and mitigate landslide disasters, it is crucial to understand the historical and current causes that trigger landslides.

Currently, there are several assessment methods being used to evaluate the susceptibility map. The qualitative or direct approach is entirely subjective and relies upon expert opinion, whereas the quantitative or indirect method is based on statistical calculation. In general, the quantitative approach is widely used for predicting future landslides by studying landslide history and the conditioning factors that provide better accurate results, especially where field knowledge of the operator is limited. In the era of machine learning, many tools were utilized to check the accuracy of the prediction of landslide susceptibility maps in which Random Forest (RF), Support Vector Machine (SVM), Artificial Neural Network (ANN), Logistic Regression (LR), K-Nearest Neighbor (KNN), Gradient Boosting and XG Boost, were most popular machine learning tool. In this research, the XGBoost machine learning model was used to map the susceptibility of landslides. XGBoost, short for "Extreme Gradient Boosting," has gained immense popularity in the world of machine learning. It is an ensemble learning algorithm which creates a strong predictive model by combining the predictions of multiple weak predictive models. It belongs to the supervised class of boosting algorithms, which iteratively trains weak models and assigns higher weights to misclassified instances to improve subsequent models. The unique characteristic of XGBoost lies in its optimization objective and regularization techniques, which make it highly efficient and accurate. This algorithm is highly effective in

managing large datasets and excels in classification and regression tasks. Currently, the landslide susceptibility map heavily relies on this model for its production. In order to produce a susceptibility map of landslide locations, we have selected sixteen causative factors, including slope, elevation, rainfall, aspect, Normalized Difference Vegetation Index (NDVI), land use land cover, Stream Power Index (SPI), Topographic Wetness Index (TWI), distance from river, geology, geomorphology, distance from road, distance from lineament, relative relief, plan curvature, and profile curvature. It was proven by various peer-reviewed journals that utilizing a maximum selection of causative factors provides a fair result of prediction compared to using fewer factors (Keshri et al., 2024; Hammad Khaliq et al., 2023; Maqsoom et al., 2022; Batar & Watanabe, 2021; Mandal et al., 2021; Sahin, 2020; G. Wang et al., 2020; Chakraborty et al., 2019; Zhang et al., 2017). The model performance will be evaluated using the accuracy score, AUC, and Kappa score. The final output will show the susceptibility level in high, medium, and low landslide susceptibility.

## 2 Study Area

The Aglar Watershed, is situated in the Dehradun and Tehri Garhwal district of the Lesser Himalaya region and has been chosen as a study area for the bypass road for Chardham Yatra. The geocoordinates of the watershed are 30°24' N to 30°35' N and 78°0' E to 78°18' E, and it covers a total area of 307.280 square km with elevations ranging from 674 to 3016 m (Fig. 1). The region is home to around two hundred and fifty six villages (Department of Drinking Water and Sanitation, Ministry of Jal Shakti, GOI) and experiences frequent annual landslides, although there have been not directly reported casualties so far. These areas has not been previously studied for landslide susceptibility, making it a prime location to identify high, moderate, and low susceptibility zones.

Aglar River is the primary tributary of Yamuna River, which runs through the center of the study area and flows from east to west, dividing the region into two parts. The river has a length of approximately 34.34 km. The Aglar River is the only perennial spring in the region, which supplies domestic water to the entire village. Precipitation is the primary source of recharge to the springs, rivers, and aquifers. The area's climatic conditions are sub-tropical to temperate, with an approximate total rainfall of 1901.7 mm based on the record of 2014–15 (Kumar & Sen, 2018). GPM monthly precipitation data from 2001 to 2021 with a spatial resolution of  $0.1^\circ \times 0.1^\circ$  has been utilized. The precipitation ranges from a minimum of 40.54 mm to a maximum of 45.24 mm (Keshri et al., 2024).

The study area is situated between major Thrust Planes to the north and south. The northern flank is bordered by the Main Central Thrust (MCT), Tons Thrust (TT), and North Almora Thrust (NAT), while the Main Boundary Thrust (MBT) is present in the southern flank. The MCT separates the study area from the Greater Himalayan region and confines it within the Lesser Himalayan zone. The area is mainly located within the lap of Tons Thrust and MBT and is surrounded by numerous minor thrust

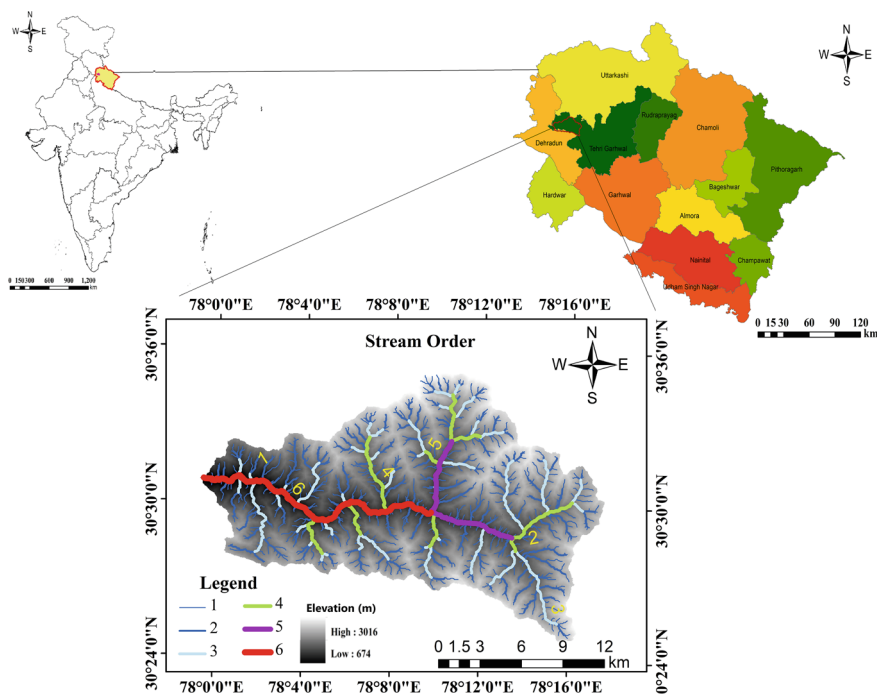


**Fig. 1** a Map of India showing the Uttarakhand state with study area; b Showing Uttarakhand state with study area; c study Area (Aglar watershed) showing the stream order with elevation

and fault planes, as highlighted in Fig. 2. The national highways NH 507 and NH707 meet near the outlet of the Aglar River. These national highways are widely used by pilgrims for Uttarakhand Chardham Yatra.

### 3 Materials and Method

#### 3.1 Data Collection and Preparation (Landslide Inventory Map and Causative Factors)

It's important to gather information about the distribution and historical characteristics of past landslides in order to create a susceptible map of particular region. Conducting a thorough and systematic investigation of the landslide inventory in specific region can provide reliable information on the distribution and characteristics of past landslide events (Fang et al., 2020; Nguyen et al., 2019; Guzzetti et al., 2007, 1995).

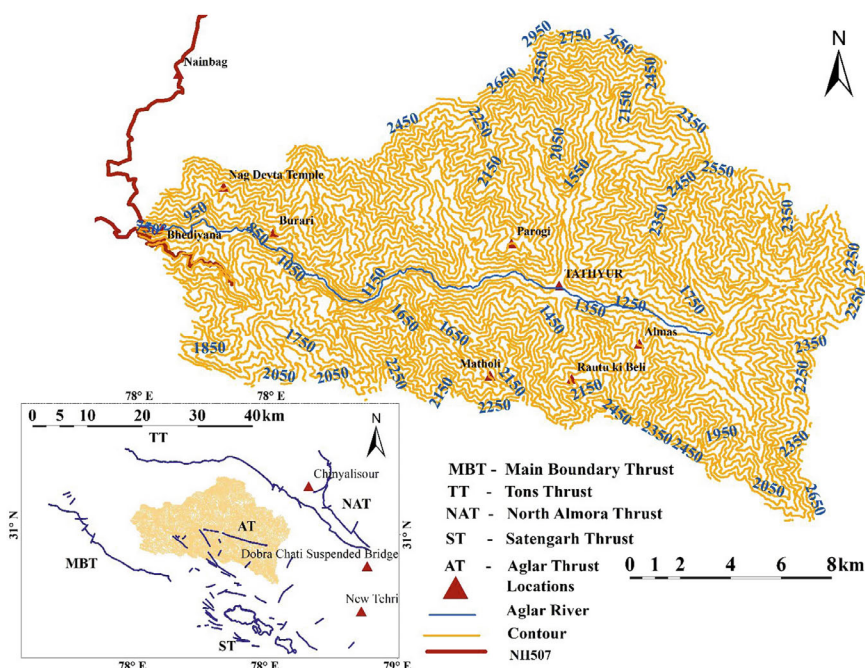


**Fig. 2** Contour map of the study area with locations and major thrust and fault planes

It seems that in this particular region, there are three different types of landslides that are typically reported. These include rock fall, debris fall, and mix complex slides. Interestingly, the height and width of these landslides vary greatly, ranging from approximately 10 m to 100 m and 60 m to 200 m, respectively. Additionally, it was noted that the majority of these landslides tend to increase in both height and width over time.

To identify these landslide events, a landslide inventory has been prepared using satellite imagery and field observational data. A total of 375 polygon of landslide events were prepared and sixteen causative factors were selected for landslide susceptibility mapping. These factors were chosen based on the geological, meteorological and topographical conditions of the region, and by reviewing the literature from various sources (Youssef & Pourghasemi, 2021; Achour & Pourghasemi, 2020; Zhou et al., 2018; Regmi et al., 2014a, b; Sarkar et al., 1995). The causative factors were then processed using GIS and remote sensing techniques (Table 1).

To develop and test the model, 375 landslide inventory polygons were split through a random sampling method and divided into 70% training datasets and 30% validation datasets. Further, the training set was used to establish the spatial relationship between causative factors and landslide inventories. Both the training and validation sets were further divided into two zones: one where landslides occurred, represented by '1', and another one where landslides did not occur, marked by '0'.

**Table 1** Data collection using multiple sources

Conditional factors	Source	Spatial resolution
Slope, aspect, elevation, profile curvature, plan curvature, relative relief	ALOS PALSAR DEM	12.5 m
Geology	Bhukosh web portal, NRSC	1:124,370
Distance from lineament, geomorphology, NDVI, proximity to road	Landsat 8 OLI-TIRS	30 m
Distance from stream, SPI, TWI	ALOS PALSAR DEM	12.5 m
Rainfall	2001–2021 GPM data with half-hourly temporal resolution	$0.1^\circ \times 0.1^\circ$
LULC	LISS-IV	5.8 m

### 3.2 Data Analysis

The process of data modelling was executed in the R Studio platform of R programming language using XGBoost and Hyper parameter optimization machine learning tool (Wei et al., 2022; Can et al., 2021; Wang et al., 2021; Sahin, 2020). All sixteen causative factors were prepared in the GIS environment, and background spatial statistics were calculated using GIS. Image layer stacking and land use land cover image classification were done using Erdas Imagine (Fig. 3). To start the analysis, all sixteen causative factors were converted into raster format. The 375 landslide inventories were superimposed onto all raster causative factor maps to get the feature attributes of the corresponding raster cells. This information was used to create training datasets for the model. These datasets were divided into a 70% training dataset and a 30% validation dataset through a random sampling method. The dataset, consisting of 784 observations and 17 variables, was randomly divided into a 70% training set and a 30% validation set for machine learning (ML) algorithm implementation. Z-score normalization was used on both the training set (548 samples, 16 features) and the validation set (236 samples, 16 features). Z-score normalization, expressed mathematically shown in Eq. 1.

$$I_s = \frac{(I_a - \mu)}{\chi} \quad (1)$$

It involves scaling the data using the mean ( $\mu$ ) and standard deviation ( $\chi$ ) of the samples. XG Boost model was trained using the training set and evaluated using the validation set to assess their predictability. Performance measures such as accuracy, and Kappa score were used to evaluate the trained models (Saha et al., 2023; Kainthura & Sharma, 2022; Nanda et al., 2020).

To increase the stability and reliability of parametric statistics, multicollinearity is assessed by calculating tolerance (TOL) and variance inflation factor (VIF) (Eq. 2



and 3) (Al-Najjar et al., 2021; Adnan et al., 2020).

$$\text{tolerance}(TOL) = 1 - X_i^2 \quad (2)$$

$$\text{variance inflation factor}(VIF) = \frac{1}{(1 - X_i^2)} \quad (3)$$

where  $X_i^2$  represents the proportion of the variance between the  $i$ th selected predictor variable that the other predictor variables can explain.

This analysis is performed in R programming. Various studies states that the acceptable limits of tolerance is greater than 0.1 and for VIF it is less than 10, respectively (Arabameri et al., 2020). In this study the minimum value of tolerance and VIF is 0.34 and 1.10 whereas the maximum value of TOL and VIF is 0.91 and 2.98 respectively, which suggests low multi-collinearity shown in Table 2. The modelling algorithms are applied firstly to train the datasets and further applied to validate datasets. The accuracy of both models is evaluated using statistics such as Accuracy score, and Kappa score. Finally, model has been applied to the entire dataset to classify the study area into low, medium, and high landslide susceptibility. The entire methodology has been shown in the Fig. 4.

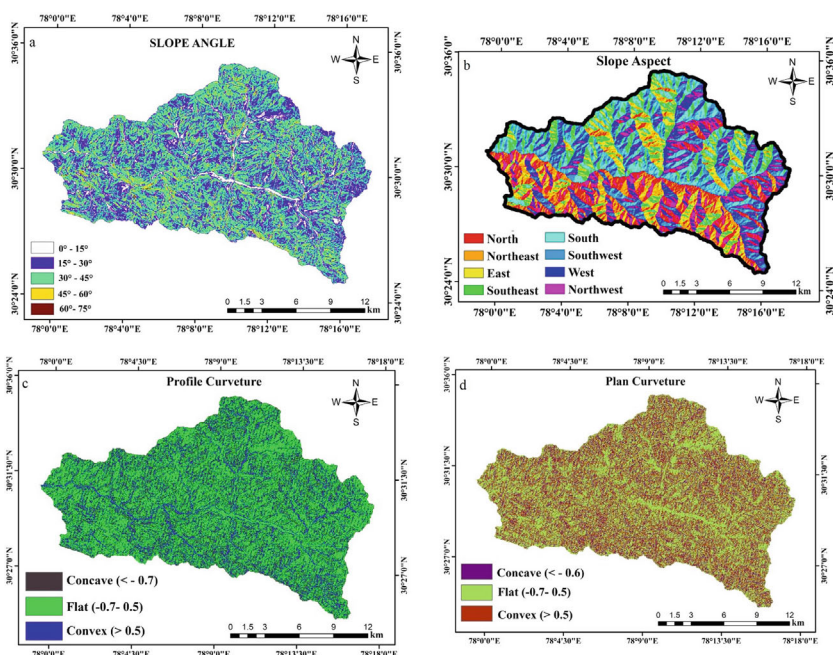


**Fig. 3** Sixteen selected causative factors for the study. **a** Slope angle, **b** Slope aspect, **c** Profile curvature, **d** Plan curvature, **e** Elevation, **f** Relative relief, **g** Geology, **h** Distance from stream, **i** Distance from road, **j** NDVI, **k** SPI, **l** TWI, **m** Rainfall, **n** Lineament, **o** Geomorphology, **p** LULC

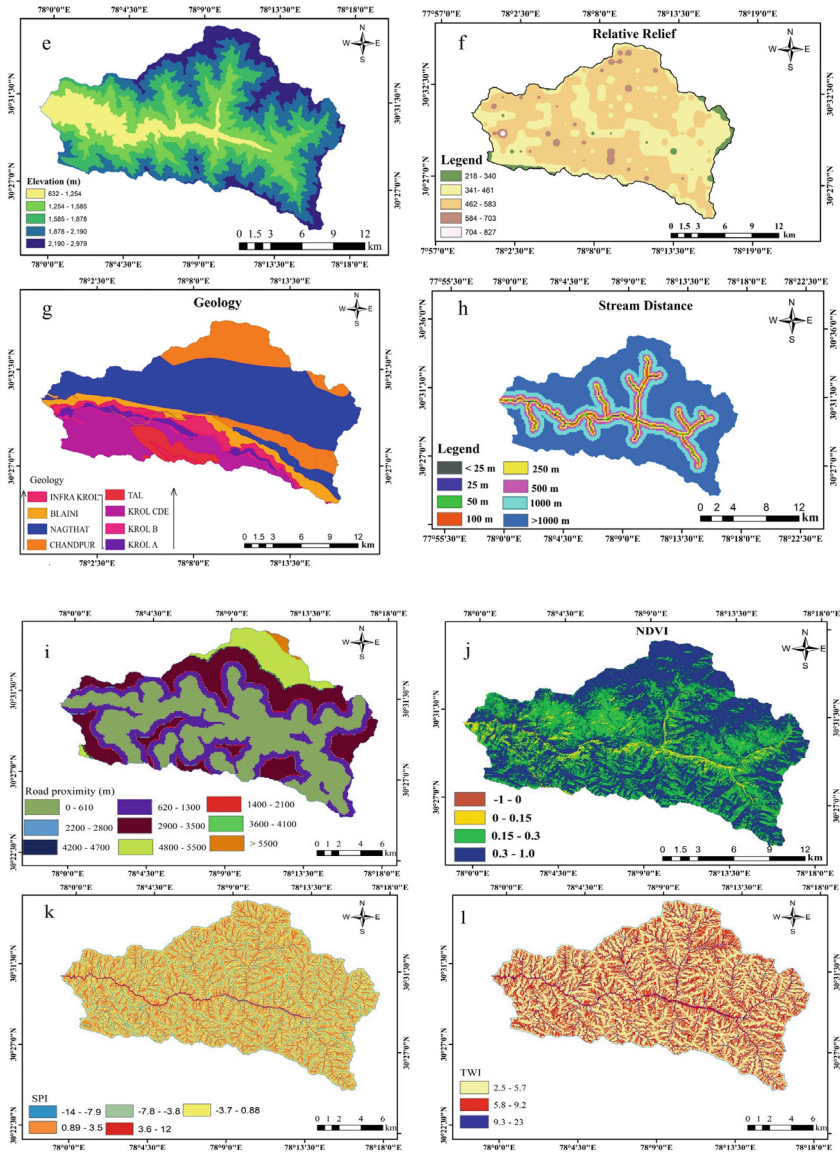


Fig. 3 (continued)

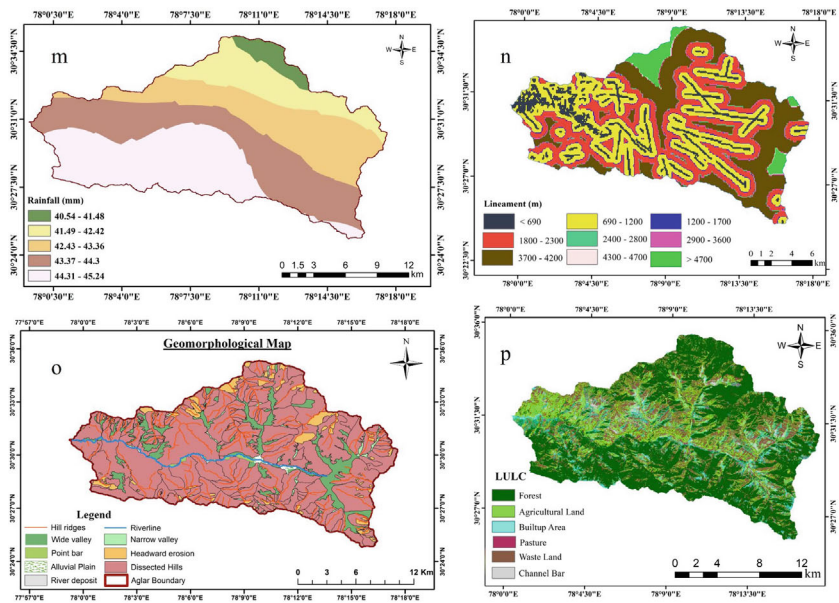
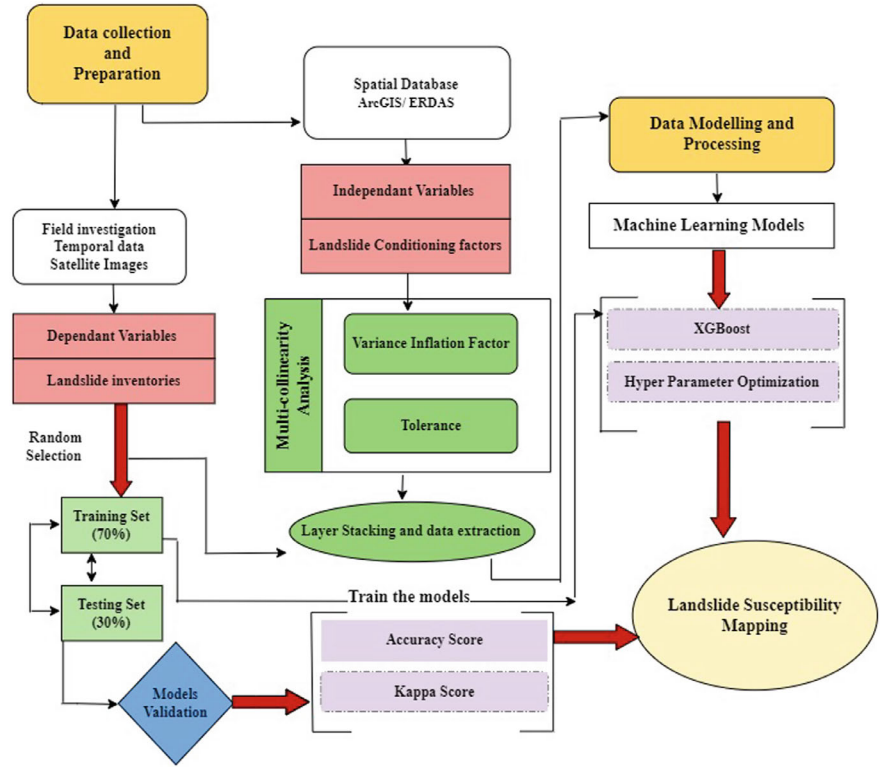


Fig. 3 (continued)

**Table 2** Multi-collinearity analysis of the causative factors

Independent variables	TOL	VIF
TWI	0.34	2.98
SPI	0.37	2.70
Elevation	0.39	2.58
Rainfall	0.42	2.37
Proximity to stream	0.46	2.17
Slope	0.51	1.95
Road	0.57	1.76
Geology	0.60	1.66
Plan curvature	0.62	1.61
Profile curvature	0.66	1.51
Geomorphology	0.71	1.41
Relative Relief	0.80	1.25
NDVI	0.81	1.24
Lineament	0.88	1.14
LULC	0.89	1.13
Aspect	0.91	1.10



**Fig. 4** Applied methodology of entire research work

## 4 Results and Discussion

The study evaluated the performance of XGBoost ensemble learning model in combination with Hyperparameter optimization techniques. The evaluation was based on accuracy score, and kappa score to determine the better performing model. Table 3 provides the performance validation of both models.

According to Table 3, the XGBoost model with the Hyperparameter optimization technique performs better than the XGBoost model without Hyperparameter optimization in validation datasets. With Hyperparameter tuning, the XGBoost model achieved a kappa score of 84.73% and an accuracy score of 92.40%. The XGBoost model without Hyperparameter tuning achieved a kappa score of 84.49% and an

**Table 3** Validation of the performance of both model

Parameters	XGBoost tuning without hyper-parameter optimization (%)	XGBoost tuning with hyper-parameter optimization (%)
Accuracy score	92.28	92.40
Kappa score	84.49	84.73

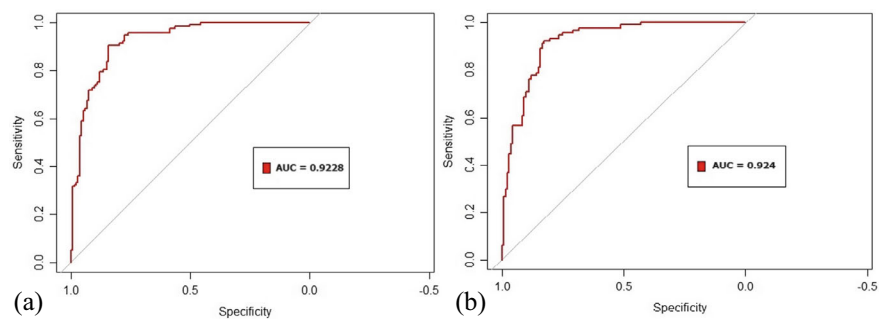


**Fig. 5** XGBoost tuning **a** without hyper-parameter optimization **b** with hyper-parameter optimization

accuracy score of 92.28%, as shown in Fig. 5. The model has also been able to select the causative factor variable importance shown in Fig. 6.

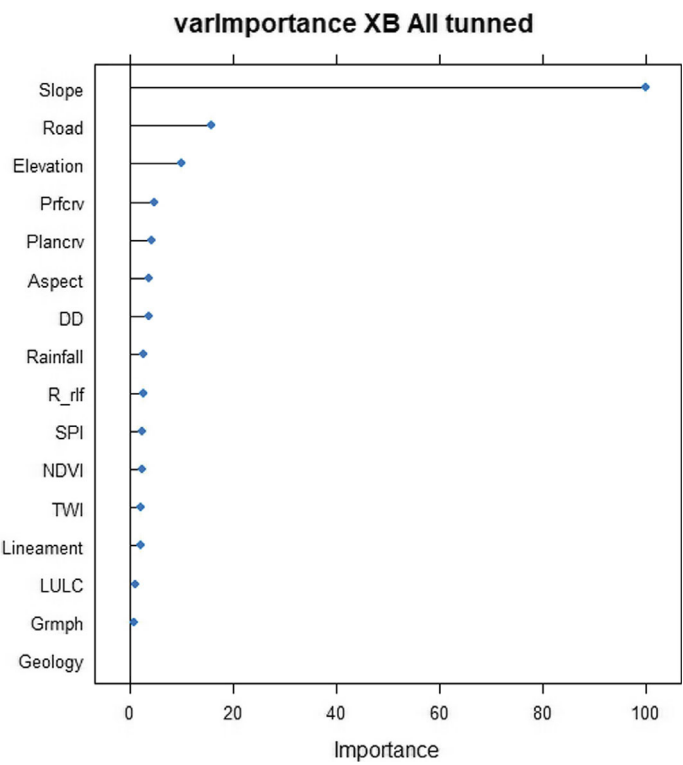


**Fig. 6** Causative factor variable importance chosen by the applied model i.e., XGBoost with hyperparameter optimization techniques

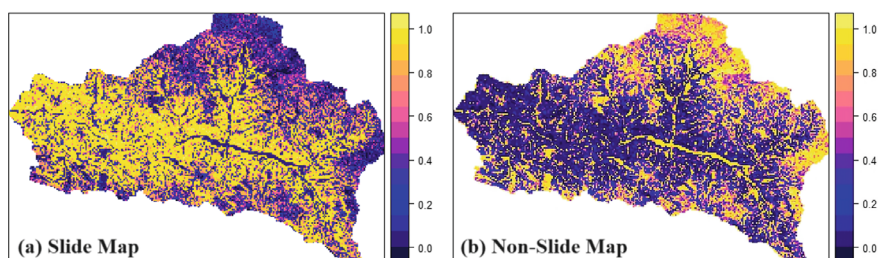


**Fig. 7** Both map has been prepared by R studio platform in R programming. **a** Map showing predicted landslide map where ‘0’ showing the areas of non-slide and 1 represent the area of highly susceptible zones for slide and vice versa in **(b)**

The study concluded that using the XGBoost model with Hyperparameter is more effective than the traditional XGBoost without Hyperparameter model for mapping landslide susceptibility. The XGBoost model was then applied to the study area to identify the landslide-prone zones, as shown in Fig. 7.

## 5 Conclusion

In areas where landslides cause damage to life and property, identifying the susceptible areas can help reduce casualties. The study area comprises approximately 256 villages with a total population of around 87,648. Modeling the landslide susceptibility of an area is a complex task that requires a thorough understanding of the region. XGBoost, a machine learning algorithm with ensemble technique, can handle complex and non-linear relationships in small or large datasets, allowing it to capture subtle patterns and connections for landslide prediction. This results in more accurate susceptibility maps. Additionally, hyper parameter optimization can lead to simpler and more interpretable models. This feature is particularly helpful in geoscience, where understanding the causative factors that contribute to model landslide susceptibility is crucial for developing effective mitigation strategies. The use of the XGBoost model, along with hyper parameter optimization techniques, enhances the accuracy, efficiency, and interpretability of landslide susceptibility mapping, resulting in more reliable and actionable results for disaster prevention. Upon calculating the area of susceptible zones of each category, it was determined that 47.93% of the study area is highly susceptible, 17.86% is moderately susceptible, and 34.19% is low susceptible zones for landslide shown in Fig. 8. The concept of building a Landslide Susceptibility Map using XGBoost with hyper-parameter optimization techniques can be extrapolated from a known region to an unknown region. This study provides valuable information to decision-makers, policymakers, and engineers for implementing landslide prevention measures, sustainable infrastructure development, land use planning, and slope stability analysis.



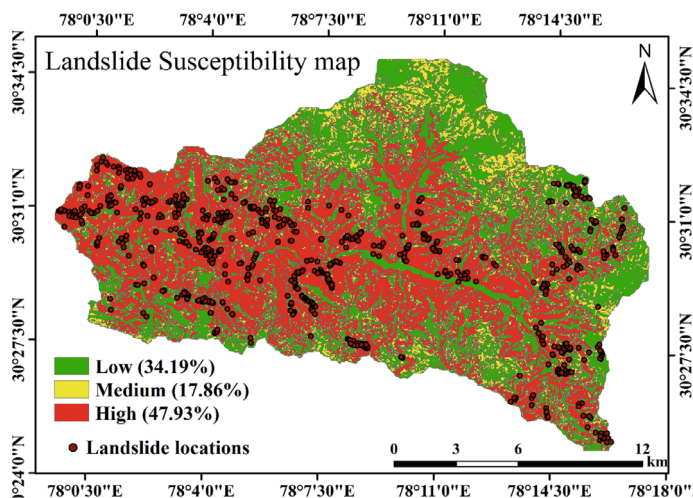


**Fig. 8** Landslide susceptibility map using XGBoost model with hyperparameter optimization techniques

**Acknowledgements** Acknowledgements to the Indian Institute of Technology (Indian School of Mines) Dhanbad; Indian Institute of Remote Sensing, Dehradun; and DIT University, Dehradun, Uttarakhand, for providing the necessary facilities to finish the work.

## References

- Adnan MSG, Rahman MS, Ahmed N, Ahmed B, Rabbi MF, Rahman RM (2020) Improving spatial agreement in machine learning-based landslide susceptibility mapping. *Remote Sens* 12(20):1–23. <https://doi.org/10.3390/rs12203347>
- Ahmed B (2015) Landslide susceptibility mapping using multi-criteria evaluation techniques in Chittagong Metropolitan area Bangladesh. *Landslides* 12(6):1077–1095
- Al-Najjar HAH, Pradhan B, Kalantar B, Sameen MI, Santosh M, Alamri A (2021) Landslide susceptibility modeling: An integrated novel method based on machine learning feature transformation. *Remote Sens* 13(16). <https://doi.org/10.3390/rs13163281>
- Arabameri A, Saha S, Roy J, Chen W, Blaschke T, Bui DT (2020) Landslide susceptibility evaluation and management using different machine learning methods in the Gallicash River Watershed, Iran. *Remote Sens* 12(3). <https://doi.org/10.3390/rs12030475>
- Chakraborty T, Alam MS, Islam MD (2019) Landslide susceptibility mapping using Xgboost model in Chittagong District, Bangladesh. In: *International conference on disaster risk management*, pp 431–434. [https://jidpus.buet.ac.bd/ICDRM2019/resources/proceedings-papers/73\\_ICDRM\\_2019\\_Proceedings.pdf](https://jidpus.buet.ac.bd/ICDRM2019/resources/proceedings-papers/73_ICDRM_2019_Proceedings.pdf)
- Champati Ray PK, Chatteraj SL, Bisht MPS, Kannaujiya S, Pandey K, Goswami A (2016) Kedarnath disaster 2013: causes and consequences using remote sensing inputs. *Nat Hazards* 81(1):227–243. <https://doi.org/10.1007/s11069-015-2076-0>



- Chattoraj SL (2017) Debris flow modelling and risk assessment of selected landslides from Uttarakhand-case studies using earth observation data. In: Remote sensing techniques and GIS applications in earth and environmental studies. IGI Global, pp 111–121
- Kainthura P, Sharma N (2022) Machine learning driven landslide susceptibility prediction for the Uttarkashi region of Uttarakhand in India. *Georisk* 16(3):570–583. <https://doi.org/10.1080/17499518.2021.1957484>
- Keshri D, Sarkar K, Chattoraj SL (2024) Landslide susceptibility mapping in parts of Aglar Watershed, Lesser Himalaya based on frequency ratio method in GIS environment. *J Earth Syst Sci* 133(1):1–26
- Kumar V, Sen, S (2018) Analysis of spring discharge in the lesser Himalayas: a case study of Mathamali Spring, Aglar Watershed, Uttarakhand. In: Water resources management: select proceedings of ICWEES-2016, pp 321–338
- Nanda A, Sen S, Sharma AN, Sudheer KP (2020) Soil temperature dynamics at hillslope scale-field observation and machine learning-based approach. *Water (Switz)* 12(3). <https://doi.org/10.3390/w12030713>
- Nayava JL, Bhusal JK, Paul JD, Buytaert W, Neupane B, Gyawali J, Poudyal S (2022) Changing precipitation patterns in far-western Nepal in relation to landslides in Bajhang and Bajura districts. *Geogr J Nepal* 15:23–40. <https://doi.org/10.3126/gjn.v15i01.42884>
- Pandey P, Chauhan P, Bhatt CM, Thakur PK, Kannaujia S, Dhote PR, Roy A, Kumar S, Chopra S, Bhardwaj A (2021) Cause and process mechanism of rockslide triggered flood event in Rishiganga and Dhauliganga River Valleys, Chamoli, Uttarakhand, India using satellite remote sensing and in situ observations. *J Indian Soci Remote Sens* 49:1011–1024
- Regmi AD, Devkota KC, Yoshida K, Pradhan B, Pourghasemi HR, Kumamoto T, Akgun A (2014a) Application of frequency ratio, statistical index, and weights-of-evidence models and their comparison in landslide susceptibility mapping in central Nepal Himalaya. *Arab J Geosci* 7(2):725–742. <https://doi.org/10.1007/s12517-012-0807-z>
- Regmi AD, Yoshida K, Pourghasemi HR, Dhital MR, Pradhan B (2014b) Landslide susceptibility mapping along Bhalubang—Shiwapur area of mid-Western Nepal using frequency ratio and conditional probability models. *J Mt Sci* 11(5):1266–1285. <https://doi.org/10.1007/s11629-013-2847-6>
- Saha S, Bera B, Shit PK, Sengupta D, Bhattacharjee S, Sengupta N, Majumdar P, Adhikary PP (2023) Modelling and predicting of landslide in Western Arunachal Himalaya, India. *Geosystems Geoenvironment* 2(2). <https://doi.org/10.1016/j.geogeo.2022.100158>
- Wang S, Zhuang J, Zheng J, Fan H, Kong J, Zhan J (2021) Application of bayesian hyperparameter optimized random forest and XGBoost model for landslide susceptibility mapping. *Front Earth Sci* 9:1–18. <https://doi.org/10.3389/feart.2021.712240>

## Website Links

Har ghar Jal, Jal Jeevan Mission, Department of Drinking Water and Sanitation, Ministry of Jal Shakti (GOI), <https://ejalshakti.gov.in/>

**Dipika Keshri** has completed Master's in Science from the University of Burdwan, West Bengal, with distinction in the Applied Geology Department. She has also completed her Master's in Technology in Petroleum Exploration from the Indian Institute of Technology, IIT (ISM), Dhanbad (India), with distinction in the Applied Geology Department. She was honored with a gold medal from the Indian Institute of Technology, IIT (ISM), Dhanbad, India, during her Master's. She is currently pursuing Ph.D. at the Indian Institute of Technology, IIT (ISM), Dhanbad (India) in the Applied Geology Department, in collaboration with ISRO-IIRS, Dehradun. She has twelve years

of experience in the academic industry at an institute of repute in India. Her current research interests include landslide hazards and risk analysis, application of machine learning tools in various domains, kinematic analysis, numerical modeling, and identifying groundwater potential zones through remote sensing.

**Kripamoy Sarkar** is an Associate professor in the Department of Applied Geology in the Indian Institute of Technology (Indian School of Mines) Dhanbad. He is an accomplished and trained Engineering Geologist by profession with unique blend of industry and academic experience, has contributed significantly in the field of natural hazard investigations and soft computing applications in landslides. A few noteworthy contributions of Prof. Sarkar include improvements in rock mass characterization systems, and application of numerical modelling techniques to solve slope instability problems in the Indian Himalayas. His list of publications includes 85 scientific papers in various national and international journals and conference proceedings of repute. He has also published 4 edited book chapters that reflect advanced studies on the assessment of the landslide hazards. Prof. Sarkar has been the principal investigator of 5 major projects on landslide vulnerability analysis and rockfall hazard assessment sponsored by the Ministry of Earth Sciences, DST, and IIT (ISM) Dhanbad in the Northern and North-Eastern parts of the Indian Himalayas. He is the recipient of the prestigious Inder Mohan Thapar Research Award (2021 & 2022) from IIT (ISM) Dhanbad. He is an Associate Editor of the Journal of Earth system Science.

**Shovan Lal Chatteraj** has been working as a Scientist in Geosciences Department, Geosciences and Disaster Management Group, Indian Institute of Remote Sensing (ISRO), Dehradun, for the last 12 years. After receiving the University Gold Medal in master's degree, he completed his PhD in sedimentary geochemistry from IIT Bombay, Mumbai. He is honoured with high ranks in Graduate Aptitude Test (GATE) and UPSC Geologist Exam. He was exposed to real-time challenges in the field of engineering geology while being associated with NHPC Ltd. as a geologist for 3 years. He has authored many research articles, published in national and international journals/periodicals and books in the field of sedimentary geology, landslide modelling, hazard assessment and applications of remote sensing in mineral exploration. He presently is serving as Associate Editor in Journal Indian Society of Remote Sensing, Springer. He is honoured with LT RAMA Rao birth Centenary award, Geological Society of India. Till date, he has supervised two Ph.D., 18 M. Tech and many PG Diploma students. His current interest lies in Numerical modeling and process-based simulation of Debris flow, Slope Stability analysis and rock strength, Hyper-spectral Remote Sensing, Mineral Exploration, Spectroscopic characterization of Minerals and Geochemistry, Metallogenesis and ore formation system, Lunar and Martian surface mineralogy, morphology and terrestrial analogues.